Resolving the organic carbon budget of a humic, oligotrophic lake in the west of Ireland.

A thesis presented to the School of Health and Science, Dundalk Institute of Technology in the fulfilment of the requirements of the degree of

Doctor of Philosophy

Brian Christopher Doyle MSc. BSc.

March 2021

Academic Supervisors: Professor Eleanor Jennings[1]

Dr Elvira de Eyto[2]

Dr Valerie McCarthy[1]

[1] Dundalk Institute of Technology, Dundalk, Co Louth, Ireland
[2] Marine Institute, Furnace, Newport, Co.Mayo, Ireland

Declaration

I hereby certify that this material, which I now submit for assessment on the programme of study leading to the award of doctor of philosophy (PhD) is entirely my own work, and that I have exercised reasonable care to ensure that the work is original, and does not to the best of my knowledge breach any law of copyright, and has not been taken from the work of others save and to the extent that such work has been cited and acknowledged within the text of my work.

Signed: 

Student ID No: D00198154

Date: 29/03/2021

Supervisor Name: _____

Supervisor Signature: _____

Date: _____

Funding

The work described in this thesis was funded by the Marine Institute as part of their Cullen PhD Fellowship and core research and development programmes, grant No. CF/15/05.

Acknowledgements

I consider that I am extremely lucky to have had such excellent support and guidance from my supervision panel throughout the course of my PhD studies. It is true to say that I simply would not have been able to complete this work without their help and encouragement. I wish to express my gratitude to Prof. Eleanor Jennings for sharing her broad span of scientific and statistical knowledge and her unparalleled editing skills! I also wish to thank Dr. Elvira de Eyto for her excellent practical scientific advice, insights, and general positivity which was truly inspiring. And I also wish to thank Dr. Valerie McCarthy for her sound advice and guidance throughout my studies.

Many thanks also to the staff in the Marine Institute, Furnace, Co Mayo, and especially to Mary Dillane, who (along with Elvira), keeps the data streaming in from the Burrishoole catchment. My thanks also to Allison Murdock for her assistance in the DKIT Laboratories.

I also wish to thank Dr. Katrin Attermeyer, Dr. Pascal Bodmer for the opportunity to collaborate in the Eurorun Project, and my gratitude also extends to Dr. Magdalena Nagler for the opportunity to contribute to her European methane biogeography project. Many thanks to Dr. Sean Kelly and Dr Elvira de Eyto, for the opportunity to collaborate on their recent papers.

I also wish to thank The Marine Institute and their Cullen Fellowship Programme for funding this PhD.

On a personal note:
The completion of this thesis would not have been possible without family support. I dedicate this work to my wife, Michelle. Your love, support, encouragement and patience is always treasured (and has been upgraded from ‘legendary’ to ‘saintly’!). Huge hugs all round and a big thanks to my children, Conor, Emér, Seán and Niamh!

Thanks to Mary and Tom for the accommodation (and great conversations) in Dublin.

Thanks for all the encouragement Colm, John and Tom!

Thanks Mam and Dad, your support and love is always cherished.

Table of Contents

List of Figures

Chapter 3

Chapter 4

Chapter 5

List of Tables

Chapter 2

Chapter 3

Chapter 4

List of Abbreviations

Abbreviation	Full Description
AIC	Akaike's Information Criterion
ANCOVA	Analysis of Covariance
AWQMS	Automatic Water Quality Monitoring Stations
ARMS	Automatic River Monitoring Stations
C	Carbon
CDOM	Chromophoric Disolved Organic Matter
CH_4	Methane
Chl	Chlorophyll
Chl *a*	Chlorophyll a pigment
Chl *b*	Chlorophyll b pigment
Chl *c*	Chlorophyll c pigment
CO_2	Carbon Dioxide
DIC	Dissolved Inorganic Carbon
DO	Dissolved Oxygen
DOC	Dissolved Organic Carbon
DOM	Dissolved Organic Matter
DVM	Diel Vertical Migration
EC	Eddy Covariance
EEMs	Excitation Emission Matrix scan
EPA	Enviromental Protection Agency
EU	European Union
FTU	Formazine Turbidity Unit
GAM	Generalised Additive Model
GAMM	Generalised Additive Mixed Model
GHG	Green House Gas
GPP	Gross Primary Production
IMS	Industrial Methylated Sprits
IPCC	Inter-Governmental Panel on Climate Change
Kd	Light Extinction Coefficient
LOD	Limit of Detection
LOI	Loss of Ignition
MeanH Chl	Daily Average of Hourly Chl Fluorescence
N	Nitrogen
(N)	Buoyancy Frequency
NEE	Net Primary Production
NEP	Net Ecosystem Production
NECB	Net Ecosystem Carbon Budget
NPP	Net Primary Production
OC	Organic Carbon
P	Phosphorus
PAR	Photosynthetically Active Radiation
POC	Particulate Organic Carbon
POM	Particulate Organic Matter
QC	Quality Control
QSU	Quinine sulphate unit
R	Respiration
RFU	Raw Fluorescence Units
SD	Secchi depth

SIA	Stable Isotope Analysis
SMD	Soil Moisture Deficit
SO_2	Sulphur Dioxide
SPI	Standardised Precipitation Index
SRFA	Swannee River Fulvic Acid
SS	Suspended Sediment
SW	Short Wave Radiation
SWT	Surface Water Temperature
THMs	Trihalomethanes
TN	Total Nitrogen
TOC	Total Organic Carbon
TP	Total Phosphorus
TTHMs	Total Trihalomethane
UK	United Kingdom
US	United States
UV	Ultraviolet
WFD	Water Framework Directive
WHO	World Health Organisation

Abstract

Waters draining peatland catchments are generally coloured due to high levels of dissolved and particulate organic carbon (DOC and POC). This flux represents a key link between soil and ocean carbon pools and fuels the aquatic food-web. Knowledge about these carbon fluxes is crucial to broaden our understanding of global C cycling. In three interconnected studies, the dynamics of aquatic carbon cycling were explored in the Burrishoole catchment (Ireland) and its main lake, Lough Feeagh. In the first study, changes in river water colour (a DOC proxy) were analysed in three streams feeding Lough Feeagh. Statistical analysis revealed that three variables, soil temperature, soil moisture deficit, and the North Atlantic Oscillation, explained 66% of colour variance. In the second study, high-frequency measurements of CO_2, in the surface waters of Lough Feeagh, were examined along with a set of environmental variables. CO_2 concentrations ranged between 491 and 1169 µatm, and the lake was a constant source of CO_2 to the atmosphere. Statistical analysis revealed that inflow DOC concentration explained 68% of the CO_2 variability. An organic carbon (OC) budget for Lough Feeagh during 2017 was estimated in the third study. The total OC load to the lake was 2544 t C (equivalent to 817 g m^2 yr^{-1} of lake area), of which 51% was transported as DOC, and 41% as POC, 4% in ground water, 3% as net ecosystem production, and 1% in rainwater. The total OC fate was estimated to be 2689 t C (equivalent to 864 g m^2 yr^{-1} of lake area) of which 49% and 12% were exported as DOC and POC respectively, 28% was deposited as sediment and 11% was emitted as CO_2 to the atmosphere. These studies provided an improved understanding of the quantity of OC in flux and insights into the mechanisms driving these fluxes.

1.0 Introduction

1.1 Background

‘All things begin in order, so they shall end, and so shall they begin again.’

The Garden of Cyrus, Thomas Browne (1658)

Along with nitrogen, sulphur and phosphorus, carbon is one of the elements essential to life on Earth (Archer, 2010). While there is a continuous supply of energy from the Sun, there is a finite and fixed store of these biologically important elements on the planet; the Earth is a closed system. For as long as life has existed, carbon has been cycled through the planet’s atmosphere, biosphere and geosphere, and without its continued re-use, all carbon would have been exhausted eons ago (Archer, 2010). The carbon cycle is therefore essential for life on Earth to continue and thrive. Also, certain carbon compounds, such as CO_2, are important greenhouse gases, which regulate the temperature on Earth (Falkowski et al., 2000). Over the long-term, the carbon cycle is balanced, with atmospheric inputs balanced by outputs to both the biosphere and geosphere. However, in recent decades it has become apparent that the carbon cycle has been disturbed: there is more carbon entering the atmosphere than there is being removed (Rockström et al., 2009). When Charles Keeling set up the Mauna Loa atmospheric research station in 1957, atmospheric CO_2 in Hawaii averaged 317 ppm, by 2013 atmospheric CO_2 concentration reached 400 ppm for the first time, and at the time of writing in December 2020 it had reached 414 ppm (NOAA, 2020). The cause of the increase in atmospheric CO_2 is by now well established: the extraction and burning of fossil fuels which release carbon from long-term stores at a much faster rate than would occur naturally (IPCC, 2014a). The principal impact of increased atmospheric CO_2 concentration is also well established — global warming and resultant climate change.

Evaluating the many impacts of climate change on ecosystem services (defined by Millennium Ecosystem Assessment (2005) as the ‘benefits people obtain from ecosystems’) and formulating appropriate adaptation and mitigation strategies are some of the greatest scientific challenges that must now be addressed. The future climate conditions that are predicted for Ireland, particularly alterations in seasonal precipitation patterns and increased temperatures, are likely to drive many changes to Irish ecosystems (Sweeney and Fealy, 2002; Desmond et al., 2017). One such ecosystem, namely

peatlands, are recognised hotspots for carbon storage (Parish et al., 2008) and are acknowledged to be particularly sensitive to climate change (Ise et al., 2008). A report from the Intergovernmental Panel on Climate Change (IPCC, 2014b) emphasised this vulnerability, stating that terrestrial carbon stores, including peatlands, may destabilise due to climate change. Of particular concern are the resultant increases in the quantity of external organic carbon (OC) entering downstream aquatic ecosystems. Allochthonous, or externally sourced carbon, is the main source of carbon fuelling all trophic levels in many freshwater systems, particularly in catchments dominated by peatland (Hope et al., 1997a). Increases in dissolved organic carbon (DOC) concentrations have been reported in aquatic systems draining peatlands (Freeman et al., 2001; Clark et al., 2007; Worrall et al., 2007; Bates et al., 2008). These increases are hypothesised to be driven in part by global warming (e.g. Freeman et al., 2001; Preston et al., 2011) and also to recovery from the effects of atmospheric acid deposition due to reductions in transboundary air pollution (Monteith et al., 2007; Erlandsson et al., 2008). Whatever the cause, these observed increases have major implications for the chemical and biological processes that occur within these systems.

Research into carbon cycling in aquatic environments, especially lakes and conducted at catchment scale, provides greater understanding of the biogeochemical transfer of carbon from long-term stores to aquatic ecosystems. The role that lakes play in making, storing and mineralising OC is substantial and relevant to regional and global carbon budgets (Hanson et al., 2014b). Lakes are important in terms of global C cycling, however, there are surprisingly few complete and fully balanced lake OC budgets (e.g. Cole et al., 1989; Sobek et al., 2006; Hanson et al., 2014b) and there have been to date, to the best of the student's knowledge, no OC lake budgets conducted in western European peatland regions. Most lake OC budgets are also incomplete owing to the practical difficulties in monitoring and quantifying the many components of aquatic carbon cycles. Complete OC budgets include quantification of 1, the major allochthonous inputs from surface water, groundwater, and atmospheric deposition; 2, losses due to outflow, sediment burial and gaseous evasion, and 3, autochthonous primary production and ecosystem respiration. Over the last 20 years, considerable progress has been made on resolving the carbon budget of one Irish lake, Lough Feeagh (Jennings et al., 2010; Sparber, 2013; Fealy et al., 2014; Ryder et al., 2014; Doyle et al., 2019), primarily through the use of the long-term environmental monitoring data that are collected by the Marine Institute in the Burrishoole catchment.

The Burrishoole catchment is a typical, western upland peatland catchment, and is an important index site, for diadromous fish monitoring and catchment change investigation e.g. (Jennings et al., 2010; Jennings et al., 2012; Dalton et al., 2014; de Eyto et al., 2016). The presence of a research station, run by the Marine Institute on the lakeshore of Lough Feeagh, and the extensive, high and low resolution monitoring that currently takes place throughout the catchment, allows the capture of important biological, environmental and meteorological data streams. Many of these data were analysed and reported in the following chapters and were ultimately used to provide the organic carbon budget for Lough Feeagh, presented in Chapter 5. The OC carbon budget, presented here, delivers a more comprehensive understanding of C cycling in peatland lakes, and provides important insights into the mechanisms and drivers of aquatic OC cycling in maritime temperate climate zones. Given the dearth of knowledge of aquatic OC cycling in an Irish climate context, the student considers that his research makes an original, significant and coherent contribution to the literature in this area. The work is also intended to contribute directly into estimates of greenhouse gas (GHG) emissions from lakes. Currently, lake C emissions are not captured in national emissions budgets for Ireland (EPA., 2019), however, such emission data may be required to be considered by the EPA in future national GHG emission inventories.

1.2 Aims and Objectives

The overarching aim of the research undertaken for this dissertation was to improve the knowledge and understanding of the cycling of aquatic carbon in a peatland catchment, which includes a freshwater lake, using both high frequency and low frequency datasets. To achieve the overarching aim, three main objectives, which focus on three separate aspects of carbon cycling dynamics within the catchment were completed.

1. The first objective was to investigate the drivers of aquatic export of DOC from the Burrishoole catchment to Lough Feeagh. To realise this objective, multi-annual colour data in stream water entering the lake were analysed along with a range of environmental variables. The DOC export from the catchment into Lough Feeagh was also quantified.
2. The second objective was to examine the dynamics of CO_2 evasion from Lough Feeagh to the atmosphere. This was achieved by monitoring the variation of the partial pressure of CO_2 ($_pCO_2$) in the lake over the study period using high frequency sensor data in conjunction with allied sets of environmental data. The

quantity of CO_2 released to the atmosphere from the lake was also estimated using using gas transfer models taken from the literature.

3. The third objective was to calculate and present an organic carbon budget of Lough Feeagh. Included in the budget were: aquatic OC fluxes entering and exiting the lake, groundwater inputs, OC sedimentation to the lake floor and CO_2 emissions to the atmosphere.

1.3 Thesis Structure

This thesis is divided into six chapters; this introductory chapter is followed by Chapter 2, which presents a review of current literature relating to aquatic carbon cycling processes in peatland catchments. This is followed by the three main data chapters.

The title of Chapter 3 is; *Synchrony in catchment stream colour levels is driven by both local and regional climate.* The focus of this published paper was an investigation of the aquatic export of dissolved organic carbon (DOC) from the Burrishoole catchment. Colour (mg PtCO l^{-1}) data in the three main rivers in the catchment — measured using spectroscopy from weekly grab-samples — were used as a proxy for DOC concentrations. Six years of data from 2011 to 2017 were used in the analyses which included spatial analysis of the catchment and also comparisons of seasonal, multi-annual, and random colour trends among the three rivers. The study also investigated the main environmental drivers of dissolved carbon export in the system. The principal aims of the study were firstly to compare random, seasonal and multi-annual trends in water colour from rivers in three sub-catchments in a blanket peatland catchment, secondly to identify and examine the effects of the principal climatic drivers of these trends and finally to estimate the fluvial export of DOC from the catchment over the study period.

Chapter 4 is titled; *Late summer peak in $_pCO_2$ corresponds with catchment export of DOC in a temperate, humic lake* - is focussed on the dynamics of CO_2 evasion from Lough Feeagh within the Burrishoole catchment. $_pCO_2$ at one-meter depth within the lake water column was measured using a high-frequency (15 minutes) aquatic CO_2 sensor placed on the data buoy in the centre of the lake. The principal aims of this chapter were firstly to examine the variation of $_pCO_2$ in the lake over the study period, secondly to model and estimate CO_2 release to the atmosphere from the lake and finally to examine the drivers of the variability of $_pCO_2$ in Lough Feeagh during the study period.

The title of Chapter 5 is *The allochthonous organic carbon budget of an oligotrophic peatland lake.* This chapter presents an allochthonous organic carbon budget of Lough

Feeagh. Aquatic carbon fluxes entering and exiting the lake were estimated using high-resolution Chromophoric Dissolved Organic Matter (CDOM) fluorometers for DOC quantification and high-resolution nephelometers for POC quantification. These high-frequency measurements were also calibrated against weekly colour and suspended sediment data. Groundwater inputs of DOC were estimated from well water sampling and lake sediment traps were used to estimate carbon sedimentation in the lake. CO_2 emissions from the lake were also estimated using a high-resolution aquatic $_pCO_2$ sensor.

Chapter 6- *Synthesis and future research* presents a summary of findings from Chapters 3, 4 and 5 and discusses the implications of these findings. The chapter includes an outline of possible future research paths that are implied by the study. The final conclusions of the thesis are also presented in this chapter.

Appendices A to D contains four published papers that the student has contributed to during the course of his studentship. Two of the papers report studies that have taken place within the Burrishoole catchment and the remaining two papers are European-wide collaborative studies where certain biogeochemical processes within the Burrishoole catchment are reported in context to a range of European sites. Details of the publications and the authors contributions are included in the following section.

1.4 List of publications and description of the author's contribution

Chapter 3 is based on the following paper, Doyle B.C, de Eyto E, Dillane M, Poole R, McCarthy V, Ryder E, Jennings E. 2019. *Synchrony in catchment stream colour levels is driven by both local and regional climate.* Biogeosciences. 16(5):1053–1071. For this paper, Brian Doyle collected environmental samples, undertook research and laboratory analysis, calibrated laboratory instruments, quality-controlled datasets, and analysed data and was the primary author of the paper. Eleanor Jennings, Elvira de Eyto and Valerie McCarthy supervised the research, provide advice on statistical analysis and manuscript writing. Mary Dillane and Elvira de Eyto maintain a wide range of environmental monitoring equipment and subsequent data-streams in the Burrishoole catchment for the Marine Institute. Russell Poole, a section manager at the Marine Institute's facility at Newport, provided editing advice.

Chapter 4 is based on the following paper, Doyle B.C, de Eyto E, McCarthy V, Dillane M, Poole R, Jennings E. (2021). *Late summer peak in $_pCO_2$ corresponds with catchment export of DOC in a temperate, humic lake*. Inland Waters, (Accepted for Publication).

For this paper Brian Doyle collected manual CO_2 lake measurements, quality-controlled a range of environmental and meteorological datasets, researched and analysed data and was the primary author of the paper. Eleanor Jennings, Elvira de Eyto and Valerie McCarthy supervised the research, provide advice on statistical analysis and manuscript writing. Mary Dillane and Elvira de Eyto maintained environmental monitoring equipment and data-streams used in this study. Russell Poole, provided editing advice.

Chapter 5 is based on the following paper, Doyle B.C, de Eyto E, McCarthy V, Dillane M. Jennings E. (2021). The organic carbon budget of an oligotrophic temperate peatland lake. Limnology and Oceanography (In Review). For this paper Brian Doyle collected, collated and quality-controlled a range of aquatic organic carbon data, including river colour, turbidity, lake sediment, CO_2 and lake metabolism data. A range of environmental, hydrological and meteorological datasets were also gathered and analysed. Brian Doyle was the primary author of the paper. Eleanor Jennings, Elvira de Eyto and Valerie McCarthy supervised the research, provide advice on statistical analysis and manuscript writing. Mary Dillane and Elvira de Eyto maintained environmental monitoring equipment and data-streams used in this study.

Appendix A contains the following paper, de Eyto E, Doyle B, King N, Kilbane T, Finlay R, Sibigtroth L, Graham C, Poole R, Ryder E, Dillane M, Jennings E., (2020) *Characterisation of salmonid food webs in the rivers and lakes of an Irish peatland ecosystem.* Biology and Environment: Proceedings of the Royal Irish Academy, Vol. 120B, No. 1, pp. 1-17. The primary author of this paper was Elvira de Eyto. For this paper Brian Doyle prepared a range of environmental samples for stable isotope analysis, including a sample population of juvenile salmonids. He also assisted the primary author with producing some of the paper's figures.

Appendix B contains the following paper, Kelly S, Doyle B, de Eyto E, Dillane M, McGinnity P, Poole R, et al. *Impacts of a record-breaking storm on physical and biogeochemical regimes along a catchment-to coast continuum.* (2020). PLoS ONE 15(7): Sean Kelly was the primary author of this paper. Brian Doyle carried out spatial and statistical data analysis on an array of rain-gauge monitors throughout the Burrishoole catchment to elucidate total rainfall volumes within specific time periods and catchment areas. He also assisted the principal author with the production of a number of figures and graphs within the publication and contributed to a portion of the manuscript text.

Appendix C contains the following paper, *Abundance and biogeography of methanogenic and methanotrophic microorganisms across European streams*. (2020). Nagler, M. Praeg, N. Niedrist, G.H. Attermeyer, K. Catalán, N. Pilotto, F. Gutmann Roberts, C. Bors, C. Fenoglio, S. Colls, M. Cauvy-Fraunié, S. Doyle, B. Romero, F. Machalett, B. Fuss, T. Bednařík, A. Klaus, M. Gilbert, P. Lamonica, D. Nydahl, A.C. González-Quijano, C.R. Bistarelli, L.T. Kenderov, L. Piano, E. Mor, JR. Evtimova, V. deEyto, E. Freixa, A. Rulík, M. Pegg, J. Ortega, S.H. Steinle, L. Bodmer, P. Journal of Biogeography; 00:1-14. For this study, which ranged across 16 European streams from northern Spain to northern Sweden and from western Ireland to western Bulgaria, community compositions of methanogenic and methanotrophic microorganisms were described at large spatial scales. Their abundances were linked to potential sediment production and oxidation rates. Brian Doyle chose a suitable location and collected stream sediment core samples for one site in the study. He also assisted in the manuscript editing process.

Appendix D contains the following manuscript, Attermeyer, K, Casas-Ruiz, JP. Fuss, T. Pastor, A. Cauvy-Fraunié, S. Sheath, D. Nydahl, A.C. Doretto, A. Portela, A.P. Doyle, B.C. Simov, N. Gutmann Roberts, C. Niedrist, G.H. Timoner, X. Evtimova, V. Barral-Fraga, L. Bašić, T. Audet, J. Deininger, A. Busst, G, Fenoglio, S. Catalán, N. de Eyto, E. Pilotto, F. Mor, JR. Monteiro, J. Fletcher, D. Noss, C. Colls, M. Nagler, M. Liu, L. González-Quijano, CR. Romero, F. Pansch, N. Ledesma, J.L.J. Pegg, J. Klaus, M. Freixa, A. Herrero Ortega, S. Mendoza-Lera, C. Bednařík, A. Fonvielle, JA. Gilbert, P. Kenderov, L.A. Rulík, M. Bodmer, P. *Substantial carbon dioxide flux changes from day to night across European streams* (2021) Nature Communications Earth & Environment (In Review). This paper presents the results of a Europe wide collaborative study, also known as the EuroRun project, comprising a year-long investigation of day and night-time CO_2 fluxes of running streams. Fluxes were directly measured once per season using drifting chambers in 34 streams across 11 European countries. As lead member of the Irish team, Brian Doyle attended a workshop at the Erken Laboratory, a facility connected to Uppsala University, located at Lake Erken in Norrtälje, Sweden. At the workshop, participants were trained to: assemble the floating chambers, measure CO_2 fluxes using the chambers and to analyse the data. Brian Doyle then conducted the CO_2 flux analysis on two streams in the Burrishoole catchment during 2017.

2.0 Literature Review

2.1 Introduction

This section reviews the current literature on carbon cycling in aquatic ecosystems within humic catchments. The review firstly presents a broad outline of biogeochemical cycles and of the carbon cycle in particular. The process of carbon storage in peatlands is discussed and recent estimates of the terrestrial stores of carbon contained in Irish peatlands are compared. In the main body of the review, relevant literature is presented regarding the mechanisms and drivers of the production and transport of organic carbon within humic catchments. Also included is an exploration of the physical, chemical and biological processes that may occur in aquatic systems as a result of these carbon inputs. The review concludes by examining the ultimate fate of organic carbon within these systems, including mineralisation to CO_2 and CH_4 within the water column and exchange with the atmosphere.

2.2 Biogeochemical Cycles

The carbon cycle, which describes the movement of carbon (C) through various reservoirs in the biosphere and geosphere, is intimately tied to life-processes. The discipline of biogeochemistry examines the carbon cycle and its links with other biogeochemical cycles such as oxygen, nitrogen and phosphorus and to a lesser extent, iron, sulphur and a variety of trace metals. Ultimately the sun provides the energy to turn the cycles, for example in the carbon cycle it fuels photosynthesis which captures carbon, transforming it into organic compounds. These organic compounds fuel the biosphere and their stored energy is released via respiration (Wetzel, 2001). The vital role of biogeochemical cycles in supporting and maintaining Earth's environments was stressed early in the 20th century by the Russian mineralogist, Vladimir Vernadsky (1863-1945), considered to be the father of biogeochemistry, when he stated: ‘living matter is the most powerful geological force’ (Paton, 2013).

2.3 The Global Carbon Cycle

The global carbon cycle involves atmospheric, terrestrial and marine biogeochemical processes and within the cycle both biological and non-biological reactions occur. It is essentially a hierarchy of three linked sub-cycles that operate on different time-scales. The terrestrial carbon cycle mostly operates within time-scales of months to thousands of years, the marine carbon cycle runs over hundreds of thousands of years, and the geological carbon cycle operates over millions of years (Field & Raupach, 2004; Archer,

2010). In the terrestrial carbon cycle, CO_2 is fixed from the atmosphere by photosynthesis and is transformed into organic compounds. A relatively small fraction of this C is quickly returned to the atmosphere *via* respiration however the majority becomes incorporated into plant tissue. Following death, the plants' C becomes incorporated into the soil C stores and microbial degradation returns it to the atmosphere as CO_2. Some carbon may escape respiration and decomposition and remain in soil carbon and some may be transported into aquatic environments. These compounds in soils stores will have differing levels of lability (Archer, 2010). The carbon cycle within the marine environment operates on intermediate time-scales. In a process known as the 'biological pump', dissolved CO_2 in marine surface waters is utilised by phytoplankton to generate organic matter and over time this organic matter sinks down through the water column while surface water CO_2 is replenished from the atmosphere (Sephton & Smith, 2002). In parallel with the terrestrial carbon cycle, a small proportion of organic matter escapes mineralisation and is buried in sediments. This 'leak' of carbon from both the terrestrial and marine carbon cycles due to burial allows carbon to enter the long-term geological carbon cycle (Sephton & Smith, 2002). Most of the carbon in the global carbon cycle is contained in rock reservoirs and this carbon is returned to the terrestrial or marine carbon cycles when carbon bearing rocks are exhumed by tectonic forces and weathered or directly oxidised to CO_2 (Archer, 2010).

2.4 Peatland as a Carbon Sink

One important pathway for carbon from the terrestrial carbon cycle into long-term storage is the build-up of carbon in peatland soils. Peatlands may be defined as wetland ecosystems where organic matter, called peat, which originates from dead and decaying vegetation accumulates under high water saturation conditions (Hammond, 1981). Estimates of peat depth accumulation rates vary between 0.5 and 1mm $year^{-1}$ or between 5 and 10 m over 10,000 years, with considerable local variation (Clymo, 1992). Historic estimates have shown that worldwide, peatlands have accumulated between 274 and 550 gigaton (GT) of carbon (Gorham, 1991; Immirzi et al., 1992; Lappalainen, 1996; Sheng et al., 2004; Vasander & Kettunen, 2006). These widely-varying estimates of the peatland carbon pool are the result of differences in the calculation of the extent and depth of peatlands, as well as a dearth of reliable data on the bulk density of different peat deposits (Charman, 2002; Turunen et al., 2002). More recent analysis indicates that although the rate of global peatland C accumulation has varied greatly over time, peatlands have, in total, accumulated greater than 600 GT of carbon over the Holocene (i.e. the last cs.

11,500 years), serving as a long-term persistent sink of approximately 5 billion tonnes of C per century on average (Yu et al., 2010). This substantial reservoir of sequestered carbon in global peatlands is large enough to have had a significant impact on the global C budget and atmospheric CO_2 change (Joos & Prentice, 2004; Elsig et al., 2009). Spatially, peatlands cover 3% of the global land area (Dise, 2009; Bain et al., 2011) and contain approximately one-third of the world's soil carbon (Bain et al., 2011).

2.5 Irish Peatlands

There are four, distinct sub-groups of Irish peatland, namely; Fen, Raised Bog, Atlantic Blanket Bog and Mountain Blanket Bog (Renou-Wilson et al., 2011). Fens are groundwater fed (minerotrophic) peatlands that form from vegetation receiving a constant influx of base-rich groundwaters. Most fen peats have a relatively high pH, but some fens have pH values within the acidic range, from 4.5 to 8.0 (Doyle & Ó Críodáin, 2003). Raised bogs, mostly common in central Ireland, originate from fens that continued to develop and grow. Intact and pristine raised bogs are dome-shaped peat masses which average around 7 m in depth (Renou-Wilson et al., 2011). The ongoing development process 'domed up' the bog surface above the surrounding groundwater level and allowed rain-fed peat-moss species to dominate the vegetation and grow upward. Moreover, the dominating Sphagnum (peat moss) species maintain the bog's acidic habitat which further favours continued Sphagnum growth (Hammond, 1981).

Generally, blanket bogs are confined to the oceanic margins of the island where there is constant high rainfall throughout the year. This habitat is most common where the annual rainfall amounts exceed 1,250 mm and there are greater than 225 days with rain (Lindsay, 1995). Similar to raised bogs, blanket bogs are rain-fed or ombrotrophic, with pH ranging between 3.5 and 4.2 (Feehan et al., 2008). Atlantic blanket bogs predominate on the western fringe of Ireland, in the valleys of mountainous areas and on coastal plains, below 200 m elevation. They contain a distinctive suite of vegetation which is clearly different from raised bog and mountain blanket bogs (White & Doyle, 1982). Mountain blanket bogs occur above 200 m elevation on gentle slopes and mountain plateaux. They are also more widely distributed than Atlantic blanket bog (Renou-Wilson et al., 2011).

2.6 Carbon Pool Estimates in Irish Peatlands

Determining the spatial extent of peat soils is essential for measuring the national stock of soil carbon; in addition, healthy peatland soils provide a wide range of ecosystem services such as climate regulation, biodiversity support, water supply, filtration, and

hydrological control (Evans et al., 2014). Assessing the national extent of peatlands across the Republic of Ireland is therefore an important exercise. The most recent estimate of national land area covered by peat soils is 20.6% or 1.4 M ha (Connolly & Holden, 2009) and is substantially larger than prior estimates, such as 17% cover by Hammond, (1981) and 13.8% cover by Connolly et al., (2007). The increase in peat soil cover estimated by Connolly and Holden (2009) can be explained by more extensive occurrence of peat in the drumlin belt counties of the north east of Ireland than had been previously mapped. The first complete soil carbon inventory of Irish peatlands was conducted over fifteen years ago (Tomlinson, 2005) and as estimating techniques have been refined, such as improved mapping of peat soil cover and depth, national soil carbon totals have increased by over 30%. Table 2.5 shows data from four separate studies estimating the total amount of carbon stored in Irish peatlands: the first three estimate amounts in the Republic of Ireland and the last study, in the North of Ireland. Recent work by Teagasc on a national soil survey may further refine both the peat soil extent and carbon pool estimates (Teagasc, 2017).

Table 2.5 Published estimates of carbon stored in Irish peatlands

Source	C Estimate (Mt)	National soil C (%)	Method
Tomlinson, 2005	1071	53	Based on General Soil Map (Gardiner and Radford, 1980)
Eaton et al., 2008	1503	62	Based on peat bog category CORINE 2000, C density (Cruickshank, 1995) and average depth values (Hammond, 1981)
Renou-Wilson et al., 2011	1566	75	Based on peat depth model (Holden and Connolly, 2011), map of peatland spatial extent (Connolly and Holden, 2009), and Tomlinson (2005) estimate for basin peat soil organic C

2.7 Carbon Storage in Peatland Catchments

Following the retreat of the ice sheets from the Irish land surface some 10,000 years ago, peatlands began to develop at variable rates and have accumulated C within peat soils since then (Renou-Wilson et al., 2011). Carbon is stored in different 'compartments' within the peatland ecosystem, namely as biomass, litter, peat soil, mineral soil, and in soil pore water. Each compartment contains varying amounts of C and has different C turnover rates. The peat soil layer is the compartment that contains the greatest amount of carbon as it largely consists of organic matter. Peat is technically defined as comprising greater than 30% dry mass organic matter with a carbon content ranging from 48% to 63% (Heathwaite & Gottlich, 2003) an average of 51% was calculated from various

analyses of Irish peat (Hammond, 1981; Tomlinson, 2005; Renou-Wilson et al., 2011). Peatland ecosystems that are undamaged generally have a consistently high water table and as a result are long-term C sinks (Belyea & Malmer, 2004; Lund et al., 2010). Their high water table creates conditions where CO_2 fixed by photosynthesising vegetation generally exceeds that being released by ecosystem respiration. For the stock of C to continue to increase in peatlands, the rate of carbon sequestration should be greater than the total rate of carbon losses. The net ecosystem exchange (NEE) − determined by subtracting the amount of carbon produced by heterotrophic respiration from the net primary production − should display a negative value (Roulet et al., 2007). It has been observed that NEE has strong diurnal and seasonal variations in peatland systems (Vasander & Kettunen, 2006) with the highest values occurring during summer daytimes. There are, however, large inter-annual variations in NEE (Roulet et al., 2007, Sottocornola & Kiely, 2010) and it is not uncommon that a peatland may switch, in consecutive years, from being a CO_2 sink to source on an annual basis (Alm et al., 1999; Holden et al., 2006; Roulet et al., 2007). The accumulating peat, however, is convincing evidence that in the medium to long-term, these ecosystems have been carbon sinks. Furthermore, peatlands are also a significant source of methane (Huttunen et al., 2003; Laine et al., 2007) as a consequence of the anoxic conditions within the peat body that provide a suitable environment for the microbial breakdown of plant litter and root exudates.

Overall, intact peatlands act as long-term carbon stores, primarily as a result of a persistently high water table, which creates conditions within the peat, whereby the amount of carbon fixed by the peatland vegetation during photosynthesis is greater than that released through ecosystem respiration, methane emissions, leaching, emissions during fire events or surface run-off of dissolved organic carbon (DOC) in streams and rivers (Renou-Wilson, 2011). For example Koehler et al., (2009) reported that a blanket bog in Co Kerry accumulated an average of 29.7 tonnes C km^{-2} yr^{-1} over six years. Similarly Dinsmore et al., (2010) showed that the Auchencorth peatland in central Scotland was a net sink for C, accumulating up to 69.5 tonnes C km^{-2} yr^{-1}. In a review carried out by Joosten (2008) it was estimated that the current rate of carbon sequestration in natural peatlands of the world is just below 100 Mt C $year^{-1}$ and, together with the large stock of C they contain, peatlands play an important role in the regulation of the global C cycle and therefore the global climate.

2.8 Sources of Organic Carbon in Aquatic Systems

Organic carbon in the aquatic environment comprises a mixture of both living and non-living plant, microbe and animal products in various states of decomposition, a portion of which may be used as an energy source for further aquatic production (Tranvik, 1988; Karlsson, 2003). There are three sources of organic carbon in natural waters: allochthonous or external sources, internal or autochthonous sources, and atmospherically deposited sources, however the latter contributes very minor amounts in comparison to the other two sources (Wetzel, 2001; Kortelainen, 2006). The first source, allochthonous organic matter, is derived from the degradation of living matter from the catchment through microbiological and physical processes and also material such as leaf litter, dead biomass that has not yet been decomposed (Dziedzic et al., 2010). This material is transferred from the terrestrial environment to rivers and streams as particulate organic matter (POM) and dissolved organic matter (DOM) (McDonald et al., 2004; Gardner et al., 2005). The diverse sources of allochthonous organic matter ensure its composition is chemically complex, however it may be divided into two broad categories: non-humic and humic substances (Wetzel, 2001; Sebek et al., 2006). Non-humic substances include compounds such as carbohydrates, peptides, amino-acids, fats, waxes, pigments and other components that are low in molecular weight (Hayes & Clapp, 2001). These substances are mostly labile and being easily utilised and degraded by microbial action, exhibit rapid flux rates. Humic compounds on the other hand are high in molecular weight, are recalcitrant and generally resist biological degradation. They are formed by the partial decomposition of plant material by microbial activity and may be stored in the soil for quite lengthy periods of time – peat soils are an excellent example – before further decomposition processes may break them down (Wetzel, 2001; Hudson et al., 2007). Humic compounds may be further divided into three categories: humic acids, fulvic acids and humins, differing from one another in molecular weight and functional group content, and also by solubility at different pH's. Humic acids are soluble in water but precipitate upon acidification, where $pH \leq 2$, fulvic acids are soluble at all pH values and humins are insoluble at all pH values (Hudson et al., 2007). Fulvic acids have the lowest molecular weight of the three compounds and the highest proportion of oxygen containing functional groups (Wetzel, 2001). Humic compounds in DOM are also named collectively as coloured, or chromophoric, dissolved organic matter (CDOM) (; McKnight, 1997; Williamson et al., 1999). These heterogeneous compounds, which range from yellow to dark brown and even black colours, are present in varying concentrations

in all natural waters. The relative proportion of humic compounds in natural waters is multi-factorial and catchment specific (Thacker et al., 2008).

The second source of organic carbon in water bodies is derived within the water body itself by autochthonous primary production. This carbon pool is produced by the fixation of aquatic CO_2 by algal and cyanobacterial phytoplankton and other aquatic plants such as macrophytes and picoplankton (Bertilsson & Travik, 2000; Cole et al., 2000). This autochthonous-fixed carbon can be in converted to POM and DOM by active secretion, decomposition and lysis of macrophytes and attached algae and bacteria. These autochthonous carbon sources are labile and in turn progressively mineralized by heterotrophic microflora to CO_2 and heat (Bertilsson & Travick, 2000). Both allochthonous and autochthonous sources of carbon contribute to ecosystem respiration (R). The difference between gross primary production and R is known as net ecosystem production (NEP) (Cole et al., 2000).

2.9 Dissolved and Particulate Organic Carbon (DOC) and (POC)

Technically, dissolved organic carbon (DOC) is defined as the carbon concentration of water passing through a 0.2 – 0.7 µm filter (Thurman, 1985) and more recently a filter mesh size of 0.45 µm has become standard (e.g. Chow et al., 2005). However, glass fibre filter papers (GF-F: 1.2 µm; GF-C: 1.7 µm) are also commonly used due to sample contamination issues with carbonate based filter papers (Fellman et al., 2009). The fraction of carbon retained on the filter following filtration constitutes the colloidal and particulate organic carbon (POC) fraction (McKnight, 1997). POC is made up of both particulate detritus (dead organic material) and living organisms (bacteria, phytoplankton, protozoa and metazoa). DOC concentrations in natural waters generally range from less than 0.5 mg l^{-1} to greater than 50 mg l^{-1}, and as DOC is closely aligned to CDOM, this natural range of DOC also generally describes the natural range of water colour, from crystal clear to dark brown waters (Mulholland et al., 2003). A cut-off of >30 mg PtCo L^{-1} (*circa* 2-3 mg l^{-1} DOC) is used by some to define humic waters e.g. (Hessen & Tranvik, 1998). DOC comprises the largest pool of organic carbon in lake water with typical values greater than 90% of the total organic C fraction (Wetzel, 2001; Thurman, 1985) and in some boreal lake water, DOC has been reported to constitute 97% of the TOC fraction (Kortelainen et al., 2006).

2.10 Sinks of Organic Carbon in Aquatic Systems

The main sinks of organic matter in aquatic systems are firstly *in-situ* microbial activity leading to mineralisation to CO_2 or CH_4 and secondly, flocculation and coagulation in the water column leading to sedimentation. The mineralisation of aquatic carbon by microbial action as a part of energy flows in the food web (Tranvik, 1989; Pace et al., 2004) results in a net flow of CO_2 from the water column to the atmosphere (Cole et al., 1994). Small lakes and headwater streams are considered to be hot spots of carbon mineralization (Cole et al., 2007) and a number of studies suggest that this pathway of carbon removal from peatlands in the northern hemisphere is important and makes a significant contribution to their C budgets (Hope et al., 2001; Billet et al., 2004). The process of flocculation, coagulation and eventual settling of organic matter out of the water column and into bottom sediments is considered to be a major sink of organic carbon especially in boreal climate zones (Molot & Dillon, 1996; Einsele et al., 2001; von Wachenfeldt & Tranvik, 2008). It is estimated that approximately half of the organic matter in aquatic systems is exported *via* streams to the sea (Cole et al., 2007).

2.11 Drivers of DOC Production in Catchments and Transport to Aquatic Systems

The volumes and quality of organic carbon produced and transported from catchments varies widely both spatially and temporally (Thacker et al., 2005) and this variation is driven by a combination of factors that also operate over a range of spatial and temporal and scales. The combination of local factors for DOC production and export are site-specific, such as geomorphology, hydrology, soil type, vegetation and land management and the unique combination of these factors at each catchment vary both the production and contribution of different carbon sources and affect linkages between terrestrial and aquatic environments e.g. (Wetzel, 2001). At a regional scale, both the production and transport of DOC are strongly influenced by climate factors such as precipitation patterns, temperature and soil moisture levels and anthropogenic factors such as decreasing atmospheric deposition of sulphur dioxide. Each factor is further discussed in the following sections, however, it is worth noting that although each of the variables are treated individually, they are interlinked and work in combination.

2.11.1 The Geomorphology and Hydrology of Catchments

The topography and hydrological characteristics of individual catchments are known to influence the generation of DOC within the catchment. The steepness of slopes influence how rainwater both infiltrates and inundates catchment soils, factors that directly affect

DOC transport (Rasmussen et al., 1989; Xenopoulos et al., 2003). For example, catchments with steep, undulating topography and non-porous crystalline bedrock tend to have more rapid-flow hydrological regimes and deliver precipitation faster and more directly to streams, thereby allowing less soil organic matter to dissolve (Frost et al., 2006). On the other hand, catchments with more gentle slopes have slower hydrological regimes and often complex drainage systems. In areas of impeded drainage where climatic factors cause precipitation to exceed evapotranspiration, wetland areas, such as blanket peatlands develop (Renou-Wilson et al., 2011). Wetland areas such as peatlands supply significant quantities of dissolved organic matter to aquatic systems (Pace & Cole, 2002; Sobek et al., 2007). DOC compounds concentrated in the porewaters of peaty soils are flushed out into aquatic pathways by precipitation, with the highest concentrations often coinciding with high flow levels (Arvola et al., 2004; Jennings et al., 2010). However DOC concentrations tend to decrease at high flow, indicating that soil C-stores can be washed-out and diluted with successive events (Worrall et al., 2002). Furthermore, Jennings et al., (2020) have found a seasonal cycle for this effect in the Burrishoole catchment. DOC concentrations in temperate-zone lakes are influenced by catchment characteristics via their effect on allochthonous inputs, and regional studies have found that lake DOC is positively related to the lake drainage/lake area ratio and negatively related to catchment slope (Weyhenmeyer & Bloesch, 2001; Sobek et al., 2007). Lake morphometry is also an important factor determining DOC concentrations and DOC has been shown to be negatively related to residence time, lake area and mean lake depth (Pace & Cole, 2002; Sobek et al., 2007). Generally, the largest lakes tend to have longer residence times of water, lower areal loading rates and higher in-lake rates of photo-degradation and microbial decomposition resulting in lower DOC and colour (Köhler, 2002; Mazzuoli, 2005).

2.11.2 Soil Type and Vegetation

The soil type and vegetation that occur within catchments are significant drivers of DOC production and export (Tranvik & Jansson, 2002; Mattsson et al., 2005). High volumes of DOC export are common from catchments with large soil carbon stores such as peatlands, wetlands and forests (Dillon & Molot, 1997; Laudon et al., 2004). Conversely, lower DOC concentrations are found in catchments where organic soils are poorly developed and vegetation is sparse. There are two distinct horizons in peat soils, the acrotelm and catotelm, each being differentiated by a distinct hydrologic conductivity (Evans et al., 1999). The uppermost acrotelm, comprises roots and decomposing plant

material while the lower catotelm is an anoxic horizon and comprises dense peat. The movement of the water table, up or down through the acrotelm, controls the amount of aerobic decomposition and oxidation occurring within the peat soils and influences DOC generation and export (Clark et al., 2005). Stands of forest and also the type and distribution of tree species within those forests influence the export of DOC in catchments (Ågren et al., 2007). According to Strobel et al., (2001) and based on a study in Denmark, DOC export from plantations of Norway spruce are higher compared to stands of Scots pine due to higher litter production in spruce stands. Different tree species produce litter with varying carbon nitrogen ratios which influences their degradability, and in turn the quality and reactivity of DOC in the forest soil. Litter from deciduous trees are the most easily degraded and DOC yields from deciduous forest soils are considerable (Hongve et al., 2000).

2.11.3 Land Use Factors

Significant factors governing DOC production and export to freshwater ecosystems are land management practices and land use (Chantigny, 2003; Worrall et al., 2003). Land management practices, such as clear-felling of forest plantations, burning of heathland and blanket peatlands, draining and cutting-over of peatlands, intensive stocking and grazing of uplands, intensive agricultural activity and urban development, influence the export of organic carbon (Worrall et al., 2003; Evans et al., 2005; Tetzlaff et al., 2007). Globally, the function of peatland as a carbon store has been negatively impacted due to extraction of peat for fuel and also by the conversion of peatland into agricultural and forestry land (Burt, 1995). Irish peatlands have been similarly impacted and as such only a small percentage of Irish peatlands are in a natural or intact condition. Renou-Wilson et al., (2011) have reported that 18% of Blanket Bogs, 11% of Fens and 7% of Raised Bogs remain intact. Changes in the land management practices, in particular the drainage of peatlands, dramatically alters the balance between aerobic and anaerobic processes within the acrotelm with resulting DOC release (Holden et al., 2004; Worrall & Burt, 2004; Jennings et al., 2010). Other land management practices, such as increased stocking rates and grazing intensity has caused critical and permanent soil erosion and increased the export of organic carbon from catchments (Bragg & Tallis, 2001; Allott et al., 2005). Forestry noticeably influences DOC release from soils and it has been observed that afforestation and clear-felling result in increased DOC and suspended sediment concentrations in waters draining these areas, and that also these increases may be observed over a number of years post deforestation (Cummins & Farrell, 2003; DeFries

& Eshleman, 2004). The practice of clear-felling in particular has been shown to increase runoff (Roberts & Crane, 1997) sedimentation (Johnson & Whitehead, 1993) acidification (Harriman et al., 2003) and increased nutrient leaching (Rodgers et al., 2010). Other land management practices that may be a factor in increased DOC concentrations in natural waters include agricultural and industrial activity. Agricultural practices such as slurry-spreading, tillage, and access of livestock to waterways has the potential to increase aquatic DOC concentrations via runoff (Kay et al., 2009). Point-source direct industrial outfall, including discharges from waste-water treatment facilities may also increase DOC loading to rivers and streams e.g. (Hudson et al., 2007).

2.11.4 Climate Factors

The sensitivity and vulnerability of upland blanket peat ecosystems to climate change is widely recognised. Rising global temperatures due to increasing CO_2 levels in the atmosphere are increasing the occurrence of extreme episodic events such as storms and floods, heat waves and droughts and these events, together with the overall rise in temperatures, have major implications for both terrestrial and aquatic peatland ecosystems (IPCC, 2013). According to an IPCC policy report (WG2 AR5) terrestrial carbon stores, including peatlands, are threatened by increasing drought frequency, temperature and precipitation, and also by ecosystem loss (IPCC, 2014b). Loss of carbon from long-term environmental stores such as peatlands is in turn directly affecting the magnitude of carbon fluxes within the global carbon cycle. Depletion of carbon stores from upland blanket peat catchments and subsequent carbon transport to downstream rivers and lakes is increasingly linked to flood and drought events, amplified by climate-change, particularly in upland regions where spate conditions prevail. A climate envelope modelling study by Jones et al. (2006) predicts that changes in climate are likely to result in a significant reduction of Irish peatland cover by 2075. In addition to warming trends, precipitation patterns across Europe have altered over the last thirty years with average precipitation increasing in the north of the continent and a corresponding decrease in the Mediterranean (IPCC, 2007). To understand why the changes in precipitation have occurred it is necessary to examine larger-scale atmospheric dynamics and also the underlying physical processes at work (Trenberth, 1990). The NAO is a large-scale pattern of air circulation and air pressure anomalies that span the North Atlantic Ocean and its periphery and significant relationships between precipitation and temperature and the NAO in winter on the west coast of Ireland have been observed (Jennings et al., 2000; McElwain & Sweeney, 2003). The NAO index is calculated as the difference in air

pressure at sea-level between the Azores high-pressure zone and the Icelandic low-pressure zone, and the observed difference is generally greatest during winter months (Hurrell et al., 2003; Hurrell & Deser, 2009). The effects of strong positive phases of the NAO are generally above-normal precipitation across northern Europe and Scandinavia and below-normal precipitation across central and southern Europe, positive NAO phases also display above-normal temperatures across northern Europe and the eastern United States and below-normal temperatures in Greenland, southern Europe and the Middle East. During strong negative phases of the NAO opposite patterns of precipitation and temperature are observed (Hurrell et al., 2003). The influence of the NAO on physical processes such as river discharge (via its influence on precipitation) and water temperature (via its influence on air temperature) has been demonstrated in Ireland and the UK. Kiely (1999) has shown that recent positive phases of the NAO has increased runoff in Irish rivers since the mid-1970's and Jennings et al (2000) have demonstrated this specifically within the Burrishoole catchment. Elliott et al. (2000) demonstrated that water temperature was highly correlated with winter NAO in Black Brows Beck, a small stream in the Lake District of north east England.

There is a complex relationship between precipitation (via runoff) and DOC concentrations in fresh water systems as there are numerous factors at play. For example, in a study of DOC release from an upland peat catchment in the UK by Worrall et al., (2002) three separate hydrological regimes with three associated DOC concentrations were identified during the autumn flushing period. Two of these hydrological regimes had low DOC concentrations. The first was associated with ground-water flow and was largely depleted of DOC, the second was associated with very high precipitation levels and overland flow and had little contact with the soil. The third regime had a high DOC footprint and was associated with interception and throughflow within the peat soil following dry antecedent conditions. This third regime was effectively a 'flushing out' event and, as such exported a substantial amount of carbon to the streams. Therefore the alteration of water budgets within catchments by the varying intensity and timing of precipitation events in turn alters the discharge of organic and inorganic matter and nutrient run-off from terrestrial into aquatic systems (Worrell et al., 2002; Erlandsson, 2008).

Air temperature and solar radiation, via their influence on soil temperature and soil moisture, are major drivers of DOC production in peatland catchments. DOC production in terrestrial systems is a biological process and the high-molecular weight, coloured

aromatic and refractory DOC released by peat soils via decomposition processes are temperature dependant (Thurman, 1985; Worrall et al., 2006). However, there is a wide variability in reported temperature sensitivities due to variation in the availability and quality of suitable substrate, limits to the access of microbial enzymes to substrate molecules and the rise and fall in microbial populations (Chapman & Thurlow, 1998; Davidson & Janssens, 2006). A factor that complicates the relationship between temperature and DOC production is the oxic status of the peat soil. For example, aerobic decomposition is generally more responsive to temperature than anaerobic decomposition (e.g. Hogg *et al.*, 1992; Weider & Yavitt, 1994; Davidson & Janssens, 2006). Aerobic decomposition is confined however to surface layers of peat soils during dry periods (e.g, Renou-Wilson et al., 2011). It has also been observed that decomposition rates can, on occasion, be greater at lower rather than higher temperature ranges (Kirschbaum, 1995; Chapman & Thurlow, 1998) and decomposition rates may fall-off after an optimum soil temperature has been reached (e.g. Fenner et al., 2005). Dawson et al. (2002) hypothesised that the longer periods of higher DOC concentrations in a stream in mid-Wales each year in comparison to a stream in north-east Scotland was largely related to warmer and wetter conditions in the former catchment in comparison to colder, drier conditions in the latter. However, the concentration of DOC in natural waters may not always show an immediate response to rising temperatures, implying a lag in soil decomposition processes or DOC mobilisation and release from soils (Clark et al., 2005). The amount of DOC exported to streams and rivers also depends on soil moisture conditions and the length of the soil-drying period, particularly in peat soils. Decreased DOC concentrations were observed in peat soils during drought conditions in the UK (Pennines range) where the drawdown of the water table caused the oxidation of organic sulphur to sulphate (Clark et al., 2005; Daniels et al., 2008). This drought-induced soil water acidification reduced DOC solubility in soil water. However, immediately following periods of dry weather or drought, pronounced increases in DOC concentrations have been observed in peatland streams (Watts et al., 2001; Jennings et al., 2010; Ryder et al., 2014), Ryder et al., (2014) reported a significant step-change increase in DOC concentrations in the Glenamong sub-catchment in the Burrishoole during moderately wet conditions during the summer of 2010 following a dry spring. In addition, land-use factors also play a role in soil moisture levels and resulting DOC export, for example Byrne et al., (2001) reported that decomposition processes are greater on forested peat than on virgin peat in Ireland, and attributed the higher rates to the drainage of forested peatland plots. Another climate factor that affects DOC concentration

in natural waters is direct solar radiation. Direct sunlight on water provides the necessary energy to break apart the double bonds of DOC (Wetzel, 2001). This photo-degradation process has been found to reduce DOC in natural waters by up to 60% over a period of 11 to 70 days (Shiller et al., 2006).

2.12 Trends of DOC Concentrations in Aquatic Systems

Increasing concentrations of fluvial DOC have been reported in many peat catchments over the last 20 years (Monteith et al., 2007; Worrall & Burt, 2007 Erlandsson et al., 2008; Jennings et al., 2010). These changes have been attributed in some part to recovery from the effects of atmospheric acid deposition on a regional scale as a result of reductions in transboundary air pollution (Monteith et al., 2007; Erlandsson et al., 2008). Some studies completely reject the acid deposition hypothesis and argue that DOC trends are more consistent with changes in precipitation (Erlandsson et al., 2008) higher temperatures (; Freeman et al., 2001; Preston et al., 2011) and the effect of drought events on peat decomposition (Clark et al., 2010b; Jennings et al., 2010; Ryder et al., 2014). Alternative drivers for long-term increasing trends of DOC have also been proposed, including changing nitrogen deposition (Findlay, 2005), increasing solar radiation (Hudson et al., 2003), and recent changes in upland management (Yallop & Clutterbuck, 2009). For example, increased incidents of heather burning in the UK have corresponded with increases in DOC concentrations (Yallop & Clutterbuck, 2009). There is therefore some disagreement regarding the main regional drivers of DOC trends. Clark et al., (2010b) suggest that *'confusion over these temporal and spatial scales of investigation has contributed unnecessarily to the disagreement over the main regional driver(s) of DOC trends, and that the data behind the majority of these studies is more compatible than is often conveyed'.* Roulet & Moore, (2006) and Sucker & Krause, (2010) emphasised that trends of DOC increase should not be attributed to any single factor and suggest that multiple drivers are required to explain increasing DOC trends. Evans et al., (2006) proposed that the observed rise in DOC trends is attributable to a complex interaction of changing atmospheric, deposition, and climate-related factors. Also, given the known linkages between DOC and climate factors, it is possible to model possible future DOC export rates with respect to climate change (Naden et al., 2010).

2.13 The Function of DOC in Aquatic Ecosystems

The fluxes of both material and energy through the aquatic ecosystem of peatland catchments are heavily influenced by inputs of allochthonous carbon and also the

generation of autochthonous carbon. Therefore changes in the rate of DOC input or manufacture within an aquatic system will directly impact the physical, chemical and biological behaviour of that system. Also these effects will be simultaneous and interlinked across all three of these domains (Jones, 1998).

2.13.1 Physical Factors

The presence and concentration of DOC in natural waters has a very marked effect on its absorption of light energy. Natural waters, particularly waters with high concentrations of humic acids have a high capacity to absorb infrared and red wavelengths, resulting in significant heating of the uppermost meter of water depth (Wetzel, 2001). This absorption also drastically reduces the transmission of light within the water column reducing energy penetration at greater depths. DOC concentrations are therefore strongly related to thermocline depth, and thus, to the mixing depth of lakes (Wetzel, 2001; Hudson et al., 2003; Maloney et al., 2005). For example, Bowling & Salonen (1990) demonstrated that thermal stratification in small humic forest lakes in southern Finland developed earlier in the year than in clear-water lakes. The relative penetration of light through water, or transparency, is calculated by determining the ratio between the irradiance at the water surface and at depth and is generally determined using a Secchi disc. The Secchi disc is used therefore to estimate the euphotic depth, i.e. the depth of the layer of water within which net photosynthetic production is possible (Håkanson & Peters, 1995). The net photosynthesis threshold is approximately 1% of full daylight (wavelengths between 400-750 nm). The bottom layer of the euphotic zone corresponds to this threshold level and may also be referred to as the attenuation depth of photosynthetically active radiation (PAR). The euphotic zone in clear water, oligotrophic lakes may extend to depths greater than10 m (Jones, 1992) and in some cases up to 50 m (Snucins & Gunn, 2000). However, in highly coloured humic lakes PAR is strongly attenuated. In lakes with DOC concentrations of between 10 and 15 mg l^{-1} the euphotic zone is generally between 1 and 2 m in depth, while in highly humic lakes where DOC concentrations exceed 15 mg l^{-1} it rarely exceeds 1 m (Lindell et al., 1996). Natural waters with high levels of dissolved organic compounds also absorb light radiation at the other end of the spectrum. In waters with high concentrations of humic compounds, absorption of ultra-violet (UV), blue and green wavelengths is essentially complete at 1 m depth (Wetzel, 2001). It is well understood that UV irradiance can photolyse portions of protein and humic macromolecules and transform them to small fatty acids — such as acetic, formic and malic, among others — a transformation that provides substrates for bacterial metabolism

(Wetzel, 2001). Irradiation of humic substances in natural waters therefore significantly increases the bio-availability of carbon substrates (Bertilsson, & Tranvik, 2000; Wetzel, 2001; Zhang et al., 2007).

2.13.2 Chemical Factors

Humic substances are a major source of acidity in peatland waters and naturally elevated DOC concentrations are a major contributor to the low pH of these aquatic systems (Turner et al., 2016). Stream and lake water acidification may be described as a net increase of H^+ ions within the water column and it occurs when an acid load into receiving waters exceeds its natural buffering capacity or if there is a decrease in the amount of exchangeable cations within the water altering its chemical equilibrium (Cresser & Edwards, 1987). The sources of acidification to aquatic systems may be both natural and anthropogenic, however the contribution of acid precipitation resulting from industrial pollution to the acidity of natural waters in western Ireland is likely to be small as the dominant air mass movement is from the west and southwest over the Atlantic (Aherne & Farrell, 2002). Low pH values are particularly common in peatland aquatic ecosystems that are dominated by littoral mats of *Sphagnum* mosses. The pH of *Sphagnum* bogs is generally within the range of pH 3.3 to pH 4.5 and significant H^+ ion concentrations in peat soil water appear to result from active cation exchange by the cell walls of *Sphagnum*, during which H^+ is released (Wetzel, 2001).

In natural waters many organic compounds form complexes with iron and as result of this process, both the solubility and availability of iron for organisms is altered (Wetzel, 2001). In surface waters with a high content of dissolved organic matter such as fulvic, humic and tannic acids, iron enrichment is common (Shaw, 1994). In fact it is these iron-organic complexes that are, in part, responsible for the deep yellow to brown colour of bog water (Wetzel, 2001). The principal method of the complexing of iron with humic derivatives, including organic acids, is peptisation, whereby iron is dispersed in a solubilised form ($Fe[OH]_3$) by adsorption of the organic acids onto the surfaces of the iron precipitate (Shapiro, 1966). The precipitation particles of iron oxide contain approximately 30 to 40% iron by weight and adsorbed humic carbon can contribute approximately 4 to 7% to the total particle weight (Wetzel, 2001). These complexes steadily sediment out of the water column and have the potential to enrich the hypolimnion with humic material (Wetzel, 2001).

The rate of oxygen depletion in lakes may be influenced by photochemical oxidation of DOC, reducing the maximum depth of oxygenation and in turn, impacting upon in-lake aquatic life (Likens, 2010; Müller et al., 2012). Nutrients also bind to and are carried by DOC and therefore DOC has a role in nutrient concentration and bioavailability in aquatic systems (Wiegner & Seitzinger, 2004). Total nitrogen concentrations (TN) in humic lakes in temperate regions in general, range between 300 and 500 µg N l^{-1} and the inorganic fractions of these totals are at detection limits. Inorganic N export to aquatic systems is minor and the bulk of dissolved N is bound in humic substances (Stepanauskas et al., 1999). Total phosphorus (TP) concentrations on the other hand may be elevated in humic lakes and generally range between 10 and 25 µg l^{-1}. The majority of this phosphorus is bound to humus colloids and forms iron-phosphorus-humus complexes. The formation of these complexes, therefore, affects the bioavailability of phosphorous as a nutrient within these aquatic systems (Tipping, 1981). In catchments that are impacted by pollution, DOC binds to aquatic contaminants including toxic organic molecules, radionuclides and metals such as iron, aluminium, iron, lead, chromium, and mercury. The process of binding these pollutants with DOC reduces their dissolved concentrations within the water column and thus their bioavailability to aquatic biota (Perdue et al., 1998; Shaw et al., 2000). The presence of high concentrations of DOC in potable water supplies has health implications because of the formation of disinfection by-products (DBPs) and trihalomethanes (THMs). Both are potentially carcinogenic compounds that form when highly coloured water is disinfected using chlorine (WHO, 2011). For this reason, DOC is usually removed by flocculation prior to chlorination. However, the quality of DOC can also affect the removal process. It was water treatment plants in Scandinavian countries that first began to report difficulties treating water with high DOC concentrations during the 1990's (Löfgren et al., 2003) and similar problems have been noted in Ireland (EPA, 2011).

2.13.3 Biological Effects

There are two main energy inputs to aquatic ecosystems that are exploited by two separate microscopic communities: autotrophic plankton utilise the sun's energy and heterotrophic bacteria exploit dissolved organic matter e.g. (Pace et al., 2004; Cole et al., 2006). Both communities occupy similar functional roles within the pelagic ecosystem and supply higher trophic levels with either physical or chemical derived energy, for example, micro-grazer communities channel a major fraction of bacterial production in lakes toward higher trophic levels (Isaksson et al., 1999). Ultimately the fate of the carbon processed

within aquatic ecosystems depends on whether the system is net autotrophic or heterotrophic (Bass et al., 2010). Ecosystems that are net autotrophic are atmospheric sinks for CO_2 while net heterotrophic systems are net releasers of both CO_2 and CH_4 to the atmosphere (Cole et al., 1994; Ojala et al., 2011). In lakes, there is a dynamic balance between net autotrophy and net heterotrophy and the balance is mainly dependent on the trophic status of the lake, for example, Sobek et al., (2005) reported that oligotrophic systems are dominated by heterotrophic processes and eutrophic systems are predominantly autotrophic. Also, certain lakes are known to switch, on a seasonal basis, between net autotrophy and net heterotrophy (Laas et al., 2012). Other factors, such as organic and inorganic nutrient supply in general (Bass et al., 2010) and DOC concentration in particular (Bloomqvist, 2001) are important in determining autotrophic / heterotrophic balance. It has been estimated that the balance may tilt towards net heterotrophy at DOC concentrations of around 5 mg l^{-1} (Jansson et al., 2000).

2.14 Gaseous C Emissions from Lakes

Terrestrial carbon is actively processed in aquatic systems and consequently these systems are frequently supersaturated with CO_2 (Cole et al., 1994), and they are therefore important sources of CO_2 to the global carbon budget (Aufdenkampe et al., 2011). Many lakes are net heterotrophic and this CO_2 excess is mainly derived from the export of OC from the surrounding catchment through respiration of organic carbon in the water column and also as CO_2 ultimately derived from soil respiration in the surrounding catchment (Cole et al., 1994; Duarte & Prairie, 2005; Battin et al., 2008). Raymond et al., (2013) estimated that globally, 2.1 Pg C yr^{-1} is emitted in the form of CO_2 from inland waters. There are many possible drivers for temporal variability of CO_2 fluxes in lakes. For example, diel differences have been observed in $_pCO_{2aq}$ (the partial pressure of CO_2 in the water column) due to the in-lake switch between respiration and photosynthesis (Sellers et al., 1995). Day-night differences in air temperature can also cause convective night-time mixing bringing up deeper CO_2-rich water (Eugster et al., 2003; Åberg et al., 2010). Precipitation and subsequent discharge events introduce new organic matter into lakes, enhancing respiration rates and increasing CO_2 release (Rantakari & Kortelainen, 2005; Vachon & del Giorgio, 2014). Seasonal occurrences such as lake mixing events in autumn introduce CO_2 rich water from bottom layers into the surface waters (Kelly et al., 2001; Weyhenmeyer et al., 2012). Wind events in Lake Como in Italy have been shown to cause thermocline tilt and upwelling by internal seiches which may also introduce CO_2 rich water to upper layers (Shintani et al., 2010). Also, the gas transfer velocity, also

known as the piston velocity (*k*) has been shown to vary with lake fetch and this has been found to have an influence on CO_2 fluxes (Schilder et al., 2013; Vachon & Prairie, 2013). In terms of spatial variability, Natchimuthu et al., (2017) reported that rates of photosynthesis, the existence of littoral zones, and the location of river inputs influenced variation in pCO_{2aq} and CO_2 fluxes across lakes in southwest Sweden.

To date, most estimates of lake CO_2 exchange have been based on calculating (*k*) using local wind speed measurements (Wanninkhof, 1992; Cole & Caraco, 1998; Crusius & Wanninkhof, 2003) in tandem with surface water CO_2 concentrations. The flux of CO_2 (*F*) is calculated according to the following equation:

$$F = k \times Kh(pCO_{2\,aq} - pCO_{2\,atm}) \quad (1)$$

where *F* is the flux (mmol m^{-2} d^{-1}), *k* is the piston velocity (m d^{-1}), *Kh* is Henry's constant (M atm^{-1}), $pCO_{2\,aq}$ is the CO_2 partial pressure in equilibrium with the surface water concentration, and $pCO_{2\,atm}$ is the partial pressure of CO_2 in the atmosphere (µatm). Generally, at any studied lake system, measurements to estimate CO_2 fluxes are made intermittently and at relatively few locations, and according to Natchimuthu et al., (2017) there is currently an unclear understanding of the spatial and temporal variation of lake CO_2 fluxes. Moreover, this lack of knowledge may be compounded by the fact that measurements of pH and alkalinity are often used to estimate $_pCO_{2aq}$ in natural waters and it has recently been highlighted that this indirect approach may overestimate $_pCO_{2aq}$ in acidic or low alkalinity humic waters (Abril et al., 2015).

Methane (CH_4) is an important greenhouse gas and is responsible for approximately 20% of the warming generated by long-lived greenhouse gases since the industrial revolution. By reacting with hydroxyl radicals in the atmosphere, CH_4 reduces the oxidising capacity of the atmosphere and also generates ozone in the troposphere (Kirschke et al., 2013). One of the largest natural sources of methane gas is lakes and ponds (Wik et al., 2016). The production of CH_4 is a microbiological process, resulting from the mineralisation of carbon under anaerobic conditions in aquatic sediments (Wetzel, 2001). CH_4 diffuses along concentration gradients within the sediments and may be oxidised, under microaerobic conditions, by methane-oxidising bacteria (Wetzel, 2001). An alternative and more direct route to the atmosphere for CH_4 may be available via the roots and intercellular spaces of aquatic plants such as emergent macrophytes, and significant volumes of CH_4 from aquatic sediments may be released in this manner e.g., (Segers, 1998). CH_4 production in the sediments can be intense and may reach as much

as 85% of the total gas volume formed in the deposits, however in low to moderately productive lakes, very little CH_4 escapes due to the activity of methane-oxidising bacteria in the sediments and water column (King & Blackburn, 1996).

2.15 Lake OC budgets

It is now recognised that lakes are active and important sites for OC storage and cycling (Cole et al., 2007; Raymond et al., 2013), entirely disproportionate to their spatial extent. Moreover, inland waters are now considered as highly relevant to the global carbon cycle (Ciais et al., 2013). Currently, global carbon flux estimates of lateral carbon and CO_2, and CH_4 evasion equate to approximately 4.8 Pg C y^{-1}, (Tranvik et al., 2009; Stanley et al., 2016; Ward et al., 2017). Quantifying lake OC budgets and gaining an understanding of the controls and processes of lake carbon cycling is considered to be of critical importance (Apps et al., 1993; Kasischke et al., 1995; Kurz et al., 2013). Mass balances or budgets are used as a tool to inform on element or nutrient transfers in lakes, and include estimates for inputs, outputs, and changes to standing stocks in the water column and sediments (Pace & Lovett., 2012). Specifically, in terms of lake OC budgets, by calculating key rates and fluxes, a greater understanding of the lake trophic state in terms of carbon, i.e., autotrophy vs. heterotrophy may be gleaned. On a broader scale, lake OC budgets can help in understanding the role that lakes' play as storage and transformation sites of OC in the landscape (Buffam et al., 2011).

Complete lake carbon budgets are rare, i.e. those that incorporate allochthonous OC inputs from surface water and groundwater, atmospheric deposition, OC exports from outflow, sediment burial, autochthonous primary production and ecosystem respiration (Hanson et al., 2014b). There are a number of reasons for this scarcity, the most important factors being the difficulty and expense of gathering the complete suite of data required to balance a lake OC budget. Hydrological inputs of OC can vary considerably in time, with peaks relating to seasonal or weather-related patterns, making them difficult to measure (Caverly et al., 2013). Diffuse inputs of OC to the lake, such as those from groundwater may be difficult to measure (Hanson et al., 2014b). Internal lake processes, including primary production and respiration, are also difficult to estimate as they are not spatially or temporally homogeneous (Hoellein et al., 2013; Solomon et al., 2013). There are also complications in the estimation of lake OC storage as the process of sedimentation is spatially hererogeneous and dependent on lake-specific aspects such as morphology (Kastowski et al., 2011; Ferland et al., 2014). Another factor that adds to the complexity of completing lake OC budgets may be the disciplinary nature of scientific

research, where methodological constraints focus on specific components of the carbon balance at the expense of other components (Falkowski et al., 2000).

There are few complete OC lake budgets in the literature, for example in a review by Hanson et al., (2014b) just three studies were cited, Likens (1985), Cole et al., (1989) and Wetzel (2001). The Likens (1985) study was one of many biogeochemical studies reported in a continuous, long-term ecological research project at the Hubbard Brook Ecosystem Research Station, which includes Mirror Lake, in New Hampshire, USA. The OC budget presented by Cole et al., (1989) involved an intensive measurement campaign of lake allochthonous and autochthonous OC components to estimate bacterial production and respiration. The study was also conducted in Mirror Lake. Wetzel (2001) republished work he had previously reported in 1972 on Laurance Lake, Michigan. That study included a detailed evaluation of a carbon budget of a hardwater lake and included OC inputs and exports, and dynamics in the littoral, pelagic and benthic zones of the lake. One other example of a complete OC budget was the study of a small humic lake in Sweden (Lake Frisksön) by Sobek et al., (2006). The study was conducted to gain an understanding of biogeochemical processes at the site, to assess its suitability as a potential final repository for radioactive waste. In a review of boreal lake C budgets by Anas et al., (2015) just four complete budgets were available (Dillon & Molot 1997; Algesten et al. 2003; Sobek et al. 2006 and Einola et al. 2011). Even though complete and detailed lake OC budgets are rare, there are numerous 'approximate' budget studies available in the literature. While these studies do not strictly contain all of the terms of a complete OC budget they are, nonetheless, extremely informative in terms of lake OC processing (Hanson et al., 2014b).

It is also important to note that there is also a strong geographical bias, in aquatic OC studies, towards the continental-temperate to boreal and sub-artic climate zones of the northern hemisphere (Webb et al., 2018). Expanding this relatively narrow spatial range and conducting more studies across broader global extents will provide a better basis for calculating the contribution of lakes to both regional and world-wide C cycles. For example, annual precipitation, a strong climate indicator, has been found to be a reliable predictor of particular carbon pools and fluxes at catchment (Oquist et al., 2014), continental (Butman et al., 2016), and global scales (Sanders et al., 2016). The following three chapters of this thesis present three interlinked studies of OC cycling dynamics (including an OC budget) for Lough Feeagh, a lake within a temperate maritime climate zone. This climate zone is strongly influenced by the ocean, thus maintaining a limited

variation of annual temperature and experiencing substantial precipitation (Köppen, 1936). The completion of these studies, and the lake OC budget, improves the knowledge of peatland catchment OC dynamics, and increases the geographical extent of lake OC cycling analysis to include this important climate setting.

Chapter 3. Synchrony in catchment stream colour levels is driven by both local and regional climate

A note on the collaborations associated with the work described in this chapter:

This chapter is based on the following paper, Doyle B.C, de Eyto E, Dillane M, Poole R, McCarthy V, Ryder E, Jennings E. 2019. *Synchrony in catchment stream colour levels is driven by both local and regional climate.* Biogeosciences. 16(5):1053–1071. For this paper, Brian Doyle collected environmental samples, undertook research and laboratory analysis, calibrated laboratory instruments, quality-controlled datasets, and analysed data and was the primary author of the paper. Eleanor Jennings, Elvira de Eyto and Valerie McCarthy supervised the research, provide advice on statistical analysis and manuscript editing. Mary Dillane and Elvira de Eyto maintain a wide range of environmental monitoring equipment and subsequent data-streams in the Burrishoole catchment for the Marine Institute. Russell Poole, a section manager at the Marine Institute's facility at Newport, provided editing advice.

3.1 Abstract

Streams draining upland catchments carry large quantities of carbon from terrestrial stocks to downstream freshwater and marine ecosystems. Here it either enters long-term storage in sediments or enters the atmosphere as gaseous carbon through a combination of biotic and abiotic processes. There are, however, increasing concerns over the long-term stability of terrestrial carbon stores in blanket peatland catchments as a result of anthropogenic pressures and climate change. We analysed sub-annual and inter-annual changes in river water colour (a reliable proxy measurement of dissolved organic carbon (DOC)) using six years of weekly data, from 2011 to 2016. This time-series data set was gathered from three contiguous river sub-catchments, the Black, the Glenamong and the Srahrevagh, in a blanket peatland catchment system in western Ireland, and used to identify the drivers that best explained observed temporal change in river colour. The data were also used to estimate annual DOC loads from each catchment. General additive mixed modelling was used to identify the principle environmental drivers of water colour in the rivers, while wavelet cross correlation analysis was used to identify common frequencies in correlations. At 130 mg Pt Co L^{-1}, the colour levels in the Srahrevagh (the sub-catchment with lowest rainfall and higher forest cover) were almost 50% higher than those from the Black and Glenamong, at 95 and 84 mg Pt Co L^{-1} respectively. The decomposition of the colour datasets revealed similar multi-annual, annual, and event-

based (random component) trends, illustrating that environmental drivers operated synchronously at each of these temporal scales. For both the Black and its nested Srahrevagh catchment, three variables (soil temperature, SMD and the weekly North Atlantic Oscillation (NAO)) combined to explain 54% and 58% of the deviance in colour respectively. In the Glenamong, which had steeper topography and a higher percentage of peat intersected by streams, soil temperature, the log of stream discharge and the NAO explained 66% of the colour concentrations. Cross-wavelet time-series analysis between river colour and each environmental driver revealed a significant high common power relationship at an annual time step. Each relationship however, varied in phase, further highlighting the complexity of the mechanisms driving river colour in the sub-catchments. The estimated mean annual DOC loads for the Black and Glenamong rivers to Lough Feeagh were similar at 15.0 and 14.7 t C km^{-2} yr^{-1} respectively. Our results show the important role of regional scale climatic drivers, in particular temperature, have in controlling aquatic carbon export, emphasising the vulnerability of blanket peatland carbon stores to projected climate change.

Key words. Carbon transport, dissolved organic carbon, blanket peatland, climate effects.

3.2 Introduction

Blanket peat ecosystems occur within a relatively narrow window of climatic conditions, characterised by warmer and wetter conditions, in temperate regions where precipitation exceeds potential evaporation by a ratio of about three to one (Wieder & Vitt 2006). Under such conditions, primary production exceeds decomposition of soil organic matter, and therefore organic carbon (C) accumulates. These ecosystems are a major terrestrial carbon store (Bain et al., 2011). Blanket peats (technically a soil with peat depth > 40cm) are now recognised as being under threat, not only from excessive erosion due to anthropogenic pressures (for example, harvesting, burning and grazing) (Renou-Wilson et al., 2011), but also from increases in C loss related to directional climate change (Gallego-Sala & Prentice., 2013). Streams and rivers are the major pathways along which organic C is conveyed from upland peatlands to downstream lakes and oceans. In most studies which have evaluated fluvial losses of both dissolved organic carbon, and particulate organic carbon, DOC has been identified as the dominant C form, representing between 60% and 88% of the total carbon load (Hope et al. 1997a; Tipping et al. 1997;

Ryder et al., 2014). Hope et al. (1997b) concluded that, for British rivers as a whole during 1993, 0.68 Mt C of the fluvial carbon load was in dissolved form, representing 77% of total C export. In the west of Ireland, DOC was estimated to account for 60.5% of the total fluvial C load from the Glenamong sub-catchment (Ryder et al., 2014), a site which is also used in the current study

Stream DOC concentrations draining blanket peatland catchments in Ireland typically show a distinct seasonal pattern, with highest values from late summer to early winter and lowest values in spring (e.g. Ryder et al., 2014). Longer term patterns in DOC concentrations or in proxies for DOC have been linked to year-to-year changes in meteorological conditions at both local and regional scales. At local scales, temperature affects peat decomposition rates and therefore the availability of DOC, while higher precipitation increases the washout of DOC from soils (Jennings et al., 2010; Ryder et al., 2014). Increases in oxygen availability within peat during droughts can also lead to higher rates of aerobic decomposition (Mitchell & McDonald, 1992; Yallop & Clutterbuck, 2009; Fenner & Freeman, 2011). At regional scales, DOC concentrations have been shown to be influenced by global weather patterns, for example, DOC concentrations in certain Canadian lakes were found to be correlated with climate indices such as the Pacific Decadal Oscillation and the Southern Oscillation Index (Zhang et al., 2010). In Europe, and Ireland in particular, such correlations would be expected to be linked to the North Atlantic Oscillation (NAO). The NAO is a weather phenomenon related to fluctuations in the difference of atmospheric pressure at sea level between the Icelandic low and the Azores high (Hurrell et al., 2003). A positive phase of the NAO reflects below-normal atmospheric pressure across Greenland and Iceland and above-normal atmospheric pressure over the central North Atlantic, the eastern United States and Western Europe. A negative phase reflects an opposite pattern of atmospheric pressure anomalies over these regions. High positive values of this index over northwest Europe are associated with warmer and wetter conditions during the winter and positive index values during the summer are linked with warm, dry and relatively cloud-free periods (Folland et al., 2008). In a 28 year study, Nõges et al (2007) found that water colour (one of the most commonly used proxies for DOC) during spring in Estonian rivers was positively related to the previous winter's North Atlantic Oscillation (NAO) index. A similar positive relationship between the winter NAO and the total organic carbon (TOC) load was reported over 25 years in Finnish rivers (Arvola et al., 2004).

Increasing trends in fluvial DOC concentrations have been observed in many peat catchments over the last 20 years (Hongve et al., 2004; Evans et al., 2005; Monteith et al., 2007; Worrall & Burt, 2007; Erlandsson et al., 2008; Jennings et al., 2010). While these changes have been attributed in part to recovery from the effects of atmospheric acid deposition on a regional scale (Monteith et al., 2007; Erlandsson et al., 2008), the trend has also been linked to changes in the key climatic drivers of DOC export. These drivers include the effect of changes in precipitation and snowmelt patterns on flushing rates (Hongve et al., 2004; Erlandsson et al., 2008), and the impact of higher temperatures (Freeman et al., 2001; Preston et al., 2011) and of drought events (Clark et al., 2005; Jennings et al., 2010;) on peat decomposition. There are, however, also studies where DOC concentrations have been shown to have decreased (Clair et al., 2008; Worrall et al., 2018), or no increase has been observed, such as within certain catchments in the U.K. (Worrall & Burt, 2007). Winterdahl et al. (2014) also reported increases in TOC in only half of 130 Swedish streams, but with no clear geographic pattern, highlighting the need for further examination of the complex relationship between DOC concentration and climate. Given the close relationship between peat formation and peat decomposition, and climate factors such as temperature, directional climate change is likely to place additional pressures on peatland systems (Clark et al., 2010a; Coll et al., 2014;). Observed and projected climate changes for Ireland include higher temperatures throughout the annual cycle, a decrease in the summer water table, and higher winter streamflow (Dwyer, 2012; Nolan, 2015), a combination that has been shown to have the potential to increase fluvial DOC export (Naden et al., 2010).

In Europe, Atlantic blanket bogs are found on the western fringes of the continent and are common only in Ireland and Scotland (Sheehy Skeffington & O'Connell, 1998), reflecting the dominant influence of the Atlantic on the local climate in these countries (Coll et al., 2005; Sweeney, 2014). In Ireland, up to 75% of soil carbon storage is in peatlands, much of which is in upland blanket peat soils (Holden & Connolly, 2011, Renou-Wilson et al., 2011). Examining riverine fluxes of carbon from these catchments provides a means to quantify export of C from long-term storage in peatland ecosystems, and to explore the effects of climatic variables on these C stores. The present study expands on the work described earlier of Ryder et al. (2014), firstly by comparing colour concentrations from three contiguous peat sub-catchments that differ in their catchment characteristics, and secondly by including the role of the regional climatic conditions, e.g. the NAO, as a possible driver. The principal aims of the current study, using river colour

data from the Burrishoole catchment in the west of Ireland were 1. to compare the sub-seasonal, seasonal and multi-annual trends in water colour 2. to identify the main climatic drivers of river colour and 3. to quantify the inter-annual variability in fluvial export of DOC over the study period.

3.3 Methods

3.3.1 Study Area

3.3.1.1 Geology and Soils

The Burrishoole catchment (~100 km^2) is a topographic basin, that has been carved into the Nephin Beg mountain range over successive ice-ages and comprises twenty-one lakes of sizes ranging from 0.04 ha to 395 ha and approximately 143 kilometres of interconnecting rivers and streams (53º 55' N 9º 55' W). Late Precambrian metamorphic rocks and smaller areas of Palaeozoic sandstone and limestone characterise the geology of the catchment (Parker 1977; Long et al., 1992). Rivers and streams on the western side of the catchment (Glenamong) are generally more acidic, with low buffering capacity (alkalinities in the order of -2.7 to 7.5 mg L^{-1} $CaCO_3$, (Marine Institute, unpublished data) and low aquatic production. Rivers draining the east of the catchment (Black and Srahrevagh) are nearer circumneutral with alkalinities in the order of 15 - 20 mg L^{-1} $CaCO_3$, with consequently higher aquatic productivity. There are also significant till subsoil-deposits throughout the catchment comprising unconsolidated material of lithology reflecting that of its underlying parent bedrock (Kiely et al., 1974). The overlying soils are predominantly poorly-drained gleys and peaty podsols, with alluvial soils on the valley floors and blanket peatlands covering upland slopes (May and Place, 2005). Land cover in the catchment comprises 52% blanket peat, 15% forestry, with the remaining 33% being made up of discrete parcels of transitional woodland and scrub, natural grasslands and agricultural land (CORINE, 2012). Much of the peatland area is commonage, and is used for sheep grazing (Weir, 1996). Vegetation cover on the blanket peats is characterised by *Calluna vulgaris*, *Molinia caerulea*, *Schoenus nigricans* and *Scirpus caespitosus* (O'Sullivan, 1993).

3.3.1.2 Climate

The Burrishoole catchment is located close to the northwest coast of Ireland and experiences a temperate, oceanic climate with mild winters and relatively cool summers. A meteorological station (Newport) has been in operation in the catchment on the shores

of Lough Feeagh since 1958. Long-term average annual precipitation at this station (1960–2014) was 1564 mm. Average daily rainfall for the same period was 4.3 mm (± 6.2 mm SD), and 75% of days had some measurable rainfall (de Eyto et al., 2016). The total annual precipitation at Newport between 2010 and 2016 ranged from a minimum of 1316 mm $year^{-1}$ (2013) to a maximum of 2020 mm $year^{-1}$ (2015), with an average of 1636 mm $year^{-1}$. It is also important to note that rainfall levels varied spatially across the catchment over the study years from an annual average of 2623 mm $year^{-1}$ (±386 mm $year^{-1}$ SD), recorded at an automatic rain gauge in the northwest of the catchment to 1508 mm $year^{-1}$ (±158 mm $year^{-1}$ SD) at the south of the catchment (MI unpublished data). Seasons were defined as follows in the current study: winter = December, January and February; spring = March, April and May; summer = June July and August; autumn = September, October and November. Maximum summer temperatures in the Burrishoole catchment rarely exceed 20°C, while minimum winter temperatures are usually between 2°C and 4°C (Marine Institute unpublished data). The average annual air temperature at Newport meteorological station from 2010 to 2016 was 10.1ºC.

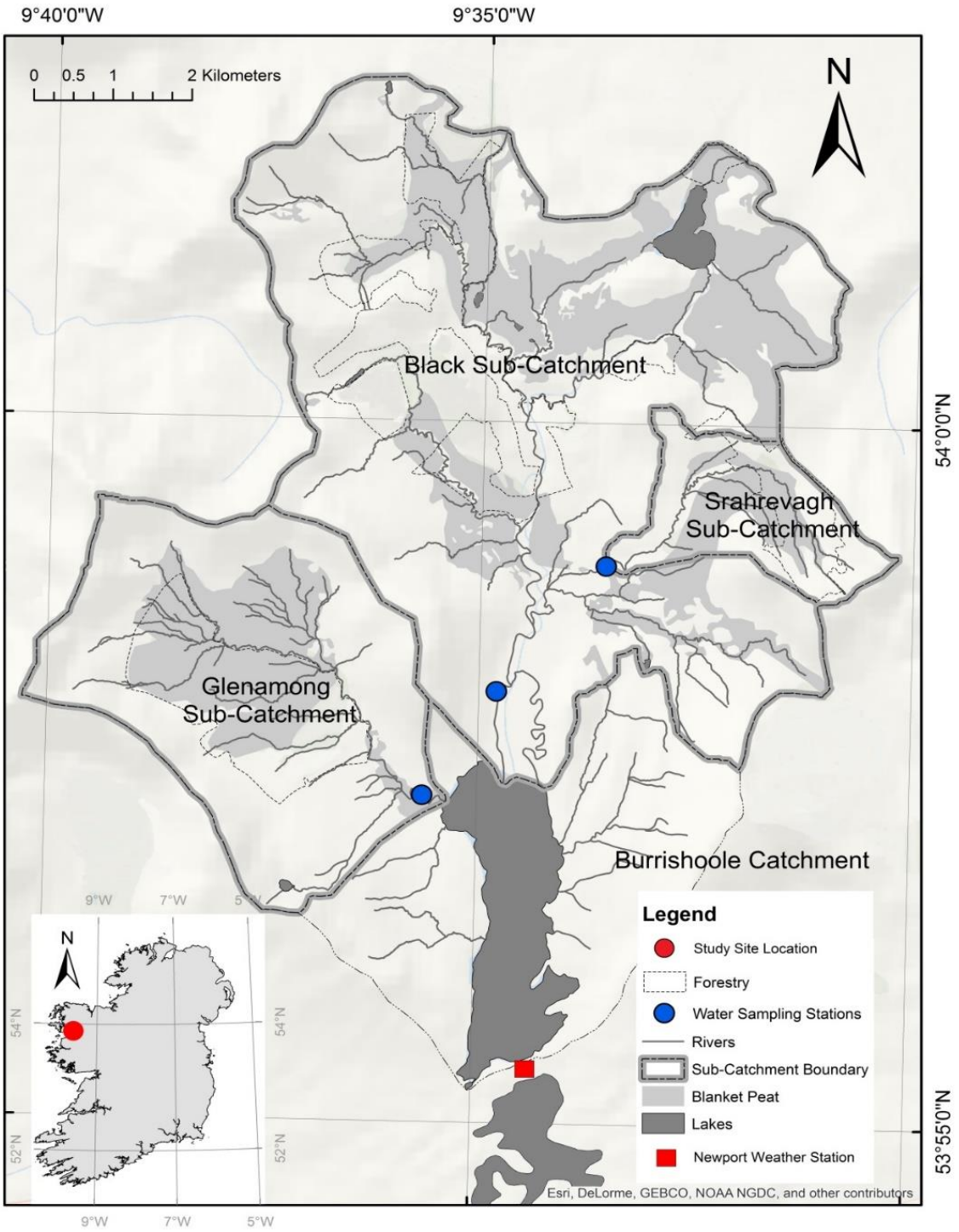

Figure 3.1 Location of the sub-catchments in the Burrishoole catchment.

3.3.1.3 Catchment characteristics

This study is focussed on three rivers and their sub-catchments in the Burrishoole catchment. The Black and the Glenamong, drain directly into Lough Feeagh whilst the third, the Srahrevagh, is nested within the larger Black sub-catchment. (Figure 3.1). The predominant land uses in all three sub-catchments are sheep grazing and forestry, however the Black also contains a small proportion of more intensively managed agricultural land. Soils with a peaty, carbon-rich top horizon are common throughout the Burrishoole catchment and blanket peat covers approximately 20% of the catchment. Blanket peat has been mapped in all three sub-catchments, with the Srahrevagh containing approximately 5% more peat relative to its area than the other two sub-catchments (Kiely et al., 1974; Gardner & Radford, 1980) (Table 3.1). The Glenamong has a greater percentage of stream length intersecting blanket peat in comparison to the Black and the Srahrevagh sub-catchments (Figure 3.1 & Table 3.1). The CORINE land-cover data shows that 32% of the Srahrevagh sub-catchment contains coniferous plantation compared to approximately 25% and 17% for the Glenamong and Black respectively (Table 3.1). The Srahrevagh sub-catchment has the greatest proportion of slopes ranging between 0 and 20 % while the Glenamong is the most mountainous of the three sub-catchments, having the greatest altitude range and containing the greatest proportion of slopes steeper than 50% (Table 3.1). Glenamong stream water is consistently more acidic than the other two sub-catchments; however the remaining stream chemistry metrics between sub-catchments are broadly similar (Table 3.1). The slope distribution (as percent) for the Burrishoole catchment and each sub-catchment was calculated from a digital elevation model (DEM) at a 10 m resolution (Marine Institute Data) using the Spatial Analyst routine in ArcMap 10.3.1 (ESRI - https://www.esri.com).

Table 3.1 Sub-catchment characteristics, climate (recorded at Newport climate station) / hydrology and stream water chemistry data for the Black, Glenamong and Srahrevagh sub-catchment

Catchment		**Black**	**Glenamong**	**Srahrevagh**
Characteristics				
Area (km^2)		48.3	17.5	4.6
Aspect		South facing	South-east facing	South-west facing
Altitude range (m)		8 - 629	8 - 710	39 - 550
Soils		Peats, Humic podzols, Regosols and Fluvisols	Peats, Humic podzols, Regosols and Fluvisols	Peats, Humic podzols and Regosols
Geology		Quartzite and schist, also interbedded volcanics, marble, dolomite, and schist	Predominantly Quartzite and schist	Quartzite and schist, also interbedded volcanics, marble, dolomite, and schist
Management		Sheep grazing, Forestry, Grass – Silage	Sheep grazing, Forestry	Sheep grazing, Forestry
Climate / Hydrology 2011 - 2017				
Rainfall (mm yr^{-1})		2623 (367)	2358 (361)	1853 (204)
Mean discharge (m^3 s^{-1})		5.37 (7.02)	0.88 (1.26)	0.42 (0.90)
Mean air temperature (°C)		10.12 (4.12)	10.12 (4.12)	10.12 (4.12)
Water temperature range (°C)		-.05 – 26.0	-.03 – 26.0	-.25 – 25.0
Mean (range) chemistry				
pH range		4.0 – 8.0	3.5 – 7.3	4.5 – 8.0
Colour range (mg PtCo l^{-1})		15 – 257	24 – 211	18 – 364
DOC range (mg l^{-1})		2.3 – 25.8	3.6 – 21.5	3.2 – 28.7
Land cover				
Blanket Peat Area %		28.7	29.7	34.4
Stream length (km)		87.8	37.9	12.3
Streams Intersecting peat (km)		37.5	25.2	6.9
Streams Intersecting peat %		42.7	66.5	56.6
CORINE Coniferous Forest %		16.6	24.9	32.2
Slope (%) distribution in each catchment				
Slope Class (%)	0 – 10	*29.2*	*24.4*	*24.2*
	10– 20	*30.3*	*33.0*	*43.0*
	20 – 30	*21.2*	*13.9*	*19.5*
	30–50	*15.7*	*17.3*	*12.8*
	50–100	*3.6*	*11.4*	*0.5*

3.3.2 Water chemistry sampling

Water samples from the rivers were taken at weekly intervals over six years (2011-2016) from the same sampling sites (Figure 3.1). Colour (mg PtCO L^{-1}) was measured within hours of sampling using a HACH Dr 2000 spectrophotometer at 455 nm on water filtered through Whatman GF/C filters (pore size: 1.22 µm). Wavelength accuracy = ± 2 nm from 400 – 700 nm and ± 3 nm from 700 – 900 nm.

3.3.3 Meteorological and hydrological measurements

Daily precipitation and soil temperature data, were available from the Newport met station (Figure 3.1). Water levels (cm) were recorded every 15 minutes at each site using OTT Hydrometry Orpheus Mini water level loggers (https://www.ott.com). The levels for the Glenamong and Srahrevagh rivers were converted to volume of discharge per second (m^3 s^{-1}) using site specific ratings curves that have been developed using data collected regularly (Marine Institute unpublished data). No reliable rating curve was available for the Black river, therefore discharge was estimated using the drainage area ratio method based on the Glenamong discharge (Hirsch, 1979).

3.3.4 Data Analysis

3.3.4.1 Statistical Tests

This analysis was conducted to ascertain if there were significant statistical differences between river colour in each catchment. A Mann-Whitney U test was used to test for statistical differences between mean colour concentrations in the Glenamong and Black and the Glenamong and Srahrevagh rivers. As the Black and Srahrevagh rivers are in the same river system, a non-parametric Wilcoxon Signed Rank Test was used to test for statistical differences between their colour concentrations.

3.3.4.2 Time series decomposition

The time series datasets of weekly colour concentrations in the three rivers were examined using Seasonal Trend Decomposition using LOESS (STL) (Cleveland et al; 1990) in R (R Core Team 2013). The STL algorithm decomposes a time series into three separable elements: the trend, the seasonal variation and the residual using an additive model (equation 1). Loess (locally weighted smoothing) regression is a nonparametric technique that uses local weighted regression to fit a smooth curve through points in a scatter plot. An additive model was preferred over a multiplicative model because no obvious non-stationarity in the time series was observed, i.e. the amplitude of the seasonal cycle remained uniform and did not increase or decrease with the trend in the data (Figure

3.3A). Variation in the time series data was decomposed into a set of constituent elements: overall mean or level (α), trend (T), seasonal component (S), and random noise (N) (Chatfield, 1984). For a specific time series, colour concentration in surface waters can be expressed as:

$$Y_{tl} = \alpha_l + T_{tl} + S_{tl} + N_{tl} \quad (1)$$

where Y_{tl} is the colour concentration at time t in location l. The overall mean colour level (α) is site specific and could vary with, for example, the soil, vegetation or land management characteristics of each catchment. Regular variation of seasonal weather, for example, precipitation and temperature, principally drive the S term, and N represents short-term, random events. Any factor that drives the production of colour in surface waters (i.e. DOC production, solubility or transport) over multiple years could drive the trend T (Clark et al., 2010b). STL analysis was also carried out on the principal explanatory drivers of water colour identified in the general additive mixed models (GAMM) analysis. The trend component of each explanatory driver, namely soil temperature, discharge, soil moisture deficit and the NAO were extracted and compared visually.

3.3.4.3 General Additive Mixed Models

To identify the main explanatory drivers of colour in the rivers, general additive mixed models (GAMM) with cubic smoothing regression splines and Gaussian distributions were developed using the mgcv package in R (Wood, 2006). Variance inflation factors (VIFs) less than 3 were used to exclude closely related variables (Montgomery & Peck., 1992, Zuur et al., 2009). All models were tested for violations of the assumptions of homogeneity, independence and normality, and correlation or variance structures included as appropriate. Models were examined for the effects of autocorrelation in residuals by plotting the autocorrelation function (acf) (Venables & Ripley, 2002). All analysis was carried out in R. The response variable was the weekly colour data from the three sub-catchments. Potential explanatory variables comprising climate and hydrological data were included as continuous variables. The climate variables, measured at the Newport meteorological station, were constructed as follows: the first set was the weekly mean of each climate variable calculated from the sampling week; the second set was the value of each variable measured on the day of sampling. The third set was constructed by lagging each climate variable by one, two and four weekly time-steps. The climate variables included were: maximum, minimum and mean air temperature (°C), total precipitation (mm), wind speed (m s^{-1}), solar radiation (kWh/m^2), relative humidity

(%), air pressure (hPa), soil temperature at 5, 10, 30, 50 and 100 cm depths and sun hours (h). Hydrological explanatory variables included river discharge (m^3 s^{-1}), soil moisture deficit (SMD) (mm day^{-1}) and actual evapotranspiration (mm day^{-1}). Soil moisture deficit was calculated using a procedure described by Brereton et al. (1996) for Irish grasslands. Potential evapotranspiration rates were first estimated based on air temperature and sunshine data using the method of Priestley & Taylor (1972) and then actual evapotranspiration was calculated as a proportion of potential evapotranspiration based on Aslyng (1965). Both weekly and monthly means of the NAO index were downloaded from the National Oceanic and Atmospheric Administration (NOAA, 2017) and used as explanatory variables in the statistical analysis. The Standardised Precipitation Index (SPI) was calculated using the R package 'SPEI' (Beguería et al., 2014; Vicente-Serrano et al., 2010) using daily precipitation data from the Newport met station over 21 years (1995 - 2016). The SPI was used to assess relative changes in rainfall and to discover the occurrence of drought events in the catchment over the study period. The SPI index creates a numeric output on a monthly time step that can be sub-divided into seven categories: extremely wet >2, severely wet 1.5 to 2, moderately wet 1 to 1.5, normal, -1 to 1, moderately dry -1 to -1.5, severely dry -1.5 to -2 and extremely dry < -2. Time series of the possible drivers of water colour, namely soil temperature, SMD, river discharge in the Glenamong and the weekly NAO were also decomposed using the Seasonal Trend Decomposition as described above.

3.3.4.4 Cross-wavelet transform analysis

A cross-wavelet transform analysis was carried out to further examine the trends and periodicities in colour concentrations with the explanatory drivers of colour in the rivers. Cross-wavelet transform analysis can be used as a method of examining pairs of time series that may be expected to be linked in some way. Continuous wavelet transforms from pairs of time series are used to construct the cross wavelet transforms, revealing their common power and relative phase in time-frequency space. In particular, the analysis examines whether regions in time frequency space with large common power have a consistent phase relationship, suggesting causality between the time series pairs (Grinstead et al., 2004). A cross-wavelet power spectrum was calculated from the cross wavelet transform results in order to estimate the covariance between each pair of time series as a function of frequency and the statistical significance was also estimated as part of the analysis. The 'biwavelet' package in R (R Core Team, 2017) was used for the bivariate wavelet analyses (Grinstead et al., 2004).

3.3.5 Estimation of DOC concentration from water colour concentration, and calculation of carbon export

DOC (mg L^{-1}) concentration was estimated from water colour concentration (PtCo mg L^{-1}) using a linear model developed between water colour and DOC from the Glenamong River between April 2010 and September 2011(Ryder, 2015). There was a strong linear relationship between colour and DOC ($r^2 = 0.88$, $p \leq 0.001$, $n = 366$) indicating that water colour measurements were a good proxy for DOC concentrations in the sub-catchment rivers. DOC analysis was carried out using a Sievers 5310C Total Organic Carbon analyser (Sievers Instruments Inc, sievers.instruments.wts@suez.com) (Range 4 ppb to 50 ppm, accuracy ± 2% or ± 5 ppb, whichever is greater; precision < 1% relative standard deviation). To verify the TOC analyser performance, 10 ppm potassium hydrogen phythalate (KHP) standards were used. The mean annual loads were calculated for the Black and Glenamong sub-catchments by multiplying the calculated stream discharge volume for each week by the weekly estimated DOC concentration and summing the totals. Mean annual yield (per km^2) was estimated by dividing the mean annual load by the upstream drainage-basin area.

3.4 Results

3.4.1 Hydrological and meteorological conditions, 2011 - 2016

Weather conditions varied during the six study years, with 2013 being the driest year, with a mean daily precipitation of 3.7 mm day^{-1} and an annual total of 1315 mm $year^{-1}$. The wettest year was 2015 with mean daily precipitation of 5.6 mm day^{-1} and an annual total of 2020 mm $year^{-1}$. The lowest number of rain days (days with >1 mm rainfall) (194) during the six study years was recorded in 2013, compared to 229 rain days recorded for 2015. The maximum air temperature at Newport meteorological station during the period was 29 °C on the 20th of July 2013 and the minimum was −3.1 °C on 3rd January 2011. The warmest summer over the study period was in 2013 with an average mean temperature of 15.7 °C and the coolest summer was in 2011 with an average of 13.3 °C. The coolest winter was in 2014 / 2015, with an average mean temperature of 5.8 °C and the warmest winter was in 2011/2012 with an average of 7.2 °C. The driest summer over the study period occurred in 2013 with 258 mm accumulated rainfall. The driest winter was also in 2012/2013 with 430 mm accumulated rainfall. The wettest summer was in 2012 with 373 mm accumulated and the wettest winter was in 2015/2016 with 744 mm accumulated rainfall.

A comparison of monthly precipitation values during the six-year study period with precipitation from the previous 15 years (1995 to 2010) at the Newport station showed that the first two study years, 2011 and 2012, had near normal precipitation totals (SPI of 1 to -1) with some short moderately wet periods (SPI of 1 to 1.5). However, the period between June 2013 and February 2015 was, when compared to the previous 15 years of data, a notable long dry spell, with SPI values ranging from near normal to periods of moderately dry (SPI of -1 to -1.5) to extremely dry values (SPI > -2). Following this predominantly dry period, there was a moderate to extreme wet period from February 2015 to August 2015. Precipitation during the remainder of 2015 and 2016 was mostly near-normal (Figure. 3.2A).

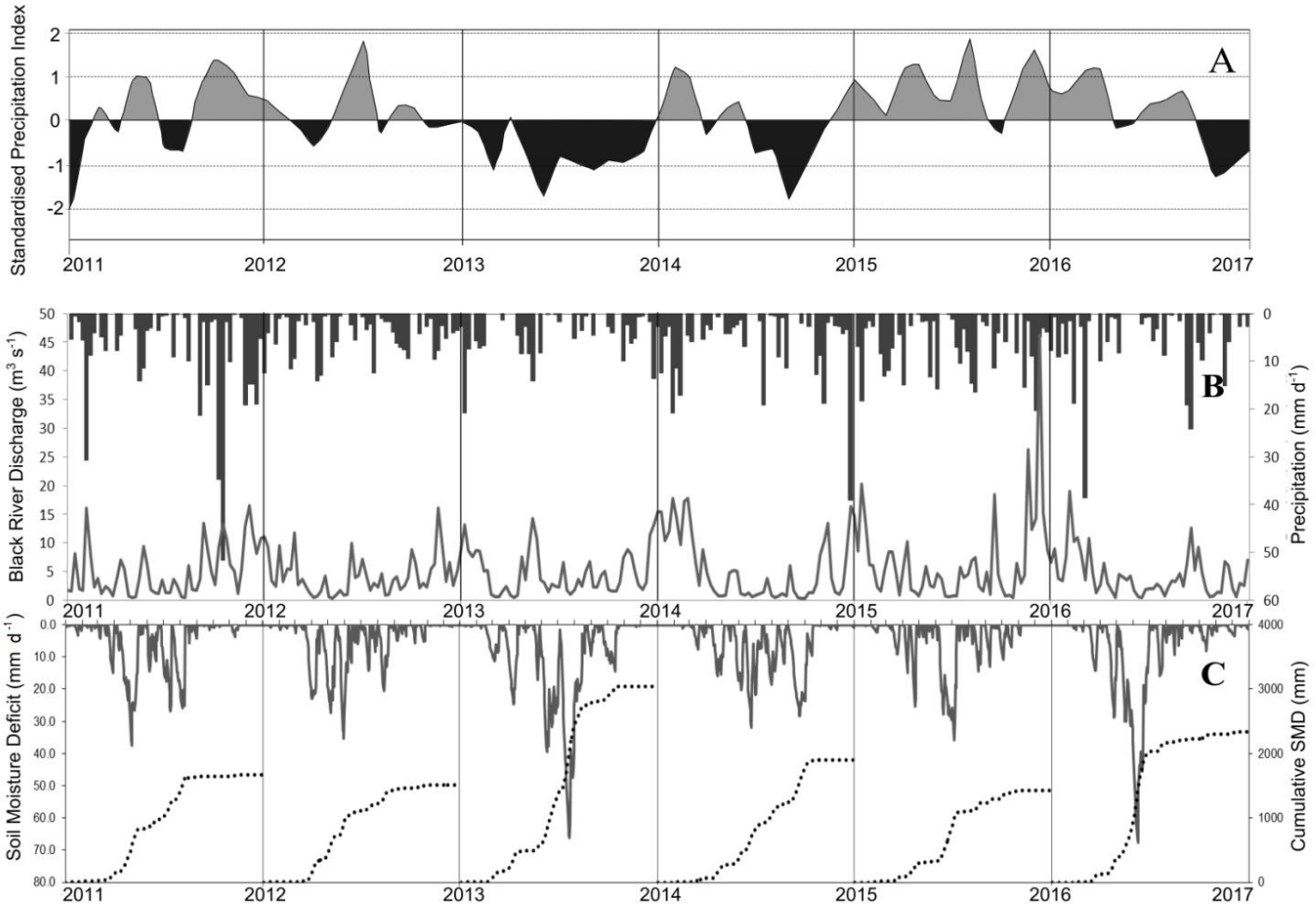

Figure 3.2 Panel A: one month Standardised Precipitation Index (SPI) calculated using precipitation data from the Newport climate station (reference period 1995 to 2010). Periods where the index is >1 represent moderately wet conditions and periods where the index <-1 indicate moderately dry conditions. Panel B: Black river discharge (grey line - m^3 s^{-1}) and mean precipitation (black bars - mm day^{-1}): panel C: cumulative soil moisture deficit (SMD) per year (mm)(dotted line) and actual soil moisture deficit (mm d^{-1} (grey line)).

The mean stream water discharge rates for the three rivers during the study period were 1.89, 0.84 and 0.36 $m^3 s^{-1}$ for the Black, Glenamong and Srahrevagh rivers respectively, reflecting the difference in area for the three catchments, as well as the higher precipitation in the Black. Values greater than the 90% percentile of discharge for the Black river were > 4.47 $m^3 s^{-1}$ while those less than the 10% percentile were < 0.26 $m^3 s^{-1}$ (Figure 3.2B). The highest discharge recorded during the study period for all three rivers occurred on the 5th of December 2015 with flows of 40.6 $m^3 s^{-1}$ recorded for the Black river, 31.8 $m^3 s^{-1}$ for the Glenamong and 9.2 $m^3 s^{-1}$ for the Srahrevagh. These exceptional flows occurred during Storm Desmond, a 1000-year return event and one of a series of storms that tracked across the country during a fourteen-week cyclonic episode that began in early November 2015, which brought severe, extensive and protracted flooding to much of Ireland, Scotland and Northern England (Marsh et.al., 2016).

The pattern in soil moisture deficit (SMD) varied considerably over the six years, largely reflecting the varying volumes of precipitation over the catchment each year. The year with the greatest cumulative SMD was 2013 with an average daily deficit of 8.3 mm. The cumulative SMD reached a maximum of 66.2 mm in July. The least accumulated deficit occurred in 2015 with an average of 3.9 mm, with a maximum of 35.7 mm recorded in July. The maximum daily SMD recorded over the study period was 67.6 mm day^{-1} which occurred in June 2016 however the average daily deficit for that year was 6.4 mm day^{-1} (Figure 3.2C).

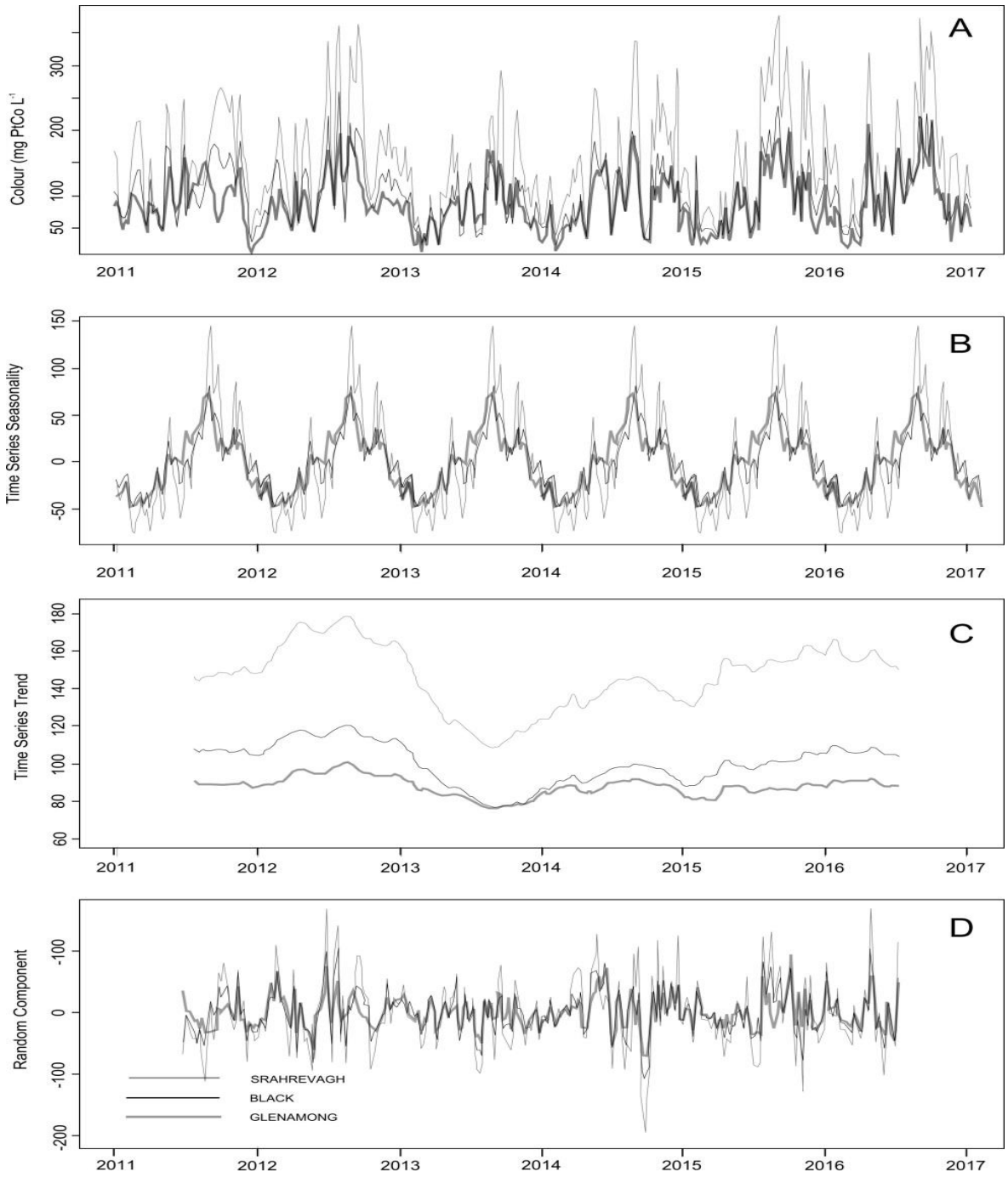

Figure 3.3 (A) Time series of colour concentrations (mg PtCo l^{-1}) measured weekly in the Black, Glenamong and Srahrevagh rivers from 2011 to 2017. Decomposition of the weekly water colour concentrations to the (B) inter-annual trend; (C) seasonal component and (D) random component

3.4.2 Colour concentrations in the three rivers

The colour concentration showed a strong synchronous annual pattern for all sub-catchments, dipping to a minimum during the winter and peaking in late summer to early autumn (Figure. 3.3A). The Srahrevagh River had the highest colour concentrations, with a median colour concentration of 130 mg Pt Co L^{-1}, the Glenamong River had the lowest concentrations with a median of 84 mg Pt Co L^{-1}, while the Black River had median values intermediate between these two of 95 mg Pt Co L^{-1}. Overall, the median colour measurements in the Srahrevagh river were significantly higher than those measured in the Glenamong river (Mann-Whitney U test, $W=20317$, $p<0.01$) and Black river (Wilcoxon signed Ranked test, $V=892.5$, $p<0.01$). Colour in the Glenamong river was also marginally significantly lower than that measured in the Black river (Mann-Whitney U test, $W=37604$, $p < 0.05$).

The inter-annual trend in colour concentration (Figure. 3.3B) was also synchronous across all three sub-catchments. There was a peak during the summer of 2012 before it descended to a minimum for all three catchments in the late summer and early autumn of 2013. The trend generally increased from this low-point to the beginning of 2016, with the exception of a minor dip in colour concentration in January 2015. The seasonal patterns were also almost identical for all three sites (Figure. 3.3C) with highest concentrations in late-summer and lowest values in January and February of each year. The Srahrevagh again displayed the greatest range of seasonal variation, and the seasonal variation of the Black and Glenamong were largely similar. The decomposed random component of the colour time-series (Figure. 3.3D) also displayed a broad synchronicity in timing across all three sub-catchments over the six years, indicating that the mechanisms controlling short-term spikes and dips in colour were also synchronous across all three sub-catchments. Similar to the pattern of the seasonal variation, the greatest range of variation in the random component was from the Srahrevagh River (-200 to 169) while the range of variation in the other two rivers were broadly similar (-109 to 107 and -71 to 96 for the Black and Glenamong respectively).

3.4.3 Drivers of water colour variation

The optimal GAMM for the colour in the Black River included three smoothers, soil temperature at 100 cm depth, soil moisture deficit, and the weekly mean NAO (Figure. 3.4). This model explained 54% of the deviance in water colour over the study period (Table 3.2). Explanatory variables that were measured on the day of sampling resulted in a better model fit than weekly means for the previous week. Lagging the explanatory

variables by one, two and four weeks did not improve the model. The smoother explaining the relationship between soil temperature and colour was linear in the model (estimated degrees of freedom = 1) and positive, indicating that colour increases with increasing temperature. The smoother describing the relationship between colour and soil moisture deficit was, in contrast, generally negative, indicating that colour concentrations in the river decreased with increasing SMD, while notably that describing the relationship between NAO and colour indicated that colour decreased in positive phases of the North Atlantic Oscillation. The optimal GAMM for the Srahrevagh River had the same three smoothers as the Black, soil temperature at 100 cm, SMD and the weekly NAO (Figure 3.4) and the model explained 58% of the deviance in water colour over the study period (Table 3.2). Again the sub-set of explanatory variables that were measured on the day of sampling provided the optimum model. The smoothers in the Srahrevagh River model also showed the same patterns in relationship to colour i.e. a positive relationship between colour and soil temperature and a negative relationship between SMD and the weekly NAO.

The optimal GAMM for colour in the Glenamong River also had three smoothers, but differed in that it included the log of river discharge rather than SMD (Figure 3.4). The model explained 66% of the deviance in water colour over the study period (Table 3.2) with again the sub-set of explanatory variables that were measured on the day of sampling providing the optimum result. The shape of the smoother describing the relationship between colour and discharge indicated that colour concentrations in the river increased to a point and then stabilised at higher discharges. The smoother describing the relationship between the NAO and colour was similar to that found in the other two models and decreased for positive phases of the North Atlantic Oscillation (Figure 3.4G).

The models described above produced the optimum R^2 values for the set of explanatory variables chosen. It is important to note that the log of river discharge was also found to be a significant variable in the models for the Black and Srahrevagh; however, as it was correlated with SMD both explanatory variables could not be used within the same model. When the SMD was used instead of the log of discharge for the Black and Srahrevagh, the revised optimum model variables still included soil temperature and the NAO in both cases with log of discharge, but explained only 48% and 47% of the variance respectively. Conversely, SMD was found to be significant when swapped with the log of river discharge in the Glenamong model, however, the R^2 value reduced slightly to 64% from the optimum value of 66%.

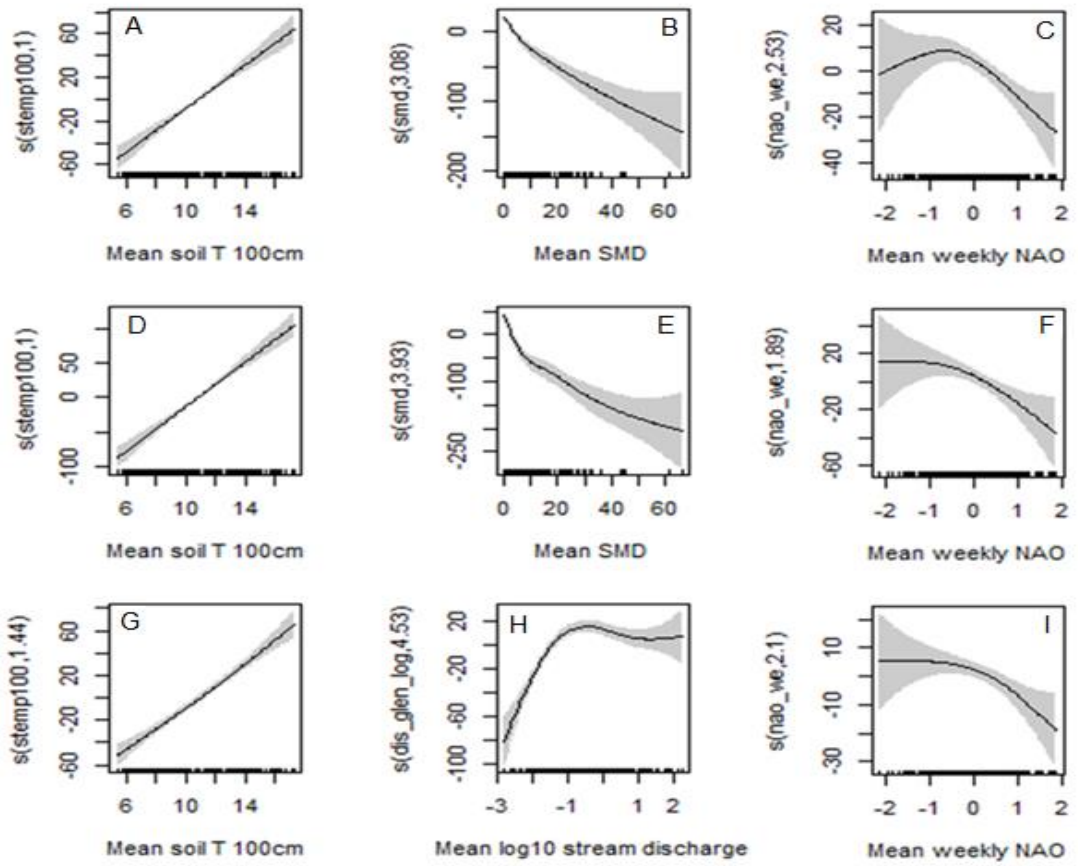

Figure 3.4 Selected smoothers for the contribution of explanatory variables for the optimal GAMM explaining water colour in each sub-catchment river: Black (A, B, C): A = soil temperature, B = soil moisture deficit (SMD), C = NAO; Srahrevagh (D, E, F): D = soil temperature, E =soil moisture deficit, F = weekly NAO; Glenamong (G, H, I): G = soil temperature, H = log of discharge, and I = NAO. The solid line is the smoother and the shaded area shows the 95% confidence bands. Y axis units are the scaled smoother (s) for each explanatory variable with the variable name followed by the estimated degrees of freedom within the prentices.

Table 3.2 Results of Generalised Additive Mixed Models (GAMM) applied to colour in the Black river (top) the Srahrevagh river (middle) and the Glenamong river (bottom) between 2011 and 2016. The (s) refers to the scaled smoother for each explanatory variable. Stemp100 refers to soil temperature at 100 cm depth, smd refers to soil moisture deficit, dis_glen_log refers to the log of the discharge of the Glenamong river, and nao_we refers to weekly mean values of the NAO index, edf = estimated degrees of freedom.

Colour – Black River		*R-sq. (adj) = 0.54*	*Scale est. = 99.816*	*n = 258*
	Estimate	Std. Error	t value	Pr (>|t|)
Intercept	100.30	3.41	29.40	< 0.0001
Approximate significance of smooth terms:	edf		F	p-value
s(stemp100)	1.00		96.75	<0.0001
s(smd)	3.08		48.64	< 0.0001
s(nao_we)	2.53		7.48	0.0006
Colour – Srahrevagh River		*R-sq.(adj) = 0.58*	*Scale est. = 2809.1*	*n = 261*
	Estimate	Std. Error	t value	Pr (>|t|)
Intercept	145.61	4.11	35.40	< 0.0001
Approximate significance of smooth terms:	edf		F	p-value
s(stemp100)	1.00		133.08	< 0.0001
s(smd)	3.93		54.62	< 0.0001
s(nao_we)	1.89		4.72	< 0.0067
Colour – Glenamong River		*R-sq. (adj) = 0.66*	*Scale est. = 647.71*	*n = 264*
	Estimate	Std. Error	t value	Pr (>|t|)
Intercept	88.52	2.27	39.06	< 0.0001
Approximate significance of smooth terms:	edf		F	p-value
s(stemp100)	1.53		128.10	< 0.0001
s(dis_glen_log)	4.53		29.23	< 0.0001
s(nao_we)	2.10		4.97	< 0.0081

Of note also was the relative importance of the explanatory variables in each of the models. For example, in the optimum model for the Black sub-catchment, out of the total of 54% of the variance explained by the model, soil temperature contributed 34%, SMD contributed 17% and the NAO contributed 3%. For the Srahrevagh, out of the 58% total, soil temperature contributed 40% of the variance, SMD contributed 16% and the NAO contributed 2%. Out of the 66% total of explained variance for the Glenamong, soil temperature contributed 52%, the log of river discharge contributed 11% and the NAO contributed 3%. The multi-annual trend plots for the NAO, soil temperature, discharge and water colour all had similar patterns that included a distinct dip in the period from late 2012 to mid-2013, and a general upward trend after these low points (Figure 3.5). These low-points were sequential for the different variables, with the dip in the NAO occurring in the early winter of 2012, that in soil temperature occurring in early 2013, and that in mean colour concentrations (mean based on data for all three sites) in mid-summer of 2013. The trends for river discharge, here using the Glenamong as an example, had a less defined low point, which ran from early- to mid-summer 2013 (Figure 3.5C). The trend in SMD displayed a distinct plateau for each year, with 2013 having the highest levels and 2015 the lowest levels (Figure 3.5D).

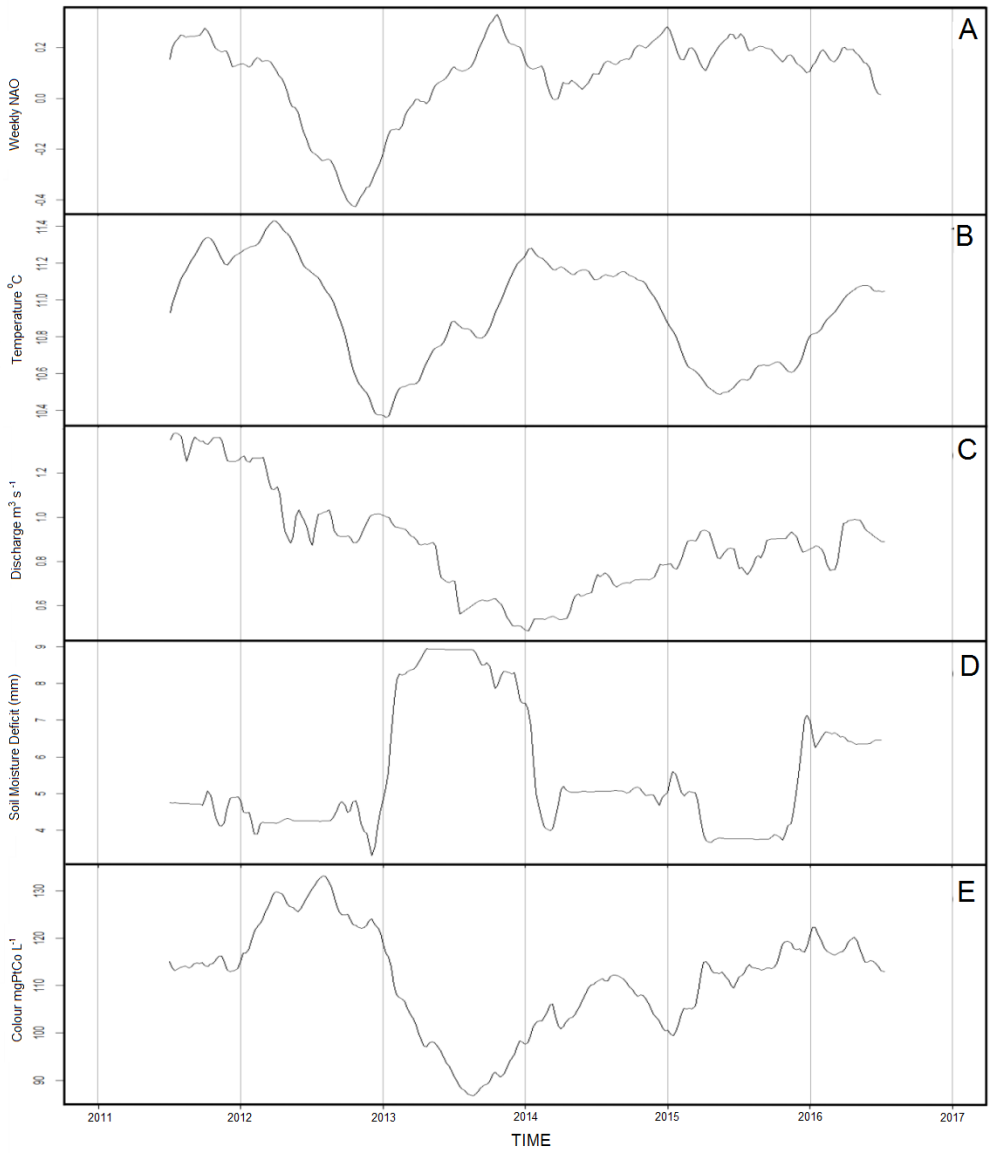

Figure 3.5 (A) Trend of weekly NAO during the study period (B) trend of weekly soil temperature (C) trend of weekly discharge in the Glenamong river (D) trend of weekly soil moisture deficit (SMD) and (E) trend of mean weekly mean colour concentration in the three sub-catchment rivers.

3.4.4 Cross-wavelet power analysis

In the cross-wavelet analysis, there was a significant common power between river colour at the annual (52 week) time scale for all four variables, with additional significant zones occurring intermittently at higher frequencies (*circa* 2-16 weeks) that were most notable for SMD and for the NAO (Figure 3.6). For soil temperature, the width of the orientation at the annual time step was relatively consistent with phase arrows that all pointed right, i.e. there was a positive correlation between soil temperature and river colour that was consistent at the annual scale (Figure 3.6A). The orientation of the phase arrows (i.e. downward) for stream discharge indicated that river colour was leading river discharge by 90°, indicating they both had seasonal cycles where river colour peaked half an annual cycle before river discharge. The orientation of the phase arrows for the NAO, in contrast, showed a consistent anti-phase or negative correlation with river colour at an annual time step. Notably this weakened between weeks 100 and 150 i.e. during 2013. For SMD (Figure 3.6B) the orientation of the phase arrows at the annual time step, in contrast, showed SMD leading river colour by 90°, therefore, colour peaked half an annual cycle after a peak in SMD. The areas of common power with river colour at higher frequencies (i.e. at periods of 2 to 16 weeks) were most notable for SMD: these were predominantly negative and occurred during summer periods, when SMD was higher. There were also regular areas of common power at frequencies between 2 and 16 weeks between the NAO and river water colour, however their phase relationship was variable from area to area, with no consistent pattern.

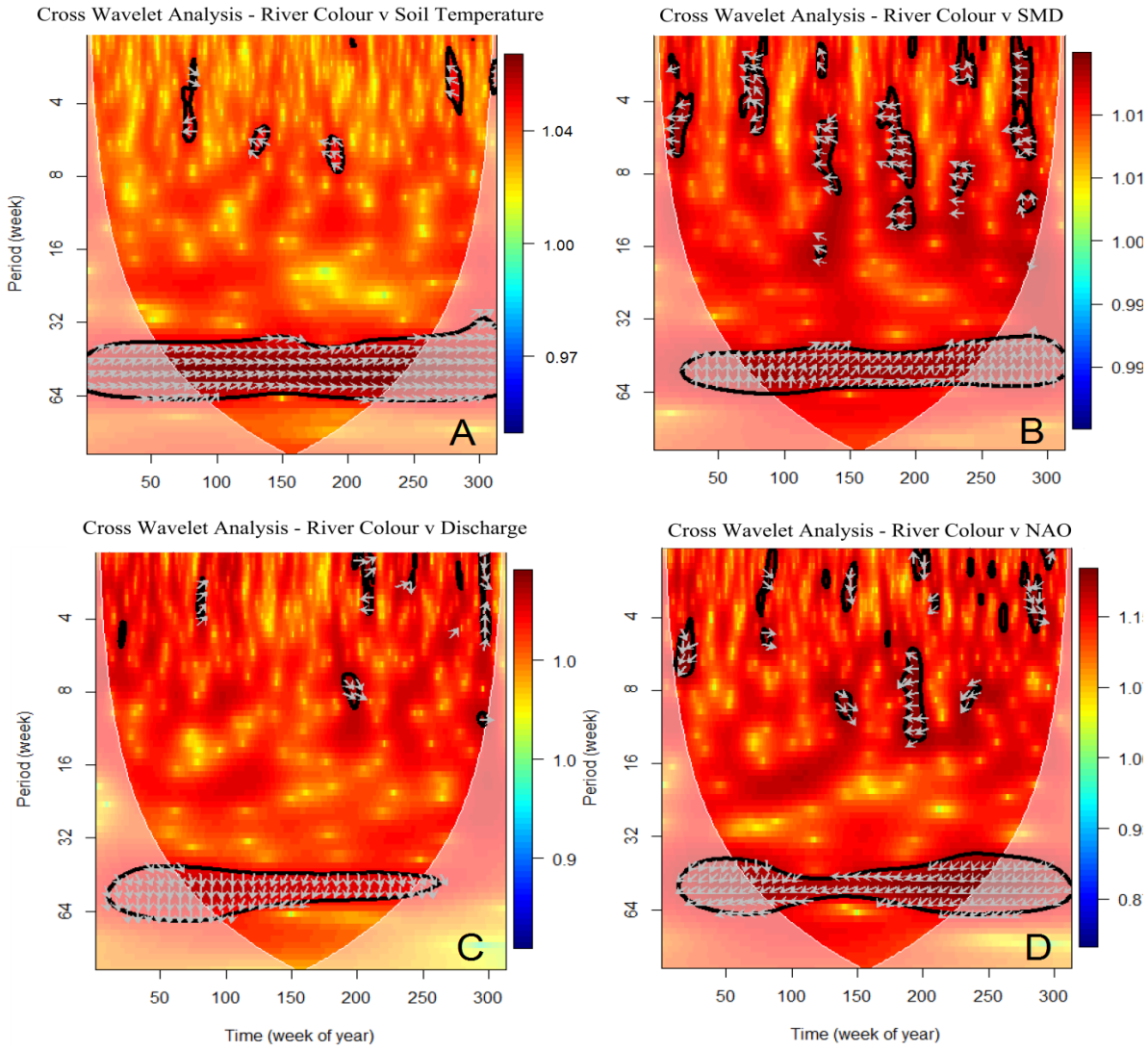

Figure 3.6 Cross-wavelet power spectrum of soil temperature at 1 m depth (A), Soil Moisture Deficit (SMD) (B), river discharge in the Glenamong (C) and NAO (D) with river colour. Colour contours represent cross-wavelet power and vectors indicate the relative phase relationship between the two time series (with in-phase pointing right, anti-phase pointing left, or a variable leading or following river colour by 90° pointing straight down/up). The 5% significance level is shown as a thick contour. Pink regions on either end indicate areas where the analysis is unreliable as there is no data before and after the study period.

3.4.5 Estimated DOC loads from the sub-catchments

There was a wide range in the annual estimated loads exported from the three sub-catchments over the six study years, both at an annual and seasonal scale (Table 3.3). The higher colour concentrations in the Srahrevagh river translate into the highest DOC exports any of the sub-catchments, even when the loads are area-weighted. The highest annual load was estimated for the Srahrevagh in 2015 (38.6 t C km^2 $year^{-1}$), while the lowest was recorded in the Glenamong in 2013 (11.6 t C km^2 $year^{-1}$). The smallest loads across all sub-catchments were recorded in 2013. Based on these data (the sum of the Black and Glenamong loads), a total of 5898 tons of DOC were exported into Lough Feeagh during the six study years. In other words, just under 1000 tons of DOC is transferred from land to water in the Burrishoole catchment every year

Table 3.3 Estimated DOC load (t C km^2 $year^{-1}$) from the Black, Srahrevagh and Glenamong catchments between 2011 and 2016. *Totals were calculated as the area-weighted average for the Black and Glenamong sub-catchments only (which are in-flows to Lough Feeagh, the main lake shown in Fig. 1). Seasonal loads are linked to the years in the table header. Winter (D, J, F) = December, January, February etc.

Catchment	**2011**			**2012**			**2013**			**2014**			**2015**			**2016**		
Black	18.5			15.2			12.0			12.6			17.3			14.5		
Srahrevagh	28.4			25.8			21.2			35.4			38.6			18.6		
Glenamong	18.5			15.0			11.6			12.6			16.3			14.4		
Total*	18.5			15.1			11.8			12.6			16.8			14.5		
Totals by Season	Black	Glenamong	Srahrevagh	Black	Glenamong	Srahrevagh	Black	Glenamong	Srahrevagh	Black	Glenamong	Srahrevagh	Black	Glenamong	Srahrevagh	Black	Glenamong	Srahrevagh
Winter (D, J, F)	-	-	-	6.5	5.4	9.4	5.1	4.8	9.0	4.6	4.5	18.4	5.2	5.1	11.9	7.0	4.8	9.4
Spring (M, A, M)	3.3	3.1	4.2	1.7	1.6	2.8	3.0	3.0	5.7	2.4	2.2	6.5	3.2	2.8	5.0	2.2	2.2	2.2
Summer (J, J, A)	2.7	3.1	2.4	3.5	3.8	5.6	2.2	2.3	3.1	1.4	2.1	3.4	4.0	3.8	5.9	3.1	3.4	2.2
Autumn (S, O, N)	7.0	7.3	11.8	4.9	4.7	8.4	2.1	2.2	3.9	3.5	3.1	5.7	3.5	5.4	16.2	4.4	4.4	8.6

3.5 Discussion

3.5.1 Introduction

This study highlighted the dominant influence of local and regional climate on water colour as a proxy for DOC levels. Weather related factors explained between 54 and 66 % of the variability in all three sub-catchment datasets, and there was strong synchronicity in these climate signals across the Burrishoole catchment. It also showed, however, that despite this synchronicity, colour concentrations in one sub-catchment (the Srahrevagh) were significantly higher than the other two monitoring sites, a difference that was consistent over seasons and the six years of the study. Colour, and therefore DOC, in these headwater rivers probably originates almost exclusively from the surrounding catchment soils and the consistent difference in colour concentrations between each sub-catchment during the study was most likely a function of individual sub-catchment properties such as the extent of peat within catchments (Hope et al., 1997a), land use (Findlay et al., 2001), local runoff (Dillon and Molot., 2005) vegetation type (Sobek et al., 2007) and the unique morphology and geology of the sub-catchment landscape (Moore, 1998). Forestry is also known to influence DOC release from soils and it has been observed that both afforestation and forest clear-felling result in increased DOC concentrations and that these increases may continue for several years after the initial event (Cummins & Farrell, 2003; Schelker et al., 2012) The extent of peat soils in the study catchments, the length of streams intersecting the peat, slope analysis and CORINE land cover may explain the higher levels of colour found in the Srahrevagh. However, an additional factor could be the distance between a given sampling point and the source of any coloured compounds. Dawson et al., (2002) previously observed decreases in TOC (both DOC and POC) concentrations in the Upper Hafren (a headwater stream in mid-Wales) downstream from the source that were stated to be related to a decrease in peat depth with altitude, combined with in-stream processing of DOC. A similar process may contribute to the difference in concentration between the upstream Srahrevagh and downstream Black sampling points, although there are other studies that reported no clear decrease in DOC concentration as water travelled downstream (Temnerud & Bishop, 2005; Creed et al., 2015;Winterdahl et al., 2016).

3.5.2 Local climate effects

The local climate effects identified in this study included strong positive linear correlations between colour concentrations in the three rivers and soil temperature. There

was also a consistent positive relationship between soil temperature and colour at the annual scale in the cross wavelet analysis. Soil temperature was common to all three GAMMs, and was the dominant explanatory variable, emphasising how dissolved organic carbon is released by peat soils via decomposition processes that are temperature dependant (Christ & David, 1996; Neff & Hooper, 2002). This temperature effect is complicated, however, by an interaction between peat decomposition and the water table level. Peat soils during low water level conditions show increased rates of decomposition, brought about by changes in the oxygen status within the peat and subsequent changes in the microbial community structures within the soil (Mäkiranta et al., 2009). The lowered water table reduces the hydrological connection i.e. the transport of DOC along active flow pathways in the soil. This breaks the connection between the source of DOC production and its eventual destination. Increasing temperature, therefore, will increase DOC production in the peat but only if the increase in temperature does not result in a large draw-down of the water table. The strong relationship displayed between soil temperature and water colour concentrations in the three rivers, and the significant and high common power with river colour at the yearly time scale in the cross-wavelet analysis, indicated that soil temperature was the primary driver of the seasonal pattern in water colour during the study period in this catchment. It is interesting to note that in general no relationship between seasonality and DOC concentration has been reported in some other studies (e.g. Winterdahl et al., 2014). However, these results are consistent with observations of DOC dynamics in some surface waters, where seasonal variation has been found to be the largest source of DOC variation in catchments with high DOC concentrations (Clark et al, 2010b; Ryder et al., 2014). Of note also were the strong similarities in the pattern in multi-annual trends of river colour and soil temperature, particularly in the first four years of the study where the pronounced sequential dip was observed in temperature and then in water colour, indicating as might be expected, that temperature also acts at a multi-annual scale.

The relationship of colour with SMD in the Black and Srahrevagh optimal GAMM models indicated that as soil moisture decreased DOC concentrations also decreased. The cross-wavelet analysis indicated a significant continuous relationship at a yearly time step where SMD led colour by 90°, that is colour peaked after higher SMDs. More notably there were intermittent, shorter periods during the summer months, where the relationship between the two variables was consistently negative, in line with the GAMM results. The multi-annual trends in decomposed colour concentrations and SMD over the study period

also broadly confirmed this negative relationship, where lower colour concentrations corresponded with higher values in SMD. A drought effect has previously been reported in the Glenamong catchment, where low DOC concentrations in the river were associated with an extremely dry winter and spring during 2010 (Ryder et al., 2014). Hydrology has a direct control on DOC *via* its influence on soil residence time and transfer from soil to stream. For example, the transfer from more lateral drainage routes to vertical pathways with decreasing precipitation would consequently increase the potential for adsorption of DOC by ion-exchange complexes in mineral soil horizons (Moore & Jackson, 1989). There are also indirect effects of hydrology on DOC concentrations such as the availability of water for biogeochemical cycling, biological production and chemical controls on solubility (Clark et al., 2010a). Decreased DOC export has been observed from peat soils during drought conditions where the drawdown of the water table causes the oxidation of organic sulphur to sulphate (Clark et al., 2005; Daniels et al., 2008). This drought-induced soil water acidification reduces DOC solubility in soil water, and therefore concentrations. However, immediately following periods of dry weather or drought, pronounced increases in DOC concentrations have been observed in peatland streams (Watts et al., 2001). Ryder et al., (2014) also reported a significant step-change increase in DOC concentrations in the Glenamong sub-catchment during moderately wet conditions during the summer of 2010 following a very dry spring that year.

River discharge was a significant explanatory variable in the optimum model for the Glenamong, and in alternative models for the Black and the Srahrevagh rivers, further emphasising the complex effects of hydrology on colour, and therefore DOC concentrations, in the catchment. The reasons why river discharge superseded SMD as an explanatory variable for the Glenamong are likely to be its more westerly location, with higher precipitation, and more mountainous topography. The effect of precipitation has been shown to operate at sub-catchment spatial scales and short temporal scales in the Burrishoole catchment. de Eyto et al., (2016) described the effects of an intense episodic rainfall event on the ecology of Lough Feeagh, where anomalous high amounts of rain fell in the east side of the catchment (the Black and Srahrevagh) while relatively moderate amounts were recorded in the west (the Glenamong). However, that event was not associated with any increase in water colour, while in contrast, Jennings et al., (2012) described a large increase in DOC concentrations in the Glenamong during increased precipitation in summer 2006. Short-duration high discharge events were also less likely to have been picked up at a weekly sampling regime of the current study. The GAMM

smoother for colour concentration in the Glenamong versus discharge showed that colour increases with increasing discharge to an optimum point where it levels off and even decreases slightly at very high discharges. The cross-wavelet time-series analysis between river colour and river discharge in the Glenamong indicates a significant continuous relationship at a yearly time step with colour concentrations leading discharge by 90°. This high common power relationship is however unlikely to be causal, since colour cannot result in changes in discharge, but emphasises the co-occurrence of seasonal patterns in both data sets.

3.5.3 Regional climatic effects and the NAO

The current study indicated variable results for the effect of NAO on water colour. There was a negative relationship with the NAO indicated in both the GAMMs, and in the common power at an annual time step in the cross wavelet analysis, but also a lagged positive effect indicated in the plots of the multi-annual trends. The effects of the NAO on the local climate and lake water temperatures have previously been described for the Burrishoole catchment (Jennings et al., 2000; Blenckner et al., 2007). Jennings et al., (2000) reported that a range of meteorological variables at two lake sites in the west of Ireland (Lough Feeagh, Co Mayo and Lough Leane, Co Kerry) were influenced by the winter NAO, including positive relationships with mean winter air temperature and surface water temperature, mean winter wind speed, and winter rainfall. These relationships were also apparent but to a lesser degree in the following spring and summer. Kiely (1999) also showed that positive phases of the winter NAO led to increased runoff in Irish rivers. During the construction of the GAMMs, both the weekly and monthly NAO index values were tested in the analysis. The models using the weekly data consistently explained more of the deviance in the model. This most likely reflects the proximity of the site to the Atlantic coast and the time frame over which weather systems associated with the NAO pressure difference generally reach the study location. Although the weekly NAO improved the optimum models by only between 2 and 4%, it was significant at the 99.9% level in all of the models. The smoothers for the weekly NAO in the GAMM's indicated that colour decreased during positive phases of the NAO. This appears to be contrary to the literature for more northern sites whereby DOC has been shown to increase during positive NAO phases, a relationship that has been linked to higher winter precipitation (Nõges et al., 2007; Arvola et al., 2004). However, some studies have also suggested that positive phases of the NAO during the summer are associated with warm and dry rather than warm and wet conditions over northwest

Europe, in particular the UK and much of Scandinavia (Folland et al., 2008). It is possible that this negative relationship was reflected in the strong effect on SMD on colour in the current study. However, the negative relationship apparent in the cross-wavelet time-series analysis at the annual time step may also merely reflect the fact that both time series have seasonal patterns, but are not linked by any causal mechanism. Examination of the multi-annual trend of the decomposed NAO values also showed a large and sustained swing in the index to negative values, beginning in late spring of 2012 until spring of 2013, with a subsequent return to positive values. Negative NAO values during the winter generally correspond to relatively cold and dry conditions, and dry weather was observed throughout 2013, reflected in the SPI Index, beginning during the winter of 2012/2013. Cold conditions were also confirmed by the sharp dip in the multi-annual trend of soil temperature observed during the same winter period. This overall trend was mirrored in the pattern in water colour but lagged by *circa* six months, suggesting that the NAO actually has a lagged but positive effect on water colour at this time scale. Further analysis with a longer multi-annual dataset would be required to explore the effect of the NAO on water colour and therefore DOC export at this site.

3.5.4 Carbon export from the sub-catchments

The minimum annual total DOC load from the Burrishoole catchment was 11.8 t C km^2 yr^{-1} in 2013 while the maximum was 18.5 t C km^2 yr^{-1} in 2011, giving a range of 6.7 t C km^2 yr^{-1} during the study period. This considerable variability in total annual load from the Burrishoole catchment was most likely linked to climate variability over the study period. For example the driest year of the study period, 2013, displayed the minimum yield. The estimated annual yields reported here are broadly in line with the 9.5 t C km^2 yr^{-1} and 13.7 t C km^2 yr^{-1} estimated DOC export from the Glenamong sub-catchment in 2010 and 2011 respectively (Ryder et al., 2014) and broadly within the ranges reported in other studies from peatland catchments (Clark et al., 2007; Koehler et al., 2009; Naden et al., 2010)

3.6 Conclusions

The results of this study emphasised how colour concentrations, and therefore DOC levels, respond to common climatic drivers which operate at both a local and regional scale. In the Burrishoole catchment, temporal changes in stream colour levels were driven by variation in soil temperature, hydrology (discharge and / or SMD), and by the NAO, an overarching regional climate pattern. These effects lead directly to variability in aquatic DOC concentrations in the sub-catchments that will ultimately affect the carbon

budget of the downstream receiving waters of Lough Feeagh. The results presented here serve to further strengthen the well-established link between climate and aquatic carbon concentrations in peatland catchments, and the vulnerability of blanket peatlands to climate change.

4.0 Late Summer Peak in $_pCO_2$ Corresponds With Catchment Export of DOC in a Temperate, Humic Lake

A note on the collaborations associated with the work described in this chapter:

The following chapter is based on the following paper, Doyle B.C, de Eyto E, McCarthy V, Dillane M, Poole R, Jennings E. (2021). *Late summer peak in $_pCO_2$ corresponds with catchment export of DOC in a temperate, humic lake*. Inland Waters, (In Review). For this paper Brian Doyle collected manual CO_2 lake measurements, quality-controlled a range of environmental and meteorological datasets, researched and analysed data and was the primary author of the paper. Eleanor Jennings, Elvira de Eyto and Valerie McCarthy supervised the research, provide advice on statistical analysis and assisted with manuscript exiting. Mary Dillane and Elvira de Eyto maintained environmental monitoring equipment and datasets used in this study. Russell Poole, provided editing advice.

4.1 Abstract

It is now widely recognised that many lakes are supersaturated with CO_2 and play an import role as net emitters of this greenhouse gas to the atmosphere. Lakes in humic systems also play a key role in the processing and fate of organic carbon (OC) mobilised from their catchments. At present, however, knowledge of lake OC dynamics in temperate lakes, especially those with maritime climates, is limited. The generally wet and cloudy conditions coupled with the relatively benign temperatures exert a significant influence on mechanisms of OC capture, storage and processing on the west coast of Ireland. Here, we examine a high-frequency dataset of partial pressure of CO_2 ($_pCO_2$) in the surface waters of Lough Feeagh collected over one year, along with an allied set of environmental explanatory variables. The annual pattern in $_pCO_2$ ranged between 491 and 1169 µatm, and was found to be strongly related to allochthonous OC inputs from the incoming rivers. In contrast to observations from lakes in colder climates where snowmelt often drives $_pCO_2$ seasonality, a single peak in $_pCO_2$ occurred in Lough Feeagh in early September. Generalised additive mixed modelling revealed that two variables, inflow water colour concentration (a reliable proxy for DOC concentrations) and lake Schmidt stability together explained 68% of $_pCO_2$ variability. Both the statistical analysis and the concurrent timing of the peak in inflow DOC with the peak in $_pCO_2$ strongly suggested that catchment carbon export drove $_pCO_2$ supersaturation in the lake, and hence CO_2 emission. We estimated that between 217 and 370 t CO_2-C (0.55 – 0.94 t CO_2-C / ha) as

CO_2 was emitted from the lake during the study period. These results highlight the interplay that exists between catchment OC fluxes and climate in determining $_pCO_2$ dynamics in maritime temperate lakes.

4.2 Introduction

Lakes actively process terrestrial carbon and, as a consequence, are important emitters of greenhouse gas (GHG) to the atmosphere (Cole et al., 2007; Tranvik et al., 2009; Bastviken et al., 2011; Deemer et al., 2016). The contribution from lakes and impoundments has been estimated to be equivalent to almost 20% of global anthropogenic fossil fuel emissions and range between 503 Tg CO_2-C yr^{-1} and 810 Tg CO_2-C yr^{-1} (DelSontro et al. 2018). When rivers and streams are included in these calculations the contribution from freshwater systems in their entirety increases to 2.1 Pg C yr^{-1} (Raymond et al., 2013). Factors such as nutrient status, lake hydrology and morphology, catchment properties and climate are known to determine lake carbon processing and cycling characteristics (Tranvik et al., 2009; Lewis Jr, 2011; Weyhenmeyer et al., 2015).

Soil OC tends to accumulate in areas where precipitation dominates over potential evaporation by a ratio of about 3:1 and subsequently primary production exceeds the decomposition of soil organic matter (Wieder & Vitt, 2006). This imbalance in accrual over decomposition for soil OC is particularly common in temperate maritime climate zones and results in the accumulation of peat soils (Moore & Bellamy, 1974). These peat soil accumulations occur as blanket bog, common in Ireland and Scotland, reflecting the strong influence of the Atlantic Ocean in both countries (Coll et al., 2014). Blanket peatlands are recognised as being under threat from excessive erosion due harvesting, burning and grazing (Renou-Wilson et al., 2011) and climate change (Gallego-Sala & Prentice, 2013). Freshwater aquatic systems in these carbon-rich peatland environments are the principal conduits along which OC is conveyed to the ocean (Hope et al., 1997; Tipping et al., 1997; Ryder et al., 2014). Whilst there is a large amount of literature focused on carbon processing in upland peatland streams (Hope et al., 1997; Jones & Mulholland, 1998; Dawson et al., 2004), less is known about carbon processing and $_pCO_2$ dynamics of peatland lakes within temperate maritime climate zones.

There are approximately 12,200 lakes greater than 0.001 ha (10 m^2) in the Republic of Ireland, with a total cumulative lake surface area of 1,288 km^2 or 1.8 % of the total land area (Dalton, 2018). Geographically, the greatest concentrations of lakes are in the

northwest and west of the country (Dalton, 2018). This spatial concentration of lakes in Ireland overlaps, to a great extent, with catchments that are dominated by blanket peatland, as peatlands are also spatially biased towards the west of Ireland. It is important, therefore, to gain a better understanding of lake C processing within this geographical setting and in peatland catchments in temperate regions generally.

Lake epilimnetic $_pCO_2$ is driven by the interplay of numerous drivers over a range of timescales, however, central to the process are photosynthesis and respiration (Dodds & Cole, 2007). Variation in $_pCO_2$ at daily time scales is predominantly linked to biological activity in the water column. Primary producers in lakes fix inorganic C during photosynthesis, thus reducing water column $_pCO_2$ (Williamson et al., 2009). Conversely, the oxidation of OC during respiration by both heterotrophic and autotrophic organisms increases lake water column $_pCO_2$ (Cole et al., 1994; Jonsson et al., 2001). The observed diel variation of $_pCO_2$ in lakes occurs as a result of the continuous oscillation between both photosynthesis and respiration during the day and respiration only at night (del Giorgio et al., 1997; Sobek et al., 2005; Huotari et al., 2009). Physical processes may also cause diel variation in $_pCO_2$, for example, convective night-time mixing causes upwelling of deeper CO_2-rich water as a result of differences in air temperature between day and night (Åberg et al., 2010). The drivers of $_pCO_2$ may also be abiotic, such as sunlight-related photochemical reactions (Bertilsson & Tranvik, 1998), wind-related water column mixing (Czikowsky et al., 2018), and discharge-related direct CO_2 inflow to the lake from rain events, surface water and groundwater (Jonsson et al., 2007).

When considering the variation of $_pCO_2$ at longer, multi-seasonal time scales, other factors become important. As biological processes, both photosynthesis and respiration are directly affected by hydrologically driven inputs of dissolved or total OC (DOC/TOC) (Jonsson et al., 2003; Weyhenmeyer et al., 2012a; Lapierre & del Giorgio, 2012), inorganic C from the catchment (Weyhenmeyer et al., 2015; Wilkinson et al., 2016) and factors such as the temperature and nutrient status of the water column (Dodds & Cole 2007). Any given lake will function as either a net source of CO_2 to the atmosphere (when the water is supersaturated with CO_2 with respect to the atmosphere), or as a sink of CO_2 from the atmosphere (when the water is CO_2 under-saturated) (Tranvik et al., 2009) depending on the relative rates of these biological processes within each system. Lake C inputs are sensitive to regional climate variation such as variations in precipitation (Rantakari and Kortelainen, 2005; Marotta et al., 2010), temperature (Staehr & Sand-Jensen, 2007) and also to individual lake and catchment-related properties such as area,

morphometry, productivity and land use (Roehm et al., 2009; Staehr et al., 2012; Maberly et al., 2013; Raymond et al., 2013; Ferland et al., 2014).

High resolution $_pCO_2$ datasets have been used to explore lake and reservoir C processing dynamics in boreal (Laas et al., 2016; Denfeld et al., 2018), temperate (Morales-Pineda et al., 2014) and tropical (Junger et al., 2019) climates. To the best of our knowledge there are no similar published studies for peatland lakes within temperate maritime climate zones. Lough Feeagh's geographic setting within a peatland-dominated catchment and temperate maritime climate zone on the west coast of Ireland make it an interesting case-study from a carbon dynamics perspective. Previous studies suggest that OC is stored in abundance in the surrounding catchment soils and continuously supplied to the lake, driven mainly by the catchment's hydrologic regime (e.g. Ryder et al., 2016; Doyle et al., 2019). Within-lake OC processing is not disrupted during the winter as the lake does not ice-over due to the relatively warm winters experienced locally. We presume therefore, in contrast to boreal or temperate - continental climate lakes, that there is no major OC release in the spring during an ice-out or turnover event. The almost continual tracking of Atlantic weather-fronts over the region, bringing cloud and wind, generally ensures a relatively weak stratification during the summer months and a mixed water column for the rest of the year (de Eyto et al., 2016; Andersen et al., 2020). The turbulence of the lake, in combination with the relatively cool summers are also in direct contrast to many studied boreal and temperate-continental lake systems where calm conditions and hot summers predominate.

Using data from an *in-situ* CO_2 sensor deployed in this temperate humic lake in the maritime temperate region of Europe, we investigated temporal changes in $_pCO_2$ in the lake surface water over one year. We assessed the relationships between these changes and a range of potential environmental drivers of $_pCO_2$ variability.

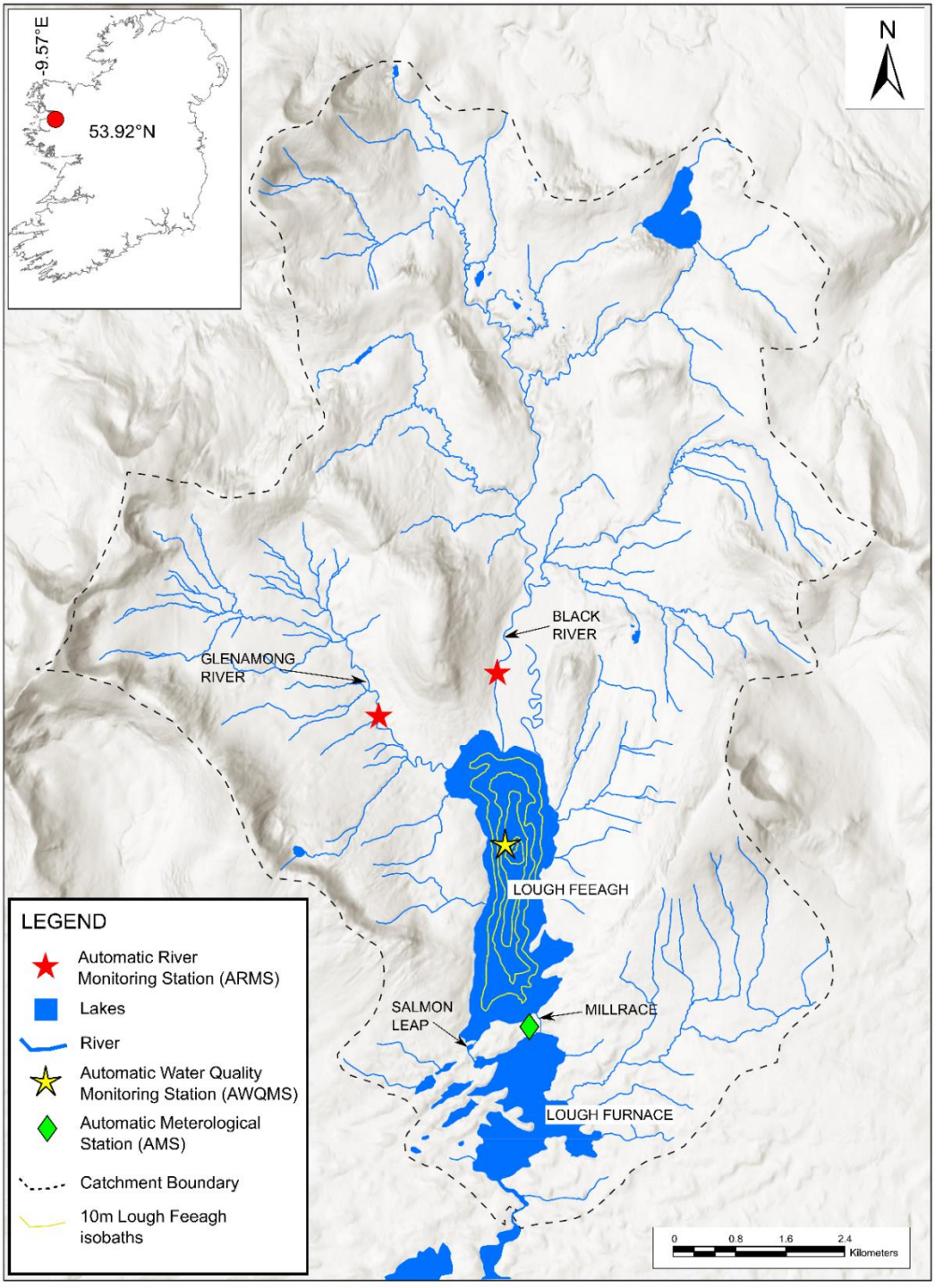

Figure 4.1 Geographical position of Lough Feeagh and the location of the Automatic Meteorological Station and lake and river monitoring stations. Flow direction is from north to south.

Our aims were (1) to investigate the temporal variation in $_pCO_2$ between February and November 2017, a 10-month study period; (2) to determine the principal environmental drivers of $_pCO_2$ in the system; and (3) to calculate the magnitude of CO_2 evasion from the lake over the study period. We hypothesised that the lake was net heterotrophic and supersaturated with CO_2 due to high year-round inputs of coloured allochthonous OC from the catchment which would both stimulate ecosystem respiration and restrict net ecosystem production. We also hypothesised that $_pCO_2$ in the lake would peak during the late summer and early autumn, responding to the regular, strong, annual peak in DOC concentrations observed in the main catchment streams entering the lake in previous studies (Ryder et al., 2014; Doyle et al., 2019; Jennings et al., 2020).

4.3 Materials and Methods

4.3.1 The Study Site

The Burrishoole, research station, run by the Irish Marine Institute, is a centre for the study of diadromous aquatic species such as salmon, sea trout, and eel in the North Atlantic (e.g. McGinnity et al., 2009; de Eyto et al., 2016a; Poole et al., 2018). As a key element of this research, the Marine Institute maintains a network of high resolution instrumentation in the catchment in tandem with a program of long-term ecological monitoring (http://burrishoole.marine.ie). Essential to the present study was the use of data from this network of high resolution monitoring equipment, especially the automatic biogeochemical sensors deployed throughout the catchment. The multi-seasonal and high-frequency data sets captured during the study were critical for assessing $_pCO_2$ dynamics and examining the processes underlying them (Hanson et al., 2006).

Lough Feeagh (53°56′44″ N, 9°34′40″ W, Figure 4.1) is a freshwater lake located at the base of the Burrishoole catchment (~ 84 km^2). It has an area of 3.92 km^2 and mean and maximum depths of 14.5 m and 46 m respectively (Table 4.1). The two main inflows into Lough Feeagh are the Black and the Glenamong Rivers which supply the lake with most of its water. There are two short outflows from the lake, named the Millrace and Salmon Leap. Both channels are approximately 200 m in length and drop approximately 10m in elevation over this distance. Both outflows discharge to Lough Furnace, a tidal lagoon to the south of Feeagh, before entering the sea through a tidal estuarine river. The catchment displays a flashy hydrological regime, mainly due to the temperate maritime climate and subsequent high temporal variability of rainfall. Frontal Atlantic rain systems continually cross the catchment and on occasion, extreme storm events may cause dramatic flooding (de Eyto et al., 2016; Kelly et al., 2020). The Newport Met Éireann automatic weather station, located

between Lough Feeagh and Lough Furnace (Figure 4.1) and operating since 2005, recorded an average annual rainfall of 1533 mm $year^{-1}$ (± 182 mm SD) between 2005 and 2017. Long-term average monthly rainfall at the station indicates that the driest month is generally April (mean monthly total: 85 mm) while December is the wettest month of the year (mean monthly total: 168 mm). The temperate maritime climate in the region manifests in both mild winters and summers with mean a December-February 2005-2018 air temperature of 6.0 °C and a mean June-August 2005-2018 air temperature of 14.3 °C (Met Éireann - www.met.ie). The area also experiences a regular diurnal sea breeze with mean wind speeds of approximately 5 m s^{-1} (Kelly et al., 2018).

The Environmental Protection Agency (2005) has defined twelve categories of Irish lakes using three separate factors: alkalinity, depth and size. Under this system, Lough Feeagh is classified as low alkalinity (< 20 mg l^{-1} $CaCO_3$), deep (> 4m average depth and >12m maximum depth) and large (> 0.5 km^2). The lake is considered oligotrophic (Table 4.1), with low productivity associated with low phosphorus and nitrogen, and humic, with highly coloured water resulting in a mean Secchi disk depth of 1.7 m (e.g. Caldero et al., 2020). The two main rivers supplying the lake, the Black and the Glenamong rivers, have alkalinities in the order of 15–20 and -2.7 to 7.5 mg l^{-1} $CaCO_3$ respectively. These ranges (< 35 mg l^{-1} $CaCO_3$) categorise the rivers as being of soft water chemistry and the catchment geology bedrock as being effectively 100% siliceous (EPA 2005).

Table 4.1 Location and General Characteristics of Lough Feeagh & the Burrishoole Catchment

General Characteristics of Lough Feeagh		**Characteristics of Burrishoole Catchment**		
Latitude / Longitude	53° 56' 44" N 9° 34' 40"W	Latitude	53°55′N	
		Longitude	9°34′W	
Lake Area (km^2)	3.92	Area (km^2)	18.2	
Maximum Depth (m), Mean Depth (m), Mean Volume (m^3)	46, 14.5, 5.9 × 10^7	Geology	Quartzite and schist, also interbedded volcanics, marble, dolomite, and schist	
Mixing type	Monomictic	Blanket Peat (%)	52	
Mean Retention Time (yr)	0.47	Forestry (%)	15	
Chl a (µg l-1)	0.52 − 2.01	Minimum Altitude (m)	8	
Secchi depth (m)	1.0 − 2.2	Maximum Altitude (m)	710	
Water Characteristics of L. Feeagh		**Water Characteristics of Burrishoole Rivers**		
			Black	**Glenamong**
pH range*	6.5 − 7.4	pH range*	4.0 – 8.0	3.5 – 7.3
Colour (mg PtCo l-1)	62 − 114	Colour (mg PtCo l-1)	15 – 257	24 – 211
DOC (mg l-1)	7.7 − 11.7	DOC (mg l-1)	2.3 – 25.8	3.6 – 21.5
Total Phosphorous (µg l-1)	4.8 − 10.1	-	-	-
Total Nitrogen (mg l-1)	0.13 − 0.78	-	-	-
Mean discharge (m^3 s^{-1})	4.37	Mean discharge (m^3 s^{-1})	3.56	0.67
Water temperature range (°C)	5.3 – 18.8	Water temperature range (°C)	-0.05–26	-0.03-26

The land cover in the Burrishoole catchment was reported by Doyle et al. (2019), from a study using CORINE data, as comprising 52% blanket peat, 15% forestry and the remaining 33% being made up of transitional woodland and scrub, natural grasslands and agricultural land. The catchment topsoils are predominantly humic, with blanket peatlands covering upland slopes and high-carbon content soils including poorly-drained gleys, podzols and alluvial soils on the valley floors (May & Place, 2005).

4.3.2 pCO2, Meteorological and Ancillary Measurements

An Automatic Water Quality Monitoring System (AWQMS) on Lough Feeagh, positioned over the deepest point of the lake (46 m), collects and transmits high frequency sensor information to the Marine Institute's research station (Figure 4.1) via GPRS (http://burrishoole.marine.ie). $_pCO_2$ in the lake water was measured at the AWQMS every 15 minutes using a membrane covered optical carbon dioxide sensor (AMT Analysenmesstechnik GmbH, Joachim-Jungius-Strasse 9D-18059 Rostock, Germany) suspended at one-meter depth. The sensor was deployed on 16th February 2017 until 05th December 2017 and ran continually except for three data-gaps of 95, 216 and 77 hours in August, October and November, respectively. A multi-parameter sonde (Hydrolab DS5,

OTT, Kempton, Germany), deployed on the AWQMS at 0.9 m below the water surface, measured pH, specific conductivity (mS cm^{-1}), temperature (°C), and dissolved oxygen (DO) (mg L^{-1} and %) every 2 minutes for the same period. Vertical temperature profiles below the AWQMS were measured during the study period using a chain of 12 platinum resistance thermistors (PRTs: Lab facility PT100 1/10DIN 4 wire sensor, www.labfacility.co.uk, Labfacility Ltd., Bognor Regis, UK). The chain spanned the full water column with sensors at depth intervals of 2.5, 5, 8, 11, 14, 16, 18, 20, 22, 27, 32, 42 m, all recording every two minutes. Sensors on the AWQMS were cleaned fortnightly, and DO on the multi-parameter sonde was calibrated once per month.

An array of instruments on the surface platform of the AWQMS measured meteorological parameters. Wind speed and direction were measured with Vector Instruments A100L2-WR and W200-P-WR respectively (www.windspeed.co.uk, Windpeed Ltd., Rhyl, North Wales, UK), and photosynthetically active radiation (PAR) was estimated using a pyranometer (Kipp & Zonen CMP6 www.kippzonen.com). Pyranometer data (W m^{-2}) was converted to PAR by multiplying by 0.45 (45% of the light measured by a pyranometer falls into the PAR region) and converting to µmol m^{-2} s^{-1} (1 W m^{-2} = 4.6 µmol m^{-2} s^{-1}). Lake water level (m) was recorded every 15 min using an OTT Hydrometry Orpheus Mini water level logger (https://www.ott.com). Air temperature (°C), air pressure (hPa), solar radiation (kWh m^{-2}), relative humidity (%), daily rainfall amount (mm) and mean soil temperature (°C) measurements were available from an automatic meteorological weather station (AWS), operated by Met Éireann (www.met.ie) and situated at the Marine Institute's research station (Figure 4.1).

In addition to the data described above, manual river water samples were taken at weekly intervals from the two main rivers entering the lake, the Black and Glenamong, and one river exiting the lake, the Millrace. These were analysed for true water colour (mg PtCo L^{-1}) within hours of sampling using a HACH Dr 2000 spectrophotometer at 455 nm on water filtered through Whatman GF/C filters (pore size: ca. 1.22 µm). Wavelength accuracy was ± 2 nm from 400 to 700 nm. DOC (mg L^{-1}) concentration was estimated from water colour concentration (Pt Co mg L^{-1}) using a linear model developed between water colour and DOC from the Glenamong River between April 2010 and September 2011 (Ryder, 2015). There was a strong linear relationship between colour and DOC (r^2 = 0.88, $p \leq 0.001$, n = 366), indicating that water colour measurements are a good proxy for DOC concentrations in the catchment rivers.

4.3.3 Data collation and analysis

Continuous *in situ* measurements of surface water CO_2 concentrations were used to estimate CO_2 emission (F-CO_2, mmol m^{-2} d^{-1}) from the lake by applying the following equation (Cole & Caraco 1998):

$$F\text{-}CO_2 = k\,[CO_{2\ water} - CO_{2\ sat}] \quad (1)$$

where k is the gas transfer velocity (cm h^{-1}), $CO_{2\ water}$ is the CO_2 concentration in the water (µatm L^{-1}); and $CO_{2\ sat}$ is the CO_2 concentration at equilibrium with the atmosphere, calculated from Henry's constant (Weiss, 1974). For $CO_{2\ sat}$ a constant ${}_pCO_2$ in equilibrium with the atmosphere of 400 µatm was assumed (http://co2now.org/). The gas transfer velocity k was estimated from k600 values derived from wind speed based on the following formula as described by Cole & Caraco (1998);

$$k_{600} = 2.07 + 0.215\ U_{10}^{\ 1.7} \quad (2)$$

where k_{600} is the gas transfer velocity at 20 °C (cm h^{-1}) and U_{10} is the wind speed over the lake at 10m height (ms^{-1}). A temperature-dependent Schmidt number (defined as the kinematic viscosity of water divided by diffusion coefficient of the gas) for CO_2 was calculated according to Jähne et al., (1987) using the following equation;

$$Sc = 1841 \times e^{(-0.0549 \times t)} \quad (3)$$

where Sc is the Schmidt number and t is the water temperature in °C. The Schmidt number was used to recalculate k_{600} (Wanninkhof, 1992) using the following equation;

$$k = k_{600} / (600 / Sc)^{-0.66} \quad (4)$$

In addition to the Cole & Caraco (1998) model used to estimate gas transfer velocity (k), we also report CO_2 emissions using an alternative bilinear approximation model described by Crusius & Wanninkhof (2003).

Raw data from the instruments on the AWQMS and the water level recorders were visually checked, cleaned and adjusted where necessary by referring to the Marine Institute's maintenance logs and using Hydras 3 v10.1software (www.ott.com/products/software-solutions/ott-hydras-3-basic). Any outliers identified in the data were removed, drift that could be attributed to biofouling of sensors between

calibration periods (particularly in the DO dataset) was corrected using the sliding correction feature in Hydras 3. Indices of lake physical structure (Schmidt stability and Brunt-Väisälä buoyancy frequency) were calculated using the r Lake Analyzer package 1.11.4.1 (Winslow et al., 2014) through R 3.6.2 (R Core Team, 2019). Schmidt Stability was calculated as defined by Schmidt (1928) as the amount of work required to transform a waterbody to a uniform density. The Brunt–Väisälä frequency, or simply buoyancy frequency, measures fluid stability against vertical displacements such as those caused by convection (Gilmour, 1973).

An estimate of the autochthonous C contribution was calculated using primary productivity in the lake. Daily estimates of Gross Primary Production (GPP), Respiration (R), and Net Ecosystem Production (NEP) were made using the R Lake Metabolizer package (Winslow et al., 2016), applying the maximum likelihood estimate method, a process-error-only model with parameters fitted via maximum likelihood estimation (Solomon et al., 2013). Lake Metabolizer was run with a 2-minute time step over the study period where data (DO, water temperature, PAR, and wind speed) were available, producing estimates of daily GPP and R (O_2 mg m^{-2} d^{-1}), and NEP (GPP − R). Negative values of GPP and positive values of R were removed from the dataset on the assumption that the model fit was poor or that some other process not included in the model was acting that day (e.g., physical entrainment of O_2 from other depths).

Comparing the lake CO_2 flux with NEP on a daily scale was used to provide insight into the contribution of aerobic in-lake metabolism to the net CO_2 efflux. Daily NEP values (O_2 mg l^{-1} d^{-1}) were converted to aerial units (O_2 mg m^{-2} d^{-1}) and converted to CO_2 assuming a respiratory quotient of 1. The daily CO_2 amounts were summed over the study period and the estimated mass of C is reported.

The DOC load to the lake over the study period was calculated for the Black and Glenamong sub-catchments by multiplying the calculated river discharge volume for each week by the weekly estimated DOC concentration using water colour data converted to DOC concentration, and summing the totals.

4.3.4 Predictors of pCO2 dynamics

To identify the principal explanatory drivers of $_pCO_2$ in the lake, a generalised additive mixed model (GAMM), with cubic regression smoothing splines and q Gaussian distributions, was developed using the mgcv package (Wood, 2006) in R, version 3.6.2, (R Core Team, 2019). Variance inflation factors (VIFs) greater than 3 were used to

exclude closely related variables (Montgomery & Peck, 1992; Zuur et al., 2009). All models were tested for violations of the assumptions of homogeneity, independence and normality, and correlation or variance structures were included as appropriate using the protocol described in Zuur et al., (2009). The response variable was the lake $_pCO_2$ data. Potential explanatory variables included a set of climatic, hydrological and lake metabolic data. As water colour was available at a weekly time-step only, weekly means were calculated for all other variables for each sampling week. The climate variables included were mean air temperature (◦C), total daily precipitation (mm day^{-1}), wind speed (m s^{-1}), relative humidity (%), air pressure (hPa) and solar irradiance using a pyranometer (W m^{-2}). Hydrological and metabolic explanatory variables included lake level (cm), conductivity (mS cm^{-1}), dissolved oxygen (mg l^{-1}), pH, chlorophyll *a* (RFU), colour in the Black River (mg L^{-1} PtCO), Gross Primary Production (GPP-mg O^2 L^{-1} d^{-1}), Respiration (R-mg O^2 L^{-1} d^{-1}), Net Ecosystem Production (NEP-mg O^2 L^{-1} d^{-1}), Schmidt Stability, and Thermocline depth (m).

The original 15-minute $_pCO_2$ dataset was converted to a mean hourly time-step and examined using seasonal trend decomposition using loess (STL) (Cleveland et al., 1990) in R (R Core Team, 2019), however, no periodicity in the dataset was uncovered. A manual decomposition technique, previously described by Morales-Pineda et al., (2014) was applied to the hourly $_pCO_2$ dataset, based on two frequencies that were assumed, a priori, to show maximum lake $_pCO_2$ variation. The two chosen frequencies were 24 hours and 48 hours, the former frequency highlighting the variation in $_pCO_2$ due to photosynthesis and the latter frequency highlighting $_pCO_2$ variation caused by weather events. Storm event durations in the Burrishoole catchment average 54.0 hours during the winter and 46.4 hours during the summer (Andersen et al.,, 2020), which was rounded to 48 hours to encompass the entire year. The daily component ($_pCO_2$ ^{daily}) was calculated by removing the 24-hour moving average (24 h $_{avg}$) from the hourly $_pCO_2$ dataset (equation 3). The 48-hour component ($_pCO_2$ ^{48hr}) was calculated by removing the 48-hour moving average (48 h $_{avg}$) from the 24-hour moving average (equation 4). The remaining, seasonal component ($_pCO_2$ ^{seasonal}) was calculated by removing the $_pCO_2$ time series data average ($_pCO_{2\ avg}$) from the 48-hour moving average (equation 5). These equations are expressed below:

$$ {}_{p}CO_2{}^{\text{daily}} = {}_{p}CO_2 - 24\ \text{h}_{\text{avg}} \quad (3) $$

$$ {}_{p}CO_2{}^{\text{48hr}} = 24\ \text{h}_{\text{avg}} - 48\ \text{h}_{\text{avg}} \quad (4) $$

$$ {}_{p}CO_2{}^{\text{seasonal}} = 48\ \text{h}_{\text{avg}} - {}_{p}CO_{2\ \text{avg}} \quad (5) $$

The hourly ${}_{p}CO_2$ dataset can be described mathematically as:

$$ {}_{p}CO_2 = {}_{p}CO_{2\ \text{avg}} + {}_{p}CO_2{}^{\text{seasonal}} + {}_{p}CO_2{}^{\text{48hr}} + {}_{p}CO_2{}^{\text{daily}} \quad (6) $$

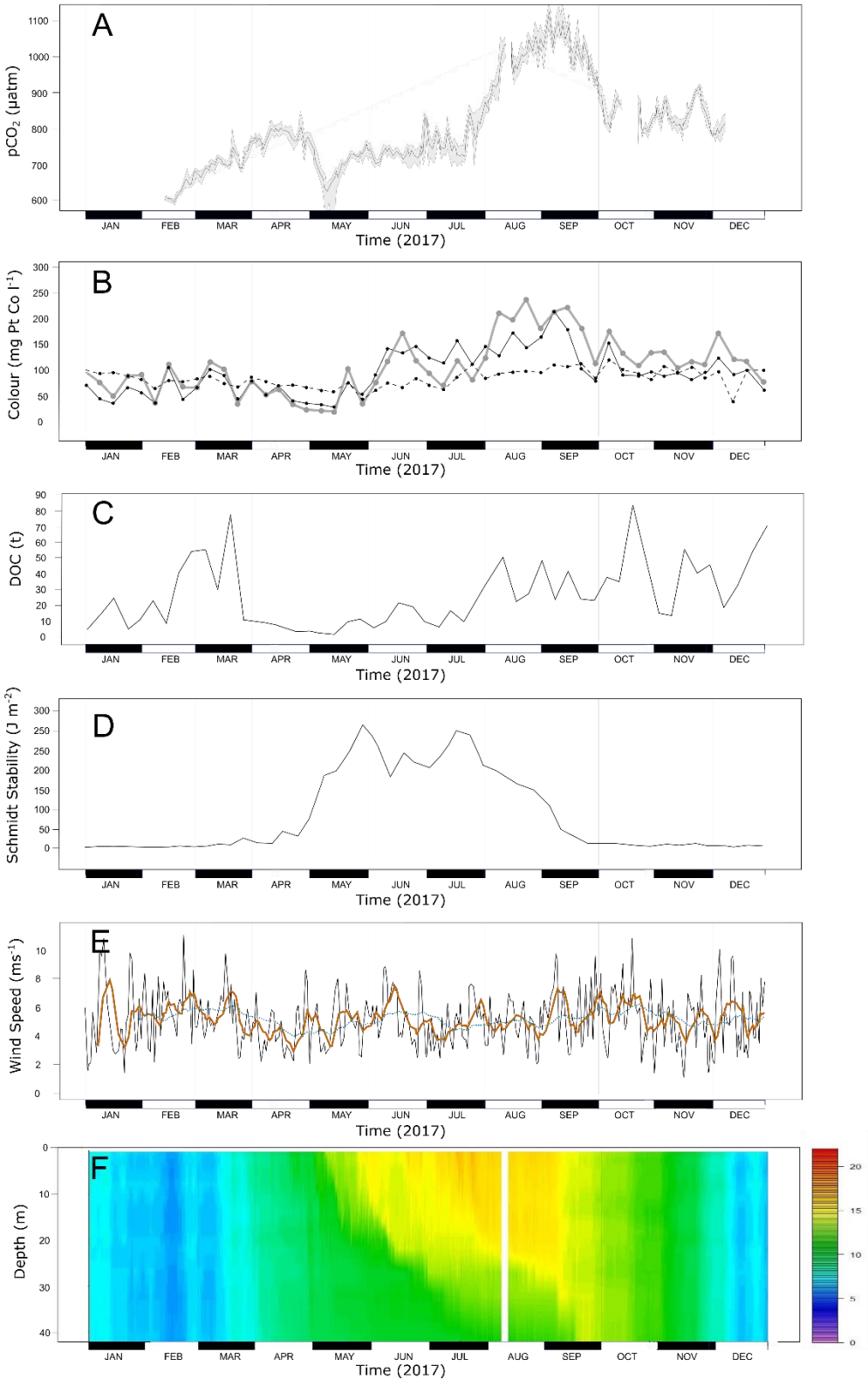

Figure 4.2. A = Average daily $_pCO_2$ (black line) within daily maximum and minimum (shaded area), B = River inflow and outflow colour concentrations (black line = Black River, grey line = Glenamong River, dashed line = Millrace outflow), C = Catchment OC load in tones DOC to the lake. D = Schmidt Stability, E = Average daily wind speed (black line), average weekly wind speed (orange line) and average monthly wind speed (dashed blue line), F = Lake temperature profile.

4.4 Results

4.4.1 Data Overview

From a possible total of 43,020 separate measurements, 39,456 valid $_pCO_2$ measurements at 15-minute resolution were taken during the 303-day study period (11th February 2017 to 11th December 2017). Data gaps accounted for 8.3% of the total data set, with three main gaps occurring between 10th and 14th August (95 hours), 11th and 20th October (216 hours) and between 19th and 22nd November (77 hours). $_pCO_2$ ranged from a minimum of 491 µatm, recorded on 10th May to a maximum of 1,169 µatm recorded on the 10th September. The average $_pCO_2$ for the whole study period (± SD) was 803 ± 122 µatm and the lake was supersaturated throughout the study period. The $_pCO_2$ had a general seasonal cycle, with lower values in earlier part of the record, reaching a maximum value in the autumn. Concentrations climbed steadily during the first three months, from around 600 µatm in early February, reaching concentrations of just over 800 µatm in the latter part of April (Figure 4.2A). Concentrations then declined sharply for three weeks, with concentrations just above 500 µatm being recorded in the second week of May. From this low point, concentrations climbed and plateaued at around 750 µatm until the end of July. They then climbed steadily, reaching a maximum in early September with values of over 1,100 µatm. Thereafter, there was a decline to around 800 µatm in late November.

Mean water colour concentrations in the two rivers entering the lake, the Black and the Glenamong, were 109 (± 54 SD, n = 44) and 96 (± 43 SD, n = 44) mg PtCo L^{-1} respectively (Figure 4.2B). Maximum and minimum values of 236 and 19 mg Pt Co L^{-1} were recorded in the Black, while those for the Glenamong were 216 and 31 mg Pt Co L^{-1}. Temporally, the colour concentrations in both inflowing rivers were broadly synchronous over the study period. From February until the beginning of May, colour concentrations in the Black and Glenamong averaged 71 and 63 Pt Co L^{-1}, respectively. Minimum colour concentrations for both inflowing rivers during the study period were recorded in early May which also corresponded with a minimum lake level recorded at this time. Colour concentrations recovered rapidly from this low point in late spring, climbing to the maxima recorded for the two rivers, in mid to late August (Figure 4.2B).

The Schmidt Stability of Lough Feeagh began to climb in early April and reached a peak of approximately 250 J m^{-2} at the start of June. Schmidt Stability values fell back and did not peak again until mid-July. From this point, values fell until around mid-September when the lake was fully mixed and Schmidt Stability values remained at 0 for the

remainder of the study period (Figure 4.2C). Greater peaks of wind-speed were noticeable during January and February and also during September. A calm period also occurred during late April and early May and coincided with the onset of thermal stratification (Figure 4.2D).

Water temperature at the lake surface ranged between 5.3 ℃ (27th February) and 18.8 ℃ (17th July) with a mean water temperature of 12.3 ℃ ± 3.3 SD over the study period. Temperature averaged just over 16 ℃ during August and declined steadily to temperatures around 7.7 ℃ at the end of the study period. The water column in the lake was mixed until 19th of April when thermal stratification commenced. The lake was thermally stratified until 20th September when the water column began to mix following a series of storm events (Figure 4.2E).

The water level in the lake fluctuated considerably over the study period, responding to periods of high and low rainfall in the catchment. A maximum level of 1.19 m was recorded on 18th March and a minimum level of 0.18 m was recorded on the 12th May. The mean lake level was 0.47 m (± 0.18 SD) and the overall level of the lake varied by 1.01 m over the study period (Figure 4.5B). An estimated total DOC load to the lake of 1182 t C during the study period (11th February to the 11th December) was calculated for the Black and Glenamong sub-catchments.

Estimated carbon emission as atmospheric CO_2 from the lake surface varied depending on the model applied. Using the Cole and Caraco (1998) model, emissions ranged from 2.8 to 195.0 mmol C m^{-2} d^{-1} (mean = 28.1 ± 15.5 mmol C m^{-2} d^{-1}), and using the model proposed by Crusius and Wanninkhof (2003) emissions ranged from 0.5 to 83.1 mmol C m^{-2} d^{-1} (mean = 16.5 ± 8.2 mmol C m^{-2} d^{-1}) (Figure 4.3A). The total estimated carbon emission over the study period from the lake was 369.6 t C using the Cole and Caraco (1998) and 216.9 t C using the Crusius and Wanninkhof (2003) models. The estimated emissions, therefore, represent 31.3% or 18.3% of the calculated DOC load entering the lake depending on the model applied.

NEP (GPP−R) was found to be predominantly negative, which is in agreement with the almost continuous O_2 under-saturation observed throughout the study period. Daily NEP values (mmol O_2 m^{2-1} d^{-1}) (Figure 4.3B), converted to CO_2 assuming a respiratory quotient of 1, and summed over the study period, were estimated to amount to 67.92 t C. This is considered to be the contribution of aerobic in-lake metabolism to the net CO_2

efflux and equates to between 18.3 and 31.3 % of the total C emission to the atmosphere during the study period, depending on the model applied.

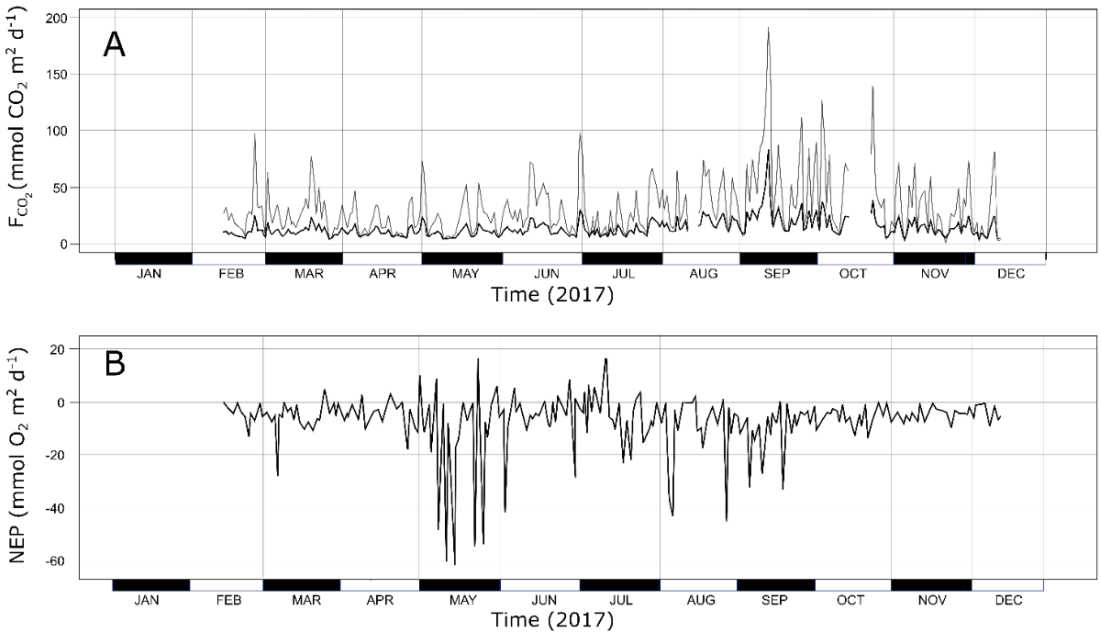

Figure 4.3 A = Water to air fluxes of CO_2 from Lough Feeagh during the study period. The dark black line corresponds to Crusius and Wanninkhof (2003) bilinear relationship and the grey line corresponds to Cole and Caraco (1998) power relationship, the fluxes equate to 217 and 370 t C respectively. B = Net Ecosystem Production (NEP) during the study period. Daily NEP converted to CO_2, summed over the study period and assuming a respiratory quotient of 1, were estimated to amount to 67.92 t C.

4.4.2 Predictors of pCO2 dynamics

The optimal GAMM for $_pCO_2$ in Lough Feeagh included two significant smoothers, colour concentrations in the Black River and Schmidt stability of the water column in Lough Feeagh. This model explained 67.8 % of the variance in $_pCO_2$ over the study period (Table 4.2). The smoother for colour concentration in the Black River indicated a linear, positive relationship with $_pCO_2$, showing that in general, the pattern of $_pCO_2$ follows the inflowing water colour concentrations over the course of the study period (Figure 4.4A). The relationship between Schmidt stability and $_pCO_2$ in the lake was more complicated, with the smoother showing a wave-like pattern (Figure 4.4B). The pattern indicated that there was a positive relationship between $_pCO_2$ and Schmidt stability when the lake was fully mixed and Schmidt stability values were close to zero. However, as Schmidt stability values increased above approximately 100 J m^{-2} the relationship with $_pCO_2$ became

negative. At Schmidt stability values above 250 J m^{-2} the relationship between the two variables became positive again. An alternative model, using solely colour concentration in the Black River *versus* $_pCO_2$, results in an r^2 value of 0.60, indicating that this explanatory variable explains approximately 60 % of the variance in the optimal model and confirms that colour in the Black River, and by proxy DOC from the surrounding catchment, is most important driver of $_pCO_2$ in the model.

Table 4.2 Results of generalised additive mixed model (GAMM) applied to $_pCO_2$ in Lough Feeagh over the study period in 2017. The (s) refers to the scaled smoother for each explanatory variable. Black_col refers to colour concentrations in the Black River and Schmidt.stability refers to the Schmidt stability of Lough Feeagh during the study period.

$_pCO_2$ – Black River n = 44			R-sq. (adj) = 0.678	Scale est. = 4276.2
	Estimate	Standard error	t-value	Pr (>|t|)
Intercept	804.131	9.972	80.64	$< 2.0 \times 10^{-16}$
Approximate significance of smooth terms:	edf	Ref.df	F	p - value
s(black_col)	1.000	1.000	61.801	1.47×10^{-10}
s(Schmidt.stability)	3.751	3.751	3.895	0.0133

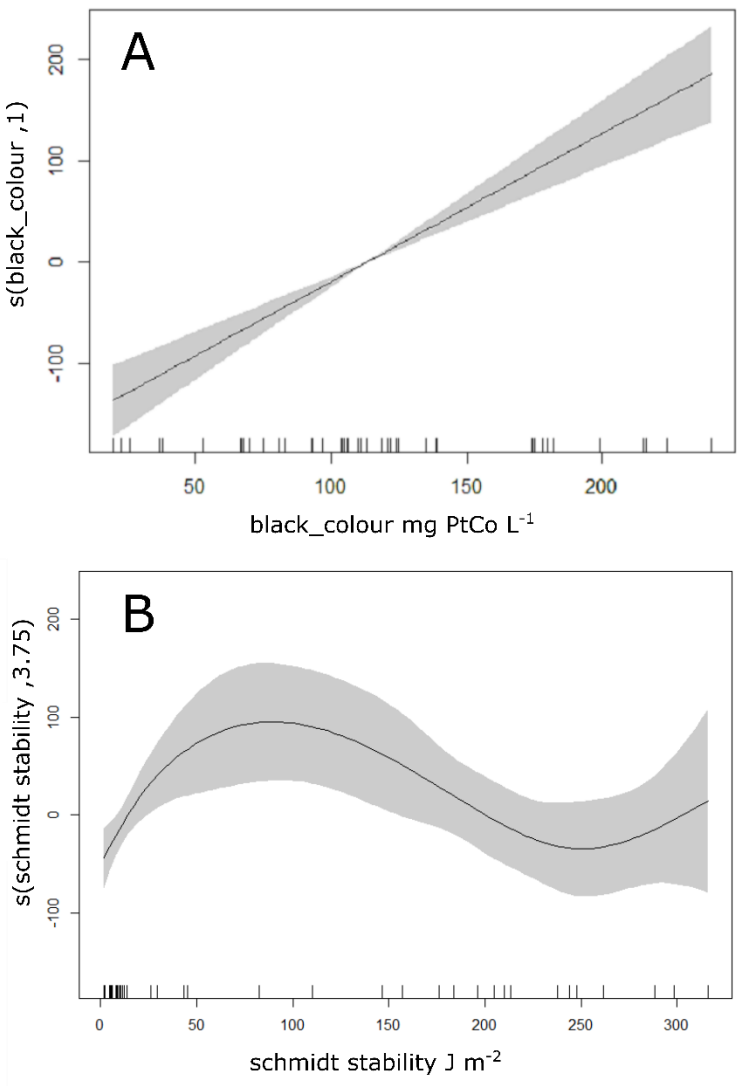

Figure 4.4 Selected smoothers for the contribution of explanatory variables for the optimal GAMM explaining $_pCO_2$ in the Lough Feeagh: (A) colour concentrations in the Black River, (B) Schmidt explanatory variable with the variable name followed by the estimated degrees of freedom (edf) within the parentheses stability in Lough Feeagh. The solid line is the smoother, and the shaded area shows the 95 % confidence bands. The y axis units are the scaled smoother (s) for each

4.4.3 pCO2 Time-Series Decomposition

The mean hourly $_pCO_2$ signal was decomposed into three temporal components, a 24-hour or daily component $_pCO_2^{daily}$ (Figure 4.5A), a 48-hour component $_pCO_2^{48hr}$ (Figure 4.5B), and a seasonal component, $_pCO_2^{seasonal}$ (Figure 4.5C). Following careful visual inspection of the $_pCO_2^{daily}$ data, no strong, regular pattern of diel variation was observed (suggesting variation in $_pCO_2$ due to photosynthesis), except during one 4-week long period between April and May. This period is shaded and marked as S1 in Figure 4.5A.

During this period, a strong and regular trend of diel $_pCO_2^{daily}$ variation is apparent in the time-series, and is synchronous with an extended period of sunny and calm weather (i.e. high pyranometer values and wind speeds below about 4 m s^{-1}). Large dips and spikes in the $_pCO_2^{daily}$ component can be observed from the end of June to around mid-August, however these variations appear to be random in time and when viewed alongside the wind and lake-level data, they appear to be related to individual storm events.

The duration of the 48-hour component was chosen to highlight how storm events might affect $_pCO_2$ variability. Many of the major dips and spikes in the $_pCO_2^{48hr}$ data appeared to be synchronous with peaks of wind speed and abrupt rises in lake level following heavy rain, and are highlighted as shaded areas (Figure 4.5B). The seasonal component, $_pCO_2^{seasonal}$ shows the $_pCO_2$ variability when both the 24-hour and 48-hour components are removed from the mean hourly $_pCO_2$ dataset (Figure 4.5C).

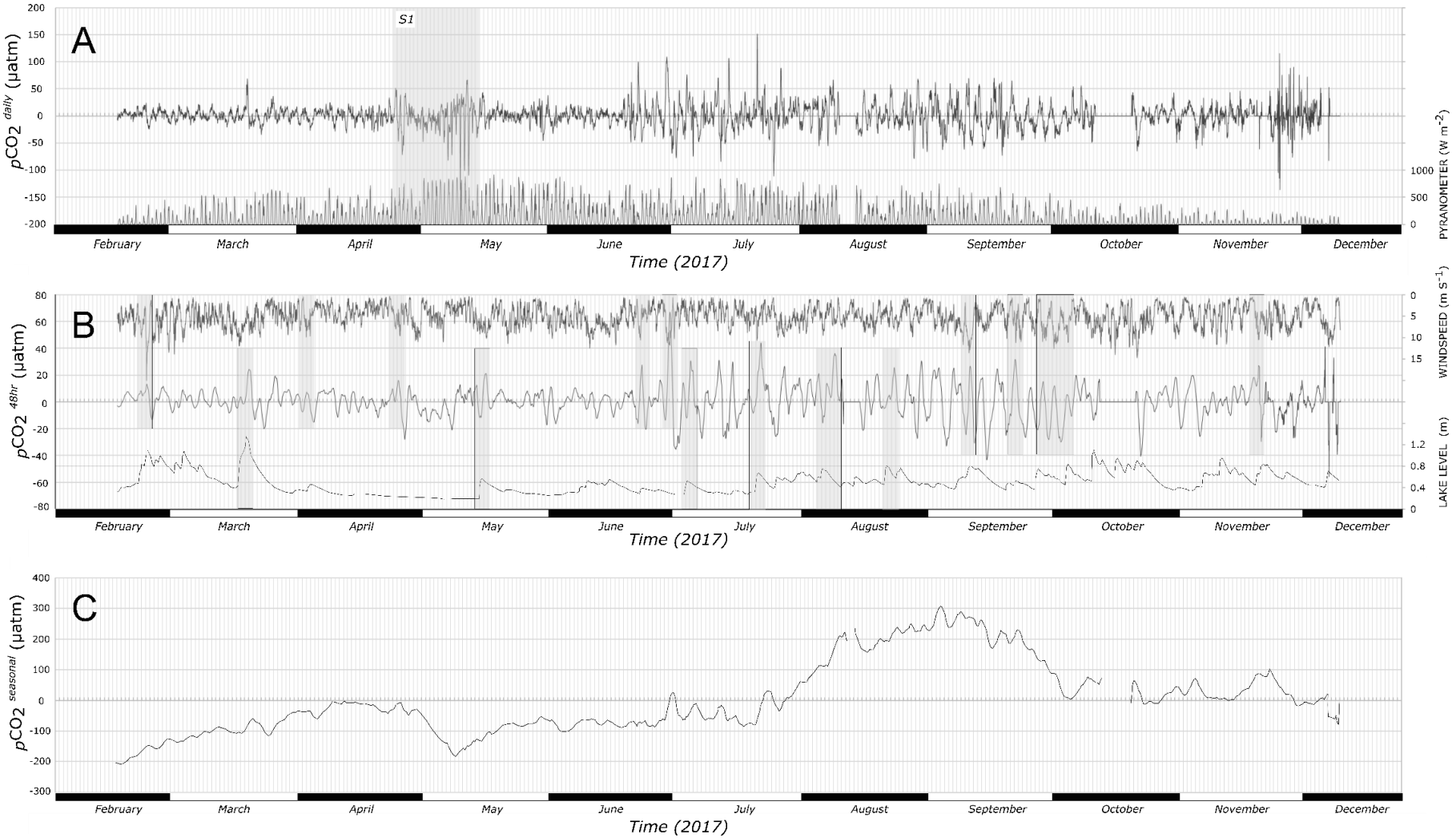

Figure 4.5. Decomposition of the original $_pCO_2$ signal to, Panel A = Daily $_pCO_2$ component ($_pCO_2^{daily}$) and Pyranometer (lower right axis). Shaded section (S1) highlights a period where diurnal periodicity is evident. Panel B = 48 hour $_pCO_2$ component ($_pCO_2^{48hr}$) with Wind Speed (upper right axis) and Lake Level (lower right axis). Areas shaded highlight peaks in $_pCO_2^{48hr}$ with concurrent peaks in either Wind Speed or Lake Level. Panel C = Seasonal $_pCO_2$ component ($_pCO_2^{seasonal}$). Note – Shaded areas were identified by visual examination. Power for $_pCO_2$ component is at the seasonal scale (Fig. 4.5C), followed by the daily scale (Fig. 4.5A) and finally the intermediate scale (Fig. 4.5B).

4.5 Discussion

Freshwater aquatic systems, including lakes, are recognised as important regulators of carbon transport and transformation along the continuum of inland waters (Cole et al., 2007; Tranvik et al., 2009; Raymond et al., 2013; Engel et al., 2019). It has also been shown that many are net contributors of C to the atmosphere (Cole et al., 1994; Bastviken et al., 2011). The $_pCO_2$ levels that we report here confirmed that Lough Feeagh was continuously emitting CO_2 during the course of the study. More interesting, however, was the temporal pattern of $_pCO_2$ in Lough Feeagh, which had a peak in late summer /early autumn with levels then dropping again towards winter. To our knowledge, this pattern has not been reported from other climate zones where data were available over the annual cycle. For example, in Boreal climate zones, $_pCO_2$ has been observed to generally peak twice during the year, once following ice melt when CO_2 is released having built up beneath the ice during the winter (Ducharme-Riel et al., 2015), and again in autumn when lake mixing brings CO_2 rich bottom water to the surface (Ojala et al., 2011; Weyhenmeyer, et al., 2012b; Finlay et al., 2019). Ice formation on Lough Feeagh is an extremely rare and brief occurrence due to the temperate maritime climate of the region and the hydrological pattern therefore differs considerably from boreal sites, with highest inflows throughout the autumn-winter and into early spring.

Surface water $_pCO_2$ in Lough Feeagh did not fall below 491 µatm at any time during the measurement cycle. At 803 µatm, mean lake $_pCO_2$ was approximately double that of atmospheric CO_2 levels in 2017 (http://co2now.org/). Surprisingly, given the humic status of the lake, the mean $_pCO_2$ values from Lough Feeagh were, however, on the lower end of the scale when compared with directly measured $_pCO_2$ values reported from other climate zones. In a study of temporal dynamics of $_pCO_2$ in two Mediterranean reservoirs, for example, mean concentrations of 695 and 1529 µatm were reported using high-frequency data over the summer months (Morales-Pineda et al., 2014). In boreal climate zones, a total of 33 lakes in Sweden, sampled four times during the year, had a mean $_pCO_2$ of 1762 µatm (Sobek et al., 2003) and a more recent study by Yang et al., (2015) reported mean $_pCO_2$ of 1100 µatm in 75 lakes in Norway and Sweden that were sampled once during July and August.

Two other studies showed $_pCO_2$ similar to those in Lough Feeagh. Larsen et al., (2011) presented mean $_pCO_2$ levels of 774 µatm for 112 lakes in Norway that were sampled once in October, while mean $_pCO_2$ of 631 µatm were reported by Roehm et al., (2009) from a 3-year sampling campaign of 78 Boreal lakes in Canada. The majority of the lakes in that

latter study were, however, sampled on one occasion during the summer or early autumn. Only one other study that presented lake $_pCO_2$ in temperate maritime zones was found in the literature. Whitfield et al., (2011) reported median $_pCO_2$ in the region of 1080 µatm for 121 lakes in Ireland, in a study where each lake was again sampled only once during the early summer. Twenty of the lakes from that study were found to be undersaturated. Although most of the sampled lakes were situated in peatland catchments, they were also much smaller than Lough Feeagh (median = 2.0 ha) and predominantly located above 200 m in altitude. The results of our study suggest that the timing of the one-off sampling period in the Whitfield study coincided with a period of the year that $_pCO_2$ would have been lower.

In Lough Feeagh, $_pCO_2$ was observed to climb steadily during the summer, during the time when the lake was stratified (Figure 4.2A and 4.2F). Conversely, in studies from other climate zones, the onset of lake thermal stratification has been reported to suppress $_pCO_2$ in the epilimnion by reducing the volume of water in which mineralisation of allochthonous OC can occur (e.g. Jonsson et al., 2007). Also, in boreal and continental temperate climates, lake thermal stratification generally coincides with periods of low discharge which result in a reduction of allochthonous C inputs to lakes. During their study in a boreal lake, for example, Jonsson et al., (2007) reported an anomalous high-rainfall/discharge event in late July where a large input of DOC-rich water entered the lake, causing a spike in $_pCO_2$ which declined slowly. The authors noted that typical, low discharge $_pCO_2$ levels were not reached until one month after the peak discharge was recorded. It is our assumption that the high rainfall regime experienced at Lough Feeagh results in the lake being continuously 'topped up' with allochthonous C from the surrounding catchment throughout the year. This can be observed by the relatively high loading of DOC to the lake (Figure 4.2B and 4.2C) (Ryder et al., 2014; Doyle et al., 2019). We suggest that this almost constant and regular OC supply allows $_pCO_2$ in Feeagh to climb even during the main period of thermal stratification.

One of the most striking features in the $_pCO_2$ time-series for the study year was the sharp decrease that occurred between mid-April and mid-May, where values dipped to 491 µatm, the minimum values recorded over the study period (Figure 4.2A). This period of sharply supressed $_pCO_2$ coincided with a 30-day rain-free period, a relatively rare occurrence in this catchment, and corresponded to minimum values for the lake-level gauge. River colour concentrations in the inflowing rivers also dropped to their lowest levels during this period. The coincident reduction of $_pCO_2$, water colour and discharge

highlights the connectivity between catchment hydrology and OC availability in this lake. During such low-discharge periods, the lowered water-table and processes such as drought-induced acidification serve to break the connection between the source of DOC production, the surrounding peatland soils, and its destination, the catchment's aquatic continuum (Clark et al., 2005). A drought effect has previously been reported in the Glenamong catchment for early summer, whereby low river DOC concentrations were associated with a dry weather event (Ryder et al., 2014). For the 30-day period described here, we assume that the lake's epilimnion was increasingly deprived of allochthonous C inputs and $_pCO_2$ in the lake dropped accordingly. However, $_pCO_2$ in the lake rapidly rebounded following the return of rain in mid-May.

Following peak $_pCO_2$ observed in early September, where concentrations reached over 1100 µatm, they declined relatively quickly to concentrations of between 800 and 900 µatm. Interestingly, this period of declining $_pCO_2$ coincided with the breakdown of thermal stratification in the lake. In other climate zones, downward epilimnion expansion has been associated with an increase in $_pCO_2$, when CO_2 contained in the hypolimnion is released. For example, Morales-Pineda et al., (2014) reported increasing $_pCO_2$ in one Spanish reservoir during early autumn as downward epilimnion expansion facilitated release of CO_2 trapped beneath the thermocline. We suggest that as bio-available C was not limited in the epilimnion of Lough Feeagh during the period of breakdown of thermal stratification, there was no major spike in $_pCO_2$ at that time.

A link between diel variations in $_pCO_2$ and solar radiation due to the changing day-night balance between production and respiration has been well described in the literature (Carignan, 1998; Hanson et al., 2006; Huotari et al., 2009). However, the expected, regular pattern of increase in $_pCO_2$ during the night, as respiration dominates production in plankton metabolism, appeared only sporadically in the Lough Feeagh record. Careful visual examination of the daily $_pCO_2$ component ($_pCO_2^{daily}$) and concurrent wind-speed and pyranometer data indicated that these distinct diel fluctuations only occurred at times when wind speed remained consistently below about 4 m s^{-1} and solar radiation levels were high, when conditions were calm and sunny. Such conditions did not occur often during the study period, but did between mid-April and mid-May, and gave rise to a strong diel $_pCO_2$ signal at that time, with sharp peaks in $_pCO_2$ at night and dips during the day. This strong signal notably occurred during a period when overall $_pCO_2$ levels in the lake were falling sharply. Our results show that the regular diel $_pCO_2$ oscillation reported from

water bodies in other climate zones (e.g. Morales-Pineda et al., 2014) were generally intermittent and weak in Lough Feeagh over the study period.

The two main predictors of $_pCO_2$ dynamics in the lake were colour concentrations in the incoming Black River and the Schmidt Stability of the lake water column. The optimal model explained 67.8 % of $_pCO_2$ variance during the study period and the relationship between colour in the Black River and $_pCO_2$ in the lake was positive and linear (Figure 4.4 A). This result suggests a close dependence between input of allochthonous DOC and heterotrophic respiration in Lough Feeagh. A regular pattern of strong, annual peaks in colour / DOC concentrations during the late summer / early autumn were found in a recent, six-year long, study on colour concentrations in the main streams entering Lough Feeagh (Doyle et al., 2019). These peaks were found to be predominantly driven by soil temperature in the catchment and to a lesser extent by soil moisture levels, stream discharge and climate. It was especially notable in the current study that the annual peak of colour/DOC in both the Black and Glenamong rivers corresponded closely to the annual peak $_pCO_2$ levels in the lake (Figure 4.2A). There have been numerous studies, mostly from northern, boreal lakes, that highlight the relationship between the biological mineralisation of allochthonous carbon and excess CO_2 in lake waters (e.g. del Giorgio & Peters, 1994; Sobek et al., 2003; Duarte & Prairie, 2005; Lapierre et al., 2013).

The Schmidt Stability of Lough Feeagh generally follows a predictable and regular pattern every year, closely following the solar cycle and peaking in July (de Eyto et al., 2016). It was notable, however, that the annual peak in Schmidt Stability was not synchronous with the annual peak in $_pCO_2$. Presumably it is the offset in timing between the peak in the Schmidt Stability of the lake and the peak in $_pCO_2$ that gives rise to the complicated relationship that is evident in the model (Figure 4.4B). Also of note is the absence of any in-lake or autochthonous drivers of $_pCO_2$ variability in the optimal model. While daily estimates of lake GPP, R and NPP were included as explanatory variables they were excluded from the final model as they were not statistically linked to $_pCO_2$ variability in the lake over the study period. The estimate of autochthonous-derived C also shows that primary production in the lake contributed between approximately 18 and 31 % of the total OC mineralisation.

The $_pCO_2^{48hr}$ data shows strong variation at this time step and much of the variation appears to be concurrent with storm events that occur over a similar time duration in the catchment. Although elevated wind speeds may have supressed variability of $_pCO_2$ over

a daily time period, it appears to be a significant forcing factor over longer time periods. Visual examination of the $_pCO_2^{48hr}$ graph, in conjunction with wind speed, showed that many of the larger peaks in $_pCO_2$ corresponded to wind speed peaks. Presumably during these storm events, downward expansion of the epilimnion released $_pCO_2$ in the hypolimnion, rapidly increasing $_pCO_2$ levels. A similar episodic relationship between wind speed and $_pCO_2$ was described by Morales-Pineda et al., (2014) in two reservoirs in the south of Spain. Variability in $_pCO_2^{48hr}$ also appears to be linked with major rainfall events in the catchment (Figure 4.5B). A repeated pattern of $_pCO_2$ variation appears with these rainfall event, whereby there is an initial dip of $_pCO_2$ as fresh water arrives in the lake, followed immediately by a sharp peak of $_pCO_2$. The initial dip in $_pCO_2$ may be explained by the rapid dilution of the epilimnion and the subsequent peak occurs as a result of increased respiration as the bacterial and planktonic communities responds to the pulse of DOC and nutrients from the catchment.

Estimating the water-to-air fluxes of C from $_pCO_2$ provides important information on the carbon budget of the lake and is useful when comparing with other freshwater systems. Two air-water flux (F-CO_2) models, one described by Cole & Caraco, (1998) and a bilinear approximation model described by Crusius & Wanninkhof (2003) were applied to hourly-averaged $_pCO_2$ over the study period. Both models are based on empirical relationships between gas transfer velocity and wind speed and are commonly used to calculate F-CO_2. Carbon emission estimates from the lake varied considerably depending on the model applied. The total estimated mass of carbon emission over the study period almost doubled in size between the Crusius & Wanninkhof (2003) and the Cole & Caraco (1998) models at 217 t and 370 t C, respectively (Figure 4.3). It must be noted that both models were developed based on empirical measurements from small, wind-sheltered lakes in the boreal climate zone of North America, and as such are not entirely comparable to the more exposed conditions at Lough Feeagh. However, in an examination of $_pCO_2$ dynamics in two reservoirs in southern Spain by Morales-Pineda et al., (2014), these two models were also applied and in that case the Crusius & Wanninkhof, (2003) model was found to more accurately capture F-CO_2 dynamics in their systems. In particular, short spikes in F-CO_2 were linked to allied decreases in $_pCO_2$ during windy events, processes that were not accurately captured by the Cole & Caraco, (1998) model. This result perhaps signals that the Crusius & Wanninkhof, (2003) model may be a better fit when applied to more turbulent systems, such as Lough Feeagh. The estimated total DOC load to the lake of 1182 t C during the study period is equivalent to a catchment load of 14.7 t C km^2, and

is comparable to previous load estimates to the lake from the catchment (Doyle et al., 2019).

There is a dearth of data on C processing in Irish lakes, which is unfortunate given that there are over 12,000 lakes in the Irish Republic covering approximately 1.8 % of the land surface. Their role in C processing and C emissions to the atmosphere is vastly disproportionate to their surface coverage, particularly as the majority of Irish lakes are located in humic, high soil OC catchments. Lake C emissions are not captured in national emissions budgets for Ireland (EPA, 2019), and we consider that this study greatly improves on existing knowledge and will assist with constraining national CO_2 emission inventories. However, further work is required on lakes within a range of sizes, trophic states and morphometries in order to form a broader, regional understanding of $_pCO_2$ dynamics and CO_2 emissions.

4.6 Conclusions

This investigation of temporal variation in $_pCO_2$ highlighted the role of the local temperate maritime climate on the temporal dynamics of lake $_pCO_2$, and the potential for use of high frequency data to inform on these patterns. Most importantly it showed that lakes in these regions can have a very different temporal pattern to sites in boreal and continental regions, with late-summer autumn peaks that are driven predominantly by catchment inflows of carbon and changes in thermal stratification. Both of our hypotheses were also confirmed; that ecosystem respiration exceeded primary production in the lake and that $_pCO_2$ peaked in the early autumn, coinciding with an annual DOC concentration peak in the incoming rivers. Our investigation also showed that the lake was supersaturated with CO_2 and was a net emitter of CO_2 to the atmosphere during the study period. We consider that this study contributes to lake carbon cycling literature by broadening the understanding of the interactions between lake $_pCO_2$ dynamics and climate.

4.7 Acknowledgements

The long-term environmental monitoring programme in Burrishoole is facilitated by the technical staff of the Marine Institute Newport (Joseph Cooney, Pat Hughes, Michael Murphy, Pat Nixon, Davy Sweeney) and Martin Rouen (Lakeland Instrumentation Ltd.). The work on Lough Feeagh was only possible thanks to technical support from Allison Murdoch (Centre for Freshwater and Environmental Studies, Dundalk Institute of Technology, Co Louth, Ireland). This work was carried out with the support of the Marine

Institute and funded under the Marine Research Programme by the Irish Government (Cullen Fellowships No. CF/15/05)

5.0 The organic carbon budget of an oligotrophic temperate peatland lake.

Brian. C. Doyle[1,2], Elvira de Eyto[2], Valerie McCarthy[1], Mary Dillane[2], Eleanor Jennings[1].

[1]Centre for Freshwater and Environmental Studies, Dundalk Institute of Technology, Louth, Ireland
[2]Marine Institute, Furnace, Newport, Mayo, Ireland

Correspondence to: Brian C Doyle (brian.doyle@dkit.ie)

Keywords

Aquatic Carbon Cycling, DOC, POC, GHG emission, CO_2, Lake Sediments

5.1 Abstract

Lakes play a key role in the global carbon cycle, transporting, processing and storing organic carbon (OC) along the land-ocean aquatic continuum. There are, however, surprisingly few complete lake OC budgets, particularly for certain lake types and geographical areas. An OC budget for Lough Feeagh (Ireland), an oligotrophic, peatland lake in a temperate oceanic location, was estimated for one year using both direct measurements and elements calculated from literature. It was constructed as a simple mass balance model that constrained the key OC processing rates. The total OC input to the lake during 2017 was estimated to be 2544 t C, of which 51% was imported as dissolved OC (DOC) in surface water, 4% in ground water, 1% in rainwater, and 3% was fixed in the lake as net ecosystem production. The remaining 41% was carried into the lake as particulate OC (POC) in surface water. The total C exported was estimated to be 2689 t C, of which 49% and 12% were exported as DOC and POC in the surface water outflow respectively, 28% was deposited as sediment and 11% was mineralised and emitted as CO_2 to the atmosphere. The excess of estimated export over import was attributed to year to year carryover. The results highlight the substantial volume of OC turned over in the lake during the study period. Moreover, it emphasises how lakes in temperate, humic systems, common in the west of Ireland, are important to the processing and fate of OC mobilised from their catchments.

5.2 Introduction

Lakes are dynamic and active landscape components that in most cases are net emitters of inorganic carbon to the atmosphere (Arvola et al., 2002; Raymond et al., 2013; Weyhenmeyer et al., 2015) as well as process, transport and store organic carbon derived from their surrounding catchments (Cole et al., 2007; Tranvik et al., 2009; Tanentzap et al., 2017). While lakes are important in terms of global C cycling, there are surprisingly few complete and fully balanced lake OC budgets (e.g. Cole et al., 1989; Sobek et al., 2006; Hanson et al., 2014b) and as such there is considerable uncertainty surrounding lake OC processing. The need for a more complete understanding of how lakes are integrated within the global C cycle is increasing, particularly in the context of a warming planet with ever increasing focus on Greenhouse Gas (GHG) emissions. Global estimates of the emission of CO_2 from lakes and reservoirs is 0.32 Pg (petagrams) C yr^{-1} (Raymond et al., 2013) while the rate at which C is stored in bottom sediments is estimated to range between 0.02 and 0.25 Pg C yr^{-1} (Mendonça et al., 2017). However, these estimates carry quite a large degree of uncertainty and therefore studies of OC dynamics, such as the work presented here, that constrain the most important lake fluxes and storage terms will increase the understanding of lake OC cycling and its influence on global C budgets (Hanson et al., 2015; Reed et al., 2018).

Most lake OC budget studies have been carried out within boreal regions (e.g. Jonsson et al. 2001; Andersson & Kumblad, 2006; Andersson & Sobek, 2006; Sobek et al., 2006) or northern continental regions (e.g. Hanson et al., 2004; Dillon & Molot, 2005; Buffam et al., 2011), resulting in a geographical bias in global estimates towards these regions. To address this bias to some extent, the following study presents an OC budget for Lough Feeagh, a lake within a temperate maritime climate zone. Temperate maritime climate zones (Köppen, 1936) are strongly influenced by the ocean, thus maintaining relatively steady temperatures ranges across the seasons but also experiencing substantial precipitation. The high volumes of rainfall, especially in upland areas on the western fringes of Europe, assist in forming catchments with elevated soil carbon levels and moorland landscapes dominated by blanket peat soils (Renou-Wilson et al., 2011). The completion of a lake OC budget within this geographical and climate setting not only provides valuable insights of peatland catchment OC dynamics, it also informs on transport of OC to the marine environment and hence the oceanic C cycle (Bauer et al., 2013).

Budgets or mass balances are used as a tool to inform on carbon or nutrient transfers in lakes, and include estimates for all inputs, outputs, and changes to standing stocks in the water column and sediments (Pace & Lovett, 2012). By constraining and quantifying key rates and fluxes, a greater understanding of the lake trophic state in terms of carbon, i.e., autotrophy vs. heterotrophy may be gleaned. On a broader scale, the role that the lake plays as a storage and transformation site of OC in the landscape may also be better understood (Buffam et al., 2011). Inputs to lake OC budgets include allochthonous (externally derived) dissolved and particulate OC (DOC and POC respectively) carried in suspension in inflowing surface and in groundwater sources. Also included in these inputs are allochthonous inputs from precipitation, and wind-blown litter fall from the lake shore. Organic C budgets may also include autochthonous (internally derived) DOC and POC from organisms such as bacteria (Kawasaki & Benner, 2006), phytoplankton (Engel 2020), and zooplankton (Bruce et al., 2006). There are three possible fates for this OC within the lake: mineralisation to inorganic carbon, burial in lake sediments, and export via surface water. In Figure 5.1, a simplified allochthonous OC budget of a lake is shown. The diagram outlines the individual pathways of allochthonous OC into the lake and the three possible fates for this OC. The OC budget presented here is constructed from both observational data that informs estimates of certain fluxes, in combination with process rates, taken from literature. The main terms or processes that comprise lake OC budgets, namely allochthonous and autochthonous inputs, sedimentation, mineralisation and export are further described below.

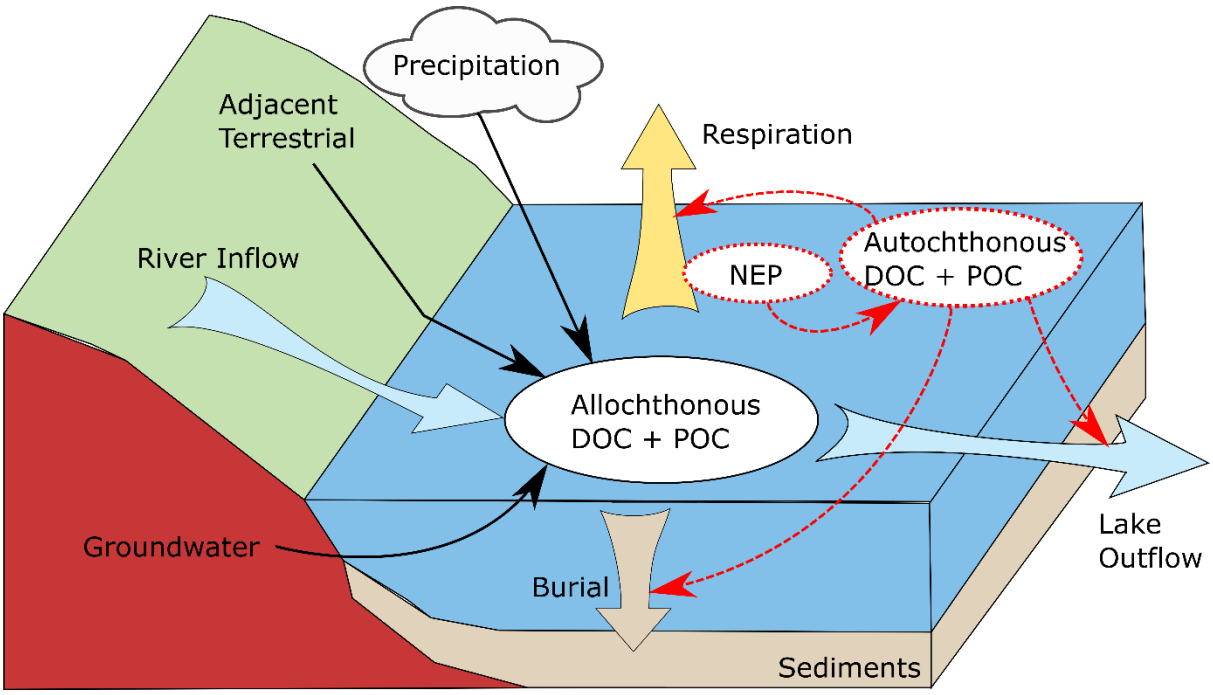

Figure 5.1. Diagram showing the principal fluxes of OC in this study. The allochthonous OC loads and fates that were either measured directly or calculated from literature values are shown. Red dashed lines show the autochthonous components OC in the lake. NEP was estimated for the study, however individual autochthonous components were not.

All externally derived OC to the lake, including terrestrial DOC and POC from surface and groundwater inflows, windblown vegetation including leaf litter and pollen, and direct-fall precipitation are considered allochthonous inputs. Direct DOC concentration measurements of inflow stream water, when available, is perhaps the most obvious method of ascertaining allochthonous DOC surface water inputs (e.g. Jonsson et al., 2001; Urban et al., 2005; Klump et al., 2009), but alternative approaches have also been reported and include OC input loads based on water colour (Doyle et al., 2019), watershed area (Sobek et al., 2006), input load estimates based on literature values (Striegl & Michmerhuizen, 1998), input load estimates based on precipitation volumes (Staehr et al., 2010), or input load estimates based on land cover and hydrological flow path analysis (Canham et al., 2004). Studies that have directly measured OC inputs to lakes via groundwater discharge are rare as accurate measurement is difficult to achieve (Hanson et al. 2014b). Atmospheric OC loads from leaf and litterfall and in rainfall are typically small in proportion to the overall loads and are generally estimated as a function of lake size and literature based loading coefficients (Hanson et al., 2004).

Autochthonous, or in-lake DOC and POC originates mainly through photosynthesis by primary producers, however bacterial exudates are also known to be a source (Cole, 1999). Ecosystem level estimates of gross primary production (GPP) are difficult to measure, therefore net primary production (NPP) — calculated as GPP minus autotrophic respiration — is generally measured as an alternative (Pace & Lovett, 2012). Reported methods of estimating NPP include high frequency measurements of dissolved O_2 or CO_2 concentrations (Cole et al., 2002; Staehr et al., 2010) and bottle incubations (Yang et al., 2008). Åberg et al., (2004) calculated NPP by estimating biomass proportions out of the overall OC pool. Other approaches include developing statistical relationships between lake temperature and total phosphorus (Hanson et al., 2004) and chlorophyll *a* (Jonsson et al., 2001; Ramlal et al., 2003).

Lakes can act as a reservoir of global C stocks through the process of long-term burial of POC in lake sediments. Knowledge of this process is very important when considering global C cycling rates, and it is also critical for our understanding of lake processing of allochthonous and autochthonous POC (Tranvik et al., 2009; Mendonça et al., 2017). The process of POC burial in lakes has been linked to a number of factors including POC particle size distributions and water column POC concentrations that control settling rates. In addition, sediment density, particle size, lake hydrodynamics and biogeochemistry that affect both settling rates and resuspension are also important factors in POC burial (Downing et al., 2008; Xu et al., 2013). Approaches to estimating sediment accumulation rates include using lake sediment cores (Klump et al., 2009; Heathcote & Downing., 2012), sediment traps placed near the lake bed (Jonsson et al., 2001; Ramlal et al., 2003; de Eyto et al., 2016), bathymetry (Downing et al., 2008), or lake area functions (Hanson et al., 2004; Canham et al., 2004). Accurate measurements of sediment accumulation rates are particularly difficult to estimate as they are known to vary, both spatially and temporally, while the data are mostly gathered from single point sources. This carbon sink could be especially important in peatland dominated catchments, however as noted earlier, OC budgets from lakes in these regions are scarce. Also, it is important to note that lake sedimentation estimates also include both allochthonous and autochthonous OC sources.

An important fate of OC is mineralisation or respiration which results in CO_2 supersaturation in the water column of many lakes (Cole et al., 1994; Sobek et al., 2003). Water column CO_2 supersaturation has mostly been attributed to the mineralisation of OC in excess of lake primary production (Cole et al., 1994). Quantifying in-lake

mineralisation as an OC flux is particularly challenging, and most studies have depended on laboratory investigations to predict ecosystem rates (Hanson et al., 2011). Lake CO_2 emission may be estimated, with some uncertainty, from surface water partial pressure, however this measurement does not accurately translate into within-lake OC process rates (Hanson et al., 2014a). While CO_2 emission estimates serve to constrain lake OC mineralisation rates, a variety of other processes such as photolysis of OC and inflows of dissolved inorganic carbon (DIC) may also contribute to CO_2 emissions. One solution, employed by a number of lake OC budget studies (e.g. Hanson et al., 2011; Hanson et al., 2014a; McCullough et al., 2018) is to apply a temperature-dependent mineralisation rate, based on literature values from bottle incubation experiments, to estimate the allochthonous and autochthonous OC mineralisation flux.

Allochthonous and autochthonous OC that is not buried in lake sediments or mineralised is exported via surface water (Cole et al., 1984). The surface water export of OC represents lateral allochthonous inputs to downstream aquatic systems, therefore this flux is an important process in ecosystem C cycling (Kling et al., 2000). OC export flux is predominantly a function of the hydrology of a lake system and can, for example, be calculated from lake DOC concentration, lake volume and hydrologic residence time (Hanson et al., 2014a).

In this study, a simple mass balance of OC is presented for Lough Feeagh over one calendar year. It was calculated using observational data from the catchment together with values from the literature. Using the approach outlined above, we aimed to use the budget to answer four principal questions, the answers to which will provide valuable insights into carbon cycling in peatland catchments in temperate maritime climate zones. The questions are; 1. how is the allochthonous OC import load partitioned among sources? 2. what is the magnitude of the autochthonous load to the lake? 3. what is the balance between the three fates of OC in the lake, namely, storage, mineralisation and export? 4. what are the implications of the study in terms of catchment scale C processing?

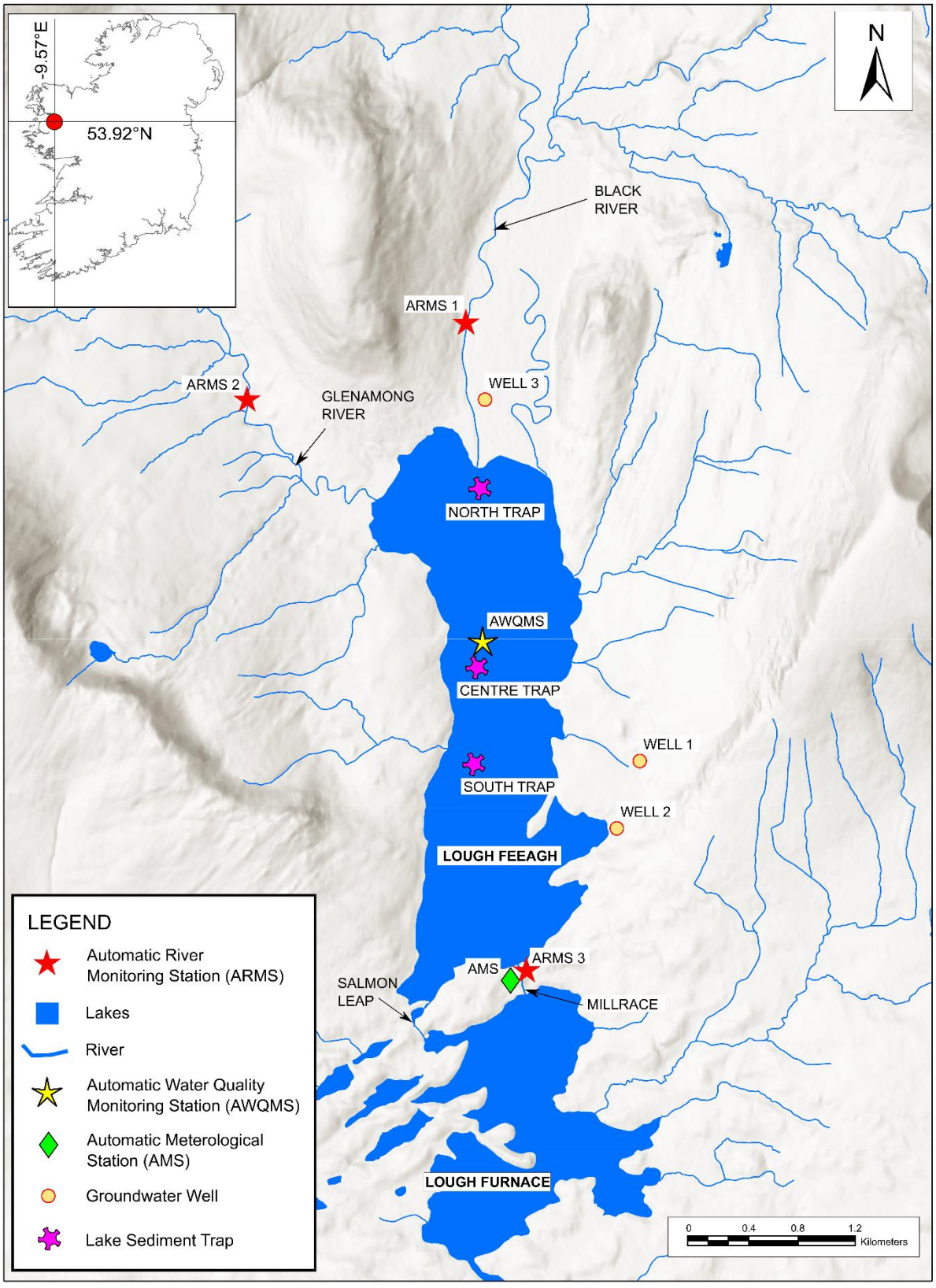

Figure 5.2 Map showing the geographical location of Lough Feeagh and the position of the various monitoring stations and monitoring equipment in relation to the lake.

5.3 Materials and Methods

5.3.1 The Study Site

The study was conducted in Lough Feeagh, a humic lake in western Ireland (53°55′N, 9°34′ W) located at the base of the Burrishoole catchment (~ 84 km^2) (Figure 5.2). Lough Feeagh has a surface area of 3.92 km^2, maximum and mean depths of 14.5 m and 46 m respectively and a volume of 5.9 x 10^7 m^3. The lake water is highly coloured (c. 80 mg l^{-1} PtCo) with a mean Secchi disk depth of 1.7 m, due to a high content of land-derived DOC (mean DOC = 8.82 mg l^{-1}). The lake water is also slightly acidic (pH = c. 6.7) with low alkalinity (< 20 mg l^{-1} $CaCO_3$) (de Eyto et al., 2016).

The two main inflows into Lough Feeagh are the Black River (catchment area = 48.3 km^2), located to the north of the lake, and the Glenamong River (catchment area = 17.5 km^2), located to the northwest of the lake, which supply the lake with most of its water. There are also seven ungauged first and second order streams on the eastern and western flanks of Lough Feeagh that discharge directly to the lake (catchment area = 18.2 km^2). There are two short outflow rivers at the south of the lake, the Millrace and the Salmon Leap, each of which are less than 200 m in total length. Both outflows discharge into Lough Furnace, an estuarine tidal lagoon, before entering the sea through a tidal river (Figure 5.2). The theoretical water retention time (volume/annual average discharge) of the lake is 172 days (de Eyto et al., 2016). Land cover in the Burrishoole catchment comprises 52% blanket peat, 15% forestry and the remaining 33% being made up of transitional woodland and scrub, natural grasslands and agricultural land (Doyle et al., 2019). The bedrock geology on the western side of the catchment is predominantly quartzite and schist, while on the eastern side, quartzite and schist are interleaved with veins of volcanic rock, dolomite and wacke, leading to higher buffering capacity and aquatic production. Soils and sub-soils in the catchment comprise poorly drained gleys, peaty podzols and blanket peats (de Eyto et al., 2020).

The Newport (Furnace) Met Éireann automatic meteorological station (AMS), located between Lough Feeagh and Lough Furnace and operating since 2005, recorded an average annual rainfall of 1533 mm $year^{-1}$ (± 182 mm SD) between 2005 and 2017. The temperate maritime climate in the region manifests in both mild winters and summers with mean air temperature from December to February (2005-2018) of 6.0 °C and from June to August (2005-2018) of 14.3 °C (Met Éireann - www.met.ie). The area also experiences a regular diurnal sea breeze with mean wind speeds of approximately 5 m s^{-1} (Kelly et al., 2018), that

are frequently interrupted by storm events originating from the Atlantic throughout the year (Andersen et al., 2020). The hydrological regime in the catchment is distinctly spatey, due to the temperate oceanic climate and subsequent high variability of rainfall. Frontal Atlantic rain systems continually cross the catchment and on occasion, extreme storm events may cause dramatic flooding (de Eyto et al., 2016; Kelly et al., 2020).

5.3.2 Lake allochthonous C budget calculation

The OC budget for Lough Feeagh was calculated over 1 year, from the 1st January 2017 to 31st December 2017. The lake organic carbon budget used in this study was based on the following equation adapted from Hanson et al., (2011):

$$I + A = S + R + E \quad (1)$$

where I is allochthonous import to the lake, A is autochthonous contribution, S is sedimentation, R is mineralisation (respiration plus photo-oxidation), and E is export from the lake.

5.3.3 Lake allochthonous carbon import

The OC import to the lake was calculated as the sum of the stream water inflow of DOC and POC, groundwater inflow, precipitation and aerial input from the lake perimeter. To estimate the surface water inflow of DOC, manual river water samples were taken at weekly intervals from the two main rivers, the Black and Glenamong, within 1 km of the point where they enter the lake (Figure 5.2 – ARMS = automatic river monitoring station). Water samples were also taken at weekly intervals from one river exiting the lake, the Millrace (Figure 5.2). The samples were analysed for true water colour (mg PtCo L^{-1}) within hours of sampling using a HACH Dr 2000 spectrophotometer at 455 nm on water filtered through Whatman GF/C filters (pore size: ca. 1.22 µm). Wavelength accuracy was ±2 nm from 400 to 700 nm. Water colour measurements have been found to be a good proxy for dissolved organic carbon (DOC) concentrations in the sub-catchment rivers. DOC (mg L^{-1}) concentration was estimated from water colour concentration (PtCo mgL^{-1}) using a linear model developed between water colour and DOC from the Glenamong River between April 2010 and September 2011 ($r^2 = 0.88$, $p \pm 0.001$, $n = 366$) (Ryder, 2015). The DOC load to the lake over the study year was calculated for the Glenamong sub-catchment by multiplying the calculated river discharge volume for each

week by the weekly estimated DOC concentration and summing the totals. The discharge for the Glenamong (Q_g) was estimated using water level data which were converted to volume of discharge per second ($m^3\ s^{-1}$) using a site-specific rating curve (Marine Institute, unpublished data). Water level was recorded every 15 min over the study period using an OTT Hydrometry Orpheus Mini water level logger (https://www.ott.com). No reliable rating curve was available for the Black River or for the smaller, seven ancillary streams that discharge directly to Lough Feeagh (Figure 5.2). Discharge from these sources were estimated using the drainage area ratio method based on the Glenamong discharge using the following equation (Hirsch, 1979).

$$Q_b = (\text{Area of Black \& Ancillary Catchment / Area of Glenamong Catchment}) \times \text{Glenamong Discharge} \quad (2)$$

Summing the Glenamong and the Black river (and ancillary streams) discharges ($Q_g + Q_b = Q_{in}$) allowed the estimation o*f* the surface water discharge to the lake. The calculated weekly Black river (and ancillary rivers) discharge volumes were multiplied by the weekly estimated DOC concentrations (calculated from weekly Black river colour measurements) to calculate the DOC import. The estimated DOC import from the Glenamong and the Black rivers, and ancillary catchment stream, were summed to calculate the total catchment DOC load to the lake over the study period.

5.3.4 POC in surface water inflow to the lake

The surface water inflow of POC was estimated from data collected using an automatic nephelometer (Chelsea Scientific Minitracka mk II nephelometer (www.chelsea.co.uk, Chelsea Technologies Group Ltd., West Molesely, UK), that was deployed in the Glenamong ARMS (Figure 5.2). The nephelometer provided high resolution *in-situ* data on the turbidity of the stream water, which may be used as a proxy for suspended sediment (SS) concentrations. A relationship between the millivolt output of the nephelometer and the measurements of river water SS concentration was quantified for the Glenamong sensor, using five serial dilutions of a spiked water sample. Sediment from the river bed and proximate river bank was used to spike the sample, creating a highly turbid water sample, following the methodology described by Rymszewicz et al., (2017). The nephelometer was suspended in each of the five dilutions in the field while still attached to the field logger, and the logger output (in mV) over 10 minutes was recorded. Each serial dilution was then transferred to the laboratory for quantification of the SS

concentration and loss on ignition (LOI) following the method of Moore & Chapman (1986). Filter papers (47 mm GF/C with a 1.2 µm pore size) were ashed in a furnace for 2 hours at 550 ℃ and placed in a desiccator. 200 ml of sample water was filtered through the pre-weighed filter papers, which were placed in a 100 ℃ oven for 24 hours. The filter papers were re-weighed once they had reached room temperature and then placed back in the furnace at 550 ℃ for 3 hours and re-weighed to give an LOI estimate. A linear rating curve was then developed for the millivolt output of the nephelometer and the river water SS concentration (n = 5, $R^2 = 0.99$). Loads of SS at an hourly time step were estimated by multiplying the mean hourly Lough Feeagh inflow river volumes (*Qin*) (see section below) by the mean hourly Glenamong estimated SS concentrations using the nephelometer data. The mean organic content of the SS load was estimated to be 83% using LOI data from a range of suspended sediment samples taken between 2010 and 2017 (n = 189). The organic portion of SS was converted to POC based on the measured carbon content of the organic fraction of SS for the Burrishoole catchment, a figure of 44.7 % calculated by Sparber (2012).

5.3.5 Inflow of DOC in groundwater to the lake

The mass load of C from groundwater to the lake was estimated from the product of the concentration of DOC in groundwater and the volume of groundwater entering the lake. The exchange of groundwater with Lough Feeagh was estimated using the following volumetric water balance equation (Hood et al., 2006):

$$\Delta S = \sum Q_{in} + P - E - Q_{out} + QGW_{in} - QGW_{out} \quad (3)$$

where ΔS is the change in lake storage, $\sum Q_{in}$ is the sum of incoming stream water, P is precipitation, E is evaporation, Q_{out} is outgoing stream water, QGW_{in} is incoming groundwater, and QGW_{out} is outgoing groundwater. Direct surface runoff to the lake is not included in equation (1) as it was not deemed significant for Lough Feeagh. Since groundwater inflow and outflow were not measured directly, the water balance equation was simplified to:

$$\Delta S = \sum Qin + P - E - Q_{out} + Q_{res} \quad (4)$$

where Q_{res}, the groundwater residual, is the net amount of groundwater inflow or outflow to the lake. Rearranging the equation to solve for Q_{res}:

$$Q_{res} = (\sum Q_{in} + P - E - Q_{out}) - \Delta S \quad (5)$$

The groundwater residual for Lough Feeagh was calculated using Equation 6 for the study period. The method for estimating lake water inflow volumes (Q_{in}) has been described above. The term P (Direct Precipitation) was calculated by multiplying the daily rainfall (mm) recorded at the Newport (Furnace) AMS by the lake surface area (m^2). Evaporation (E) was calculated using net shortwave and longwave radiation, wind speed, relative humidity, air temperature and surface water temperature following Woolway et al., (2015).

Lake water outflow volume (Q_{out}) was calculated using a streamflow ratings curve (R^2 = 0.97) described by Kelly et al., (2020) between the lake level and measurements of river flow in the Salmon Leap and the Millrace, the two outflows that exit Lough Feeagh. Lake level measurements (m) were recorded every 15 min over the study period using an OTT Hydrometry Orpheus Mini water level logger (https://www.ott.com).

DOC concentrations were measured at a monthly time-step in groundwater samples taken from three wells proximate to the lake between June 2016 and September 2017. Analysis for DOC was carried out using a Sievers 5310C total organic carbon analyser (Sievers Instruments Inc, sievers.instruments.wts@suez.com) (range 4ppb to 50ppm; accuracy ±2% or ±5ppb, whichever is greater; precision <1% relative standard deviation). To verify the TOC analyser performance, 10ppm potassium hydrogen phthalate (KHP) standards were used. The water samples were stored in a fridge in dark glass bottles and analysed in batches every 3 to 4 months. The monthly DOC concentrations in each groundwater well were averaged and then multiplied by the estimated monthly groundwater inflow volume to calculate the groundwater OC import. The location of the three groundwater wells in relation to the lake are shown in Figure 5.2. Well No.1 supplies potable water to a private dwelling situated approximately 730m from the eastern shore of the lake. It is approximately 50m in elevation above lake level. Well No.2 is a historical, roadside public well with the wellhead located adjacent to a local road. The wellhead is approximately 15m from the eastern lake shore and 2 m above lake level. Well No.3 supplies potable water to a private dwelling situated approximately 390m from the northern shore of the lake, close to the inlet of the Black River. The wellhead is approximately 2 m above lake level.

5.3.6 Aerial inputs of OC to the lake

Aerial inputs of OC to the lake are assumed to be leaf-fall, pollen and other wind-blown material from trees and vegetation growing close to the lake perimeter. The shoreline aerial load was assumed to be the sum of two components, discriminated by the proportion of the lake shoreline that had forest canopy and that which did not. The following equation was used to calculate the aerial load (Hanson et al., 2014a)

$$\text{Load}\,(\text{g yr}^{-1}) = [\text{PC} \times A_{oc} \times \text{perimeter}] + [(1 - \text{PC}) \times 0.2 \times A_{oc} \times \text{perimeter}] \quad (6)$$

where PC is the proportion of the shore with canopy, A_{oc} is the aerial loading factor in g C m^{-1} yr^{-1}, and perimeter is the lake perimeter in m. The aerial loading factor A_{oc} for this study was taken from Hanson et al., (2014a) where a mean A_{oc} of 1 g C m^{-1} yr^{-1} was used. Equation 3 also contains a term for a nominal load ($0.2 \times A_{oc}$) for the shoreline without canopy (1 – PC) (Preston et al., 2008).

5.3.7 Inputs of DOC to the lake from direct precipitation

The mass load of carbon from direct precipitation is the product of the OC concentration in rainwater and the volume of rainwater falling directly on the lake (P). A concentration value of 2.60 ± 2.4 mg C L^{-1} was used for this study. The value was taken from a review paper by Iavorivska et al., (2016) where mean organic carbon concentrations in rainwater are grouped by world regions, from 83 studies of DOC and TOC published between 1985 and 2015. The value (Table 2 of that paper) was the mean organic carbon concentrations in European rainwater.

5.3.8 Sedimentation of lake allochthonous C

Sediment deposition was measured using purpose-built sediment traps (Dalton et al., 2018) which have been deployed in Lough Feeagh on a continual basis since 2009. The traps were deployed in three locations along the north-south axis of the lake (Figure 5.2). Each sediment trap comprised 3 vertical tubes, each with a surface area of 1964 mm^2, suspended 4 m off the bottom of the lake on a frame. The sediment traps were emptied every 9 - 12 months (September 2016, June 2017 and June 2018) into prewashed plastic bottles, and the samples from each tube were then dried at 40 °C. The dry weight was recorded, and used to estimate the rate of sediment deposition in g m^{-2} d^{-1}, where the amount of sediment deposited on the surface area of each trap was divided by the number

of days that each trap was deployed to quantify a deposition rate. Sediment deposition for the entire lake area were calculated from average deposition rates of the three traps between September 2016 and June 2018, interpolated to the surface area of the lake, and curtailed to include the 365 days of 2017. The organic fraction of the sediment was calculated based on the % LOI of the material collected in the tube and the estimated organic material was again converted to OC based on the measured carbon content of 44.7 % of the organic fraction of SS (Sparber, 2012).

5.3.9 Export of lake allochthonous DOC and POC

The methods for estimating surface water concentrations of DOC and POC in the outflow rivers were the same as those used for estimating DOC and POC concentrations in the incoming streams as described in previous sections. Water colour and nephelometer readings were measured at the Mill Race ARMS (Fig. 5.2). The OC concentrations were multiplied by the lake water outflow volume (Q_{out}) to calculate the export.

5.3.10 Mineralisation of allochthonous OC

The mineralisation of allochthonous organic OC to CO_2 was estimated by measuring the partial pressure of CO_2 (pCO_2) in the lake and estimating the emission of CO_2 from the lake using data collected from an Automatic Water Quality Monitoring System (AWQMS) on Lough Feeagh, positioned over the deepest point of the lake (46 m). This station collects and transmits high frequency sensor information to the Marine Institute's research station via GPRS (http://burrishoole.marine.ie). ${}_pCO_2$ in the lake water was measured at the AWQMS every 15 minutes using a membrane covered optical carbon dioxide sensor (AMT Analysenmesstechnik GmbH, Joachim-Jungius-Strasse 9D-18059 Rostock, Germany) suspended at one-meter depth. The sensor was deployed on 16th February 2017 until 05th December 2017 and ran continually except for three data-gaps of 95, 216 and 77 hours in August, October and November respectively. Gaps in the time series were filled by using a linear relationship between colour concentrations in the Black river, measured weekly, and mean ${}_pCO_2$ concentrations in the lake over a 24-hour period from the same day of sampling ($R^2 = 0.66$, No = 37) (Doyle et al., 2021). Thus missing data in January 2017 and December 2017 were extrapolated to complete the ${}_pCO_2$ data set for 2017.

Two air-water flux (F-CO_2) models were used to separately estimate CO_2 emissions from the lake. The CO_2 emission (F-CO_2, mmol m^{-2} d^{-1}) from the lake was calculated by applying the following equation (Cole & Caraco, 1998):

$$F\text{-}CO_2 = k\,[CO_{2\ water} - CO_{2\ sat}] \quad (7)$$

where k is the gas transfer velocity (cm h^{-1}), $CO_{2\ water}$ is the CO_2 concentration in the water (µatm L^{-1}); and $CO_{2\ sat}$ is the CO_2 concentration at equilibrium with the atmosphere, calculated from Henry's constant (Weiss, 1974). For $CO_{2\ sat}$ a constant ${}_pCO_2$ in equilibrium with the atmosphere of 400 µatm was assumed (http://co2now.org/). The gas transfer velocity k was estimated from k600 values derived from wind speed based on a bilinear function described by Crusius & Wanninkhof (2003). For simplicity, this model will be referred to as $CW03_{bi}$ in the remaining text, is expressed as follows;

$$k_{600} = 0.72 \times U_{10} \quad (8)$$

an alternative, commonly applied model was also used for the basis of comparison, a power function described by Cole & Caraco (1998), referred to as CC98 in the remaining text, using the following equation;

$$k_{600} = 2.07 + 0.215\ U_{10}^{\ 1.7} \quad (9)$$

where k_{600} is the gas transfer velocity at 20 °C (cm h^{-1}) and U_{10} is the wind speed over the lake at 10m height (ms^{-1}). A temperature-dependent Schmidt number (defined as the kinematic viscosity of water divided by diffusion coefficient of the gas) for CO_2 was calculated according to Jähne et al., (1987) using the following equation;

$$Sc = 1841 \times e^{(-0.0549 \times t)} \quad (10)$$

where Sc is the Schmidt number and t is the water temperature in °C. The Schmidt number was used to recalculate k_{600} (Wanninkhof, 1992) using the following equation;

$$k = k_{600} / (600 / Sc)^{-0.66} \quad (11)$$

The CO_2 emission data is used to constrain the mineralisation term of the allochthonous OC balance equation.

A mineralisation rate, $RDOC_{20}$ (d^{-1}) for the lake is also reported. Firstly, RDOC is scaled according to the general biogeochemical temperature scaling function (Hanson et al., 2011):

$$RDOC\ (yr^{-1}, T) = RDOC_{20} \times \theta^{(T-20)} \quad (12)$$

where $RDOC_{20}$ is the mineralisation rate at 20°C, T is the observed water temperature in °C and θ is a temperature scaling factor, set to 1.073, which equates to a Q10 temperature coefficient value of 2.0 when scaled according to the exponent T with reference to 20°C. The rate was calculated by dividing the mean daily CO_2 emission by the mean daily standing stock of DOC in the lake and adjusting for the annual mean water temperature.

5.3.11 Estimation of autochthonous organic C

To assist with the calculation of allochthonous OC balance calculations, an estimate of the autochthonous contribution was calculated using primary productivity in the lake. A multi-parameter sonde (Hydrolab DS5, OTT, Kempton, Germany), deployed on the AWQMS at 0.9 m below the water surface, measured pH, specific conductivity (mS cm^{-1}), temperature (°C), and dissolved oxygen (DO) (mg L^{-1} and %) every 2 minutes over the study period. Vertical temperature profiles below the AWQMS were measured during the study period using a chain of 12 platinum resistance thermistors (PRTs: Lab facility PT100 1/10DIN 4 wire sensor, www.labfacility.co.uk, Labfacility Ltd., Bognor Regis, UK). The chain spanned the full water column with sensors at depth intervals of 2.5, 5, 8, 11, 14, 16, 18, 20, 22, 27, 32, 42 m, all recording every 2 minutes. Sensors on the AWQMS were cleaned fortnightly, and the DO sensor on the multi-parameter sonde was calibrated once per month.

Daily estimates of the thermocline depth were made using R Lake Analyzer package (Winslow et al., 2014). The resulting depths were used as an indicator of the mixed layer depth of the lake over the study period. Daily estimates of GPP, R, and NEP within the mixed layer were made using the R Lake Metabolizer package (Winslow et al., 2016), applying the maximum likelihood estimate method, a process-error-only model with parameters fitted via maximum likelihood estimation (Solomon et al., 2013). Lake Metabolizer was run with a 2-minute time step over the study period where data (DO, water temperature, PAR, and wind speed) were available, producing estimates of daily GPP, R and NEP (GPP − R) in (O_2 mg l^{-1} d^{-1}). Negative values of GPP and R were removed from the dataset on the assumption that the model fit was poor or that some other

process not included in the model was acting that day (e.g., physical entrainment of O_2 from other depths).

Comparing the lake CO_2 flux with NEP on a daily scale provides insight into the contribution of aerobic in-lake metabolism to the net CO_2 efflux. Daily NEP values (O_2 mg l^{-1} d^{-1}) were converted to aerial units (O_2 mg m^{-2} d^{-1}) and converted to CO_2 assuming a respiratory quotient of 1. The daily CO_2 amounts were summed over the study period and the estimated mass of C is reported.

5.4 Results

5.4.1 DOC in surface water inflow to the lake

True water colour from the weekly manual river water samples collected from the two main rivers entering the lake ranged between 26 and 240 mg PtCo L^{-1} for the Black River and between 27 and 215 mg PtCo L^{-1} for the Glenamong River equating to between 8.2 and 12.9 mg DOC l^{-1} for the Black River 8.2 and 12.4 mg DOC l^{-1} for the Glenamong river. The colour concentration showed a strong synchronous annual pattern for the two rivers, dipping to a minimum during the winter and peaking in late summer to early autumn (Figure 5.3 – Panel A). The estimated DOC load from the Black River and ancillary catchment rivers was calculated to be 987.7 t C yr^{-1} while the estimated DOC load from the Glenamong River was calculated to be 293.0 t C yr^{-1}. The total surface water input of DOC to Lough Feeagh during 2017 was 1293.7 t C yr^{-1}, equating to 15.4 t C km^{-2} yr^{-1} for the Burrishoole catchment area.

5.4.2 POC in surface water inflow to the lake

The total load of suspended sediment, estimated by multiplying the mean hourly inflow river volumes (*Qin*) by the mean hourly Glenamong SS concentration, was 2824.6 t yr^{-1}. The total estimated POC load to the lake via surface water inflow was 1047.9 t POC yr^{-1}. equating to 12.5 t C km^{-2} yr^{-1} for the Burrishoole catchment area.

5.4.3 DOC in groundwater to the lake

The water balance yielded a positive groundwater residual for 180 days during the study period. The calculated rate of groundwater inflow ranged between 0 and 16.2 m^3 s^{-1} with a mean inflow of 1.01 m^3 s^{-1} for 2017. The groundwater residual can be considered a minimum estimate of groundwater inflow, as groundwater outflow may dominate over inflow during periods of low rainfall. Calculating groundwater inflow during these

periods was not possible from the available data. Whilst the groundwater residual shows that there was a significant flux of groundwater into the lake over the whole year, during one particularly dry period in April and May, groundwater outflow dominated over groundwater inflow. Similar to the rivers flowing into Feeagh, mean DOC concentrations in the three groundwater wells around the lake displayed a strong, synchronous pattern over the yearly cycle, dipping in concentration during the winter months and reaching a peak in late summer and early autumn. Well No.1 had the highest concentration of DOC, peaking at *circa* 8.5 mg l^{-1} during September of 2016 and 2017 while Well No.2 showed the lowest concentrations, peaking between 3.3 and 4.1 in September of both years (Figure 5.3 Panel C). Multiplying the average monthly concentrations from all wells by the calculated groundwater inflows for each moth yielded a total groundwater carbon input to the lake of 110.7 t C yr^{-1}.

5.4.4 Aerial inputs of OC to the lake

Lough Feeagh's shoreline is 13.42 km long, however only 2.25 km of the shoreline is forested, a proportion of approximately 16.8%. The total aerial C load to the lake was estimated to be 0.004 t C yr^{-1} using the equation introduced by Hanson et al., (2014a), which was extremely small in comparison to the other allochthonous inputs.

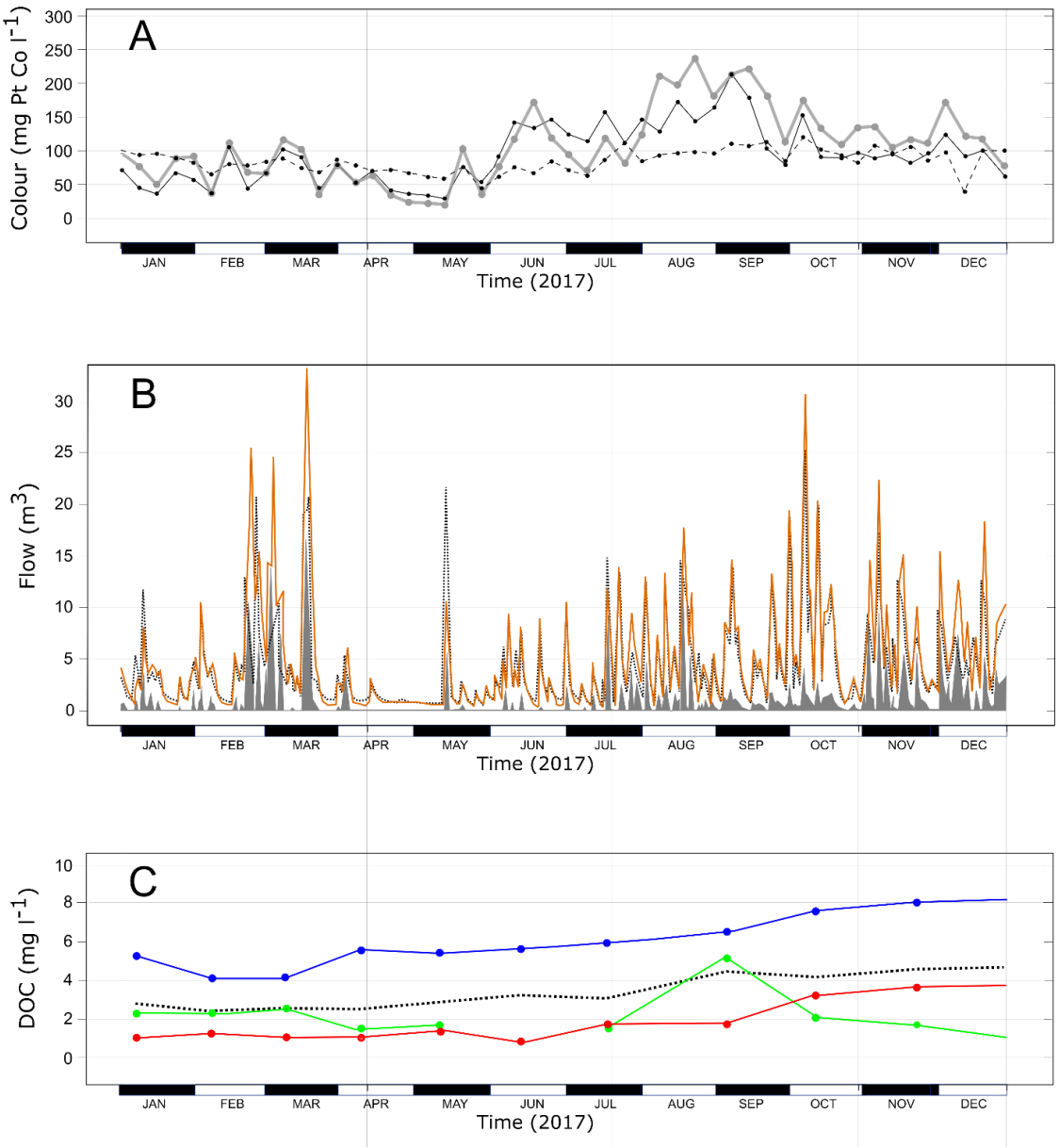

Figure 5.3. Panel A, colour concentrations (mg PtCo L^{-1}) in the rivers entering (Black = solid grey line and Glenamong = solid black line) and exiting (Millrace = dashed line) Lough Feeagh. Panel B, estimated inflow water volume (dashed line), outflow (orange line), and inflowing groundwater volume (solid grey) in m^3 s^{-1} d^{-1}. Panel C, DOC concentrations mg l^{-1} in three groundwater wells in the Lough Feeagh catchment, well 1 = blue line, well 2 = red line and well 3 = green line, dashed line shows the mean concentrations from the three wells. Y-axis on all panels = Time, 2017

5.4.5 Inputs of DOC to the lake from direct precipitation

A total of 1720 mm of rain was recorded at the Furnace Meteorological Station during 2017, equating to an average of 4.7mm of rain d^{-1}. The mass load of carbon to the lake in precipitation, calculated from the product of the OC concentration in rainwater and the volume of rain water falling directly on the lake, was estimated to be 13.9 t C yr^{-1}.

5.4.6 Sedimentation of lake allochthonous C

The average sediment deposition rate over the study period, measured in the north, middle and south sediment traps was 3.5 g m^{-2} d^{-1} (dry mass of sediment per m^2 of lake surface), with rates diminishing from north (5.6 g m^{-2} d^{-1}) to the middle (3.4 g m^{-2} d^{-1}) to the south trap (1.6 g m^{-2} d^{-1}). The loss on ignition of the sediments indicated that 33% of the sediment comprised of organic material. The total mass of OC deposited as sediment for 2017 was calculated as 753.5 t C yr^{-1} within a range of 427.4 to 963.5 t C yr^{-1} calculated from the three traps.

5.4.7 Export of lake allochthonous DOC

True water colour from the weekly manual river water samples from the Millrace, one of the two outflows from the lake, ranged between 40 and 125 mg PtCo L^{-1} which equated to between 8.5 and 10.4 mg DOC l^{-1} over the study period. When compared with the two rivers entering the lake, the trend of colour concentration over the year was much weaker and showed very little variation over the annual cycle. The calculated mass of DOC exiting the lake from the Millrace and the Salmon Leap Rivers was estimated to be 1320.6 t C yr^{-1} The total surface water DOC export from the lake on a catchment area basis equalled 16.5 t C km^{-2} yr^{-1}. As a simple check on this figure, mean monthly colour concentrations taken from grab samples from the lake were converted to DOC concentrations and multiplied by the river water volumes, giving an estimated DOC mass of 1324.2 t C yr^{-1}, a figure that is very similar to the original estimate.

5.4.8 Export of lake allochthonous POC

The total load of suspended sediment exported from the lake, estimated by multiplying the mean hourly outflow river volumes (Q_{out}) by the mean hourly Millrace SS concentration, equated to 894.4 t yr^{-1}. Using the same calculation as for the inflowing rivers, and outlined previously, the total POC load exiting the lake via surface water outflow was 331.8 t POC yr^{-1}.

5.4.9 Lake CO2 emission

The $_pCO_2$sensor recorded concentrations ranging from a minimum of 491 µatm to a maximum of 1,169 µatm. The average $_pCO_2$ for the whole study period (± SD) was 803 ± 122 µatm and the lake was supersaturated throughout the study period. The $_pCO_2$ concentration time series displayed a seasonal cycle, with lower values in earlier part of the record, reaching a maximum value in the autumn and declining thereafter. There was however a dip or decline in $_pCO_2$ concentration for approximately four weeks, from mid-April to mid-May, which coincided with a prolonged period of dry and sunny weather and decreasing lake-levels at this time. Wind speed values at Lough Feeagh are stochastic and broadly random in time. Greater peaks of wind speed are noticeable during January and February and also during September. A calm period was also apparent during late April and early May and coincided with the onset of thermal stratification. Water temperature at the lake surface ranged between 6.0 ℃ (27th February) and 18.8 ℃ (17th July) with a mean water temperature of 11.5 ℃ ± 3.5 SD over the year. The water column in the lake was mixed until 19th of April when thermal stratification commenced. The lake was thermally stratified until 20th September when the water column began to mix following a series of storm events.

Using the $CW03_{bi}$ model, the calculated emissions of CO_2 ranged from 3.8 to 56.1 mmol C m^{-2} d^{-1} (mean = 16.5 ± 8.1 mmol C m^{-2} d^{-1}), equating to a total estimated carbon emission for 2017 of 282.0 t C yr^{-1}. Using the CC98 model, the calculated emissions of CO_2 ranged from 6.5 to 112.8 mmol C m^{-2} d^{-1} (mean = 28.2 ± 15.5 mmol C m^{-2} d^{-1}) resulting in a total carbon emission of 484.8 t C yr^{-1}.

The estimated mineralisation rate $RDOC_{20}$ for the lake over the study period was calculated by dividing the daily estimated emission of CO_2-C (0.77 t C d^{-1}) by the average daily standing stock of DOC in the lake (5203.8 t C d^{-1}) = 0.00014 d^{-1}. Adjusting for the mean temperature of the lake over 2017 (11.5 °C) by using the general biogeochemical temperature scaling function (Hanson et al., 2011)

$$RDOC = 0.00014 \times 1.07^{(11.5 - 20)} = 0.000083\ d^{-1} \quad (13)$$

If the total emission of 484.8 t C yr^{-1} estimated by applying the Cole & Caraco (1998) model, the $RDOC_{20}$ estimate increases to 0.000143 d^{-1}.

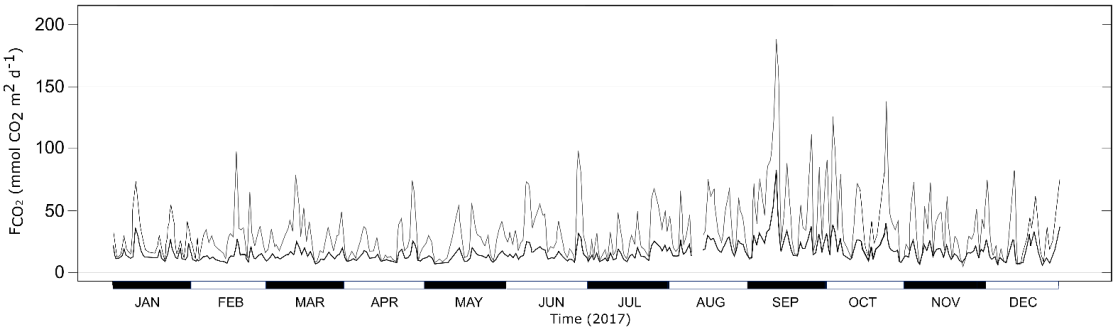

Figure 5.4 Estimated emission of CO_2 (mmol C m^{-2} d^{-1}) using two air-water flux (F-CO_2) models, the Cole and Caraco (1998) model = solid grey line and the bilinear approximation model proposed by Crusius and Wanninkhof (2003) = solid black line. The Y-axis = Time (2017).

5.4.10 Estimation of autochthonous organic C

Ecosystem metabolism was successfully estimated for 325 days of the study period. GPP and R showed a distinct seasonal trend despite substantial day-to-day variations, increasing during spring, peaking during the summer and decreased towards late autumn and winter. The higher rates of GPP and R during spring and summer were due to increasing light intensity, higher water temperatures and increased lake biomass. The relationship (slope) between GPP and R was systematically above 1.0 and R generally exceeded GPP. As a consequence, NEP (GPP−R) was predominantly negative throughout the year. This is in agreement with the almost continuous O_2 under-saturation observed throughout the study period. The strong ecosystem heterotrophy contributed to the supersaturation of CO_2 and its subsequent release to the atmosphere.

Daily NEP values (O_2 mg l^{-1} d^{-1}), converted to CO_2 assuming a respiratory quotient of 1, and summed over the study period, were estimated to be 77.2 t C yr^{-1}. This amount is considered to be the contribution of aerobic in-lake metabolism to the net CO_2 efflux.

5.5 Discussion

Lake carbon budgets contribute to understanding the role of lakes in the global carbon cycle (Likens., 1985; Hanson et al., 2014b; Evans et al., 2017). These budgets are, however. still scarce and there are particular knowledge gaps in relation to humic lakes in temperate oceanic regions. Our study is, to the best of our knowledge, one of the first to estimate a C budget of such a lake, and provided estimates for exports to the atmosphere, sediments and to downstream ecosystems. It confirmed the dominance of

allochthonous inputs as a C source in this oligotrophic lake, and showed that while most of the DOC that entered the lake was exported downstream, most of the particulate carbon was lost to the bottom sediments. Also, the low mineralisation rates and CO_2 emission relative to the substantial OC throughput confirmed the oligotrophic status of the lake.

In the case of this budget, a simplified, mass balance approach was used, whereby the OC imports to the lake were offset by the three OC fates in the lake, namely, sedimentation, emission and surface water export. There are many challenges in quantifying lake carbon budgets and many of the components that comprise an OC budget are difficult to quantify and generally have high uncertainties. We have, however, high confidence that the elements of the allochthonous OC budget that were transported in the surface water were reasonable and accurate, namely DOC and POC import and export. Our confidence is due to the long term, high-frequency monitoring of incoming and outgoing stream water levels, and lake level, along with well-established rating curves that effectively captures the hydrology of Lough Feeagh system. The high-frequency monitoring of the system's hydrology in tandem with the lake-shore location of the meteorological station also allowed reasonable estimates for precipitation and groundwater inputs to be made. The direct measurements of OC sedimentation gleaned from the sediment traps also helps to constrain the POC input.

While the organic carbon budget presented in this study did not strictly balance, with the OC fates, (2689 t C yr^{-1}) being greater than the OC loads, (2547 t C yr^{-1}) by approximately 142 t C, the difference is contained within a cumulative margin of error surrounding the estimates for each individual element of the overall budget. Less certain however are lake shore aerial inputs, where transfer rates from the literature was used to estimate the OC load. There is also less certainty regarding the estimates of CO_2 emission from the lake. The emissions were not measured directly, but based on literature derived gas transfer models. A literature-derived gas transfer model was also used in the calculation of the autochthonous contribution to the OC budget, computed from daily estimates of NEP (GPP − R). The implications for using literature based models are discussed in the relevant sections below. Using a mass balance approach allows import elements of the budget to be cross-checked and 'balanced' against export elements. For example, POC import was compared to sedimentation and POC export, and found to reasonably balance, which allows a degree of confidence in the estimates. Also, the mineralisation rate of OC conversion to CO_2 could be constrained by high-frequency measurements of the partial pressure of CO_2 ($_pCO_2$) in the surface water of the lake.

The first question we aimed to answer using the budget data was how was the allochthonous OC import load partitioned among sources? We found that DOC entering the lake in surface water was the largest contributor of C to the lake, but that particulate OC also represented a large component. The total mass of DOC entering the lake was estimated to be 1293.7 t C in 2017, which equals 51% of the OC import and equates to a catchment area export rate of 15.4 t C $km^{2\ -1}$ yr^{-1}. This estimated rate is within the range of other studies for the catchment rivers, for example, previous export estimates of 9.5 and 13.7 t C $km^{2\ -1}$ yr^{-1} from the Glenamong for 2010 and 2011, respectively were reported by Ryder et al., (2014), while Doyle et al., (2019) estimated that annual DOC fluxes from the Black and Glenamong catchment to Lough Feeagh ranged from 11.8 to 18.5 t C $km^{2\ -1}$ yr^{-1} between 2011 and 2016. The strong, synchronous seasonal trend in water colour concentrations was also previously reported by Doyle et al., (2019) and linked to soil temperature in the catchment.

The total POC load to the lake of 1047.9 t C equalled 41% of the OC import and equated to approximately 65% of the surface water DOC load to the lake over the same period. This percentage is identical to a previous study by Ryder et al., (2014) for the Glenamong river for 2010-2011. The present estimate represents a catchment POC export rate of approximately 10.0 t C $km^{2\ -1}$ yr^{-1}. POC export rates vary enormously in peatland catchments. For example, at the upper end of the scale, Worrall et al., (2003) estimated an annual catchment POC export rate of up to 31.3 t C km^{-2} yr^{-1} from an upland peatland site in the UK, a rate that was approximately double the DOC export (up to 15 t C $km^{2\ -1}$ yr^{-1}) for the same site. The contribution of organic C to the overall suspended sediment load in a river is unique to each catchment (Dawson et al., 2011). The location along an aquatic system is also important for DOC:POC ratios, for example Pawson et al., (2012) noted that DOC:POC ratios decrease from values of 1:4 at peatland stream headwaters to close to unity at catchment outlets.

Ryder et al., (2014) also investigated the principal factors contributing to variability in POC flux entering Lough Feeagh, reporting that while stream discharge was the most important explanatory factor, soil temperature and rainfall were also important explanatory variables. Also, in an earlier study of sediment transport in the Burrishoole catchment by May & Place (2005) it was noted that volumes declined during prolonged wet spells. They found that prolonged rainfall resulted in an initial washout of erodible material followed by a subsequent decline of SS as the source of available material

declined. Therefore, the rate of discharge alone did not fully explain sediment transport, as antecedent weather conditions also play a significant role.

Groundwater flows and inputs to lakes are extremely difficult to measure directly and require a great deal of resources, including equipment, time, and expertise. Full hydrology budgets are rarely included in lake OC budgets because of these difficulties (Winter & Likens, 2009; Hanson et al., 2014b). In the case of this study, the volume of groundwater entering the lake was calculated indirectly, by estimating the difference, or residual, between the measured inflows and outflows from the lake, accounting for direct precipitation and evaporation (Figure 5.3B). At 110.7 t, the amount of DOC entering the lake via groundwater was approximately 4% of the total calculated OC load to the lake over the study period. The measured mean DOC concentrations from the three groundwater wells were quite low, ranging between approximately 2 and 6 mg l^{-1}. Interestingly, the strong seasonal pattern of peaking colour/DOC concentrations in the late summer that can be observed in the inflowing streams is repeated, albeit faintly, in the groundwater DOC concentrations (Figure 5.3C). There is some evidence therefore that catchment groundwater accumulates OC before reaching the lake. The groundwater in the wells are therefore hydrologically linked to the upper soil layers in the catchment, suggesting that the groundwater origins are relatively shallow, in the subsoils, and not from deep within the bedrock (Junk et al., 1980). The overall contribution of groundwater DOC to the overall OC load is quite modest, reflecting both the low mean groundwater inflow rate of 1.01 m^3 s^{-1} to the lake, and low mean DOC concentration of the groundwater.

An estimated 13.9 t of OC, carried directly in rainfall, entered the lake in 2017, this mass equates to approximately 1% of the OC import. The load was calculated from the product of the volume of rainfall falling on the surface of the lake and a concentration value of 2.60 mg C l^{-1} (Iavorivska et al., 2016). The calculated mass of OC may be slightly overestimated as the concentration value is derived from mean OC concentrations in European rainwater, which may differ slightly from OC concentrations in rain water derived over the Atlantic Ocean. The aerial inputs of 0.004 t C yr^{-1} OC to the lake calculated from literature values are miniscule in comparison to the other allochthonous loads. The main reason for the low estimated OC load is the small proportion of forested land adjacent to the lake. The calculations are based on literature values derived from aerial deposition studies from North American lakes (Hanson et al., 2014b).

The second question we posed was, what is the magnitude of the autochthonous load to the lake? The estimate of autochthonous-derived C was derived from the assumption that changes in DO can be used as a surrogate for CO_2 based on the stoichiometric relationship between the 2 gases as part of gross primary production (GPP) and aerobic ecosystem respiration (R) (Odum, 1956; Hanson et al., 2008). The estimate of 77.2 t C yr^{-1} contributed by ecosystem metabolism equates to approximately 3% of the OC load to the lake and approximately 27% of the total C emission to the atmosphere during 2017. These figures are comparable to other reported lakes, for example Lake Ortrasket in Sweden, a high-DOC, oligotrophic lake where Jonsson et al., (2001) showed that primary production in the lake contributed at most 5% of the total organic carbon input and about 20% of the total organic carbon mineralisation.

Our third question was focused on establishing the balance between the three fates of OC in the lake, namely, storage, mineralisation and export. Given the relatively large fluvial inputs to the lake, it is not surprising that sedimentation of POC was found to be an important fate for OC in Lough Feeagh. The total of 753.5 t C that was estimated to have been deposited on the lake bed in 2017 represented approximately 28% of the estimated total OC fate in the lake. Flocculation of a portion of the DOC fraction may also help to explain the high sedimentation rates in the lake. For example, von Wachenfeldt & Tranvik (2008) also found substantial sedimentation of DOC in highly humic lakes. The spatial pattern of sedimentation was not homogeneous across Lough Feeagh, however, as indicated by the variation in deposition rates in the three traps positioned in the north, centre and south of the lake (Figure 5.2). This strong north-south spatial variation in deposition rates strongly suggests that the dominant mechanism was sedimentation from riverine input rather than any autochthonous or within-lake processes. Lough Feeagh is an oligotrophic lakes and chlorophyll *a* levels less than 2 mg m^{-3} are usually reported (e.g. Caldero-Pascual et al., 2020), levels that were confirmed in this study by low GPP estimates. The strong spatial pattern of varying sedimentation rates across the lake may also be amplified by lake morphology and the location of the inflows and outflows at either end of the lake's longer north-south axis.

It must be noted, however, that a portion of the estimated total amount of OC in the sediments will be processed further and will be mineralised to CO_2 in oxic conditions and CO_2 and CH_4 in anoxic conditions (Tranvik et al., 2009; Aufdenkampe et al., 2011; Raymond et al., 2013). The portion of OC that remains in the sediments over long periods of time is considered 'buried'. In fact, long-term burial of OC in lake sediments is the

mechanism by which C is removed by lakes from the global C cycle, and is also a critical component in the understanding of the fate of both allochthonous and autochthonous OC in the landscape (Downing et al., 2008; Xu et al., 2013).

The sedimentation rate of OC in Lough Feeagh (1292 g C m^{-2} yr^{-1}) appears to be quite large when compared to reported sedimentation rates from other lakes. For example, in a whole year study, Chimel et al., (2016) reported a rate of 43.9 g C m^{-2} yr^{-1} in a small, shallow, humic lake in boreal Sweden while Ferland et al., (2014) reported a mean sedimentation rate of 25.68 g C m^{-2} yr^{-1} from 11 lakes of varying sizes in boreal Québec. Sedimentation rates among lakes should be compared with caution, owing to the many different factors involved, including lake-to-catchment ratios. However, in both those studies, the sediment burial efficiency ratios (defined as the ratio between the long-term C accumulation in surface sediments and the sedimentation rate of OC) were similar, at 1:0.178 and 1:0.206 respectively. OC burial rates were not calculated for this study, however if a similar burial efficiency ratio was applied, OC burial rates for Lough Feeagh would be in the region of 230 g C m^{-2} yr^{-1}. To put this figure in context, in a global review by Mendoça et al., (2017) of lakes and reservoirs, whole-system OC burial rates varied from 0.2 to 17,392 g C m^{-2} yr^{-1} with an average value of 250 and a median of 40 g C m^{-2} yr^{-1}. In a global context, the estimated burial rates for Lough Feeagh would be at the upper end of scale due to the combination of substantial hydrological inputs and high inputs of eroded peat soils from the catchment.

The $_pCO_2$ concentrations that we report show that Lough Feeagh was continuously emitting CO_2 during the course of the study. Calculated CO_2 emission from the lake at 282 t C using the $CW03_{bi}$ model accounts for approximately 11% of the fate of OC in the annual budget. At 803 µatm, mean lake $_pCO_2$ concentrations were approximately double that of atmospheric CO_2 levels during 2017 (http://co2now.org/). Temporally, the annual pattern of $_pCO_2$ concentration broadly followed a simple, seasonal pattern, climbing through the Spring and Summer, reaching a peak in late Summer / early Autumn and then falling back again towards Winter. This matches the annual pattern of DOC concentrations in the incoming rivers and emphasises the intimate link between the rate of allochthonous OC input and the rate of OC mineralisation in the lake. This link is further underscored by a sharp decrease of $_pCO_2$ that coincided with a 30-day rain-free period between mid-April and mid-May, where values dipped to the minimum values recorded over the study period (Doyle et al., 2021). This temporary dip in $_pCO_2$ is attributed to an interruption of the OC supply to the lake due to low DOC concentrations

in the incoming rivers coupled with low incoming water flows during this period. $_pCO_2$ concentrations in the lake rapidly rebounded following the return of rain in mid-May.

The flux of CO_2 from lakes to the atmosphere can be estimated from free-water gas measurements through the use of gas exchange models, which rely on a gas transfer coefficient (k) to model gas exchange with the atmosphere. The two models used to calculate the lake CO_2 flux (abbreviated as CC98 and $CW03_{bi}$) were chosen because they are in common use in the literature (e.g. (Staehr et al., 2012; Trolle et al., 2012; Morales-Pineda et al., 2014). They are also relatively simple univariate models that are based solely on wind speed. The limitations of using such models must also be highlighted however (Dugan et al., 2016). For example, the chosen models were developed from SF_6 tracer data collected on relatively small (< 0.20 km^2) and sheltered lakes in the boreal climate zone of North America (Cole & Caraco, 1998; Crusius & Wanninkhof, 2003) and as such all three models are optimised for lower wind speeds than those generally prevalent on Lough Feeagh. While a number of direct flux measurements were obtained for the present study using floating chambers similar to those described by Bastviken et al., (2015), the data were considered insufficient to model k directly and thus calculate a CO_2 flux for the study period. As observational data were unobtainable, k had to be estimated using models.

Carbon emission estimates from the lake varied considerably depending on the model applied. The CC98 model returned an annual emission estimate of 484.8 t C yr^{-1}, a figure that represents approximately 18 % of the estimated carbon fate in the lake. The emission estimate using the CC98 model appears to be quite high, relative to the surface water export and sedimentation of OC, given the oligotrophic status of the lake and its relatively short residence time. By comparison, Lake Ortrasket in Sweden, an oligotrophic, high-DOC lake a with substantial fluvial source of OC and a short residence time, displayed a ratio of approximately 9% mineralisation to OC fate (Jonsson et al., 2001), similar to the ratio calculated from the $CW03_{bi}$ model (11 %). The $CW03_{bi}$ model was considered the optimal choice because the annual emission estimate of 282.0 t C yr^{-1} aligns with other elements of the budget, in particular, the autochthonous contribution of OC to the system.

The $RDOC_{20}$ mineralisation rate for Lough Feeagh, at 0.00014 d^{-1} is quite low, but it is comparable to other oligotrophic systems. For example, an $RDOC_{20}$ of 0.00083 d^{-1} was reported for Sparkling Lake in northern Wisconsin, USA by Hanson et al., (2014b). Ecosystem mineralisation rates reported in the literature vary to a great extent, for

example Sobek (2003) estimated OC mineralisation rates in a Swedish lake to be in the region of 0.001 to 0.003 d^{-1}. Another study investigating long-term degradation experiments have estimated decay rates of 0.0007 d^{-1} for riverine DOC (Hernes & Benner, 2003) and a rate of 0.0008 d^{-1} was estimated for DOC derived from a wetland source (Vähätalo & Wetzel, 2008).

We found that DOC and POC exported from the lake in the Millrace and Salmon Leap rivers together accounted for 61% of the fate of OC in the lake. At 49%, outflowing DOC was the dominant fate of OC, accounting for almost half of the departing OC. The mass of DOC (1321 t C) in the outflowing rivers was approximately 2% greater than the total DOC load imported to the lake within the inflowing rivers. The quantity of exported DOC is intimately linked to the hydrology of the lake. The lake water residence time of 172 days is relatively short and allows little time for processing and mineralisation of DOC, resulting in the proportionately large export of DOC when compared with the other fates of OC in the lake. Similar observations have been made elsewhere, for example, in a study of seven lakes in temperate North America, Hanson et al., (2014a) found that the lakes with the shortest residence times had the greatest surface water export rates. Also, in a global review of OC decay rates in inland waters, Catalán et al., (2016) found that the rate of OC decay is negatively related to water retention time. This suggests a decrease in OC reactivity along the inland waters continuum, in other words the OC pool is gradually losing its most-reactive components as it travels downstream.

The calculated mass of SS exiting Lough Feeagh during the study period was estimated to be 894.4 t yr^{-1} equating to 332 t POC yr^{-1} or 12% of the total OC fate, an amount equivalent to just 25% of the imported POC load. While it is true that some POC will simply flow through the lake, a portion of the POC in the river outflow will also be of autochthonous origin i.e. related to in-lake primary productivity. This substantial decrease, together with the data from the sediment traps, suggests that the bulk of POC entering the lake contributes to the lake sediments. While the long-term C burial rate has not been calculated in this budget, sediment cores from the lake show allochthonous OC burial over millennia (Dalton et al., 2018). Over millennial time scales, lakes have been shown to be second only to peat in terms of organic carbon storage (Buffam et al., 2011). It is reasonable to assume therefore that a proportion of the mobilised catchment OC, formerly in long-term storage in peat soils, returns to long-term storage as lacustrine sediments in the lake basin.

The final, fourth question was to identify the implications of the study in terms of catchment scale C processing. The allochthonous OC budget of Lough Feeagh is influenced by a number of key geographic factors that determine both the magnitude and partitioning of the loads entering the lake and the ultimate fate of OC within the lake. The location of Lough Feeagh on Northern Europe's rainy Atlantic margins establishes the catchment's dynamic and spatey hydrology. The high rainfall levels have also ensured that peat soils blanket the catchment and govern the considerable fluxes of DOC and POC entering the lake. The catchment's hydrology and morphology also regulates the lake's low residence time of barely half a year, which allows most of the DOC entering the lake to simply flow through the system and out to the ocean. Heavier carbon particulates, brought in by the rivers in suspension settle out in the lake and make up to 30% of the total OC fate in the lake. Long-term OC storage or burial in the lake sediment was not quantified in this study, and burial rates across European lakes vary by up to 3 orders of magnitude (Kastowski et al., 2011). The proportion of OC falling as sediment in Lough Feeagh (roughly one third) appears to be quite large in comparison to other oligotrophic systems (e.g. Jonsson et al., 2001). Similar ratios appear more common in mesotrophic and hyper-eutrophic systems (Likens., 1985; Dillon and Molot., 1997). While direct comparisons with other lakes are problematical, the high relative proportion of sedimentation can be explained by the equally high proportion of peat-derived material being carried into the lake. It is presumed that a substantial portion of the outflowing POC is predominantly bacteria, phytoplankton and alga of autochthonous origin. The relatively low mineralisation rate of DOC in the lake may be explained by a number of factors, including the low hydrologic residence time, low lake productivity and a high recalcitrance of the allochthonous DOC load, being largely derived from humic, peaty material.

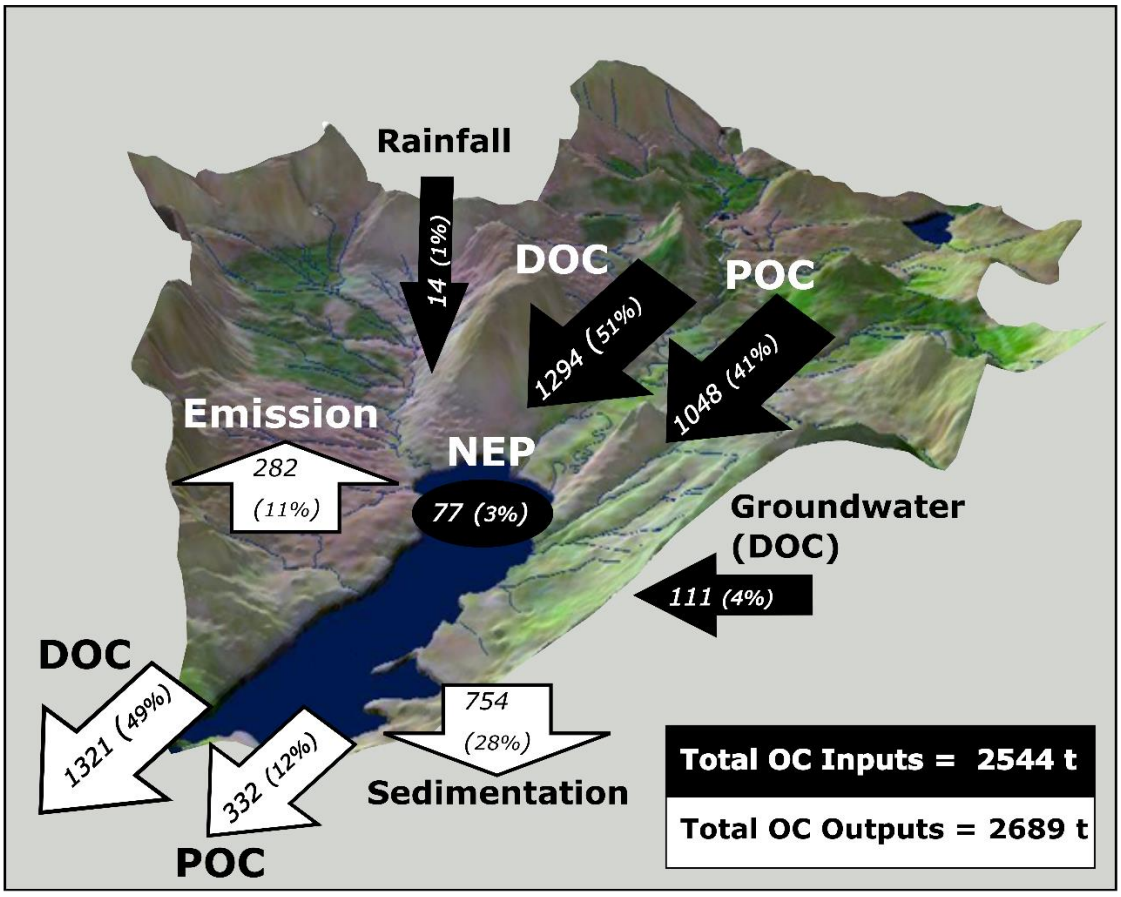

Figure 5.5 Organic Carbon budget of Lough Feeagh. Black arrows pointing toward the lake represent allochthonous inputs or loads, and white arrows pointing away from the lake represent outputs or fates. Autochthonous C, calculated from Net Ecosystem Production (black ellipse) is also shown as a load within the lake. The numbers show the total tons of C for the study period (2017). Percentages indicate the average fraction of inputs and outputs represented by each of the budget elements. DOC: dissolved organic C, POC: particulate organic C, NEP: Net Ecosystem Production.

5.6 Conclusion

In broad terms our study showed that this oligotrophic humic lake overturned approximately 2500 tonnes of C during 2017. It found that the high hydrological inputs of OC dominated the budget and that by far the most important source of OC to the lake was DOC, comprising approximately 51% of the incoming C load. More importantly much of this dissolved fraction flowed through the lake, as DOC also comprised approximately 49% of total exports, thus representing C that would become available in downstream aquatic systems. Our budget for Lough Feeagh also underscored the substantial fraction of OC that entered the lake as POC and settled out as sediment, contributing to long-term C stores in the system. An investigation of long-term carbon

burial rates would establish the role of this mechanism for removal from the global carbon cycle. While there was some uncertainty in the atmospheric emissions estimate used for this study, we also confirmed that emissions were similar to those measured from other sites. Overall, the study fills knowledge gaps in our understanding of the fate of C in humic temperate systems, especially those in peatland catchments.

5.7 Acknowledgements

The long-term environmental monitoring programme in Burrishoole is facilitated by the technical staff of the Marine Institute Newport (Joseph Cooney, Pat Hughes, Michael Murphy, Pat Nixon, Davy Sweeney) and Martin Rouen (Lakeland Instrumentation Ltd.). Russell Poole provides logistical support. The work on Lough Feeagh was only possible thanks to technical support from Allison Murdoch (Centre for Freshwater and Environmental Studies, Dundalk Institute of Technology, Co Louth, Ireland). This work was carried out with the support of the Marine Institute and funded under the Marine Research Programme by the Irish Government (Cullen Fellowships No. CF/15/05).

6.0 Synthesis

6.1 Introduction

All life on the planet is in some way dependent on water. It provides habitats, is the medium for biochemical reactions, electrochemical transformations, reproduction, transport, and many other essential services to biota (Likens, 2009). The relative extent and volume of freshwater lakes and rivers are small — comprising ~3% of the terrestrial surface of the Earth — however, their importance and value to humans is immense (Wetzel, 2001). Inland waters are used by humans for many functions, including, a source of drinking water, transportation, a food source, recreation, and aesthetics (Likens, 2009). Historically, inland waters formed the cradle for the earliest civilisations and presently, over 50% of the global population lives within 3 km of a freshwater body (Kummu et al., 2011). However, human proximity to natural inland waters has, in many locations, had a detrimental effect, and currently, freshwater ecosystems are much degraded as a result of human activities. Activities such as urbanisation, agriculture, and industrial development have caused increased impacts of freshwater ecosystem services (Dodds et al., 2013)

Of even greater concern however is the discovery, in recent decades, of the human-caused unbalancing of the global carbon cycle (Curtis & Gough, 2018; Kirschbaum et al., 2019), and subsequent global warming. One major effect of global warming is its disruption to the global hydrological cycle (Tapiador et al., 2016; Szilagyi, 2018). A more rapidly changing hydrologic cycle is predicted as the planet warms, a warming which is generating higher rates of evapotranspiration and increased rainfall across many regions. Global climate models (GCMs) suggest that climate warming will lead to a 10 to 40% increase in surface runoff by mid-century (Milly et al., 2005; Knutson et al., 2013; Knutti & Sedlacek, 2013). These global changes to rainfall and temperature patterns have concerning implications for many ecosystems, especially those that depend on delicately balanced climatic conditions. Blanket peatlands in temperate maritime climates are an excellent example, depending, as they do, on a climate ‘sweetspot’ where precipitation exceeds potential evaporation by factor of 3 to 1 (Wieder & Vitt, 2006). Blanket peatlands are hotspots of C capture and storage in the landscape, for example, in Ireland, up to 75% of soil C storage occurs in peatlands, a large proportion of which are blanket peatlands (Holden & Connolly, 2011; Renou-Wilson et al., 2011). It is now well established that blanket peatlands are under threat from a range of anthropogenic pressures (Renou-Wilson et al., 2011), including direct loss of C related to directional climate change (Gallego-Sala & Prentice, 2013).

By far, the most dominant pathways of C loss from blanket peatlands are via dissolved and particulate OC in streams and rivers that drain these terrestrial C stores (Hope et al., 1997a; Tipping et al., 1997). Over the last 20 years or so, increasing trends in fluvial DOC concentrations have been observed in rivers and streams draining many peatland catchments (Hongve et al., 2004; Evans et al., 2005; Jennings et al., 2006; Monteith et al., 2007; Worrall and Burt, 2007; Erlandsson et al., 2008). While a number of theories have been proposed to explain this trend, such as a recovery from acidification (Monteith et al., 2007), it has been linked to changes in the climatic drivers of DOC export. These drivers include precipitation patterns (Hongve et al., 2004; Erlandsson et al., 2008) increasing temperature (Freeman et al., 2001; Preston et al., 2011) and the increasing frequency of drought events (Clark et al.,2005; Jennings et al., 2006). Also, the expected changes in climate that have been predicted for Ireland include higher ambient air and water temperatures throughout the year, higher winter streamflow and an increasing depth of the water table during the summer (Dwyer, 2012; Nolan, 2015). This combination of effects has been demonstrated to potentially increase fluvial DOC export (Naden et al., 2010).

The observation of an increasing trend in DOC concentrations in tandem with the potential destabilisation of the terrestrial stores of C, locked up in blanket peatlands, has potential negative consequences for downstream aquatic habitats. Changes in the rate of DOC input to an aquatic system will simultaneously effect the system's physical, chemical and biological domains in many ways, and the effects may also interlink across these domains (Jones, 1998). One important physical change associated with increasing DOC concentration is a marked increase in the potential to absorb light energy within the water column, resulting in an increase in water temperature (Wetzel, 2001). Chemically, an increase in humic substances, a major constituent of DOC derived from peatland waters, has the potential to further lower the pH of these aquatic systems (Turner et al., 2016). Biologically, increasing DOC concentrations have the potential to upset the autotrophic / heterotrophic balance of aquatic systems as heterotrophic bacteria exploit increasing supplies of dissolved organic matter entering aquatic systems e.g. (Pace et al., 2004; Cole et al., 2006). These examples are just a few of the many potential effects of increasing aquatic DOC concentrations at an ecosystem-scale.

There is an increasing awareness of how aquatic systems act as active zones of organic matter transformation, CO_2 emissions and carbon burial and not, as simple passive 'pipes' for organic carbon transport (e.g. Cole et al., 2007; Battin et al., 2009; Tranvik et al.,

2009). For ecosystems such as blanket peatlands, DOC and POC export represent both a direct loss of C and, if it is subsequently converted to CO_2 or CH_4, a pathway for GHG emissions. Globally, the equivalent to almost 20% of global anthropogenic fossil fuel emissions has been estimated to have been emitted every year from lakes and impoundments (DelSontro et al., 2018). Yet despite the high level understanding outlined above, the knowledge of OC processing in aquatic systems appears to be weighted towards particular regions and water-body types, for example high-latitude boreal lakes and large river systems (Evans & Thomas, 2016). It is important therefore, to understand more thoroughly the role of specific ecosystems, in this case blanket peatlands, and specific climate systems in OC processing. This is relevant in the wider context of national and global estimates of GHG emissions and also in the more focused context of the effects of changes in OC transport and cycling to aquatic ecosystem function.

The work described in this thesis, therefore improves the knowledge and understanding of aquatic C cycling in a temperate peatland catchment. Each of the main chapters in the dissertation, namely chapters 3, 4 and 5, offers a complementary set of studies describing a range of processes affecting the cycling and fate of terrigenous-derived OC within the aquatic Burrishoole catchment. Chapter 3 explored the intricacies of OC export from a peatland catchment and examined the processes that drive the variance in export over a range of time scales. Chapter 4 presents an investigation of the temporal variation of $_pCO_2$ in Lough Feeagh's surface waters during a 10-month study period in 2017. The principal environmental drivers of $_pCO_2$ in the system were also determined and the magnitude of CO_2 evasion from the lake was calculated over the study period. In chapter 5, an organic carbon budget for Lough Feeagh was expounded. The major terms of the budget, such as aquatic inputs and outputs, sedimentation and CO_2 evasion were measured directly while some minor terms were estimated from relevant literature values. The following sections discuss the broader implications of the findings from each of these studies.

6.2 Summary of findings

The overarching aim of the research undertaken for this dissertation was to quantify the major fluxes of OC being imported, exported and processed within Lough Feeagh, and to uncover the main drivers of these fluxes. These studies, collectively intend to improve the knowledge and understanding of the cycling of aquatic OC in a temperate, peatland catchment. It is considered that the three main studies presented in this thesis, taken together, have achieved this aim and have added original and relevant knowledge to this important environmental topic. The studies have also brought to light aspects of lake and

river OC cycling that somewhat differ to processes described in other climate zones and ecosystems, due, in no small part, to the unpredictability of the local climate.

6.2.1 Analysis of the transport of DOC in upland streams

In Chapter 3, the analysis of aquatic export of DOC from the Burrishoole catchment to Lough Feeagh, an average yield of 14.8 t C km^2 yr^{-1} was reported from the catchment. This value equates to an average mass of approximately 1180 t C yr^{-1} entering the lake as DOC each year, over the six years of analysis. Regular, strong, annual peaks in stream DOC during the late summer / early autumn were found to be an established pattern. One result of note in this analysis, which also has implications for the other two studies, is the variation in yield over the six years (2011 to 2016), which ranged from a minimum of 11.8 t C km^2 in 2013 to a maximum of 18.5 t C km^2 in 2011. These figures show a standard deviation (σ) of 2.29 t C km^2 with a variance (σ^2) of 5.27 t C km^2 in yield which equates to a variance of approximately 420 t C over the six years of the study. The 2017 DOC import estimate of 1294 t C, reported in the OC budget in Chapter 5, while greater than average, falls within the observed year-to-year variance.

The results of the OC budget presented in Chapter 5 showed that surface-water DOC import was the greatest source of allochthonous OC to the lake, amounting to 51% of the total OC input during 2017. When POC is included, the total surface-water fluvial OC load equalled 92% for that year. While there are a number of other lake OC budgets that show high fluvial OC lake inputs (e.g. Jonsson et al., 2001), the dominance of surface-water fluvial allochthonous OC import to Lough Feeagh is quite striking. The dominance of DOC import, within the overall budget, further emphasises the year-to-year variance of this OC source to the lake. The possible variation in DOC import of up to 420 t C per year shown in Chapter 3 (and potentially a similar, relative, variation in year-to-year POC import) has, presumably, a major effect on in-lake OC processing. This includes fuelling the lake food web by providing a substrate for heterotrophic production (Hulatt et al., 2014), affecting the lake's light regime (Kritzberg et al., 2014), and thermal regime (Forsius et al., 2010). These major observed yearly variations in DOC import will also influence rates of CO_2 emission, carbon sedimentation and fluvial OC export from the lake.

The observed, and noteworthy, year-to-year variation in fluvial DOC import to the lake also highlights the importance of understanding the underlying mechanisms driving these variations. The results outlined in Chapter 3 showed that the principal drivers of DOC

variance in the incoming rivers were soil temperature, SMD (soil moisture deficit) / river discharge, and the weekly mean NAO (North Atlantic Oscillation) values. These findings emphasise how drivers which operate at both a local and regional spatial scale, and also at different temporal scales, influence the amount of OC being transported in the Burrishoole catchment. These different drivers, working together, lead directly to variability in aquatic DOC concentrations in the catchment rivers that ultimately affect the organic carbon budget of downstream Lough Feeagh. One particular finding in Chapter 3, the statistical connection between the NAO and variation in river-water DOC concentrations, is particularly interesting. This connection copper-fastens the link between climate patterns and aquatic carbon transport in peatland catchments and signals the potential vulnerability of blanket peatlands to climate change.

6.2.2 Drivers of $_pCO_2$ variability in Lough Feeagh

In Chapter 4, CO_2 evasion from Lough Feeagh to the atmosphere over a 10-month study period in 2017 was calculated and the drivers of $_pCO_2$ variability in the lake were investigated. The total estimated carbon emission over the study period ranged between 217 t and 370 t C, depending on the gas transfer model applied. The study showed that Lough Feeagh was supersaturated with CO_2 throughout the study period and was therefore a continuous source of CO_2 to the atmosphere. The variance of $_pCO_2$ was found to be controlled by two principal drivers, namely DOC input to the lake and the Schmidt stability of the water column.

A noteworthy finding of the study was the discovery of a direct link between the regular pattern of strong, annual peaks in DOC concentrations in the incoming streams during the late summer / early autumn (Chapter 3) and a synchronous annual peak of $_pCO_2$ in the lake (Chapter 4). This finding highlights the close connection between inputs of allochthonous DOC and the biological mineralisation of allochthonous carbon, leading to an excess of CO_2 in lake waters (e.g. Duarte & Prairie 2005; Lapierre et al., 2013). The close connection between the catchment's hydrology and OC processing in the lake was further emphasised during a month-long period of low discharge, when $_pCO_2$ in the lake dropped to its lowest level. An intimate connection has therefore been established between the catchment's hydrology and climate, which drives the lateral transport of OC to the lake, and in-lake mineralisation of OC. While the study, described in Chapter 4 was conducted over a 10-month time period, it is expected that the observed annual variation in DOC import to the lake will influence the year-to-year rate of CO_2 evasion from the lake.

Interestingly, a number of findings in the study highlighted some key differences between aquatic OC processing dynamics in temperate maritime climate zones, in comparison to boreal and continental temperate zones, which dominate the literature. For example, following the peak $_pCO_2$ observed in early September, concentrations declined relatively quickly and coincided with the breakdown of thermal stratification. In other climate zones, the breakdown of thermal stratification has been associated with an increase in $_pCO_2$ (Morales-Pineda et al., 2014). Also, results from the study showed that the regular diel $_pCO_2$ oscillation reported from water bodies in other climate zones due to the changing day-night balance between production and respiration (e.g. Huotari et al., 2009), were generally intermittent and weak in Lough Feeagh over the study period. These key differences in lake $_pCO_2$ processing observed in Lough Feeagh and those in the literature are ascribed to the local temperate maritime climate and very low level of primary production. Chlorophyll *a* in Lough Feeagh rarely exceed 2µg L^{-1}, which indicates that photosynthesis in the euphotic zone is unlikely to lead to large diel variation in $_pCO_2$. The regular rainfall continuously 'tops up' OC levels in the lake's epilimnion, generally ensuring that it is not deprived of allochthonous OC inputs. Also, the often turbulent nature of the lake's water supresses diel $_pCO_2$ oscillation that are so apparent at other lake systems.

6.2.3 The organic carbon budget for Lough Feeagh

An organic carbon budget of Lough Feeagh was presented in Chapter 5. It was constructed using a simple mass balance model and estimated the key OC processing rates in the lake. The total calculated OC load to the lake was estimated to be 2544 t C, of which 51% and 41% were carried into the lake as DOC and POC in surface water respectively, 4% in ground water, 1% in rainwater, and 3% was fixed in the lake as net ecosystem production. The total C exported was estimated to be 2689 t C, of which 49% and 12% were exported as DOC and POC in the surface water outflow respectively, 28% was deposited as sediment and 11% was mineralised and emitted as CO_2 to the atmosphere. The study was, to the best of the author's knowledge, the first OC budget presented for a peatland lake in a temperate maritime climate.

The budget contained a number of findings of note. Surface water imports and exports of OC dominated the budget. Organic Carbon in surface waters equated to 92% of the total import while outgoing OC in surface waters equalled 62% of the total export. This difference (30%) is quite small in comparison to other studies. For example, studies by Dillon & Molot (1997), Algesten et al., (2003) and Tranvik et al., (2009) broadly showed

OC levels reducing by approximately 50% between import and export, while Sobek et al., (2006) reported OC levels reducing by approximately 60%. On the other hand, Einola et al., (2011), in three boreal lakes in Finland, reported OC levels reducing by just 10%. The relatively low loss of OC from import to export for Lough Feeagh reflects both the short residence time (172 days) and the low mineralisation rate observed, highlighting both the high hydrological throughputs and oligotrophic status of the lake.

Of interest also is the finding that 11% of the total OC export was emitted as CO_2, an amount of 282 t C in absolute terms. While this percentage has been found to be comparable to some examples in the literature — Lake Ortrasket in Sweden, an oligotrophic, high-DOC lake a with substantial fluvial source of OC and a short residence time, displayed approximately 9% mineralisation to OC fate (Jonsson et al., 2001) — it is a much smaller percentage than many other reported studies. For example, Sobek et al., (2006) and Algesten et al., (2003) reported mineralisation to OC fate percentages of approximately 43% and 41% respectively. Tranvik et al., (2009) in their estimated carbon budget for all global inland waters, calculated a 48% CO_2 evasion rate. The budget also revealed that NEP in the lake amounted to 77.2 t C over the study period. This amount, approximately 27% of the net CO_2 efflux, is the contribution of aerobic in-lake metabolism. Both the low ratio of emitted CO_2 to OC fate in the lake and low contribution of NEP confirm the lake's unproductive, oligotrophic status.

The budget also revealed that the fate of approximately one third of the OC was sedimentation in the Lough Feeagh basin. While this proportion is quite large in comparison to other oligotrophic systems (Jonsson et al., 2001) it is more common in mesotrophic and hyper-eutrophic systems (Likens., 1985; Dillon & Molot., 1997). While more investigations are warranted, the relatively high proportion of sedimentation may be explained by the equally high proportion of peat-derived material being eroded and carried into the lake during rain events. The budget underscores the substantial fraction of OC that entered the lake as POC and settled out as sediment, contributing to long-term C stores in the system. Overall, the study fills a considerable knowledge gap in the understanding of OC processing in temperate peatland catchments.

6.3 Potential future research

The work presented in this thesis has highlighted a number of data gaps where further investigations are warranted. For example, in the organic budget presented in Chapter 5, OC in rainwater and aerial inputs of OC (wind-blown debris including pollen and leaf-

litter) were calculated using values derived from literature. Both of these terms could be measured directly and thus contribute to the budget completeness. Also, the considerable variation in year-to-year surface water DOC inputs to the lake, that were shown in Chapter 3, are expected to have major implications for annual variation in each of the OC export terms, i.e. OC in surface water outflow, sedimentation and CO_2 emissions. Additional OC whole-lake budgets are therefore justified, which would capture yearly variance and form the basis for OC modelling calibrations, thus assisting and simplifying future budget estimates.

Further investigation of DOC inputs and outputs via groundwater is another possible route of investigation. The study of DOC concentrations in three groundwater wells, carried out as part of the OC budget, showed that the yearly peak of DOC in surface water is mirrored in catchment groundwater. While a more robust calculation of groundwater flows into and out of the lake is desirable, it must be balanced by the knowledge that groundwater flows are difficult to measure directly, and require a great deal of resources and expertise to calculate properly.

In both the chapters on $_pCO_2$ variability and the OC budget of this thesis (Chapters 4 and 5), calculations of the CO_2 emission from the lake were presented. The flux of CO_2 from Lough Feeagh to the atmosphere were estimated using gas exchange models taken from the literature. These models use gas transfer coefficients (k) that were developed on relatively sheltered lakes in the boreal climate zone of North America and were chosen because they are in common use in the literature (e.g. Staehr et al., 2012; Trolle et al., 2012; Morales-Pineda et al., 2014). If, in the future, further investigations of CO_2 emissions were proposed, it would be advantageous to conduct direct flux measurements on the lake, using floating chambers. In addition to being able to calculate a 'bespoke' k value directly for Lough Feeagh, the floating chamber measurements would allow insights into the nuances of the spatial variation of CO_2 emission over the lake surface.

While the OC budget presented in this thesis calculated the amounts of carbon in flux in and out of the lake, no data on the nature of the carbon was proffered. A study of Emission Excitation Matrix scans (EEM's) of DOC inputs and outputs would allow the characterisation of this carbon and provide valuable additional information. For example, EEM's data can reveal the relative concentrations of aquatic humic substances in a sample, elucidating, for example, if the carbon is 'old' and originating from mature peat, or 'young' and originating from recently decayed vegetative matter. Across a catchment,

temporal changes to DOC composition may be determined such as seasonal, yearly and multi-year cycles. Spatial changes to DOC may also be revealed, showing how DOC origin has an influence on its rate of decomposition.

Future carbon budget research in the Burrishoole catchment could also be scaled up to include both aquatic and terrestrial ecosystems. There is an increasing interest in resolving integrated ecosystem carbon budgets which has resulted in a growing number of studies incorporating both aquatic and terrestrial OC budgets (e.g. Stets et al., 2009; Ran et al., 2015). According to Webb et al., (2018) '*the overall importance of aquatic pathways to ecosystem carbon budgets remains unresolved'* and '*at present, aquatic carbon fluxes are inconsistently evaluated in the context of landscape carbon budgets'*. The wider Burrishoole catchment could be used therefore to amalgamate both land-based carbon budgets, such as plantation forestry or blanket peatland terrestrial OC budgets with lake and stream OC budgets.

The installation of an Eddy Covariance (EC) tower would be required if a catchment-scale budget were to be attempted. EC towers are commonly used as a tool to study H_2O budgets and CO_2 and CH_4 emissions in agricultural, forestry and wetland research. An EC tower can directly measure CO_2 and CH_4 emissions from the lake, at high frequency, in all weather conditions. The tower would negate the requirement to measure gas fluxes on the lake using floating chambers, a technique that generally requires calm conditions. Such conditions are relatively rare on the windswept western coast of Ireland, and the turbulent, choppy waters of Lough Feeagh make the use of floating chambers difficult. The flux tower could also be moved periodically to capture CO_2 and CH_4 exchanges on the various ecosystems that make up the Burrishoole catchment.

6.4 Personal Development

Successful limnological studies depend upon an understanding of the interactions of processes in aquatic systems, under a broad range of scientific disciplines, including; physics, chemistry, biology, geology, meteorology, and hydrology. To do limnological research well, studies must incorporate a broad range of specialities holistically in order to make sense of the function, structure, and temporal change of an aquatic system. Limnological investigations draw, quite uniquely, upon a diverse range of skills and also foster teamwork, incorporating groups of scientists with diverse interests and expertise. I believe that the major drivers of my personal development as an environmental scientist

during the course of my study, has been both the diverse and broad range of disciplines that were required to be studied and integrated, and the collaborative nature of the work.

Teamwork was a major element in the successful completion of the three main chapters of this thesis. In addition to this main body of work, I also collaborated on four further research publications during the course of my studies. Two of these publications were based on data from the Burrishoole catchment and two were based on collaborative research from the so-called 'EuroRun' and 'EuroMethane' projects that allowed me to team up with scientists researching similar topics across Europe. The four publications are described and presented in the appendices. My attendance at one of the Global Lake Ecological Observation Network (GLEON) yearly meetings enabled my introduction to scientists that are at the forefront of research developments within lake science. While all of these collaborations were a crucial to broadening and deepening my understanding of the subject of limnology, they were also vital to improving my critical thinking skills and helping to develop my abilities as a scientist.

7 Concluding Statements

This thesis amalgamates three separate studies of C processing and cycling in the Burrishoole catchment and Lough Feeagh. These studies are important from a number of perspectives. Firstly, there is a gap in the literature, where knowledge of C transport and processing in humic lakes in temperate maritime climate zones is poorly understood. These studies contribute to the literature and improve the dearth of knowledge in this area.

Secondly, the work has uncovered some unique and interesting findings. For example, in the first study (Chapter 3), the statistical linking of the NAO to the multi-annual variation of lateral carbon transport, copper-fastens the connection between global climate and C dynamics in peatland catchments. These links are further explored in the second study (Chapter 4), where the annual, single peak of lake $_pCO_2$ – in itself an interesting finding – was explained by incoming DOC from the catchment. The sharp drop of $_pCO_2$ that coincided with a period of drought and reduced DOC input, confirmed the relationship and also signalled how the effects of climate change may impact C processing in the future.

Thirdly, the measurement of $_pCO_2$ in the lake and subsequent modelling of CO_2 emissions that were reported in Chapters 4 and 5 showed that Lough Feeagh was supersaturated with CO_2 and was therefore a continuous source of GHG emission. The calculation of this emission as an element in the OC budget of the lake also helps in the accounting of

waterborne greenhouse gas emissions from peatland ecosystems at a regional and national scale and further informs GHG budgets and policy.

Finally, the work presented in the third study (Chapter 5) is, to the best of the author's knowledge, the first organic carbon budget of a lake in Ireland. The results of the budget highlight the sheer mass of organic C overturned in the lake during a solar cycle and provide valuable insights into the redistribution and ultimate fate of OC in the catchment. This study therefore contributes to the general understanding of OC aquatic cycling in humic systems.

References

Aberg, J., Bergström, A.K., Algesten, G., Söderback, K., & Jansson, M. (2004). A comparison of the carbon balances of a natural lake (L. Örträsket) and a hydroelectric reservoir (L. Skinnmuddselet) in northern Sweden. *Water Research*. 38:531–8.

Åberg, J., Jansson, M., & Jonsson, A. (2010). Importance of water temperature and thermal stratification dynamics for temporal variation of surface water CO_2 in a boreal lake. *Journal of Geophysical Research - Biogeosciences* 115(G2): G02024, doi: 10.1029/2009jg001085.

Abril, G., Bouillon, S., Darchambeau, F., Teodoru, C.R., Marwick, T.R., Tamooh, F., Ochieng Omengo, F., Geeraert, N., Deirmendjian, L., Polsenaere, P., & Borges, A.V. (2015). Technical Note: Large overestimation of pCO_2 calculated from pH and alkalinity in acidic, organic-rich freshwaters. *Biogeosciences.* 12(1):67–78. doi: 10.5194/bg-12-67-2015.

Ågren, A., Buffam, I., Jansson, M. J., & Laudon, H. (2007). Importance of seasonality and small streams for the landscape regulation of dissolved organic carbon export. *Journal of Geophysical Research - Biogeosciences* 112: 1-11.

Aherne, J., & Farrell, E. P. (2002). Deposition of sulphur, nitrogen and acidity in precipitation over Ireland: chemistry, spatial distribution and long-term trends. *Atmospheric Environment* 36: 1379-1389.

Algesten, G., Sobek, S., Bergström, A.-K., Agren, A., Tranvik, L.J., & Jansson, M. (2003). Role of lakes for organic carbon cycling in the boreal zone. *Global Change Biology.* 10: 141–147. doi:10.1111/j.1365-2486.2003.00721.x.

Allott, N., McGinnity, P. & O'Hea, B. (2005). Factors influencing the downstream transport of sediment in the Lough Feeagh catchment, Burrishoole, Co. Mayo, Ireland. *Freshwater Forum* 23: 126-138.174

Alm, J., Schulman, L., Walden, J., Nykänen, H., Martikainen, P.J. & Silvola, J. (1999). Carbon balance of a boreal bog during a year with an exceptionally dry summer. *Ecology* 80(1): 161–174.

Anas, M.U., Scott, K.A., & Wissel, B. (2015). Carbon budgets of boreal lakes: state of knowledge, challenges, and implications. *Environmental Reviews* 23(3): 275-287 https://doi.org/10.1139/er-2014-0074

Andersen, M.R., de Eyto, E., Dillane, M., Poole, R., & Jennings, E. (2020). 13 Years of Storms: An Analysis of the Effects of Storms on Lake Physics on the Atlantic Fringe of Europe. *Water.* 12(2):318.

Andersson, E., & Kumblad, L. (2006). A carbon budget for an oligotrophic clearwater lake in mid-Sweden. *Aquatic Science*. 68(1):52–64.

Andersson, E., & Sobek, S. (2006). Comparison of a Mass Balance and an Ecosystem Model Approach when Evaluating the Carbon Cycling in a Lake Ecosystem. *Ambio; Journal of the Human Environment.* 35(8):476–483.

Apps, M.J., Kurz, W.A., Luxmoore, R.J., Nilsson, L.O., Sedjo, R.A., Schmidt, R., et al. (1993). Boreal forests and tundra. *Water, Air, Soil Pollution*. 70: 39–53. doi:10.1007/BF01104987.

Archer, D., (2010). *The global carbon cycle*, Princeton University Press. Available at: https://books.google.ie/books?id=2OUFwR3NrpkC&dq=The+global+carbon+cycle&lr=&source=gbs_navlinks_s.

Arvola, L., Kortelainen, P., Bergström, I., Kankaala, P., Ojala, A., Pajunen, H., Käki, T., Mäkelä, S., & Rantakari, M. (2002). Carbon pathways through boreal lakes: A multi-scale approach (CARBO). In: Understanding Global Systems from a Finnish Perspective: J. Käyhkö, L. Talve (EDS.).

Arvola, L., Räike, A., Kortelainen, P., & Järvinen, M. (2004). The effect of climate and landuse on TOC concentrations in Finnish rivers, *Boreal Environment Research* 9: 381-387.

Aslyng, H.C., (1965) Evaporation, evapotranspiration and water balance investigations at Copenhagen 1955–64. *Acta Agriculturae Scandinavica* 15: 284-300.

Aufdenkampe, A.K., Mayorga, E., Raymond, P.A., Melack, J.M., Doney, S.C., Alin, S.R., Aalto, R.E., & Yoo, K. (2011). Riverine coupling of biogeochemical cycles between land, oceans, and atmosphere. *Frontiers in Ecology and the Environment*. 9(1):53–60. doi: 10.1890/100014.

Bain, C.G., Bonn, A., Stoneman, R., Chapman, S., Coupar, A., Evans, M., Gearey, B., Howat, M., Joosten, H., Keenleyside, C., Labadz, J., Lindsay, R., Littlewood, N., Lunt, P., Miller, C.J., Moxey, A., Orr, H., Reed, M., Smith, P., Swales, V., Thompson, D.B.A., Thompson, P.S., Van de Noort, R., Wilson, J.D. & Worrall, F. (2011) IUCN UK Commission of Inquiry on Peatlands. IUCN UK Peatland Programme, Edinburgh

Bass, A.M., Waldron, S., Preston, T., & Adams, C.E. (2010). Net pelagic heterotrophy in mesotrophic and oligotrophic basins of a large, temperate lake. *Hydrobiologia* 652: 363-375.

Bastviken, D., Sundgren, I., Natchimuthu, S., Reyier, H., & Gålfalk, M. (2015). Technical Note: Cost-efficient approaches to measure carbon dioxide fluxes and concentrations in terrestrial and aquatic environments using mini loggers. *Biogeosciences.* 12(12):3849–3859.

Bastviken, D., Tranvik, L.J., Downing, J.A., Crill, P.M., & Enrich-Prast, A. (2011). Freshwater Methane Emissions Offset the Continental Carbon Sink. *Science.* 331(6013):50–50.

Battin, T. J., Kaplan, L.A., Findlay, S., Hopkinson, C.S., Marti, E., Packman, A,I. Newbold, J.D., & Sabater, F. (2008), Biophysical controls on organic carbon fluxes in fluvial networks, *Nature Geoscience, 1*(2): 95-100, doi: 10.1038/ngeo101.

Beguería, S., Vicente-Serrano, S.M., Reig, F., & Latorre, B. (2014) Standardized precipitation evapotranspiration index (SPEI) revisited: parameter fitting, evapotranspiration models, tools, datasets and drought monitoring. *International Journal of Climatology* 34 (10), 3001-3023

Belyea, L.R. & Malmer, N., (2004). Carbon sequestration in peatland: patterns and mechanisms of response to climate change. *Global Change Biology* 10: 1043–1052.

Bertilsson, S., & Tranvik, L.J. (1998). Photochemically produced carboxylic acids as substrates for freshwater bacterioplankton. *American Society Limnology Oceanography jnc* 43(5):885–895.

Bertilsson, S., & Tranvik, L.J. (2000). Photochemical transformation of dissolved organic matter in lakes. *Limnology and Oceanography* 45(4): 753 - 762.

Billett, M.F., Palmer, S.M., Hope, D., Deacon, C., Storeton-West, R., Hargreaves, K.J., Flechard, C. & Fowler, D. (2004). Linking land-atmosphere-stream carbon fluxes in a lowland peatland system. *Global Biogeochemical Cycles* 18: 30-39.

Blenckner, T., Adrian, R., Livingstone, D.M., Jennings, E., Weyhenmeyer, G.A., Nic Aonghusa, C., George, D.G., Jankowski, T., Järvinen, M., Nõges, T., Straile, D. & Teubner, K. (2007). Large-scale climatic signatures in lakes across Europe, a meta-analysis. *Global Change Biology* 13: 1313-1314.

Bowling, L.C., & Salonen, K. (1990). Heat uptake and resistance to mixing in small humic forest lakes in southern Finland. *Australian Journal Marine & Freshwater Research* 41: 747-759.

Bragg, O.M., & Tallis, J.H. (2001). The sensitivity of peat-covered upland landscapes. *Catena* 42: 345-360.

Brereton, A .J., Danilov, S.A., & Scott, D. (1996) Agrometerology of grass and grasslands in middle latitudes. Technical note no. 197. World Meterological Organization, Geneva, p.p. 36.

Bruce, L.C., Hamilton, D., Imberger, J., Gal, G., Gophen, M., Zohary, T., & Hambright, K.D. (2006). A numerical simulation of the role of zooplankton in C, N and P cycling in Lake Kinneret, Israel. *Ecological Modelling.* 193(3):412–436.

Buffam, I., Turner, M., Desai, A., Hanson, P., Rusak, J., Lottig, N., Stanley, E., & Carpenter, S. (2011). Integrating Aquatic and Terrestrial Components to Construct a Complete Carbon Budget for a North Temperate Lake District. *Global Change Biology*. 17:1193–1211.

Burt, T.P. (1995). The role of wetlands in runoff generation from headwater catchments. In: J.M. R. Hughes, Heathwaite, A.L. (ed.) *Hydrology and Hydrochemistry of British Wetlands*. John Wiley and Sons, Chichester, 21-38.

Butman, D., Stackpoole, S., Stets, E., McDonald, C.P., Clow, D.W., & Striegl, R.G. (2016). Aquatic carbon cycling in the conterminous United States and implications for terrestrial carbon accounting. *Proceedings of the National Academy of Sciences* 113:58–63.

Byrne, K., Farrell, E.P., Papen, H. & Butterbach-Bahl, K. (2001). The influence of temperature on carbon dioxide production in laboratory columns of virgin and forested blanket peat. *International Peat Journal* 11: 35-42.

Calderó-Pascual, M., de Eyto, E., Jennings, E., Dillane, M., Andersen. M.R., Kelly, S., Wilson, H.L., & McCarthy, V. (2020). Effects of Consecutive Extreme Weather Events on a Temperate Dystrophic Lake: A Detailed Insight into Physical, Chemical and Biological Responses. *Water*. 12(5):1411. https://doi.org/10.3390/w12051411

Canham, C., Pace, M., Papaik, M., Avram, P., Roy, K., Maranger, R., Curran, R., & Spada, D. (2004). A Spatially Explicit Watershed-Scale Analysis Of Dissolved Organic Carbon In Adirondack Lakes.Ecological Applications 14(3) :839–854.

Carignan, R. (1998). Automated determination of carbon dioxide, oxygen, and nitrogen partial pressures in surface waters. *Limnology and Oceanography* 43(5):969–975.

Caverly, E., Kaste, J.M., Hancock, G.S., & Chambers, R. (2013). Dissolved and particulate organic carbon fluxes from an agricultural watershed during consecutive tropical storms. *Geophysical Research Letters* 40:51 47-52. Doi:10.10002/grl.50982

Chantigny, M.H. (2003). Dissolved and water-extractable organic matter in soils: a review on the influence of land use and management practices. *Geoderma* 113: 357-380.

Chapman, S.J. & Thurlow, M. (1998). Peat respiration at low temperatures. *Soil Biology and Biochemistry* 30: 1013-1021.

Charman, D., (2002). *Peatlands and Environmental Change.* John Wiley & Sons, Chichester, UK.

Chatfield, C., (1984) *The analysis of time series: an introduction.* Chapman and Hall: London: 286 pp.

Chmiel, H.E., Kokic, J., Denfeld, B.A., Einarsdóttir, K., Wallin, M.B., Koehler, B., Isidorova, A., Bastviken, D., Ferland, M.È., & Sobek, S. (2016). The role of sediments in the carbon budget of a small boreal lake: Role of Sediments in Lake C Budget. *Limnology and Oceanography* 61(5):1814–1825.

Chow, A., Guo, F., Gao, S., Breuer, R., & Dahlgren, R.A. (2005). Filter pore size selection for characterizing dissolved organic carbon and trihalomethane precursors from soils. *Water Resources*. 39(7): 1255-1264.

Christ, M. J., & David, M.B. (1996) Temperature and moisture effects on the production of dissolved organic carbon in a Spodosol, *Soil Biology and Biochemistry*, 28(9), 1191-1199.

Christensen, T.R., Johansson, T., Olsrud, M., Ström, L., Lindroth, A., Mastepanov, M., Malmer, N., Friborg, T., Crill, P., & Callaghan, T.V. (2007). A catchment-scale carbon and greenhouse gas budget of a subarctic landscape. *Philosophical Transactions of the Royal Society* A.3651643–1656 http://doi.org/10.1098/rsta.2007.2035

Ciais, P., Sabine, C., Bala, G., Bopp, L., Brovkin, V., Canadell, J., et al. (2013). *Carbon and other biogeochemical cycles.* In Climate change 2013: the physical science basis. Edited by T.F. Stocker, D. Qin, G.-K. Plattner, M. Tignor, S.K. Allen, J. Boschung, et al. Cambridge university press, Cambridge, UK. pp. 465–570.

Clair, T.A., Dennis, I.F., Vet, R., & Laudon, H. (2008). Long-term trends in catchment organic carbon and nitrogen exports from three acidified catchments in Nova Scotia, Canada, *Biogeochemistry*, 87(1): 83–99.

Clark, J.M., Chapman, P.J., Adamson, J.K., & Lane, S.N. (2005). Influence of drought-induced acidification on the mobility of dissolved organic carbon in peat soils, *Global Change Biology.* 11,791– 809.

Clark, J.M., Lane, S.N., Chapman, P.J., & Adamson, J.K. (2007) Export of dissolved organic carbon from an upland peatland during storm events: implications for flux estimates, *Journal of Hydrology*. 347: 438—47, 2007.

Clark, J.M., Gallego-Sala, A.V., Allott, T.E.H., Chapman, S.J. et al. (2010a). Assessing the vulnerability of blanket peat to climate change using an ensemble of statistical bioclimatic envelope models, *Climate Research*. 45: 131–150.

Clark, J.M., Bottrell, S.H., Evans, C.D., Monteith, D.T., Bartlett, R., Rose, R., Newton, R.J., & Chapman, P.J. (2010b). The importance of the relationship between scale and process in understanding long-term DOC dynamics, *Science of the Total Environment*, 408: 2768—2775,

Cleveland, R. B., Cleveland, W.S., McRae, J.E., & Terpenning, I. (1990). Stl: A seasonal-trend decomposition procedure based on loess. *Journal of Offical Statistics.* 6(1):3–73.

Clymo, R.S. (1992) Models of Peat Growth. *Suo*. 43:127-36

Cole, J.J., McDowell, W.H., & Likens, G.E. (1984). Sources and Molecular Weight of "Dissolved" Organic Carbon in an Oligotrophic Lake. *Oikos*. 42(1):1–9.

Cole, J.J., Caraco, N.F., Strayer, D.L., Ochs, C., & Nolan, S. (1989). A detailed organic carbon budget as an ecosystem-level calibration of bacterial respiration in an oligotrophic lake during midsummer. *Limnology and Oceanography*. 34(2):286–296. DOI : 10.4319/ lo.1989 .34.2.0286

Cole, J. J., Caraco, N.F., Kling, G.W., & Kratz, T.K. (1994), Carbon dioxide supersaturation in the surface waters of lakes, *Science*, 265(5178), 1568-1570, doi: 10.1126/science.265.5178.1568.

Cole, J.J., & Caraco, N.F. (1998), Atmospheric exchange of carbon dioxide in a low-wind oligotrophic lake measured by the addition of SF6, *Limnology and Oceanography*. *43*(4): 647-656, doi: 10.4319/lo.1998.43.4.0647.

Cole, J.J. (1999). Aquatic Microbiology for Ecosystem Scientists: New and Recycled Paradigms in Ecological Microbiology. *Ecosystems.* 2(3):215–225.

Cole, J.J., Pace, M.L., Carpenter, S.R., & Kitchell, J.F. (2000). Persistence of net heterotrophy inlakes during nutrient addition and food web manipulation. *Limnology and Oceanography* 45: 1718-1730.

Cole, J.J., Carpenter, S.R., Kitchell, J.F., & Pace, M.L. (2002). Pathways of organic carbon utilization in small lakes: Results from a whole-lake 13C addition and coupled model. *Limnology and Oceanography*. 47(6):1664–1675.

Cole, J.J., Carpenter, S.R., Pace, M.L., Van de Bogert, M.C., Kitchell, J.L. & Hodgson, D.R. (2006). Differential support of lake food webs by three types of terrestrial organic carbon. *Ecology Letters* 9: 558-568.

Cole, J.J., Prairie, Y.T., Caraco, N.F., McDowell, W.H., Tranvik, L.J., Striegl, R.G., Duarte, C.M., Kortelainen, P., Downing, J.A., Middelburg, J.J., & Melack, J. (2007). Plumbing the Global Carbon Cycle: Integrating Inland Waters into the Terrestrial Carbon Budget. *Ecosystems.* 10(1):172–185.

Coll, J., Gibb, S.W., & Harrison, J. (2005) Modelling future climates in the Scottish Highlands - an approach integrating local climatic variables and regional climate model outputs. In: Thompson D.B.A., Price M.F., Galbraith C.A. (eds) *Mountains of northern Europe: conservation, management, people and nature*. TSO Scotland, Edinburgh, 103–119

Coll, J., Bourke, D., Skeffington, S.M., & Gormally, M. (2014). Projected loss of active blanket bogs in Ireland. *Climate Research* 59: 103–115. DOI: 10.3354/ cr01202.

Connolly, J., & Holden, N.M. (2009). Mapping peat soils in Ireland: updating the Derived Irish Peat Map. *Irish Geography* 42(3): 343–352.

Connolly, J., Holden, N.M. & Ward, S.M. (2007). Mapping peatlands in Ireland using a rule-based methodology and digital data. *Soil Science Society of America Journal* 71(2): 492–499.

CORINE (2012) Datasets downloaded from the Environmental Protection Agency, Ireland (EPA) Geoportal website. Available online: http://gis.epa.ie/Lydon, K., Smith, G. (2014). Corine Landcover, 2012, Ireland, Final Report. Environmental Protection Agency, Johnstown Castle, Co.Wexford, Ireland. https://www.epa.ie/pubs/data/corinedata/CLC2012_IE_Final_Report.pdf

Creed, I. F., McKnight, D.M., Pellerin, B.A., Green, M.B., Bergamaschi, B.A., Aiken, G.A., Burns, D.A., Findlay, S.E.G., Shanley, J.B., Striegl, G.G., Aulenbach, B.T., Clow, D.W., Laudon, H., McGlynn, B.L., McGuire, K.J., Smith, R.A., & Stackpoole, S.M. (2015) The river as a chemostat: fresh perspectives on dissolved organic matter flowing down the river continuum, *Canadian Journal of Fisheries and Aquatic Sciences*, 72(8), 1272-1285, doi: 10.1139/cjfas-2014-0400.

Cresser, M.S. & Edwards, A. (1987). *Acidification of freshwaters.* Environmental Chemistry Series, Cambridge, 219 pp.

Cruickshank, M.M., Tomlinson, R.W., Devine, P.M., & Milne, R., (1998). Carbon in the vegetation and soils of Northern Ireland. *Biology and Environment– Proceedings of the Royal Irish Academy* 98B(1): 9–21.

Crusius, J., & Wanninkhof, R. (2003), Gas transfer velocities measured at low wind speed over a lake. *Limnology and Oceanography*, *48*(3): 1010-1017, doi: 10.4319/lo.2003.48.3.1010.

Cummins, T., & Farrell, E.P. (2003). Biogeochemical impacts of clearfelling and reforestation on blanket-peatland streams - II. major ions and dissolved organic carbon. *Forest Ecology and Management* 180: 557-570.

Curtis, P. S., & Gough, C. M. (2018) Forest aging, disturbance and the carbon cycle, *New Phytologist*, 219(4), pp. 1188–1193. doi: 10.1111/nph.15227.

Czikowsky, M.J., MacIntyre, S., Tedford, E.W., Vidal, J., & Miller, S.D. (2018). Effects of Wind and Buoyancy on Carbon Dioxide Distribution and Air-Water Flux of a Stratified Temperate Lake. *Journal of Geophysical Research Biogeosciences.* 123(8):2305–2322.

Dalton, C., Sparber, K., & de Eyto, E. (2018). Assessing sedimentation in a temperate dystrophic lake in the NE Atlantic seaboard region. *Journal of Paleolimnology*. 60(2):117–131.

Dalton, C. (2018). Natural capital: An inventory of Irish lakes. *Irish Geography*. 51(1):75–92.

Daniels, S.M., Agnew, C.T., Allott, T.E.H., & Evans, M.G. (2008) Water table variability and runoff generation in an eroded peatland, South Pennines, UK. *Journal of Hydrology* 361: 214–226

Daniels, S.M., Evans, M.G., Agnew, C.T., & Allott, T.E.H. (2008) Sulphur leaching from headwater catchments in an eroded peatland, South Pennines, U.K., *Science of the Total Environment*, 407 (1):481–96.

Davidson, E.A., & Janssens, I.A. (2006) Temperature sensitivity of soil carbon decomposition and feedbacks to climate change, *Nature* 440: 165-173.

Dawson, J.J.C., Billett, M.F., Neal, C., & Hill, S. (2002) A comparison of particulate, dissolved and gaseous carbon in two contrasting upland streams in the UK. *Journal of Hydrology* 257: 226–246. doi:10.1016/S0022-1694(01)00545-5

Dawson, J.J.C., Tetzlaff, D., Speed, M., Hrachowitz, M., & Soulsby, C. (2011). Seasonal controls on DOC dynamics in nested upland catchments in NE Scotland. *Hydrological Processes*. 25(10):1647–1658.

de Eyto, E., Jennings, E., Ryder, E., Sparber, K., Dillane, M., Dalton. C., & Poole, R. (2016). Response of a humic lake ecosystem to an extreme precipitation event: physical, chemical, and biological implications. *Inland Waters.* 6(4):483–498.

de Eyto, E., Doyle, B.C., King, N., Kilbane, T., Finlay, R., Sibigtroth, L., Graham, C., Poole, R., Ryder, E., Dillane, M., & Jennings, E. (2020). Characterisation of salmonid food webs in the rivers and lakes of an Irish peatland ecosystem. *Biology and Environment Proceedings of the Royal Irish Academy.* 120B(1):1–17.

Deemer, B.R., Harrison, J.A., Li, S., Beaulieu, J.J., DelSontro, T., Barros, N., Bezerra-Neto, J.F., Powers, S.M., dos Santos, M.A., & Vonk, J.A. (2016). Greenhouse Gas Emissions from Reservoir Water Surfaces: A New Global Synthesis. *BioScience.* 66(11):949–964.

DeFries, R., & Eshleman, K.N. (2004). Land-use change and hydrologic processes: a major focus for the future. *Hydrological Processes* 18: 2183-2186.

Del Giorgio, P.A., & Peters, R.H. (1994). Patterns in planktonic P:R ratios in lakes: Influence of lake trophy and dissolved organic carbon. *Limnology and Oceanography*. 39(4):772–787.

Del Giorgio, P.A., Cole, J.J., & Cimbleris, A. (1997). Respiration rates in bacteria exceed phytoplankton production in unproductive aquatic systems. *Nature.* 385(6612):148–151.

DelSontro, T., Beaulieu, J.J., & Downing, J.A. (2018). Greenhouse gas emissions from lakes and impoundments: Upscaling in the face of global change: GHG emissions from lakes and impoundments. *Limnology and Oceanography Letters.* 3(3):64–75.

Denfeld, B.A., Baulch, H.M., del Giorgio, P.A., Hampton, S.E., & Karlsson, J. (2018). A synthesis of carbon dioxide and methane dynamics during the ice-covered period of northern lakes: Under-ice CO_2 and CH_4 dynamics. *Limnology and Oceanography Letters.* 3(3):117–131.

Dillon, P.J., & Molot, L.A. (2005). Long-term trends in catchment export and lake retention of dissolved organic carbon, dissolved organic nitrogen, total iron, and total phosphorus: The Dorset, Ontario, study, 1978–1998. *Journal of Geophysical Research Biogeosciences*
https://agupubs.onlinelibrary.wiley.com/doi/abs/10.1029/2004JG000003

Dillon, P.J., & Molot, L.A. (1997). The effect of landscape form on export of dissolved organic carbon, iron, and phosphorus from forested stream catchments. *Water Resources Research* 33: 2591-2600.

Dinsmore, K.J., Billett, M.F., Skiba, U.M., Rees, R.M., & Helfter, C. (2010) Role of the aquatic pathway in the carbon and greenhouse gas budgets of a peatland catchment. *Global Change Biology* 16: 2750 –2762

Dinsmore, K.J., Billett, M.F., & Dyson, K.E. (2013) Temperature and precipitation drive temporal variability in aquatic carbon and GHG concentrations and fluxes in a peatland catchment *Global Change Biology* 19:2133-2148 doi:10.1111/gcb.12209

Dioumaeva, I., Trumbore, S., Schuur, E.A.G., Goulden, M.L., Litvak, M., & Hirsch, A. I. (2002) Decomposition of peat from upland boreal forest: Temperature dependence and sources of respired carbon, *Journal of Geophysical Research,* 107:8222, doi:10.1029/2001JD000848.

Dise, N.B. (2009). Peatland response to global change. *Science* 326(5954): 810–811.

Dodds, W.K., & Cole, J.J. (2007). Expanding the concept of trophic state in aquatic ecosystems: It's not just the autotrophs. *Aquatic Science.* 69(4):427–439.

Dodds, W.K., Perkin, J.S. & Gerken, J.E. (2013) Human Impact on Freshwater Ecosystem Services: A Global Perspective. *Environmental Science and Technology.* 47:16, 9061–9068. https://doi.org/10.1021/es4021052

Douglas, C., Valverde, F.F., & Ryan, J. (2008). Peatland habitat conservation in Ireland. In: Farrell, C.A. and Feehan, J. (Eds), After Wise Use – The Future of Peatlands. Proceedings of the 13th International Peat Congress Tullamore, Co. Offaly, Ireland. The International Peat Society, Finland. pp. 681–685.

Downing, J.A., Prairie, Y.T., Cole J.J., Duarte, C., Marques, M., Tranvik L.J., Striegl, R.G., McDowell, W.H., Kortelainen, P., Caraco N.F., Melack, J.M., & Middelburg, J.J. (2006) The global abundance and size distribution of lakes, ponds, and impoundments. *Limnology and Oceanography,* 51(5), 2006, 2388–2397

Downing, J.A., Cole, J.J., Middelburg, J.J., Striegl, R.G., Duarte, C.M., Kortelainen, P., Prairie, Y.T., & Laube, K.A. (2008). Sediment organic carbon burial in agriculturally eutrophic impoundments over the last century. *Global Biogeochemical Cycles* https://agupubs.onlinelibrary.wiley.com/doi/abs/10.1029/2006GB002854

Doyle, B.C., Dillane, M., de Eyto, E., Cooney, J., Hughes, P., Murphy, M., Nixon, P., Sweeney, D., Poole, R., Ryder, E., and Jennings, E. (2018). Burrishoole catchment water colour measurements, and associated environmental drivers: Marine Institute, Ireland. doi: 10.20393/fa37ec81-7aec-4e9d-92f2-c79ff36716fb,

Doyle, B.C., de Eyto, E., Dillane, M., Poole, R., McCarthy, V., Ryder, E., & Jennings, E. (2019). Synchrony in catchment stream colour levels is driven by both local and regional climate. *Biogeosciences.* 16(5):1053–1071.

Doyle, B.C., de Eyto, E., Dillane, M., McCarthy, V., & Jennings, E. (2021). Late summer peak in $_pCO_2$ corresponds with catchment export of DOC in a temperate, humic lake. *Inland Waters.* (In Publication)

Doyle, G.J., & Ó Críodáin, C., (2003). *Peatlands – fens and bogs.* In: Otte, M.L. (Ed.), Wetlands of Ireland. University College Dublin Press, Dublin, Ireland. pp. 79–108.

Duarte, C. M., & Prairie, Y.T. (2005). Prevalence of heterotrophy and atmospheric CO2 emissions from aquatic ecosystems, *Ecosystems*, 8(7): 862-870, doi: 10.1007/s10021-005-0177-4.

Ducharme-Riel, V., Vachon, D., del Giorgio, P., & Prairie, Y.T. (2015). The Relative Contribution of Winter Under-Ice and Summer Hypolimnetic CO_2 Accumulation to the Annual CO_2 Emissions from Northern Lakes, *Ecosystems*, 18(4), 547-559, doi: 10.1007/s10021-015-9846-0.

Dugan, H.A., Woolway, R.I., Santoso, A.B., Corman, J.R., Jaimes, A., Nodine, E.R., Patil, V.P., Zwart, J.A., Brentrup, J.A., Hetherington, A.L., et al. (2016). Consequences of gas flux model choice on the interpretation of metabolic balance across 15 lakes. *Inland Waters.* 6(4):581–592.

Dunne, S., Hanafin, J., Lynch, P., McGrath, R., Nishimura, E., Nolan, P., Venkata Ratnam, J., Semmler, T., Sweeney. C, .Varghese, S., & Wang, S. (2009). Ireland in a Warmer World—scientific predictions of the Irish climate in the twenty-first century. Environmental Protection Agency, Met Éireann and University College Dublin. http://www.epa.ie/pubs/reports/research/climate/STRIVE_27_Dunne_C4I_web.pdf.

Dwyer, N., (2012). *The Status of Ireland's Climate,* EPA Report No. 26. Environmental Protection Agency, Johnstown Castle, Ireland. Available online: http:// www.met.ie/UserMediaUpl/file/CCRP_26.pdf

Dziedzic, J., Wodka, D., Nowak, P., Warszynski, P., Simon, C., & Kumakiri, L. (2010). Photocatalytic degradation of the humic species as a method of their removal from water – comparison of UV and artificial sunlight irradiation. *Physicochemical problems of mineral processing.* 45: 15-28.

Eaton, J.M., McGoff, N.M., Byrne, K.A., Leahy, P. & Kiely, G., (2008). Land cover change and soil organic carbon stocks in the Republic of Ireland 1851–2000. *Climatic Change* 91(3–4): 317–334.

Einola, E., Rantakari, M., Kankaala, P., Kortelainen, P., Ojala, A., Pajunen, H., et al. (2011). Carbon pools and fluxes in a chain of five boreal lakes: a dry and wet year comparison. *Journal of Geophysical Research Biogeosciences.* 116: G03009. doi:10.1029/2010JG001636.

Einsele, G., Yan J. & Hinderer, M. (2001). Atmospheric carbon burial in modern lake basins and its significance for the global carbon budget. *Global and Planetary Change* 30: 167-195.

Elliott, J. M., Hurley, M.A., & Maberly, S.C. (2000) The emergence period of sea trout fry in a Lake District stream correlates with the North Atlantic Oscillation, *Journal of Fish Biology,* 56: 208-210.

Elsig, J., et al. (2009), Stable isotope constraints on Holocene carbon cycle changes from an Antarctic ice core, *Nature*, 461: 507–510, doi:10.1038/nature08393.

Emery, W. J., & Thomson, R.E. (2004), *Data analysis methods in physical oceanography*, 2nd ed., Elsevier B.V.

Engel, F., Drakare, S., & Weyhenmeyer, G.A. (2019). Environmental conditions for phytoplankton influenced carbon dynamics in boreal lakes. *Aquatic Science.* 81(2):35.

Engel, F. (2020). The role of freshwater phytoplankton in the global carbon cycle (PhD dissertation, Acta Universitatis Upsaliensis). Retrieved from http://urn.kb.se/resolve?urn=urn:nbn:se:uu:diva-418658

EPA. (2005). The Characterisation and Analysis of Ireland's River Basin Districts. National Summary Report (Ireland). Environmental Protection Agency; http://www.wfdireland.ie/Documents/Characterisation%20Report/Ireland_Article_5_WFD.pdf

EPA. (2011). *Water Treatment Manual: Disinfection*, Environmental Protection Agency, Johnstown Castle, Co. Wexford. https://www.epa.ie/pubs/advice/drinkingwater/Disinfection2_web.pdf

EPA. (2019). *Greenhouse Gas Emissions – The current situation*. Website. EPA, Environmental Protection Agency. https://www.epa.ie/ghg/currentsituation. Accessed 28/01/2021

Erlandsson, M., Buffam, I., Fölster, J., Laudon, H., Temnerud, J., Weyhenmeyer, G.A. & Bishop, K. (2008). 35 years of synchrony in the organic matter concentrations of Swedish rivers explained by variation in flow and sulphate. *Global Change Biology* doi:10.1111/j.1365-2486.2008.01551.x.

Eugster, W., Kling, G., Jonas, T., McFadden, J. P., Wüest, A., MacIntyre, S., & Chapin F. S. (2003). CO_2 exchange between air and water in an Arctic Alaskan and midlatitude Swiss lake: Importance of convective mixing, *Journal of Geophysical Resources: Atmosphere*, *108* (D12): 4362, doi: 10.1029/2002JD002653.

Evans, C. D., Page, E.S., Jones, T., Moore, S. Gauci, V., Laiho, R., Hruška, J., Allott, T.E.H., Billett, M.F., Tipping, E., Freeman, C., & Garnett, M.H. (2014), Contrasting vulnerability of drained tropical and high-latitude peatlands to fluvial loss of stored carbon, *Global Biogeochemical Cycles*, 28: 1215–1234.

Evans, C.D., Chapman, P.J., Clark, J.M., Monteith, D.T. & Cresser, M.S. (2006). Alternative explanations for rising dissolved organic carbon export from organic soils. *Global Change Biology* 12: 2044-2053.

Evans, C.D., Monteith, D.T. & Cooper, D.M. (2005). Long-term increases in surface water dissolved organic carbon: observations, possible causes and environmental impacts. *Environmental Pollution* 137: 55-71.

Evans, C.D., & Thomas, D.N., (2016) Controls on the processing and fate of terrestrially-derived organic carbon in aquatic ecosystems: synthesis of special issue, *Aquatic Sciences*, 78: 415 – 418.

Evans, M.G., Burt, T.P., & Holden, J. (1999). Runoff generation and water table fluctuations in blanket peat: evidence from UK data spanning the dry summer of 1995. *Journal of Hydrology* 221: 141-160.

Falkowski, P., Scholes, R. J., Boyle, E., Canadell, J., Canfield, D., Elser, J., Gruber, N., Hibbard, K., Högberg, P., Linder, S., MacKenzie, F. T., Moore, B., Pedersen, T., Rosenthal, Y.. Seitzinger, S., Smetacek, V., & Steffen, W. (2000). The Global Carbon Cycle: A Test of Our Knowledge of Earth as a System. *Science.* 290 (5490): 291–296.

Feehan, J., O'Donovan, G., Renou-Wilson, F. & Wilson, D. (2008). The Bogs of Ireland – An Introduction to the Natural, Cultural and Industrial Heritage of Irish Peatlands. 2nd Edition, Digital Format. University College Dublin, Dublin, Ireland

Fellman, J.B., Miller, M.P., Cory, R.M., D'amore, D.V., & White, D. (2009). Characterizing Dissolved Organic Matter Using PARAFAC Modeling of Fluorescence Spectroscopy: A Comparison of Two Models Environ. *Science and Technology*. 43: 6228–6234.

Fenner, N., Freeman, C., & Reynolds, B. (2005). Observations of a seasonally shifting thermal optimum in peatland carbon-cycling processes; implications for the global carbon cycle and soil enzyme methodologies, *Soil Biology and Biochemistry* 37: 1814-1821.

Fenner, N., & Freeman, C. (2011). Drought-induced carbon loss in peatlands *Nature Geoscience* 4, 895–900 doi:10.1038/ngeo1323

Ferland, M.E, Prairie, Y.T., Teodoru, C., & del Giorgio, P.A. (2014). Linking organic carbon sedimentation, burial efficiency, and long-term accumulation in boreal lakes. *Journal of Geophysical Research Biogeosciences*. 119(5):836–847.

Field, C.B., Raupach, M.R. (Eds). (2004). *The Global Carbon Cycle: Integrating Humans, Climate, and the Natural World*. Island Press. Washington, DC, USA. 568pp. ISBN : 978-1559635271

Findlay, S., Quinn, C.W., Hickey, G., Burrell,G., Downes, M. (2001) Effects of landuse and riparian flowpath on delivery of dissolved organic carbon to streams. *Limnology and Oceanography*. 46: 345 – 355.

Findlay, S. (2005). Increased carbon transport in the Hudson River: unexpected consequence of nitrogen deposition? *Frontiers in Ecology and the Environment.* 3: 133-137.

Folland, C.K., Knight, J., Linderholm, H.W., Fereday, D., Ineson, S., Hurrell, J.W. (2008) The Summer North Atlantic Oscillation: Past, Present, and Future. *Journal of Climate.* 22: 1082 – 1103

Forsius, M., Saloranta, T., Arvola, L., Salo, S., Verta, M., Ala-Opas, P., Rask, M., & Vuorenmaa, J. (2010) Physical and chemical consequences of artificially deepened thermocline in a small humic lake—a paired whole-lake climate change experiment. *Hydrology and Earth System Science* 14:2629–2642

Freeman, C., Evans, C.D., Monteith, D.T., Reynolds, B., & Fenner, N. (2001) Export of organic carbon from peat soils, *Nature*, 412: (6849): 785.

Frost, P.C., Larson J.H., Johnston, C.A., Young, K.C., Maurice, P.A., Lamberti G.A. & Bridgham, S.D. (2006). Landscape predictors of stream dissolved organic matter concentration and physicochemistry in a Lake Superior river watershed. *Aquatic Sciences.* 68: 40-51.

Gallego-Sala, A., & Prentice, I.C. (2013). Blanket peat biome endangered by climate change. *Nature Climate Change* 3(2):152-155 DOI: 10.1038/nclimate1672

Gardner, G. B., Chen, R. F. and Berry, A. (2005). High-resolution measurements of chromophoric dissolved organic matter (CDOM) in the Neponset River Estuary, Boston Harbor, MA. *Marine Chemistry* 96(1-2): 137-154.

Gardiner, M.J. & Radford, T. (1980). Soil associations of Ireland and their land use potential, *Soil Survey Bulletin* No. 36, Dublin.

Gilmour, A.E. (1973). Calculation of väisalä-brunt frequencies and specific volume distributions of sea water. *New Zealand Journal of Marine and Freshwater Research.* 7(3):217–222.

Gorham, E., (1991). Northern peatlands: Role in the carbon cycle and probably responses to climate warming. *Ecological Applications,* 1(2): 182–195.

Grinsted, A., Moore, J.C., & Jevrejeva, S. (2004). Application of the cross wavelet transform and wavelet coherence to geophysical time series, Nonlinear Processes in Geophysics, European Geosciences Union (EGU), 11: (5/6), pp.561–566.

Håkanson, L., & Peters, R.H. (1995). *Predictive Limnology. Methods for Predictive Modelling,* SPB Academic Publishing, Amsterdam, 460 pp.

Hammond, R.F., (1981). *The Peatlands of Ireland.* Soil Survey Bulletin No. 35. An Foras Talúntais, Dublin, Ireland, 649 pp.

Hanson, P.C., Pollard, A.I., Bade, D.L., Predick, K., Carpenter, S.R., & Foley, J.A. (2004). A model of carbon evasion and sedimentation in temperate lakes. *Global Change Biology*. 10(8):1285–1298.

Hanson, P.C., Carpenter, S.R., Armstrong, D.E., Stanley, E.H., Kratz, T.K. (2006). Lake Dissolved Inorganic Carbon and Dissolved Oxygen: Changing Drivers from Days to Decades. *Ecological Monographs.* 76(3):343–363.

Hanson. P.C., Carpenter, S.R., Kimura, N., Wu, C., Cornelius, S.P., & Kratz, T.K. (2008). Evaluation of metabolism models for free-water dissolved oxygen methods in lakes. *Limnology and Oceanography Methods.* 6(9):454–465.

Hanson, P.C., Hamilton, D.P., Stanley, E.H., Preston, N., Langman, O.C., & Kara, E.L. (2011). Fate of Allochthonous Dissolved Organic Carbon in Lakes: A Quantitative Approach. *PLoS ONE*. 6(7). https://www.ncbi.nlm.nih.gov/pmc/articles/PMC3136486/

Hanson, P.C., Buffam, I., Rusak, J.A., Stanley, E.H., & Watras, C. (2014a). Quantifying lake allochthonous organic carbon budgets using a simple equilibrium model. *Limnology and Oceanography.* 59(1):167–181.

Hanson, P.C., Pace, M.L., Carpenter, S.R., Cole, J.J, & Stanley, E. H. (2014b) Integrating Landscape Carbon Cycling: Research Needs for Resolving Organic Carbon Budgets of Lakes. *Ecosystems*., DOI: 10.1007/s10021-014-9826-9

Harriman, R., Watt, A.W., Christie, A.E.G., Moore, D.W., McCartney, A.G. & Taylor, E.M. (2003). Quantifying the effects of forestry practices on the recovery of upland streams and lochs from acidification. *Science of the Total Environment* 310: 101-111.

Harrison, A.F. et al. (2008). Potential effects of climate change on DOC release from three different soil types on the Northern Pennines UK: examination using field manipulation experiments *Global Change Biology* 14:687-702 doi:10.1111/j.1365-2486.2007.01504.x

Hayes, M.H.B. & Clapp, E.C. (2001). Humic Substances: Considerations of compositions, aspects of structure, and environmental influences. *Soil Science:* 166 (11): 723-737

Heathcote, A.J., & Downing, J.A. (2012). Impacts of Eutrophication on Carbon Burial in Freshwater Lakes in an Intensively Agricultural Landscape. *Ecosystems.* 15(1):60–70.

Heathwaite, A.L. & Gottlich, K. (Eds), (2003). *Mires –Process, Exploitation and conservation.* Wiley, Chichester, UK.

Hernes, P.J., & Benner, R. (2003). Photochemical and microbial degradation of dissolved lignin phenols: Implications for the fate of terrigenous dissolved organic matter in marine environments. *Journal of Geophysical Research - Oceans.* 108 (C9). https://agupubs.onlinelibrary.wiley.com/doi/abs/10.1029/2002JC001421

Hessen, D.O., & Tranvik, L.J. (Editors) (1998). *Aquatic humic substances: ecology and biogeochemistry*. Berlin: Springer. ISBN 3-540-63910-1.

Hirsch, R.M. (1979). An evaluation of some record reconstruction techniques, *Water Resource Research,* 15 (6): 1781–1790, https://agupubs.onlinelibrary.wiley.com/doi/pdf/10.1029/WR015i006p01781.

Hoellein, T.J., Breuesewitz, D., & Richardson, D.C. (2013). Revisiting Odum (1956): A synthesis of aquatic ecosystem metabolism. *Liminology and Oceanography.* 58:2089-100.

Hogg, E.H., Lieffers, V.J. & Wein, R.W. (1992). Potential carbon losses from peat profiles: effects of temperature, drought cycles and fire, *Ecological Applications* 2: 298-306.

Holden, J., Chapman, P. & Labadz, J.C. (2004). Artificial drainage of peatlands: hydrological process and wetland restoration. *Progress in Physical Geography* 28: 95-123.

Holden, J., Chapman, P., Evans, M.G., Hubacek, K., Kay, P., & Warburton, J., (2006). Vulnerability of Organic Soils in England and Wales. Final Technical Report. Project SP0532. DEFRA, Leeds, UK.

Holden, N.M., & Connolly, J., (2011). Estimating the carbon stock of a blanket peat region using a peat depth inference model, *Catena*.2011: 86(2), 75–85.

Hongve, D., Riise, G., & Kristiansen, J.F. (2004). Increased colour and organic acid concentrations in Norwegian forest lakes and drinking water - a result of increased precipitation? *Aquatic Sciences* 66: 231-238.

Hongve, D., van Hees, P.A.W. & Lundstrom, U.S. (2000). Dissolved components in precipitation water percolated through forest litter. *European Journal of Soil Science* 51: 667-677.

Hood, J.L., Roy, J.W., & Hayashi, M. (2006). Importance of groundwater in the water balance of an alpine headwater lake. *Geophysical Research Letters.* 33(13). http://doi.wiley.com/10.1029/2006GL026611

Hope, D., Billett, M.F., & Cresser, M.S. (1997a) Exports of organic carbon in two river systems in NE Scotland. *Journal of Hydrology* 193: 61–82.

Hope, D., Billett, M.F., Milne, R., & Brown, T.A.W. (1997b) Exports of organic carbon in British Rivers. *Hydrological Processes* 11: 325–344.

Hope, D., Palmer, S.M., Billett, M.F., & Dawson, J.J.C. (2001). Carbon dioxide and methane oxidation evasion from a temperate peatland stream. *Limnology and Oceanography* 46: 847–857

Hudson, J.J., Dillon, P.J., & Somers, K.M. (2003). Long-term patterns in dissolved organic carbon in boreal lakes: the role of incident radiation, precipitation, air temperature, southern oscillation and acid deposition. *Hydrology and Earth System*

Sciences 7: 390-398.

Hudson, N., Baker, A., & Reynolds, D. (2007). Fluorescence analysis of dissolved organic matter in natural, waste and polluted waters - a review. *River Research and Applications* 23: 631

Hulatt, C.J., Kaartokallio, H., Asmala, E., Autio, R., Stedmon, C.A., Sonninen, E., & Thomas, D.N. (2014). Bioavailability and radiocarbon age of fluvial dissolved organic matter (DOM) from a northern peatland-dominated catchment: effect of land-use change. *Aquatic Science* 76:393–404

Huotari, J., Ojala, A., Peltomaa, E., Pumpanen, J., Hari, P., & Vesala, T. (2009). Temporal variations in surface water CO_2 concentrations in a boreal humic lake base on high-frequency measurements. *Boreal Environmental Research*. 14:48–60.

Hurrell, J.W., Kushnir, Y., Ottersen, G., & Visbeck, M. (2003). An overview of the North Atlantic Oscillation. In: Y. K. J.W. Hurrel, G. Ottersen & M. Visbeck (ed.) *The North Atlantic Oscillation; Climate Significance and Environmental Impacts.* 134. Geophysical Monographs Series, American Geophysical Union, Washington, DC, 1-35.

Hurrell, J.W. & Deser, C. (2009). North Atlantic climate variability: the role of the North Atlantic. *Journal of Marine Systems* 79: 231-244.

Huttunen, J.T., Nykänen, H., Turunen, J. & Martikainen, P.J., (2003). Methane emissions from natural peatlands in the northern boreal zone in Finland, Fennoscandia. *Atmospheric Environment* 37: 147–151.

Iavorivska, L., Boyer, E., & Dewalle, D. (2016). Atmospheric deposition of organic carbon in precipitation. *Atmospheric Environment*. 146: 156-163.

Immirzi, C.P., Maltby, E. & Clymo, R.S., (1992). *The Global Status of Peatlands and Their Role in Carbon Cycling: a Report for Friends of the Earth*. Friends of the Earth, London, UK.

IPCC (2007). Contribution of Working Group I to the Fourth Assessment Report of the Intergovernmental Panel on Climate Change. Cambridge University Press, Cambridge,

United Kingdom and New York, NY, USA.

IPCC (2013). Supplement to the 2006 IPCC Guidelines for National Greenhouse Gas Inventories: Wetlands

IPCC (2014a). Carbon and Other Biogeochemical Cycles. Climate Change 2013 - the Physical Science Basis. pp. 465–570. doi:10.1017/CBO9781107415324.015. hdl:11858/00-001M-0000-0023-E34E-5. ISBN 9781107415324.

IPCC (2014b). WGII Fifth Assessment Report Summary for Policymakers: Climate Change 2014: Impacts, Adaptation, and Vulnerability.

Isaksson, A., Bergstrom, A.K., Blomqvist, P. & Jansson, M. (1999). Bacterial grazing by phagotrophic phytoflagellates in a deep lake in northern Sweden. *Journal of Plankton Research* 21: 247-268.

Jähne, B., Heinz, G., & Dietrich, W. (1987). Measurement of the diffusion coefficients of sparingly soluble gases in water. *Journal of Geophysical Research Oceans.* 92(C10):10767–10776.

Jähne, B., Münnich, K.O., Bösinger, R., Dutzi, A., Huber, W., & Libner, P. (1987). On the parameters influencing air-water gas exchange. *Journal of Geophysical Research Oceans.* 92(C2):1937–1949.

Jansson, M., Bergström, A.K., Blomqvist, P. & Drakare, S. (2000). Allochthonous organic carbon and phytoplankton/bacterioplankton production relationships in lakes. *Ecology* 81: 3250-3255.

Jennings, E., Allott, N., McGinnity, P., Poole, R., Quirke, W., Twomey, H., et al. (2000) The North Atlantic Oscillation: Effects on Freshwater Systems in Ireland. *Biology and Environment: Proceedings of the Royal Irish Academy* 100B, 149–57

Jennings, E., Järvinen, M., Allott, N., & Arvola, L. (2010a) *The impact of the changing climate on the flux of dissolved organic carbon from catchments* In: The impact of climate change on European lakes / [ed] Glen George, Springer, 199-220

Jennings, E., NicAonghusa, C., Allott, N., Naden, P., O'Hea B., Pierson, D. & Schneiderman, E. (2010b). *Future climate change and water colour in Irish peatland*

catchments: results from the CLIME project. Proceedings of National Hydrology Seminar Water Resources in Ireland and Climate Change.

Jennings, E., Jones, S., Arvola, L., Staehr, P., Gaiser, A., Jones, I.D., Weathers, K., Weyhenmeyer, G. A., Chiu, C., & De Eyto, E. (2012) :Effects of weather-related episodic events in lakes: an analysis based on high-frequency data: *Freshwater Biology*, 57 (3). 589-601, doi: 10.1111/j.1365-2427.2011.02729.x.

Jennings, E., de Eyto, E., Moore, T., Dillane, M., Ryder, E., Allott, N., Nic Aonghusa, C., Rouen, M., Poole, R., & Pierson, D.C. (2020) From Highs to Lows: Changes in Dissolved Organic Carbon in a Peatland Catchment and Lake Following Extreme Flow Events. *Water*.12(10):2843. https://doi.org/10.3390/w12102843

Johnson, R.C. & Whitehead, P.G. (1993). An introduction to the research in the Balquhidder experimental catchments. *Journal of Hydrology* 145: 231-238.

Jones, M.B., Donnelly, A., Albanito, F. (2006). Responses of Irish vegetation to future climate change. *Biology and Environment: Proceedings of the Royal Irish Academy* 106B (3): 323–334.

Jones, R.I. (1992). The influence of humic substances on lacustrine planktonic food chains. *Hydrobiologia* 229: 73-91.

Jones, R.I. (1998). *Phytoplankton, primary production and nutrient cycling.* In D.O. Hessen and L.J. Tranvik (eds.), Aquatic humic substances: ecology and biogeochemistry, Springer-Verlag, Berlin Heidelberg, pp.145-175.

Jonsson, A., Aberg, J., & Jansson, M. (2007). Variations in pCO_2 during summer in the surface water of an unproductive lake in northern Sweden. *Tellus B: Chemical and Physical Meteorology* 59(5):797–803.

Jonsson, A., Meili, M., Bergström, A-K., & Jansson, M. (2001). Whole-lake mineralization of allochthonous and autochthonous organic carbon in a large humic lake (örträsket, N. Sweden). *Limnology and Oceanography*. 46(7):1691–1700.

Jonsson, A., Karlsson, J., & Jansson, M. (2003). Sources of Carbon Dioxide Supersaturation in Clearwater and Humic Lakes in Northern Sweden. *Ecosystems.* 6(3):224–235.

Joos, F., & Prentice, C. (2004). *A paleo-perspective on changes in atmospheric CO_2*

and climate, in The Global Carbon Cycle Integrating Humans, Climate and the Natural World (SCOPE series), , edited by C. B. Field and M. R. Raupach, 165-186.

Joosten, H. (2008). *Peatlands and Carbon*. In: Parish, F., Sirin, A.A., Charman, D., et al. (Eds), Assessment on Peatlands, Biodiversity and Climate Change. Global Environment Centre and Wetlands International, Malaysia and Wageningen, The Netherlands. pp. 99–117.

Junger, P., Dantas, F., Nobre, R., Kosten, S., Venticinque, E., Araujo, F.D.C., Sarmento, H., Angelini, R., Terra, I., Gaudêncio, A., et al. (2019). Effects of seasonality, trophic state and landscape properties on CO_2 saturation in low-latitude lakes and reservoirs. *Science of the Total Environment.* 664:283–295.

Junk, G.A., Spalding, R.F., & Richard, J.J. (1980). Areal, vertical and temporal differences in ground water chemistry, II. Organic constituents. *Journal of Environmental Quality*. 9:479–483.

Kasischke, E.S., Christensen, N.L., & Stocks, B.J. (1995). Fire, global warming, and the carbon balance of boreal forests. *Ecological Applications.* 5: 437–451. doi:10.2307/1942034.

Kastowski, M., Hinderer, M., & Vecsei, A. (2011). Long-term carbon burial in European lakes: Analysis andestimate, *Global Biogeochemical Cycles*, 25, GB3019, doi:10.1029/2010GB003874.

Karlsson, J., Jonsson, A. & Jansson, M. (2003). Control of zooplankton dependence on allochthonous organic carbon in humic and clear-water lakes in northern Sweden. *Limnology and Oceanography* 48: 269-276.

Kawasaki, N., & Benner, R. (2006). Bacterial release of dissolved organic matter during cell growth and decline: Molecular origin and composition. *Limnology and Oceanography*. 51(5):2170–2180.

Kay, P., Edwards, AC., & Foulger, M. (2009). A review of the efficacy of contemporary agricultural stewardship measures for ameliorating water pollution problems of key concern to the UK water industry. *Agricultural Systems*, 99 (2-3): 67-75.

Kelly, S., de Eyto, E., Dillane, M., Poole, R., Brett, G., White, M. (2018). Hydrographic maintenance of deep anoxia in a tidally influenced saline lagoon. *Marine and Freshwater Research*. 69(3):432–445.

Kelly, S., Doyle, B.C., de Eyto, E., Dillane, M., McGinnity, P., Poole, R., White, M., & Jennings, E. (2020). Impacts of a record-breaking storm on physical and biogeochemical regimes along a catchment-to-coast continuum. *PLOS ONE.* 15(7):e0235963.

Kelly, C. A., Fee, E., Ramlal, P.S., Rudd, J.W.M., Hesslein, R.H., Anema, C., & Schindler, E.U. (2001). Natural variability of carbon dioxide and net epilimnetic production in the surface waters of boreal lakes of different sizes, *Liminology and Oceanography*, *46*(5): 1054-1064, doi: 10.4319/lo.2001.46.5.1054.

Kiely, G. (1999). Climate change in Ireland from precipitation and streamflow observations. *Advanced Water Resources* 23:141–151

Kiely, J., Diamond, S., Burke, P.J., & Collins, T. (1974). Soil Map of West Mayo, An Foras Talúntais, Dublin.

King, G.M. & Blackburn, T.H. (1996). Controls of methane oxidation in sediments. *Verhandlungen des Internationalen Verein Limnologie.* 25: 25-38

Kirschbaum, M.U.F. (1995). The temperature dependence of soil organic matter decomposition, and the effect of global warming on soil organic C storage, *Soil Biology and Biochemistry* 27: 753-760.

Kirschbaum, M.U.F., Zeng, G., Ximenes, F., Giltrap, D.L. & Zeldis, J.R. (2019). Towards a more complete quantification of the global carbon cycle, *Biogeosciences*, 16(3), pp. 831–846. doi: 10.5194/bg-16-831-2019.

Kirschke, S., Bousquet, P., Ciais, P., Saunois, M. et al. (2013). Three decades of global methane sources and sinks. *Nature Geoscience.* 6: 813–823

Kling, G.W., Kipphut, G.W., Miller, M.M., & O'Brien, W.N. (2000). Integration of lakes and streams in a landscape perspective: the importance of material processing on spatial patterns and temporal coherence: Integration of lakes and streams: effects of material processing. *Freshwater Biology.* 43(3):477–497.

Klump, J., Fitzgerald, S., & Waples, J. (2009). Benthic biogeochemical cycling, nutrient stoichiometry, and carbon and nitrogen mass balances in a eutrophic freshwater bay. *Limnology and Oceanography*. 54. (3):692-712 doi: 10.4319/lo.2009.54.3.0692

Knutson, T. R., Zeng, F. R., & Wittenberg, A. T. (2013). Multimodel assessment of regional surface temperature trends: CMIP3 and CMIP5 twentieth-century simulations. *Journal of Climate*. 26, 8709–8743. doi: 10.1175/Jcli-D-12-00567.1

Knutti, R., & Sedlacek, J. (2013). Robustness and uncertainties in the new CMIP5 climate model projections. *Nature Climate Change.* 3, 369–373. doi: 10.1038/Nclimate1716

Koehler, A.-K., Murphy, K., Kiely, G. & Sottocornola, M., (2009). Seasonal variation of DOC concentration and annual loss of DOC form an Atlantic blanket bog in South Western Ireland. *Biogeochemistry* DOI 10.1007/s10533-009-9333-9:

Köhler, S., Buffam, I., Jonsson, A., & Bishop, K. (2002). Photochemical and microbial processing of streams and soil water dissolved organic matter in a boreal forested catchment in northern Sweden. *Aquatic Sciences* 64: 269-281.

Köppen, W. (1936). *Das geographische System der Klimate*. In:Köppen W, Geiger R (eds) Handbuch der Klimato - logie. Gebrüder Borntraeger, Berlin, p 1−44

Kortelainen, P. (1999). *Occurrence of humic waters.* In: P. E. J. Keskitalo (ed.) Limnology of humic waters. Backhuys, Leiden, The Netherlands. 46-55.

Kortelainen, P., Mattsson, T., Finer, L., Ahtiainen, M., Saukkonen, S., & Sallantaus, T. (2006). Controls on the export of C, N, P and Fe from undisturbed boreal catchments. *Finnish Aquatic Sciences* 68. 453-468.

Kritzberg, E.S., Granéli, W., Björk, J., Brönmark, C., Hallgren, P., Nicolle, A., Persson, A., & Hansson, L-A. (2014). Warming and browning of lakes: consequences for pelagic carbon metabolism and sediment delivery. *Freshwater Biology* 59:325–336

Kummu, M., de Moel, H., Ward, P.J., & Varis, O. (2011). How close do we live to water? a global analysis of population distance to freshwater bodies, *PLoS ONE*, 6(6). doi: 10.1371/journal.pone.0020578.

Kurbatova, J., Li, C., Tatarinov, F., Varlagin, A., Shalukhina, N., & Olchev, A. (2009). Modeling of the carbon dioxide fluxes in European Russia peat bogs *Environmental Research Letters*, 4 (4), 1-5.

Kurz, W.A., Shaw, C.H., Boisvenue, C., Stinson, G., Metsaranta, J., Leckie, D., et al. (2013). Carbon in Canada's boreal forest–a synthesis. *Environmental Review*. 21: 260–292.

Laas, A., Nõges, P., Kõiv, T., & Nõges, T. (2012). High-frequency metabolism study in a large and shallow temperate lake reveals seasonal switching between net autotrophy and net heterotrophy. *Hydrobiologia* 694, 57–74. https://doi.org/10.1007/s10750-012-1131-z

Laas, A., Cremona, F., Meinson, P., Rõõm, E-I., Nõges, T., & Nõges, P. (2016). Summer depth distribution profiles of dissolved CO_2 and O_2 in shallow temperate lakes reveal trophic state and lake type specific differences. *Science of the Total Environment*. 566–567:63–75.

Laine, A., Wilson, D., Kiely, G. & Byrne, K.A. (2007). Methane flux dynamics in an Irish lowland blanket bog. *Plant and Soil:* doi 10.1007/s11104-007-9374-6.

Lapierre, J-F., & del Giorgio, P.A. (2012). Geographical and environmental drivers of regional differences in the lake pCO_2 versus DOC relationship across northern landscapes. *Geophysical Research: Biogeosciences.* 117, G03015.

Lapierre, J-F., Guillemette, F., Berggren, M., & del Giorgio, P.A. (2013). Increases in terrestrially derived carbon stimulate organic carbon processing and CO_2 emissions in boreal aquatic ecosystems. *Nature Communications*. 4(1):1–7.

Lappalainen, E. (Ed.) (1996). *Global Peat Resources.* The International Peat Society, Finland.

Larsen, S., Andersen, T., & Hessen, D.O. (2011). The pCO_2 in boreal lakes: Organic carbon as a universal predictor? *Global Biogeochemical Cycles*. 25, GB2012.

Laudon, H., Kohler, S. & Buffam, I. (2004). Seasonal TOC export from seven boreal catchments in northern Sweden. *Aquatic Sciences* 66: 223-230.

Lewis Jr, W.M. (2011). Global primary production of lakes: 19th Baldi Memorial Lecture. *Inland Waters*. 1(1):1–28.

Likens, G.E. (1979). The role of watershed and airshed in lake metabolism. *Archiv für Hydrobiologie, Beihefte Ergebnisse der Limnologie* 13: 195-211.

Likens, G.E. (1985). *An ecosystem approach to aquatic ecology: Mirror Lake and its environment.* New York: Springer.

Likens, G.E. (Ed.) (2009). *Encyclopedia of Inland Waters.* Academic Press Inc. p.p 2588 ISBN 978-0-12-370626-3

Lindell, M.J., Granéli, H.W., & Tranvik, L.J. (1996). Effects of sunlight on bacterial growth in lakes of different humic content. *Aquatic Microbial Ecology* 11: 135-141.

Lindsay, R., (1995). *Bogs: the Ecology, Classification and Conservation of Ombrotrophic Mires.* Scottish Natural Heritage, Edinburgh, Scotland.

Löfgren, S., Forsius, M., & och Andersen, T. (2003). Climate induced water colour increase in Nordic lakes and streams due to humus, pp. 12. (Report) Nordtest, Tekniikantie 12, FIN-02150 Espoo Finland, Available : www.nordtest.org

Long, C.B., MacDermot, C.V., Morris, J.H., Sleeman, A.G., Tietzsch-Tyler, D., Aldwell, C.R., Daly, D., Flegg, A.M., McArdle, P.M. & Warren, W.P. (1992). *Geology of north Mayo.* Geological Survey of Ireland. Vol. Part, 56 pp.

López-Moreno, J.I. (2010). A multiscalar drought index sensitive to global warming: the standardized precipitation evapotranspiration index. *Journal of climate* 23 (7), 1696-1718

Lund, M., Christensen, T.R., Lindroth, A., & Schubert, P. (2012). Effects of drought conditions on the carbon dioxide dynamics in a temperate peatland. *Environmental Research Letters.* 7: 045704

Maberly, S.C., Barker, P.A., Stott, A.W., & De Ville, M.M. (2013). Catchment productivity controls CO_2 emissions from lakes. *Nature Climate Change.* 3(4):391–394.

Mäkiranta, P., Laiho, R., Fritze, H., Hytones, J., Laine, J., & Minkkinen, K. (2009). Indirect regulation of heterotrophic peat soil respiration by water level via microbial community structure and temperature sensitivity. *Soil Biology and Biochemistry* 41:695–703.

Maloney, K.O., Morris, D.P., Moses, C.O., & Osburn, C.L. (2005). The role of iron and dissolved organic carbon in the absorption of ultraviolet radiation in humic lake water. *Biogeochemistry* 75: 393-407.

Marotta, H., Duarte, C.M., Pinho, L., & Enrich-Prast, A. (2010). Rainfall leads to increased pCO_2 in Brazilian coastal lakes. *Biogeosciences.* 7(5):1607–1614.

Marsh, T.J., Kirby, C., Muchan, K., Barker, L., Henderson, E., & Hannaford, J. (2016). The winter floods of 2015/2016 in the UK - a review. *Centre for Ecology & Hydrology*, Wallingford, UK. 37 pp.

Mattsson, T., Kortelainen, P., & Raike, A. (2005). Export of DOM from boreal catchments: impacts of land use cover and climate. *Biogeochemistry* 76: 373- 394.

May, L., & Place, C. (2005). A GIS-based model of soil erosion and transport. *Freshwater Forum* https://www.fba.org.uk/journals/index.php/FF/article/view/316

Mazzuoli, S., Focardi, S., Bracchini, L., Falcucci, M., Loiselle, S.A. & Rossi, C. (2005). Spatial and temporal characterisations of the degradation of dissolved humic substances in freshwater lake. *Ecological Modelling* 186: 55-61.

McCullough, I.M., Dugan, H.A., Farrell, K.J., Morales-Williams, A.M., Ouyang, Z., Roberts, D., Scordo, F., Bartlett, S.L., Burke, S.M., Doubek, J.P., et al. (2018). Dynamic modeling of organic carbon fates in lake ecosystems. *Ecological Modelling* 386:71–82.

McDonald, S., Bishop, A.G., Prenzler, P.D., & Robard, K. (2004). Analytical chemistry of freshwater humic substances. *Analytica Chimica Acta* 527: 105–124.

McElwain, L., & Sweeney, J. (2003). Climate change in Ireland- recent trends in temperature and precipitation. *Irish Geography*, 36(2): 97-111

McGinnity, P., Jennings, E., de Eyto, E., Allott, N., Samuelsson, P., Rogan, G., Whelan, K., & Cross, T. (2009). Impact of naturally spawning captive-bred Atlantic salmon on wild populations: depressed recruitment and increased risk of climate-mediated extinction. *Proceedings of the Royal Society: Biological Science.* 276(1673):3601–3610.

McKnight, D.M., Harnish, R., Wershaw, R.L., Baron, J.S., & Schiff, S. (1997). Chemical Characteristics of Particulate, Colloidal and Dissolved Organic Material in Loch Vale Watershed, Rocky Mountain National Park. *Biogeochemistry* 36: 99-124.

Mendonça, R., Müller, R.A., Clow, D., Verpoorter, C., Raymond, P., Tranvik, L.J., & Sobek, S. (2017). Organic carbon burial in global lakes and reservoirs. *Nature Communications*. 8(1):1694.

Millennium Ecosystem Assessment (MA). (2005). Ecosystems and Human Well-Being: Synthesis (PDF). Island Press, Washington. 155pp

Milly, P.C.D., Dunne, K.A., & Vecchia, A.V. (2005). Global pattern of trends in streamflow and water availability in a changing climate. *Nature Letters* 428(17): 347 – 350, doi:10.1038/nature04312

Mitchell, G. & McDonald, A.T. (1992). Discoloration of water by peat following induced drought and rainfall simulation. *Water Research* 26: 321-326.

Molot, L.A. & Dillon, P.J. (1996). Storage of terrestrial carbon in boreal lake sediments and evasion to the atmosphere. *Global Biogeochemical Cycles* 10: 483-492.

Monteith, D., Stoddard, J.L., Evans, C.D., de Wit, H.A., Forsius, M., Høgåsen, T., Winander, A., Skjelkvåle, B.L., Jeffries, D.S., Vuorenmaa, J., Keller, B., Kopácek, J. & Vesely, J. (2007). Dissolved organic carbon trends resulting from changes in atmospheric deposition chemistry. *Nature* 450, doi:10.1083/natare06316.

Montgomery, D.C., & Peck, E. A. (1992). *Introduction to linear regression analysis* (2nd ed.). New York: John Wiley & Sons.

Moore, P.D., & Bellamy, D.H. (1974). *Peatlands*. London: Paul Elek Scientific Books Ltd.

Moore, P.D., & Chapman, S.B. (1986). *Methods in Plant Ecology*. Blackwell Scientific.

Moore, T.R., & Jackson, R.J. (1989). Dynamics of dissolved organic carbon in forested and disturbed catchments, Westland, New Zealand: 2. *Larry River Water Resources Research* 25:1331-1339 doi:10.1029/WR025i006p01331

Moore, T.R. (1998). *Dissolved organic carbon: sources, sinks, and fluxes and the role in the soil carbon cycle,* pp 281-292. In R.Lal [ed.], Soil processes and the carbon cycle. CRC Press.

Morales-Pineda, M., Cózar, A., Laiz, I., Úbeda, B., & Gálvez, J.Á. (2014). Daily, biweekly, and seasonal temporal scales of pCO_2 variability in two stratified Mediterranean reservoirs. *Journal of Geophysical Research: Biogeosciences.* 119(4):509–520.

Mulholland, P.J. (2003). *Large-scale patterns in dissolved organic carbon concentration, flux, and sources.* In: S.E.G. Findlay, & R. Sinsabaugh, (ed.) Aquatic ecosystems: Interactivity of dissolved organic matter. Academic Press, San Diego, 139-157.

Naden, P.S., & McDonald, A. (1989). Statistical modelling of water colour in the uplands: the Upper Nidd catchment. *Environmental Pollution* 60: 141-163.

Naden, P.S., Allott, N., Arvola, L., Järvinen, M., Jennings, E., Moore, K., Nic Aonghusa, C., Pierson, D., & Schneiderman, E. (2010). *Modelling the Impacts of Climate Change on Dissolved Organic Carbon.* In: G. Glen (ed.) The Impact of Climate Change on European Lakes Springer, Dordrecht, Heidelberg, London, New York, 221-253.

Natchimuthu, S., Sundgren, I., Gålfalk, M., Klemedtsson, L., & Bastviken, D. (2017). Spatio-temporal variability of lake pCO_2 and CO_2 fluxes in a hemiboreal catchment. *Biogeosciences* 122 (1): 30–49

Neff, J.C., & Hooper, D.U. (2002). Vegetation and climate controls on potential CO_2, DOC and DON production in northern latitude soils. *Global Change Biology* 8:872–84.

NOAA, (2017). National Oceanic and Atmospheric Administration, National weather service, Climate Prediction Centre. http://www.cpc.ncep.noaa.gov/products/ precip /CWlink/pna/nao.shtml.

Nõges, P., Kägu, M., & Nõges, T. (2007). Role of climate and agricultural practice in determining matter discharge into large, shallow Lake Võrtsjärv, Estonia *Hydrobiologia* 581: 125. https://doi.org/10.1007/s10750-006-0504-6

Nolan, P. (2015). *Ensemble of Regional Climate Model Projections for Ireland*. Report No. 159. Environmental Protection Agency, Johnstown Castle, Ireland. ISBN: 978-1-84095-609-2

O'Sullivan, A. (1993). Site synopsis, Owenduff/Nephin Complex. National Parks and Wildlife Service, 51 St Stephens Green, Dublin 2, Ireland.

Odum, H.T. (1956). Primary Production in Flowing Waters. *Limnology and Oceanography.* 1(2):102–117.

Ojala, A., López Bellido, J., Tulonen, T., Kankaala, P. & Huotari, J. (2011). Carbon gas fluxes from a brown-water and a clear-water lake in the boreal zone during a summer with extreme rain events. *Limnology and Oceanography* 56: 61-76.

Oquist, M., Bishop, K., Grelle, A., Klemedtsson, L., Kohler, S., Laudon, H., Lindroth, A., Ottosson Lofvenius, M., Wallin, M.B., & Nilsson, M.B. (2014). The full annual carbon balance of boreal forests is highly sensitive to precipitation. *Environmental Science & Technology Letters* 1:315–19.

Ottersen, G., Planque, B., Bergrano, A., Post, E., Reid, P.C., & Stenseth, N.C. (2001). Ecological Effects of the North Atlantic Oscillation. *Oecologia* 128: 1-14.

Pace, M.L. & Cole, J.J. (2002). Synchronous variation of dissolved organic carbon and color in lakes. *Limnology and Oceanography* 47: 333-342.

Pace, M.L., Cole, J.J., Carpenter, S.R., Kitchell, J.F., Hodgson, J.R., Van de Bogert, M.C., Bade, D.L., Kritzberg, E.S., & Bastviken, D. (2004). Whole-lake carbon-13 additions reveal terrestrial support of aquatic food webs. *Nature* 427: 240-243.

Pace, M.L, & Lovett, G.M. (2012). Primary production: The foundation of ecosystems. *Fundamentals of Ecosystem Science*.:27–51.

Parker, M.M. (1977). Lough Furnace, County Mayo; physical and chemical studies of an Irish saline lake, with reference to the biology of Neomysis integer. PhD Thesis, Dublin University.

Paton, B.E. (2013). *Herald of the Russian Academy of Sciences*. 83: 173. https://doi.org/10.1134/S1019331613020056

Pawson, R.R., Evans, M.G., & Allott, T.E.H.A. (2012). Fluvial carbon flux from headwater peatland streams: significance of particulate carbon flux. *Earth Surface Processes and Landforms.* 37(11):1203–1212.

Perdue, E.M. (1998). *Chemical composition, structure, and metal binding properties.* In: Hessen, D.O. and Tranvik, L. (ed.) Aquatic humic substances. Springer Verlag, Leiden, 41-46.

Poole, W.R., Diserud, O.H., Thorstad, E.B., Durif, C.M., Dolan, C., Sandlund, O.T, Bergesen, K., Rogan, G., Kelly, S., & Vøllestad, L.A. (2018). Long-term variation in numbers and biomass of silver eels being produced in two European river systems. Secor, D., editor. ICES *Journal of Marine Science*. 75(5):1627–1637.

Preston, N., Carpenter, S., Cole, J., & Pace, M. (2008). Airborne carbon deposition on a remote forested lake. *Aquatic Science*. 70:213–224.

Preston, M.D., Eimers, M.C., & Watmough, S.A. (2011). Effect of moisture and temperature variation on DOC release from a peatland: Conflicting results from laboratory, field and historical data analysis. *Science of the Total Environment* 409(7): 1235-1242.

Priestley, C.H.B., & Taylor, R.J. (1972). On the assessment of surface heat flux and evaporation using large-scale parameters, *Monthly Weather Review.* 100:81–2.

R Core Team. (2019). R: A language and environment for statistical computing, R Foundation for statistical Computing, Vienna, Austria, available at :https://www.R-project.org/

Ramlal, P.S., Hecky, R.E., Bootsma, H.A., Schiff, S.L., & Kingdon, M.J. (2003). Sources and Fluxes of Organic Carbon in Lake Malawi/Nyasa. *Journal of Great Lakes Research.* 29:107–120.

Ran, L., Lu, X.X., Yang, H., Li, L., Yu, R., Sun, H., & Han, J. (2015). CO_2 outgassing from the Yellow River network and its implications for riverine carbon cycle. *Journal of Geophysical Research:Biogeosciences* 120:1334–47.

Rantakari, M., & Kortelainen, P. (2005). Interannual variation and climatic regulation of the CO_2 emission from large boreal lakes, *Global Change Biology.*, *11*(8): 1368-1380, doi: 10.1111/j.1365-2486.2005.00982.x.

Rasmussen, J.B., Godbout, L., & Schallenberg, M. (1989). The humic content of lake water and its relationship to watershed and lake morphometry. *Limnology and Oceanography* 34: 1336-1343.

Raymond, P.A., Hartmann, J., Lauerwald, R., Sobek, S., McDonald, C., Hoover, M., Butman, D., Striegl, R., Mayorga, E., Humborg, C., et al. (2013). Global carbon dioxide emissions from inland waters. *Nature.* 503(7476):355–359.

Reed, D.E., Dugan, H.A., Flannery, A.L., & Desai, A.R. (2018). Carbon sink and source dynamics of a eutrophic deep lake using multiple flux observations over multiple years. *Limnology & Oceanography Letters*. 3(3):285–292.

Renou-Wilson, F., Bolger, T., Bullock, C.H., & Convery, F. (2011). *BOGLAND: Sustainable Management of Peatlands in Ireland (REPORT)*. Available at: Secure Archive for Environmental Research Data (SAFER) managed by Environmental Protection Agency Ireland http://erc.epa.ie/safer/resource?id=a07e0103-46da-102f-8c70-b53a025bc1b8

Renou-Wilson, F. (2018). *Peatlands.* In: Creamer R., O'Sullivan L. (eds) *The Soils of Ireland.* World Soils Book Series. Springer, Cham. https://doi.org/10.1007/978-3-319-71189-8_8

Roberts, G. & Crane, S.B. (1997). The effects of clear-felling established forestry on stream-flow losses from the Hore sub-catchment. *Hydrology and Earth System Sciences* 1: 477-482.

Rodgers, M., Xiao, L., O'Connor, M., O'Driscoll, C., & Asam, Z. (2010). Assessment and mitigation of soil and nutrient losses from acid-sensitive forest catchments. *Forests and Water. Coford*, 85-88.

Rockström, J., Steffen,W., Noone, K., Persson, Å., Chapin III, F.S., Lambin, E., Lenton, T.M., Scheffer, M., Folke, C., Schellnhuber, H., Nykvist, B., De Wit, C.A., Hughes, T., van der Leeuw, S., Rodhe, H., Sörlin, S., Snyder, P.K., Costanza, R., Svedin, U., Falkenmark, M., Karlberg, L., Corell, R.W., Fabry, V.J., Hansen, J., Walker, B., Liverman, D., Richardson, K., Crutzen, P., & Foley, J. (2009). Planetary boundaries:exploring the safe operating space for humanity. *Ecology and Society* 14(2): 32. URL: http://www.ecologyandsociety.org/vol14/iss2/art32/

Roehm, C.L., Prairie, Y.T., & del Giorgio, P.A. (2009). The pCO_2 dynamics in lakes in the boreal region of northern Québec, Canada. *Global Biogeochemical Cycles*. 23, GB3013.

Roulet, N., & Moore, T.R. (2006). Environmental chemistry: browning the waters. *Nature* 444: 283-284

Roulet, N.T., Lafleur, P., Richard, P.J.H., Moore, T.R., Humphreys, E.R. & Bubier, J., (2007). Contemporary carbon balance and late Holocene carbon accumulation in a northern peatland. *Global Change Biology* 13: 397–411.

Ryder, E., de Eyto, E., Dillane, M., Poole, R., & Jennings, E. (2014). Identifying the role of environmental drivers in organic carbon export from a forested peat catchment. *Science of the Total Environment.* 490:28–36.

Ryder, E. (2015). Estimating carbon pools and processing in a humic Irish lake. PhD thesis, Dundalk Institute of Technology, Dundalk, Ireland.

Rymszewicz, A., O'Sullivan, J., Bruen, M., Turner, J., Lawler, D., Conroy, E., & Kelly-Quinn, M. (2017). Measurement differences between turbidity instruments, and their implications for suspended sediment concentration and load calculations: A sensor inter-comparison study. *Journal of Environmental Management.* 199:99–108.

Sanders, C.J., Maher, D.T., Tait, D.R., Williams, D., Holloway, C., Sippo, J.Z., & Santos, I.R. (2016). Are global mangrove carbon stocks driven by rainfall? *Journal of Geophysical Research: Biogeosciences* 121:2600–9.

Schelker, J., Eklöf, K., Bishop, K., & Laudon, H. (2012). Effects of forestry operations on dissolved organic carbon concentrations and export in boreal first-order streams. *Journal of Geophysical Research.* ;117:G01011. doi: 10.1029/2011JG001827.

Schilder, J., Bastviken, D., van Hardenbroek, M., Kankaala, P., Rinta, P., Stotter, T., & Heiri, O. (2013). Spatial heterogeneity and lake morphology affect diffusive greenhouse gas emission estimates of lakes, *Geophysical Research Letters. 40*(21), 5752-5756, doi: 10.1002/2013gl057669.

Schmidt, W. (1928). Ueber temperatur und stabilitaetsverhaltnisse von Seen. Geogr Ann A. 10:145–177.

Segers, R. (1998). Methane production and methane consumption: A review of processes underlying wetland methane fluxes. *Biogeochemistry*, 41: 23-51

Sellers, P., Hesslein, R.H., & Kelly, C.A. (1995). Continuous measurement of CO_2 for estimation of air-water fluxes in lakes: An in situ technique, *Limnology and Oceanography*, *40*(3): 575-581, doi: 10.4319/lo.1995.40.3.0575.

Sephton, M., & Smith, S. (2002). *Landforms and Cycles,* Part 2 Cycles: The Open University, Walton Hall, Milton Keynes. ISBN 0 7492 5207 3

Shapiro, J. (1966). The relation of humic color to iron in natural waters. *Verhandlungen des Internationalen Verein Limnologie.* 16: 477–484.

Shaw, P.J. (1994). The effect of pH, dissolved humic substances, and ionic composition on the transfer of iron and phosphate to particulate size fractions in epilimnetic lake water. *Limnology and Oceanography*, 39: 1734 - 1743

Shaw, P.J., Jones, R.I., & DeHaan, H.E. (2000). The influence of humic substances on the molecular weight distributions of phosphate and iron in epilimnetic lake waters. *Freshwater Biology* 45: 383-393.

Sheehy Skeffington, M.J. & O'Connell, C. (1998). Peatlands of Ireland. *Studies in Irish Limnology.* P. Giller (ed.). Dublin, *Societas Internationalis Limnologiae* (SIL). pp. 39-66.

Sheng, Y.W., Smith, L.C., MacDonald, G.M., Kremenetski, K.V., Frey, K.E., Velichko, A.A., Lee, M., Beilman, D.W., & Dubinin, P. (2004). A high resolution GIS-based inventory of the west Siberian peat carbon pool. *Global Biogeochemical Cycles* 18(3): GB3004.

Shiller, A.M., Duan, S.W., van Erp, P., & Bianchi, T.S. (2006). Photo-oxidation of dissolved organic matter in river water and its effect on trace element speciation. *Limnology and Oceanography* 51: 1716-1728.

Shintani, T., de la Fuente, A., Nino, Y., & Imberger, J. (2010). Generalizations of the Wedderburn number: Parameterizing upwelling in stratified lakes55(3), *Limnology and Oceanography* 55(3): 1377-1389, doi: 10.4319/lo.2010.55.3.1377.

Snucins, E. & Gunn, J. (2000). Interannual variation in the thermal structure of clear and colored lakes. *Limnology and Oceanography* 45: 1639-1649.

Sobek, S., Algesten, G., Bergström, A-K., Jansson, M., & Tranvik, L. (2003). The catchment and climate regulation of pCO_2 in boreal lakes. *Global Change Biology*. 9:630–641.

Sobek, S., Tranvik, L.J., & Cole, J.J. (2005). Temperature independence of carbon dioxide supersaturation in global lakes. *Global Biogeochemical Cycles.* 19(2):886–900.

Sobek, S., Söderbäck, B., Karlsson, S., Andersson, E., & Brunberg, A.K. (2006). A Carbon Budget of a Small Humic Lake: An Example of the Importance of Lakes for Organic Matter Cycling in Boreal Catchments. *AMBIO Journal of the Human Environment.* 35(8):469–475.

Sobek, S., Tranvik, L.J., Prairie, Y.T., Kortelainen, P., & Cole J.J. (2007). Patterns and regulation of dissolved organic carbon: an analysis of 7,500 widely distributed lakes. *Limnology and Oceanography* 52: 1208-1219.

Solomon, C.T., Bruesewitz, D.A., Richardson, D.C., Rose, K.C., Van de Bogert, M.C., Hanson, P.C., Kratz, T.K., Larget, B., Adrian, R., Babin, B.L., et al. (2013). Ecosystem respiration: Drivers of daily variability and background respiration in lakes around the globe. *Limnology and Oceanography.* 58(3):849–866.

Sottocornola, M. & Kiely, G., (2010). Hydrometeorological controls on the CO_2 exchange variation in an Irish blanket bog. *Agricultural and Forest Meteorology* 150: 287–297. doi: 10.1013/jargrformet.2009.11.013:

Sparber, K. (2012). Neo and palaeolimnological investigations in a humic and clear water lake in the west of Ireland [PhD thesis]. Limerick, Ireland: Mary Immaculate College, University of Limerick.

Staehr, P.A., Baastrup-Spohr, L., Sand-Jensen, K., & Stedmon, C. (2012). Lake metabolism scales with lake morphometry and catchment conditions. *Aquatic Science.* 74(1):155–169.

Staehr, P.A., Bade, D., Bogert, M.C.V. de, Koch, G.R., Williamson, C., Hanson, P., Cole, J.J., & Kratz, T. (2010). Lake metabolism and the diel oxygen technique: State of the science. *Limnology and Oceanography Methods.* 8(11):628–644.

Staehr, P.A., & Sand-Jensen, K. (2007). Temporal dynamics and regulation of lake metabolism. *Limnology and Oceanography* 52(1):108–120.

Stanley, E.H., Casson, N.J., Christel, S.T., Crawford, J.T., Loken, L.C., & Oliver, S.K. (2016). The ecology of methane in streams and rivers: patterns, controls, and global significance. *Ecological Monographs* 86:146–71.

Stepanauskas, R., Leonardson, L. & Tranvik, L.J. (1999). Bioavailability of wetland-derived DON to freshwater and marine bacterioplankton. *Limnology and Oceanography* 44: 1477-1485.

Stets, E.G., Striegl, R.G., Aiken, G.R., Rosenberry, D.O., & Winter, T.C. (2009). Hydrologic support of carbon dioxide flux revealed by whole-lake carbon budgets. *Journal of Geophysical Research: Biogeosciences* 2005–2012:114.

Striegl, R.G., & Michmerhuizen, C.M. (1998). Hydrologic influence on methane and carbon dioxide dynamics at two north-central Minnesota lakes. *Limnology and Oceanography* 43(7):1519–1529.

Strobel, B.W., Hansen, H.C.B., Borggaard, O.K., Andersen, M.K. & Raulund-Rasmussen, K. (2001). Composition and reactivity of DOC in forest floor soil solutions in relation to tree species and soil type. *Biogeochemistry* 56: 1-26.

Sucker, C. & Krause, K. (2010). Increasing dissolved organic carbon concentrations in freshwater: what is the actual driver? *Biogeosciences and Forestry* 3: 103-108.

Sweeney, J. (2014). Regional weather and climates of the British Isles – Part 6: Ireland. *Weather*, 69(1), 20-27.

Szilagyi, J. (2018). Anthropogenic hydrological cycle disturbance at a regional scale: State-wide evapotranspiration trends (1979–2015) across Nebraska, USA, *Journal of Hydrology*, 557, pp. 600–612. doi: 10.1016/j.jhydrol.2017.12.062

Tanentzap, A.J., Kielstra, B.W., Wilkinson, G.M., Berggren, M., Craig, N., Giorgio, P.A., del Grey, J., Gunn, J.M., Jones, S.E., Karlsson, J., et al. (2017). Terrestrial support of lake food webs: Synthesis reveals controls over cross-ecosystem resource use. *Science Advances.* 3(3):e1601765.

Tapiador, F.J., Behrangi, A., Haddad, Z.S., Katsanos, D. & Castro, M. (2016). Disruptions in precipitation cycles: Attribution to anthropogenic forcing, *Journal of Geophysical Research : Atmospheres,* (121), pp. 2161–2177. doi: 10.1038/175238c0.

Teagasc (2017). Irish Soil Information System (Website) http://gis.teagasc.ie/soils/

Temnerud, J., & Bishop, K., (2005). Spatial variation of streamwater chemistry in two boreal catchments: Implications for environmental assessment, *Environmental Science & Technology*, 39(6), 1463-1469, doi: 10.1021/es040045q.

Tetzlaff, D., Malcolm, I.A. & Soulsby, C. (2007). Influence of forestry, environmental change and climatic variability on the hydrology, hydrochemistry and residence times of upland catchments. *Journal of Hydrology* 346: 93-111.

Thacker, S.A., Tipping, E., Baker, A. & Gondar, D. (2005). Development and application of functional assays for freshwater dissolved organic matter. *Water Research* 39: 4559-4573. 209

Thacker, S.A., Tipping, E., Gondar, D. & Baker, A. (2008). Functional properties of DOM in a stream draining blanket peat. *Science of the Total Environment* 407: 566-573.

Thurman, E.M. (1985). *Organic geochemistry of natural waters*. Junk Publishers, Dordrecht pp.497.

Tipping, E., Marker, A.F.H., Butterwick, C., Collett, G.D., Cranwell, P.A., Ingram, J.K.G., Leach, D.V., Lishman, J.P., Pinder, A.C., Rigg, E., & Simon, B.M. (1997). Organic carbon in the Humber rivers. *Science of the Total Environment*. 194–195:345–355.

Tipping, E. (1981). The absorption of aquatic humic substances by iron oxides. *Geochimica et Cosmochimica Acta* 45(2) 191-199.

Tipping, E., Marker, A.F.H., Butterwick, C., Collett, G.D., Cranwell, P.A., Ingram, J.K.G., Leach, D.V., Lishman, J.P., Pinder, A.C., Rigg, E., & Simon, B.M. (1997). Organic carbon in the Humber rivers. *Science of The Total Environment.* 194–195: 345-355

Tomlinson, R.W. (2005). Soil carbon stocks and changes in the Republic of Ireland. *Journal of Environmental Management* 76: 77–93.

Tranvik, L.J. (1988). Availability of dissolved organic carbon for planktonic carbon for planktonic bacteria in oligotrophic lakes of differing humic content. *Microbial Ecology* 16: 311- 322.

Tranvik, L.J. (1989). Bacterioplankton growth, grazing mortality and quantitative relationship to primary production in a humic and a clearwater lake. *Journal of Plankton Research* 11: 985-1000.

Tranvik, L.J. & Jansson, M. (2002). Climate change - Terrestrial export of organic carbon. *Nature* 415: 861-862.

Tranvik, L.J., Downing, J.A., Cotner, J.B., Loiselle, S.A., Striegl, R.G., Ballatore, T.J., Dillon, P., Finlay, K., Fortino, K., Knoll, L.B., Kortelainen, P.L., Kutser, T., Larsen, S., Laurion, I., Leech, D.M., McCallister, S.L, McKnight, D.M., Melack, J. M., Overholt, E., Porter, J.A., Prairie,Y., Renwick, W.H., Roland, F., Sherman, B.S., Schindler, D.W., Sobek, S., Tremblay, A., Vanni, M.J., Verschoor, A.M., von Wachenfeldt, E., & Weyhenmeyer, G.A. (2006). Lakes and reservoirs as regulators of carbon cycling and climate *Limnology and Oceanography*, 54: 2298–2314

Trenberth, K.E. (1990). Recent observed interdecadal climate changes in the Northern Hemisphere, *Bulletin American Meteorological Society*, 71 (7): 988-993.

Trolle, D., Staehr, P., Davidson, T., Bjerring, R., Lauridsen, T., Søndergaard, M., & Jeppesen, E. (2012). Seasonal Dynamics of CO_2 Flux Across the Surface of Shallow Temperate Lakes. *Ecosystems,* 15(2), 336-347. http://www.jstor.org/stable/41413047

Turner, T.E., Billett, M.F., Baird, A.J., Chapman, P.J., Dinsmore, K.J., & Holden, J. (2016). Regional variation in the biogeochemical and physical characteristics of natural peatland pools. *Science of The Total Environment* : 545-54 : 84-94

Turunen, J., Tomppo, E., Tolonen, K., & Reinikainen, A., (2002). Estimating carbon accumulation rates of undrained mires in Finland – application to boreal and subarctic regions. *Holocene* 12 (1): 69–80.

Urban, N.R., Auer, M.T., Green, S.A., Lu, X., Apul, D.S., Powell, K.D., & Bub, L. (2005). Carbon cycling in Lake Superior. *Journal of Geophysical Reseach: Oceans* https://agupubs.onlinelibrary.wiley.com/doi/abs/10.1029/2003JC002230

Vachon, D., & del Giorgio, P. (2014). Whole-Lake CO_2 Dynamics in Response to Storm Events in Two Morphologically Different Lakes, *Ecosystems*, *17*(8): 1338-1353, doi: 10.1007/s10021-014-9799-8.

Vachon, D., & Prairie, Y.T. (2013). The ecosystem size and shape dependence of gas transfer velocity versus wind speed relationships in lakes, *Canadian Journal Of Fisheries And Aquatic Sciences 70*(12): 1757-1764, doi: 10.1139/cjfas-2013-0241.

Vähätalo, A.V., & Wetzel, R.G. (2008). Long-term photochemical and microbial decomposition of wetland-derived dissolved organic matter with alteration of 13C:12C mass ratio. *Limnology and Oceanography*. 53(4):1387–1392.

Vasander, H. & Kettunen, A. (2006). *Carbon in Boreal peatlands.* In: Wieder, R.K. and Vitt, D.H. (Eds), Boreal Peatland Ecosystems. Springer-Verlag, Berlin, Germany. pp. 165–194.

Venables, W.N. & Ripley, B.D. (2002). *Modern Applied Statistics with S*. Fourth Edition, Springer. ISBN 0-387-95457-0.

Vicente-Serrano, S.M., Beguería, S., & López-Moreno, J.I. (2010). A Multiscalar Drought Index Sensitive to Global Warming: The Standardized Precipitation Evapotranspiration Index. *Journal of Climate.* 23, 1696–1718, https://doi.org/10.1175/2009JCLI2909.1.

Von Wachenfeldt, E., & Tranvik, L.J. (2008). Sedimentation in Boreal Lakes—The Role of Flocculation of Allochthonous Dissolved Organic Matter in the Water Column. *Ecosystems.* 11(5):803–814.

Wanninkhof, R. (1992). Relationship between Wind-Speed and Gas-Exchange over the Ocean. *Journal of Geophysical Research: Oceans, 97*(C5): 7373-7382, doi: 10.1029/92jc00188.

Wanninkhof, R., & Knox, M. (1996). Chemical enhancement of CO_2 exchange in natural waters, *Limnology and Oceanography*. 41(4), 689–697.

Ward, N.D., Bianchi, T.S., Medeiros, P.M., Seidel, M., Richey, J.E., Keil, R.G., & Sawakuchi, H.O. (2017). Where carbon goes when water flows: carbon cycling across the aquatic continuum. *Frontiers in Marine Science* 4:7.

Watts, C.D., Naden, P.S., Machell, J., & Banks, J. (2001). Long term variation in water colour from Yorkshire catchment. *Science of the Total Environment* 278: 57-72.

Webb, J.R., Santos, I.R., Maher, D.T. et al. (2019). The Importance of Aquatic Carbon Fluxes in Net Ecosystem Carbon Budgets: A Catchment-Scale Review. *Ecosystems* 22, 508–527. https://doi.org/10.1007/s10021-018-0284-7

Weider, R.K. & Yavitt, J.B. (1994). Peatlands and global climate change: insights from comparative studies of sites along a latitudinal gradient, *Wetlands* 14: 229-238.

Weir, G. (1996). Sheep overgrazing in the Nephin Begs. M.Sc. Thesis. Trinity College Dublin.

Weiss, R. F. (1974). Carbon dioxide in water and seawater: The solubility of a non-ideal gas, *Marine Chemistry*, 2, 203–215.

Wetzel, R.G. (2001). *Limnology: Lake and river ecosystems.* Third Edition, Academic Press, San Diego, California. pp. 1006.

Weyhenmeyer, G.A., & Bloesch, J. (2001). The pattern of particle flux variability in Swedish and Swiss lakes. *The Science of the Total Environment* 266: 69-78.

Weyhenmeyer, G.A., Fröberg, M., Karltun, E., Khalili, M., Kothawala, D., Temnerud, J., & Tranvik, L.J. (2012a). Selective decay of terrestrial organic carbon during transport from land to sea. *Global Change Biology.* 18(1):349–355.

Weyhenmeyer, G.A., Kortelainen, P., Sobek, S., Müller, R., & Rantakari, M. (2012b). Carbon Dioxide in Boreal Surface Waters: A Comparison of Lakes and Streams. *Ecosystems.* 15(8):1295–1307.

Weyhenmeyer, G.A., Kosten, S., Wallin, M.B., Tranvik, L.J., Jeppesen, E., & Roland, F. (2015). Significant fraction of CO_2 emissions from boreal lakes derived from hydrologic inorganic carbon inputs. *Nature Geoscience.* 8(12):933–936.

White, J., & Doyle, G.J. (1982). The vegetation of Ireland: a catalogue raisonné. *Journal of Life Sciences: Royal Dublin Society* 3: 289–368

Whitfield, C.J., Aherne, J., & Baulch, H.M. (2011). Controls on greenhouse gas concentrations in polymictic headwater lakes in Ireland. *Science of the Total Environment.* 410–411:217–225.

WHO. (2011). *Guidelines for Drinking Water Quality*, 4th. Edition, Annex 1: Water treatment and pathogen control: Process efficiency in achieving safe drinking water, Geneva.

Wieder, R.K., & Vitt, D.H., (Eds). (2006). *Boreal Peatland Ecosystems*. Springer Berlin Heidelberg; http://link.springer.com/10.1007/978-3-540-31913-9.

Wiegner, T.N., & Seitzinger, S.P. (2004). Seasonal Bioavailability of Dissolved Organic Carbon and Nitrogen from Pristine and Polluted Freshwater Wetlands. *Limnology and Oceanography* 49(5): 1703-1712 DOI: 10.4319/lo.2004.49.5.1703

Wik, M., Varner, R.K., Anthony, K.W., MacIntyre, S., & Bastviken, D. (2016). Climate-sensitive northern lakes and ponds are critical components of methane release. *Nature Geoscience* 9: 99 – 105.

Wilkinson, G.M., Buelo, C.D., Cole, J.J., 7 Pace, M.L. (2016). Exogenously produced CO_2 doubles the CO_2 efflux from three north temperate lakes. *Geophysical Research Letters*. 43(5):1996–2003.

Williamson, C.E., Saros, J.E., Vincent, W.F., & Smol, J.P. (2009). Lakes and reservoirs as sentinels, integrators, and regulators of climate change. *Limnology and Oceanography*. 54(part2):2273–2282.

Williamson, C.E., Morris, D.E., Pace, M.L. & Olson, O.G. (1999). Dissolved organic carbon and nutrients as regulators of lake ecosystems: Resurrection of a more integrated paradigm. *Limnology and Oceanography* 44: 795-803.

Winslow, L., Read, J., Woolway, R., Brentrup, J., Leach, T., & Zwart, J. (2014). *rLakeAnalyzer: package for the analysis of lake physics.* R package version 1.4.

Winslow, L.A., Zwart, J.A., Batt, R.D., Dugan, H.A., Woolway, R.I., Corman, J.R., Hanson, P.C., & Read, J.S. (2016). LakeMetabolizer: an R package for estimating lake metabolism from free-water oxygen using diverse statistical models. *Inland Waters.* 6(4):622–636.

Winter, T.C., & Likens, G.E. (2009). *Mirror Lake: Interactions among Air, Land, and Water.* University of California Press.

Winterdahl, M., Erlandsson, M., Futter, M.N., Weyhenmeyer, G.A., & Bishop, K. (2014). Intra-annual variability of organic carbon concentrations in running waters: Drivers along a climatic gradient, *Global Biogeochemical Cycles*, 28(4), 451-464, doi: 10.1002/2013GB004770.

Wood, S.N. (2006). *Generalized Additive Models: An Introduction R.* Chapman and Hall/CRC, Boca Raton, FL, USA, ISBN 1-58488474-6.

Woolway, R.I., Jones, I.D., Hamilton, D.P., Maberly, S.C., Muraoka, K., Read, J.S., Smyth, R.L., & Winslow, L.A. (2015). Automated calculation of surface energy fluxes with high-frequency lake buoy data. *Environmental Modelling & Software*. 70:191–198.

Worrall, F., Burt, T.P., Jeaban, R.Y., Warburton, J., & Shedden, R. (2002). The release of dissolved organic carbon from upland peat. *Hydrological Processes* 16: 3487-3504.

Worrall, F., Burt, T.P., & Adamson, J. (2003). Controls on the chemistry of runoff from an upland peat catchment. *Hydological Processes* 17: 2063-2083.

Worrall, F., & Burt, T.P. (2004). Predicting the future DOC flux from upland peat catchments. *Journal of Hydrology* 300: 126-139.

Worrall, F., Burt, T.P., & Adamson, J. (2006). Long-term changes in hydrological pathways in an upland peat catchment - recovery from severe drought? *Journal of Hydrology* 321: 5-20.

Worrall, F., & Burt, T.P. (2007). Flux of dissolved organic carbon from U.K. rivers. *Global Biogeochemical Cycles*, 21, GB1013, doi:10.1029/2006GB002709.

Worrall, F., Chapman, P., Holden, J., Evans, C., Artz, R., Smith, P., & Grayson, R. (2011). A review of current evidence on carbon fluxes and greenhouse gas emissions from UK peatlands. JNCC Report, No. 442.

Worrall, F., Howden, N.J.K., Burt, T.P., & Bartlett, R. (2018). Declines in the dissolved organic carbon (DOC) concentration and flux from the UK, *Journal of Hydrology.* 556, 775-789, doi: 10.1016/j.jhydrol.2017.12.001.

Xenopoulos, M.A., Lodge, D.M., Frentress, J., Kreps, T.A., Bridgham, S.D., Grossman, E., & Jackson, C.J. (2003). Regional comparisons of watershed determinants of dissolved organic carbon in temperate lakes of the Upper Great Lakes region and selected regions globally. *Limnology and Oceanography* 48: 2321- 2334.

Xu, H., Lan, J., Liu, B., Sheng, E., & Yeager, K.M. (2013). Modern carbon burial in Lake Qinghai, China. *Applied Geochemistry.* 39:150–155.

Yallop, A.R., & Clutterbuck, B. (2009). Land management as a factor controlling dissolved organic carbon release from upland peat soils 1: Spatial variation in DOC productivity. *Science of the Total Environment* Thematic Issue - BioMicroWorld Conference 407(12): 3803-3813.

Yang, H., Andersen, T., Dörsch, P., Tominaga, K., Thrane, J-E., & Hessen, D.O. (2015). Greenhouse gas metabolism in Nordic boreal lakes. *Biogeochemistry.* 126(1):211–225.

Yang, H., Xing, Y., Xie, P., Ni, L., & Rong, K. (2008). Carbon source/sink function of a subtropical, eutrophic lake determined from an overall mass balance and a gas exchange and carbon burial balance. *Environmental Pollution.* 151(3):559–568.

Yu, Z., Loisel, J., Brosseau, D.P., Beilman, D.W., & Hunt, S.J. (2010). Global peatland dynamics since the Last Glacial Maximum. *Geophysical Research Letters,* 37(13): p.L13402. Available at: http://onlinelibrary.wiley.com/doi/10.1029/2010GL043584

Zhang, J., Hudson, J., Neal, R., Sereda, J., Clair, T., Turner, M., Jeffries, D., Dillon, P., Molot, L., Somers, K., & Hesslein, R. (2010). Long-term patterns of dissolved organic carbon in lakes across eastern Canada: Evidence of a pronounced climate effect. *Limnology and Oceanography*., 55(1), 30-42

Zhang, Y., Zhang, B., Wang, X., Junsheng, L., Feng, S., Zhao, Q., Liu, M., & Oin, B. (2007). A study of absorption characteristics of chromophoric dissolved organic matter and particles in Lake Taihu, China. *Hydrobiologia* 592: 105–120.

Zuur, A., Ieno, E.N., Walker, N., Saveliev, A.A., & Smith, G.M. (2009). *Mixed Effects Models and Extensions in Ecology with R.* New York: Springer-Verlag; https://www.springer.com/gp/book/9780387874579

Appendices

Appendix A

Appendix A contains the following paper, de Eyto E, Doyle B, King N, Kilbane T, Finlay R, Sibigtroth L, Graham C, Poole R, Ryder E, Dillane M, Jennings E., (2020) *Characterisation of salmonid food webs in the rivers and lakes of an Irish peatland ecosystem.* Biology and Environment: Proceedings of the Royal Irish Academy, Vol. 120B, No. 1, pp. 1-17. The primary author of this paper was Elvira de Eyto. For this paper Brian Doyle prepared a range of environmental samples for stable isotope analysis, including a sample population of juvenile salmonids. He also assisted the primary author with producing some of the paper's fugures.

Appendix B

Appendix B contains the following paper, Kelly S, Doyle B, de Eyto E, Dillane M, McGinnity P, Poole R, et al. *Impacts of a record-breaking storm on physical and biogeochemical regimes along a catchment-to coast continuum.* (2020). PLoS ONE 15(7): Sean Kelly was the primary author of this paper. Brian Doyle carried out spatial and statistical data analysis on an array of rain-gauge monitors throughout the Burrishoole catchment to elucidate total rainfall volumes within specific time periods and catchment areas. He also assisted the principal author with the production of a number of figures and graphs within the publication and contributed to a portion of the manuscript text.

Appendix C

Appendix C contains the following paper, *Abundance and biogeography of methanogenic and methanotrophic microorganisms across European streams.* (2020). Nagler, M. Praeg, N. Niedrist, G.H. Attermeyer, K. Catalán, N. Pilotto, F. Gutmann Roberts, C. Bors, C. Fenoglio, S. Colls, M. Cauvy-Fraunié, S. Doyle, B. Romero, F. Machalett, B. Fuss, T. Bednařík, A. Klaus, M. Gilbert, P. Lamonica, D. Nydahl, A.C. González-Quijano, C.R. Bistarelli, L.T. Kenderov, L. Piano, E. Mor, JR. Evtimova, V. deEyto, E. Freixa, A. Rulík, M. Pegg, J. Ortega, S.H. Steinle, L. Bodmer, P. Journal of Biogeography; 00:1-14. For this study, which ranged across 16 European streams from northern Spain to northern Sweden and from western Ireland to western Bulgaria, community compositions of methanogenic and methanotrophic microorganisms were described at large spatial scales. Their abundances were linked to potential sediment production and oxidation rates. Brian Doyle chose a suitable location and collected stream sediment core samples for one site in the study. He also assisted in the manuscript editing process.

Appendix D

Appendix D contains the following manuscript, Attermeyer, K, Casas-Ruiz, JP. Fuss, T. Pastor, A. Cauvy-Fraunié, S. Sheath, D. Nydahl, A.C. Doretto, A. Portela, A.P. Doyle, B.C. Simov, N. Gutmann Roberts, C. Niedrist, G.H. Timoner, X. Evtimova, V. Barral-Fraga, L. Bašić, T. Audet, J. Deininger, A. Busst, G, Fenoglio, S. Catalán, N. de Eyto, E. Pilotto, F. Mor, JR. Monteiro, J. Fletcher, D. Noss, C. Colls, M. Nagler, M. Liu, L. González-Quijano, CR. Romero, F. Pansch, N. Ledesma, J.L.J. Pegg, J. Klaus, M. Freixa, A. Herrero Ortega, S. Mendoza-Lera, C. Bednařík, A. Fonvielle, JA. Gilbert, P. Kenderov, L.A. Rulík, M. Bodmer, P. *Substantial carbon dioxide flux changes from day to night across European streams* (2021) Nature Communications Earth & Environment (In Review). This paper presents the results of a Europe wide collaborative study, also known as the EuroRun project, comprising a year-long investigation of day and night-time CO_2 fluxes of running streams. Fluxes were directly measured once per season using drifting chambers in 34 streams across 11 European countries. As lead member of the Irish team, Brian Doyle attended a workshop at the Erken Laboratory, a facility connected to Uppsala University, located at Lake Erken in Norrtälje, Sweden. At the workshop, participants were trained to: assemble the floating chambers, measure CO_2 fluxes using the chambers and to analyse the data. Brian Doyle then conducted the CO_2 flux analysis on two streams in the Burrishoole catchment during 2017.

Regional CO_2 fluxes are important for the understanding of the global carbon cycle and greenhouse gas balances. The aim of the Eurorun project was to assess seasonal and annual CO_2 fluxes from running waters at multiple locations across Europe. The project was the first coordinated European-wide study to examine fluvial CO_2 fluxes. The temporal extent of the sampling regime allowed the comparison of seasonal and diurnal fluvial CO_2 fluxes and the spatial spread of sites allowed the examination of differences between northern and southern Europe. The measurements were conducted with floating chambers equipped with mini-loggers to continuously measure CO_2 in the chamber headspace. Initially the project participants attended a workshop where they constructed a flux chamber and were trained how to measure and analyse their data correctly. Following training, the participants conducted aquatic flux measurements in their home country in different running waters within coordinated periods during the day and night. A unique dataset was generated that allowed the estimation of CO_2 fluxes from a sample of European running waters.

The principal aims of the Eurorun project was to achieve a better estimation and understanding of riverine CO_2 fluxes and their underlying mechanisms, as well as improving current regional and global carbon budgets. Team members in the Eurorun project represented a wide range of European countries including: Ireland, the United Kingdom, France, Germany, Sweden, Bulgaria, Spain, Switzerland, Denmark, Italy, Austria and The Czech Republic. The project began with a workshop, the focus of which was to learn the required knowledge and skills to assemble a proprietary floating chamber to measure and analyse CO_2 fluxes from aquatic environments. The 3-day workshop included practical, hands-on lessons in assembling and building, calibrating and deploying carbon dioxide sensors. There were also demonstrations on the use of software that is distributed with the sensors. At the end of the workshop, each team member had built and tested their own sensor to bring away and use in the field. The workshop also gave the participants opportunity to meet and strengthen collaborations among early careers limnologists. On return to their own countries, each team then performed simultaneous measurements, on four separate occasions between October 2016 and June 2017. In each field campaign CO_2 emissions from running streams were measured at daytime and night time.

For the Eurorun project, CO_2 fluxes are measured on the rivers using floating chambers with CO_2 sensors (CO_2 Engine® ELG, SenseAir AB) installed inside the chambers. The sensors are powered by 9V batteries, and log the CO_2 concentrations inside the chambers. The chambers and sensors were assembled according to instructions set out in Bastviken et al (2015).

CHARACTERISATION OF SALMONID FOOD WEBS IN THE RIVERS AND LAKES OF AN IRISH PEATLAND ECOSYSTEM

Elvira de Eyto, Brian Doyle, Niall King, Tommy Kilbane, Ross Finlay, Lauren Sibigtroth, Conor Graham, Russell Poole, Elizabeth Ryder, Mary Dillane and Eleanor Jennings

Elvira de Eyto (corresponding author; email: elvira.deeyto@marine.ie, Orcid iD: https://orcid.org/0000–0003–2281–2491), Marine Institute, Newport, Co. Mayo; Brian Doyle, Marine Institute, Newport, Co. Mayo; Dundalk Institute of Technology; Tommy Kilbane, Galway Mayo Institute of Technology; Ross Finlay, Marine Institute, Newport, Co. Mayo; University College Cork; Lauren Sibigtroth, University College Dublin; Conor Graham, Galway Mayo Institute of Technology; Elizabeth Ryder, Marine Institute, Newport, Co. Mayo; Dundalk Institute of Technology; University College Cork; Mary Dillane, Marine Institute, Newport, Co. Mayo; Eleanor Jennings, Dundalk Institute of Technology.

Cite as follows: de Eyto, E., doyle, B., King, N., Kilbane, T., Finlay, R., Sibigtroth, L., Graham, C., Poole, R., Ryder, E., Dillane, M., and Jennings, E. 2020 Characterisation of salmonid food webs in the rivers and lakes of an Irish peatland ecosystem. *Biology and Environment: Proceedings of the Royal Irish Academy* 2020. DOI: 10.3318/BIOE.2020.01

Received 18 June 2019. Accepted 11 February 2020. Published 09 March 2020.

ABSTRACT

Peatlands are being degraded by the combined impacts of land use and climate change. Carbon stored in peat is a key constituent of aquatic food webs in rivers and lakes of humic catchments, and changes in the downstream transport of this allochthonous carbon may have considerable implications for the production of Atlantic salmon and brown trout. Understanding the food web of these keystone species is therefore crucial to their conservation in a changing world. Here, we use a combination of stomach content analysis (SCA) and stable isotope analysis (SIA) to characterise the diet of juvenile salmonids in aquatic habitats of a typical Irish peatland catchment (Burrishoole). SCA showed that Diptera, Ephemeroptera, Plecoptera and Trichoptera were the main components of the diet of juvenile salmonids. *Daphnia* were the primary prey item in salmon smolt stomachs. The average stable isotope signature of salmonids was 9.26 ± 0.87‰ δ^{15}N and -25.6 ± 1.99‰ δ^{13}C, but differed between species, age class and habitat (river vs lake). Salmonids were supported by a wide range of carbon energy sources, with δ^{13}C increasing as fish moved downstream out of the headwater rivers and into a large downstream lake.

INTRODUCTION

Peatlands occupy approximately 20% or 14,000km^2 of the land area of Ireland (Connolly and Holden 2009), holding up to 75% of national soil carbon stocks (Renou-Wilson *et al.* 2011). Healthy peatlands provide a wide range of ecosystem services, including carbon storage, climate regulation, biodiversity support, water filtration and supply, and hydrological control (Bonn *et al.* 2009). The waters draining peatlands underpin many of these services, and the ecological quality of the rivers and lakes in peatland catchments are crucial to the functional integrity of peatlands as a whole. The rivers and streams draining peatlands are important conduits linking terrestrial and oceanic ecosystems by transporting soil organic carbon from land to sea (Asmala, Carstensen and Räike 2019). It is widely acknowledged that peatlands and their aquatic ecosystems are especially sensitive to climate change (Ise *et al.* 2008), and that resultant changes in these important long-term stores are occurring. For example, increases in organic carbon (OC) concentrations has already been reported in many aquatic peatland ecosystems in the Northern Hemisphere (Freeman *et al.* 2001; Jennings *et al.* 2010; Couture, Houle and Gagnon 2012; Asmala *et al.* 2019).

Salmonids (Atlantic salmon *Salmo salar* L., brown trout *Salmo trutta* L.) and European eel (*Anguilla anguilla* L.) are keystone native species in the aquatic habitats of peatland catchments spanning the Atlantic seaboard of western Europe. These species exert considerable top down control on all aspects of the ecology of rivers and lakes in these catchments (O'Gorman, Lantry and Schneider 2004; Layer *et al.* 2011). Terrestrial (allochthonous) support of aquatic food webs, such as pulses of organic matter (both particulate and dissolved) can be significant (e.g. Solomon *et al.* 2011; Bartels *et al.* 2012; Wilkinson *et al.* 2013), meaning that changes such as peatland degradation or increased afforestation can have significant implications for the production of juvenile fish (Tanentzap *et al.* 2014).

It is currently unknown how changes in the terrestrial carbon cycling in peatlands will affect the production of salmon and trout, although recent work indicates that it is likely to be a complex response (Finstad *et al.* 2014). In addition, the role that salmonids have on controlling carbon cycling through river and lakes has yet to be determined. Recent research has quantified the role that marine fish populations have on the carbon cycle of oceanic waters (Trueman *et al.* 2014), where it was estimated that benthopelagic fishes from the

UK-Irish continental slope capture and store a volume of carbon equivalent to over 1 million tonnes of CO^2 every year. It is possible that the freshwater fish of peatland habitats can exert a similar influence, but the magnitude of the transfer of carbon to fish biomass along the LOAC (land-ocean-aquatic continuum) is, as yet, unknown. The Burrishoole catchment on the western seaboard of Ireland is an internationally important index site for diadromous fish monitoring, with long-term records of salmon, trout and eel densities and migration (Poole *et al*., 2006, 2018; McGinnity *et al*. 2009; de Eyto *et al*. 2016a). Over the last 20 years, considerable progress has been made on resolving the carbon cycle of the aquatic ecosystems in the catchment through the use of the long-term environmental monitoring data. It has already been shown that the supply of allochthonous carbon to surface waters is largely determined by hydrological and meteorological factors (discharge, air temperature) (Ryder *et al*. 2014; Doyle *et al*. 2019), which are projected to change as climate change accelerates (Fealy *et al*. 2014). This is predicted to result in larger exports of organic carbon from peat to rivers and lakes (Jennings *et al*. 2010). Palaeolimnological investigations of the two largest freshwater lakes in the catchment (Feeagh and Bunaveela) have revealed a changing aquatic environment, primarily related to land use changes in the second half of the twentieth century (Dalton *et al*. 2014). Commercial coniferous forestry was established from the 1950s and currently covers 23% of the catchment area. In addition, sheep numbers in the catchment increased rapidly from about 500 in the 1970s to a high of ~10,000 by 2000, before decreasing as a result of destocking incentives. Organic matter (% LOI: loss on ignition) fluctuated throughout sediment cores taken from the lakes, but increased in the second half of the century, coincident with increased erosion of upland peats. Increases in levels of %C (~10 to 20) and $\delta^{15}N$ (<2 to 2.5‰) in the sediments of Feeagh coincided with organic matter increases and are within the range characteristic of terrestrial plants, and ratios of C:N greater than twenty indicated a predominantly terrestrial source for organic matter (Meyers 2003). These land use changes manifested as increased erosion of peat, increased export of sediment into the lakes and a reduction in water clarity (Sparber 2012). Biological communities in Lough Feeagh (diatoms and cladocerans) have been impacted by these changes (Dalton *et al*. 2014), and we know that the pelagic communities in Lough Feeagh are currently primarily supported by allochthonous carbon at specific times in the year (Ryder 2015).

There is, therefore, much evidence to suggest that the aquatic food webs of Burrishoole are dependent on, or influenced by, terrestrial allochthonous sources, and that this influence may have increased over the last six decades. This influence is likely to increase further as peatlands destabilise with climate warming (Jones, Donnelly and Albanito 2006; Gallego-Sala *et al*. 2010). However, a current gap in our knowledge is the role that fish play in the aquatic food web, and to what extent their production is determined by carbon sources. A first step in filling this gap is to fully characterise the food web of the rivers and lakes in Burrishoole, which is the aim of this study. Stable isotope analysis (SIA) and stomach content analysis (SCA) were carried out on the same fish samples, with the aim of cataloguing and understanding how the feeding ecology of salmonids in Burrishoole varies with species (salmon and trout), age class (0+, 1+ and smolt) and habitat (river, littoral lake and pelagic lake) over the short (days) to medium (months) term. SCA was used to provide a snapshot of the diet of fish at a given time and inform the SIA. Shifts in diet along the headwater to sea gradient were also inferred from the SIA, along with the trophic position of invertebrates and fish. In conducting this study, we wish to provide a baseline against which future changes can be assessed, and background for the design of studies with more specific research questions.

MATERIAL AND METHODS

Burrishoole is a small (100km^2) upland catchment (53° 56' N, 9° 35' W) draining into the North-east Atlantic through Clew Bay (Fig. 1). Climatically influenced by the Atlantic Ocean (Jennings *et al*., 2000; Allott, McGinnity and O'Hea, 2005; Blenckner *et al*., 2007), the catchment experiences a temperate, oceanic climate with mild winters and relatively cool summers. Maximum summer air temperatures rarely exceed 20°C, while minimum winter temperatures are usually between 2°C and 4°C. The base geology on the western side of the catchment is predominantly quartzite and schist, leading to acidic runoff with poor buffering capacity. By comparison, the geology on the eastern side is more complex as quartzite and schist are interspersed with veins of volcanic rock, dolomite and wacke, leading to higher buffering capacity and aquatic production. Soils in the catchment comprise poorly drained gleys, peaty podzols and blanket peats. Lough Feeagh is the largest freshwater lake in the catchment (Surface area = 4km^2, maximum depth = 45m), and is oligotrophic (total phosphorous <10 $\mu g\ l^{-1}$), highly coloured (*c*. 80mg l^{-1} PtCo) due to high levels of dissolved organic carbon (DOC), and slightly acidic (pH = *c*. 6.7) with low alkalinity (<20mgl^{-1} $CaCO_3$) (de Eyto *et al*. 2016b).

BIOLOGICAL ANALYSIS

Samples for isotopic determination were collected concurrently around Lough Feeagh in 2015 and

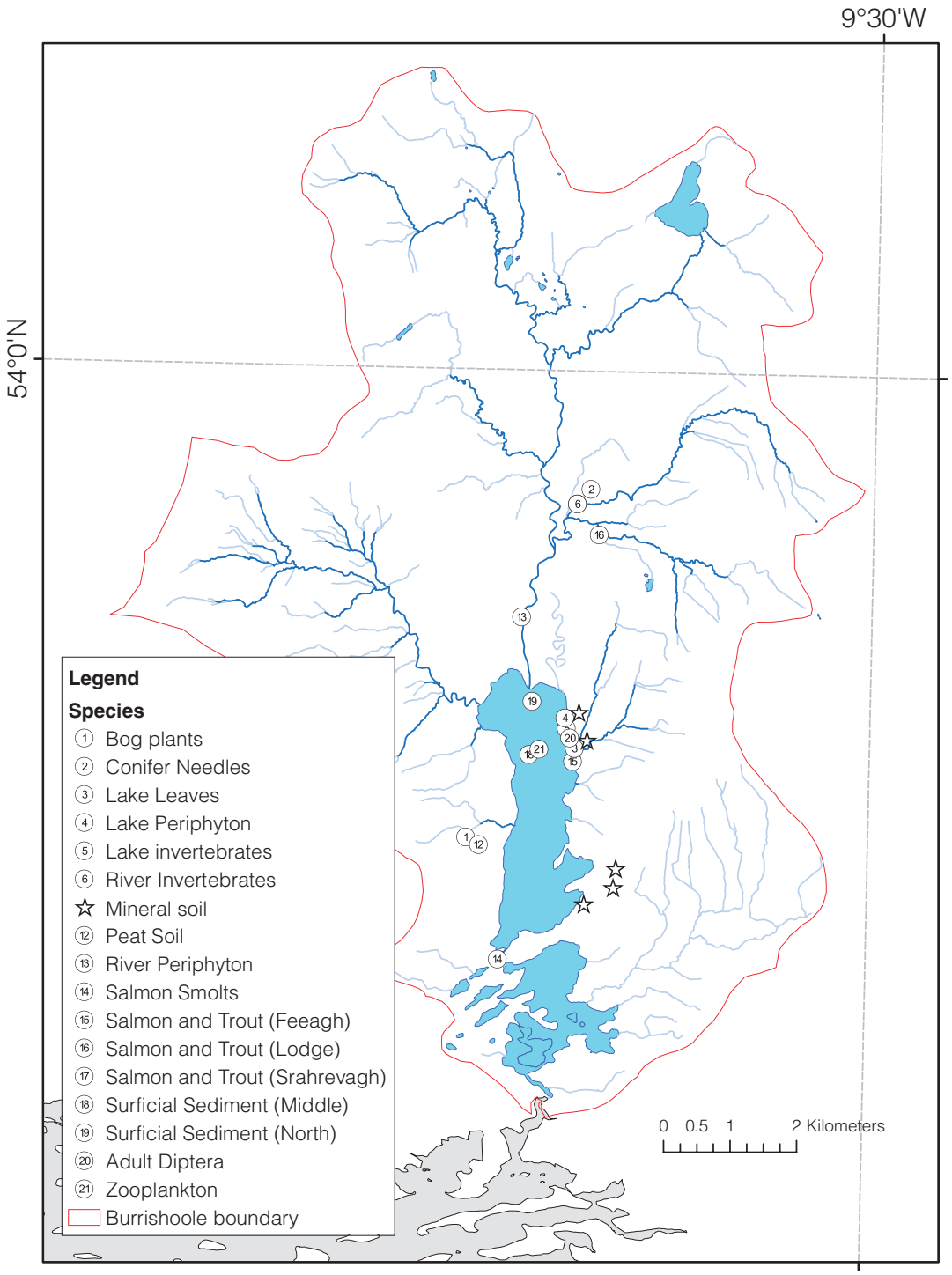

Figure 1—Map showing the location of samples collected in and adjacent to Lough Feeagh for stable isotope analysis.

2016 (Fig. 1) according to methods described below (and listed in Table 1) and following techniques described in Solomon *et al.* (2011), Karlsson *et al.* (2012) and Tanentzap *et al.* (2014). All samples were dried in an oven for 24 hours at 50°C, then crushed to a fine powder in a pestle and mortar, and weighed into individual pre-weighed tin cups.

Five samples of peat soils were collected on Lettermaghera bog (Fig. 1) in October 2015 using a plastic corer. Cores were taken from bare peat only.

Table 1—Samples collected for Stable Isotope Analysis including number of individuals, location and date of sampling

	Sampling method	*Number of samples*	*Location (Fig 1)*	*Date*
Consumer				
Lake Trout (0+)	Draft net	10	15	7 Oct 2015
Lake Trout (1+)	Draft net	10	15	7 Oct 2015
Lake Salmon (0+)	Draft net	10	15	7 Oct 2015
Lake Salmon (1+)	Draft net	10	15	7 Oct 2015
River Trout (0+)	Electrofishing	5	16 and 17	12 Oct 2016
River Trout (1+)	Electrofishing	5	16 and 17	12 Oct 2016
River Salmon (0+)	Electrofishing	5	16 and 17	12 Oct 2016
River Salmon (1+)	Electrofishing	5	16 and 17	12 Oct 2016
Migrating Salmon (smolts)	Lake Outflow Trap	20	14	3-25 May 2016
Source				
Terrestrial				
Peat	Cores	5	12	19 Oct 2015
Lake leaves	Hand collection	5	3	19 Oct 2015
Mineral Soils	Cores	5	*	19 Jan 2015
Bog plants	Hand picked	5	1	19 Oct 2015
Conifer needles	Hand picked	5	2	19 Oct 2015
Diptera (adult flies)	Hand picked	4	20	31 Oct 2016
Pelagic				
Zooplankton (*Daphnia* sp.)	Vertical haul	3	21	19 Oct 2015
Zooplankton (Cyclopoid sp.)	Vertical haul	3	21	19 Oct 2015
Benthic				
River periphyton	Scrapped off rocks	5	13	19 Oct 2015
Lake periphyton	Tiles	5	4	19 Oct 2015
Lake invertebrates (*Gammarus duebenii*)	Sweep net	3	5	19 Oct 2015
Lake invertebrates (*Heptagenia* sp.)	Sweep net	5	5	19 Oct 2015
River invertebrates (Mayfly sp.)	Sweep net	3	6	27 Oct 2016
Profundal				
Surficial sediment	Sediment traps	5	18 and 19	19 Oct 2015

Mineral soils were collected at five separate locations on the eastern side of Lough Feeagh. The chosen soil samples represent a range of mineral soils that occur in the lake catchment. The mineral soils sampled were mostly podzols with strongly stratified horizons. The mineral soils were sampled at locations shown in Fig. 1. Surficial lake sediment was taken from traps in the north and centre of Lough Feeagh, which were in place between 15 June and 20 October 2015. Sediment from five traps was emptied into separate bottles. A subsample of each bottle was filtered through GF/F filter paper and the filtered solid used for analysis.

Terrestrial primary producers (leaves) were sampled in October 2015. Representative bog plants were sampled by selecting fresh (growing) vegetation from hummocks on Lettermaghera bog (Fig. 1). The leaves and young branches of *Calluna vulgaris* (L.) Hull, *Molinia caerulea* (L.) Moench and *Sphagnum* spp. were cut and put into a zip lock bag. Conifer needles were cut directly from a stand of *Pinus contorta* Douglas ex Loudon conifers adjacent to the Srahrevagh river. In addition, decomposing leaf litter was collected from dead leaves floating in the littoral area of Lough Feeagh. Leaves were mostly from *Fraxinus* (L.), *Salix* (L.), *Betula* (L.), and *Quercus* (L.) species. All samples were cut into small pieces for processing.

Five samples of river periphyton were collected from the Black River (Fig. 1) in October 2015. One rock submerged in the river channel was chosen per sample. Each rock was placed in a white tray, scrubbed with a tooth brush and washed with distilled water. The water from each sample was stored in a pre-washed separate bottle. In the laboratory each of the five samples was filtered thorough GF/F filers and the filtered solid used for analysis. Lake periphyton was sampled from tiles were placed in

the littoral zone of Lough Feeagh in on 5 August 2015 and removed on 20 October 2015. Each tile was scrubbed with a toothbrush and rinsed with distilled water into a separate pre-washed bottle. In the laboratory each sample was filtered through GF/F filter paper and oven-dried. Following drying it was discovered that the required mass of material could not be scraped off the filters for analysis. Instead, several cores of each sample were taken from each of the filter papers and weighed into a pre-weighed tin cup. Cores were also cut from unused, dried filters and an average weight was measured (N = 10). The mass of each lake periphyton sample were calculated as:

(Mass of sample + core) –
(Average mass of unused core) = Mass of sample

Zooplankton were sampled in October 2015 using a vertical haul through the water column from 20m with a conical zooplankton net (53µm mesh). 100 individual cyclopoid copepods, calanoid copepods and *Daphnia* sp. were counted into beakers containing filtered lake water and left overnight to allow their guts to evacuate. Three samples of each group (nine beakers in total) were prepared. Each sample was then washed with deionised water and placed in porcelain crucibles for processing.

A kick-sample net was used to sample benthic invertebrates in the lake littoral region in October 2015. Individuals of *Gammarus duebenii celticus* Stock and Pinkster 1970 and *Heptagenia* sp. Walsh, 1863 were picked out by hand and left in filtered lake water overnight for them to expel their gut contents. For *Heptagenia* (mayfly), ten individuals were considered as a sample. Five *Gammarus* individuals were considered a sample. River invertebrates (a mix of three may fly species, *Baetis rhodani* (Pictet 1843), *Heptagenia* sp. and *Rhithrogenia semicolorata* (Curtis 1834)) were similarly sampled and processed. Winged (adult) Diptera were sampled by handpicking them from the lake shore as they were caught in spider webs suspended at approximately 1 metre height. Five to ten flies were grouped for a sample, and four samples were collected.

Littoral lake samples of salmon and trout (+0 and +1) were caught in a draft net in October 2015 (Fig. 1). River samples of salmon and trout (+0 and +1) were caught by electrofishing in October 2016 from two upland rivers above Lough Feeagh (the Lodge and Srahrevagh river). Salmon smolts (2+) were sampled as they migrated downstream through fish traps at the seaward end of Lough Feeagh during the smolt run of May 2016 and these were classified as having come from pelagic lake habitat. Fish sample sizes are given in Table 1. As the trout population of Burrishoole is primarily resident (i.e. non-anadromous), only 0+ and 1+ fish were sampled for this study, both from river and littoral lake habitats (Table 2). The fish were immediately stored in a freezer (-18 °C) until the time of dissection. The fish were later (within 3 months of being caught) defrosted and their digestive tracts removed. A sample of white flesh was removed from each fish and care was taken to avoid bone, skin, scales and other non-muscle material. The stomach content of each fish was dissected, and the occurrence of various prey items was counted. Individuals were generally identified to order.

Table 2—Stomach contents of salmon and trout of differing ages and habitats in the Burrishoole catchment. Values are the number of fish stomachs which contained each taxa.

	Salmon					*Trout*				*Total*	*% occurrence*
Age	0+	1+	0+	1+	2+ (smolt)	0+	1+	0+	1+		
Habitat	littoral	littoral	river	river	pelagic	littoral	littoral	river	river		
n	7	10	5	5	24	12	10	6	5	84	
Diptera	3	10	3	1	16	5	8	5	5	56	67%
Ephemeroptera	5	8	0	0	3	7	6	2	1	32	38%
Plecoptera	3	3	2	4	2	6	7	2	2	31	37%
Trichoptera	0	7	3	2	6	0	3	1	4	26	31%
Coleoptera	0	2	4	2	0	3	5	2	3	21	25%
Daphnia	0	0	0	0	21	0	0	0	0	21	25%
Mollusca	0	7	1	2	0	0	1	0	1	12	14%
Amphipoda	1	0	0	0	0	2	3	0	0	6	7%
Bosmina	0	0	0	0	6	0	0	0	0	6	7%
Cyclopoid	0	0	0	0	5	0	0	0	0	5	6%
Hymenoptera	1	0	0	0	0	0	3	0	0	4	5%
Lepidoptera	1	0	0	0	0	1	1	0	0	3	4%

All pre-weighed samples were analysed by the Colorado State Plateau Stable Isotope Laboratory at Northern Arizona University, using a Thermo-Electron Delta V Advantage IRMS configured through a Finnigan CONFLO III for automated continuous-flow analysis of $\delta^{15}N$ and $\delta^{13}C$, and a Carlo Erba NC2100 elemental analyser for combustion and separation of C and N. Stable isotope ratios were expressed in δ notations as parts per thousand (‰) using the following equation:

$$\delta X = [(R_{sample}/R_{standard})-1] \times 1000$$

The standard for carbon was the Vienna Pee Dee belemnite (VPDB) and atmospheric nitrogen (AIR) for nitrogen. NIST 1547 (peach leaves) was used as the internal laboratory working standard to check on measurement reproducibility throughout each run. The isotope correction standards used were IAEA CH6 and CH7 for $\delta^{13}C$, and IAEA N1 and N2 $\delta^{15}N$. The precision for this analysis run (calculated from the standard deviations for the NIST peach leaves) was ±0.09‰ for $\delta^{13}C$ and ± 0.08‰ for $\delta^{15}N$.

DATA ANALYSIS

The stomach contents of groups of fish were visualised using nMDS (following double square root transformation and calculation of Bray-Curtis dissimilarities) with the R package *vegan* (Oksanen *et al.* 2015) and analysed for differences between groups using the *adonis* function (analysis of variance using distance matrices) (McArdle and Anderson 2001). The input data for this analysis was the number of individuals of each taxon that were found in each fish stomach (Supplemental information II)

Following the recommendation of Post *et al.* (2007), animal samples with a C:N ratio >3.5 were lipid corrected, as lipids are depleted in $\delta^{13}C$, using the equation:

$$\delta^{13}C_{normalized} = \delta^{13}C_{untreated} -3.3 + 0.99 \star C{:}N$$

Trophic position (TP) was estimated within each sampled habitat (river and lake) using either periphyton or a primary consumer as a baseline, using the equation:

$$TP_{consumer} = ([\delta^{15}N_{consumer} - \delta 15N_{baseline}]/3.23) + \lambda$$

where 3.23 ‰ is the trophic-enrichment factor taken from the literature, $\delta^{15}N$ baseline is the mean $\delta^{15}N$ value of the baseline resource of the system, and λ is the trophic position of the baseline resource (1 for periphyton, 2 for primary consumer) (Vander Zanden and Rasmussen 2001; Manetta, Benedito-Cecilio and Martinelli 2003; Dekar *et al.* 2011; Wieczorek *et al.* 2018).

We used mixing models with the SIAR package in R to determine the most likely dietary sources for river and lake fish and hence evaluate the production base supporting juvenile salmonids in both habitats. SIAR is a Bayesian mixed model that uses Markov Chain Monte Carlo simulations to determine the probable contribution to diet of different prey sources (Parnell *et al.*, 2008). We used consumer-based dual- isotope models ($\delta^{13}C$ and $\delta^{15}N$) for fish from each habitat, with the end members being the signatures of aquatic macroinvertebrates, adult flies and pelagic zooplankton. All sampled food sources were included in the lake model (both river and lake invertebrates) as theoretically, lake fish may only have been in the lake for a very short period of time and may still maintain a 'riverine' dietary signal. In contrast, we assume that fish caught in the rivers had never spent time in the lake, and so the end members for the river model were only those invertebrates sampled in the river (mayfly) and adult flies. We used trophic enrichment values of 0.91 ‰ ± 1.04 for $\delta^{13}C$ and 3.23 ‰ ± 0.41 for $\delta^{15}N$ (Dekar *et al.*, 2011).

RESULTS

STOMACH CONTENT ANALYSIS

We carried out stomach analysis on 84 fish as part of this study, and 12 different taxa were represented across all fish (Table 2). One individual each of Hymenoptera (ants) and Lepidoptera (moths and butterflies) were found in the stomachs of the river salmon – these were excluded from analysis owing to their rarity. Diptera (flies) were the most common food item found in the stomachs, with a mix of both terrestrial and aquatic life stages. 67% of fish had Diptera in their stomachs at the time of sampling, followed by Ephemeroptera (mayflies: 38%), Plecoptera (stoneflies: 37%) and Trichoptera (caddisflies: 31%). When all 84 fish were analysed together, there were significant differences in the stomach contents of the various groups of fish (*adonis*, p=0.001, F=6.13, n=84), the most notable difference being the diet of 2+ salmon (smolts migrating from the pelagic zone of Lough Feeagh) when compared with all other groups (Fig. 2). For fish sampled in the Lodge and Srahrevagh rivers, species was a significant source of variation in observed stomach contents (*adonis*, p=0.03, F=3.27, n=21), with trout stomachs containing relatively more Diptera, while salmon were eating more Plecoptera (Fig. i, Supplemental Information). Age class was not a significant source of variation in the diets of river fish, with large overlap between the food items of 0+ and 1+ fish. In contrast, in the littoral region of Lough Feeagh, the age of the fish (0+ vs 1+) was a more important discriminant of diet (*adonis*, p=0.009,

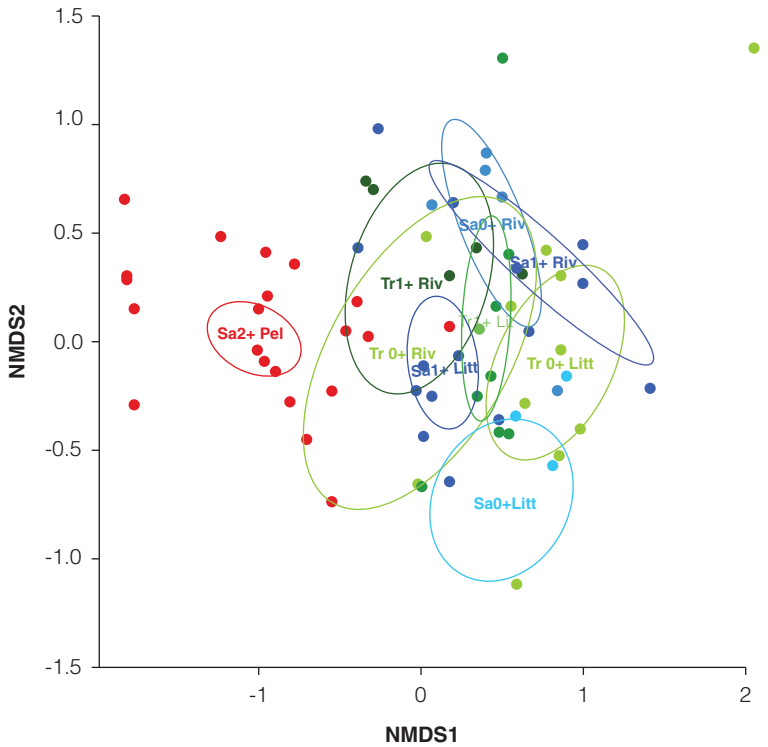

Figure 2—nMDS ordination of the stomach contents of salmon and trout sampled in the Burrishoole catchment from river and littoral lake habitats. Ellipses are plotted as the standard error of the (weighted) average of scores, and the grey lines indicate segments connecting each sample to the group centroid. Stress = 0.15, n= 84.

F=3.02, n=39) than the species (salmon vs trout), with the 0+ feeding more on Ephemeroptera and Plecoptera, and 1+ fish of both species feeding more on Trichoptera and Diptera (Fig. ii, S.I.).

In order to examine the changes in diet as fish aged, salmon and trout were also analysed separately. There was a difference between the stomach contents of the pelagic salmon smolts (2+) and the 0+ and 1+ salmon from river and lake littoral habitats (*adonis*, $p<0.001$, F=14.77, n=49) (Fig. iii, S.I.). The smolts were eating mainly zooplankton, predominantly *Daphnia* sp., with an average number of 200 individual *Daphnia* per smolt stomach. 21 out of 23 salmon smolts examined had large numbers of *Daphnia* in their stomachs. Two other zooplankton taxa, *Bosmina* sp. and cyclopoid copepods, were also found in the salmon smolt stomachs, along with Diptera and small numbers of EPT (Ephemeroptera, Plecoptera and Trichoptera). When analysed separately from the salmon smolts, there was some separation between the stomach contents of salmon sampled in rivers and those sampled in the lake littoral region (Fig. 3) (*adonis*, $p<0.001$, F=7.17, n=27). Coleoptera and Plecoptera were found more frequently in the river salmon, while the lake salmon had higher occurrences of molluscs. Ephemeroptera were not found in the stomachs of any salmon sampled in the rivers, although they were very common in the lake fish. While the diet of 0+ and 1+ river salmon overlap considerably, there was quite a divergence between 0+ and 1+ diets in the lake fish, with Trichoptera and Mollusca being absent from 0+ stomachs, but occurring in 70% of the 1+ stomachs.

Although there was more overlap in the stomach contents of trout than those of salmon described above, there were still some significant differences in the taxa found in the stomachs of lake trout compared to those of river trout (*adonis*, $p<0.01$, F=2.14, n=33) (Fig. 4). In particular, Amphipoda (*Gammarus duebenii*) were found in several lake trout, but not at all in river trout, while lake trout also had higher occurrences of Plecoptera and Ephemeroptera (Table 2). When amphipods were found in trout stomachs, it was in large numbers (17, 53 and 101 individuals in three fish)

STABLE ISOTOPE ANALYSIS

All the invertebrate samples (but not the fish) had a C:N ratio of >3.5, and so were lipid normalised. The $\delta^{13}C$ of samples ranged between -19.70‰ (lake periphyton) and -31.92‰ (conifer needles), and the $\delta^{15}N$ ranged between -3.26‰ (bog plants)

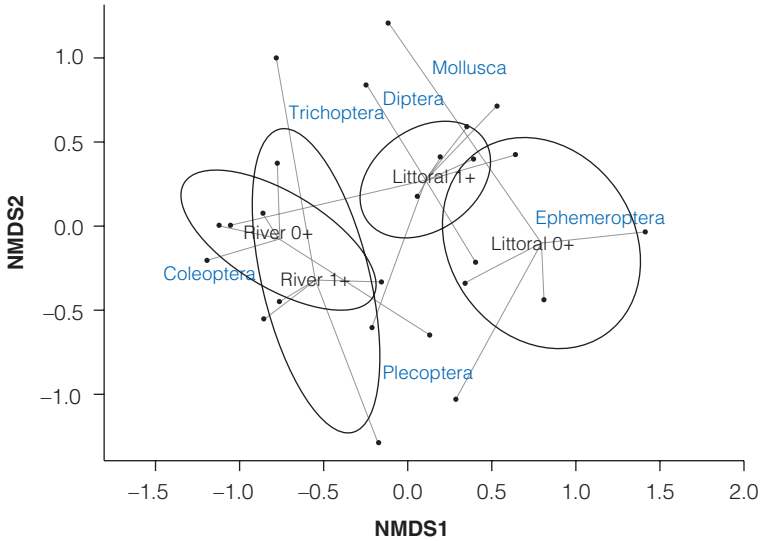

Figure 3—nMDS ordination of the stomach contents of salmon sampled in the Burrishoole catchment from river and littoral lake habitats (i.e. excluding smolts). Ellipses are plotted as the standard error of the (weighted) average of scores, and the grey lines indicate segments connecting each sample to the group centroid. Stress = 0.16, n= 27.

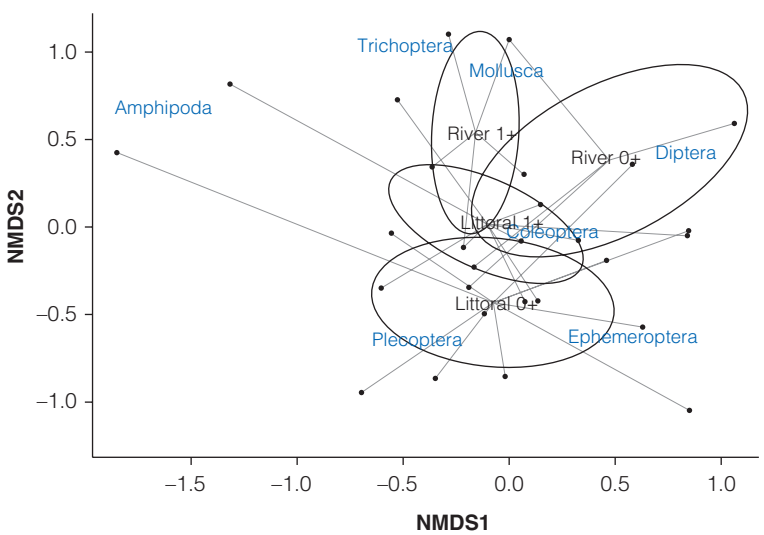

Figure 4—nMDS ordination of the stomach contents of trout sampled in the Burrishoole catchment from river and littoral lake habitats. Ellipses are plotted as the standard error of the (weighted) average of scores, and the grey lines indicate segments connecting each sample to the group centroid. Stress = 0.16, n= 27.

and 10.02‰ (Salmon 1+ lake) (Table 3). While the $\delta^{13}C$ of the lake periphyton seems to be an outlier in comparison to all other samples, it is within the range of other measurements in freshwater ecosystems (Jardine *et al.* 2003) and so we have included it in further analysis. The $\delta^{13}C$ measured in the fish ranged between -31.32 and -21.54, with fish becoming less depleted in $\delta^{13}C$ as they moved down the catchment from headwaters towards the sea. The dual isotope plots clearly show the trophic structure of the river and lake aquatic ecosystems in the catchment, with at least three trophic levels being characterised. Terrestrial primary producers (plants) are clearly separated at the base of the food web, with $\delta^{15}N$ values less than 0‰, while fish are grouped together at the top, with $\delta^{15}N$ between 8‰ and 10‰. In the middle of these two extremes are invertebrate consumers and a mix of periphyton, soils and sediments perhaps colonised with complex microbial assemblages (Fig. 5). The trophic position

Table 3—Average stable isotope results from samples taken around the Burrishoole catchment in 2015/2016.

Sample	*n*	*δ13C ‰*	*δ13Cnorm‰*	*δ15N ‰*	*%C*	*%N*	*C:N*
Basal resources							
Peat Soil	5	-28.17		-0.07	59.50	2.45	24.37
Mineral soil	5	-27.77		3.51	12.15	0.50	22.50
Surficial Sediment	5	-28.59		3.55	13.18	0.82	16.29
Bog plants	5	-29.38		-3.26	49.72	1.16	42.92
Conifer Needles	5	-31.92		-1.84	49.04	1.16	42.18
Lake leaves	5	-31.76		-0.82	44.87	1.52	29.48
River Periphyton	5	-27.73		2.77	7.04	0.51	16.16
Lake Periphyton	4	-19.70		4.52	10.10	1.36	7.59
Invertebrates							
Adult DIptera	4	-31.50	-30.40	4.08	46.80	10.53	4.47
Mayflies (River)	3	-27.46	-24.58	4.82	51.54	8.27	6.27
Gammarids (lake)	3	-23.77	-22.69	7.02	35.75	8.06	4.44
Mayfly (lake)	5	-27.33	-26.64	8.38	48.66	12.03	4.05
Daphnia	3	-30.17	-27.50	7.34	33.29	5.79	6.05
Cyclopoid	3	-28.08	-26.22	9.64	46.35	8.84	5.23
Fish							
Trout 0+ (river)	6	-27.07		8.29	41.83	13.12	3.19
Salmon 1+ (river)	5	-27.65		8.50	42.31	13.06	3.24
Trout 0+ (lake)	17	-25.52		8.67	43.54	13.31	3.34
Salmon 0+ (river)	5	-28.96		8.76	40.98	12.68	3.23
Salmon 0+ (lake)	10	-26.18		8.92	42.78	12.78	3.35
Trout 1+ (river)	5	-27.08		9.03	40.00	12.47	3.21
Trout 1+ (lake)	10	-26.33		9.44	46.04	14.30	3.22
Salmon 2+ (smolt)	24	-24.62		9.67	42.58	13.61	3.14
Salmon 1+ (lake)	20	-24.15		10.02	44.82	13.72	3.27

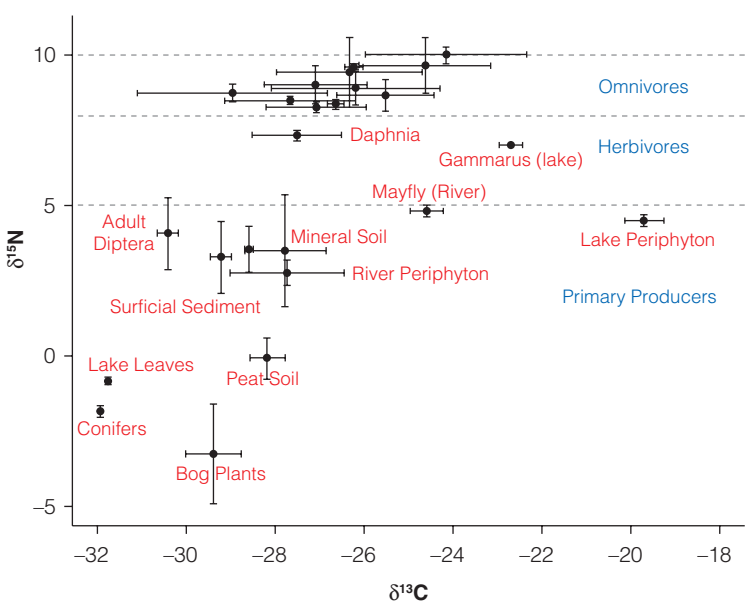

Figure 5—Dual isotope plot ($\delta^{13}C$ and $\delta^{15}N$) for basal resources, invertebrates (labelled) and fish (unlabelled – see Fig. 6) sampled in the Burrishoole catchment. Grey dashed lines indicate arbitrary ranges for trophic groups ($\delta^{15}N$) from Jardine et al. (Jardine *et al.*, 2003) and are for indicative purposes only. Error bars indicate one standard deviation.

of lake primary producers, primary consumers and predators appears to be elevated in comparison to the same groups in rivers, indicating a more complex food web downstream in the catchment (Fig. 5). The $\delta^{15}N$ of river periphyton was 2.77‰, compared to 4.51‰ for lake periphyton. River mayflies (primary consumers) had a $\delta^{15}N$ of 4.82‰, while *Gammarus* in the littoral regions of Lough Feeagh had a $\delta^{15}N$ of 7.02‰. Interestingly, mayfly in Lough Feeagh appear to be feeding at more than one trophic position higher than the same family in river, with a $\delta^{15}N$ of 8.38‰, which was within the range of $\delta^{15}N$ measured in fish (Fig. 6). Similarly, cyclopoid copepods in Feeagh, which are generally considered to be primary consumers had an average $\delta^{15}N$ of 9.57‰, which was considerably higher than the other pelagic consumer, *Daphnia*, which had an average $\delta^{15}N$ value of 7.33‰.

If periphyton is used as the baseline for the aquatic food webs in Burrishoole's rivers and lakes, salmon and trout occupy a trophic position between 2 and 3, with a considerable range, particularly in lake fish (Fig. xi, S.I.). When a primary consumer is used as the baseline, with a trophic position of 2, there is a slight shift upwards in the trophic position of fish inhabiting the lake, but still occupying a range between 2 and 3. Lake mayfly appear to be feeding at the same trophic position as the 0+ trout and salmon. As we did not sample the true phytoplankton baseline that we would expect zooplankton to be feeding on, the trophic position of *Daphnia* and Cyclopoid copepods in Figure 7 should be treated with caution, but we note that cyclopoids do seem to be feeding at a slightly higher trophic level than their pelagic co-inhabitants *Daphnia*. In the river food web, using a primary consumer (a mix of mayfly species) as a baseline leads to estimated trophic positions of greater than three for all four fish groups (0+ and 1+ salmon and trout) (Fig. xi, S.I.).

A total of nine fish groups were sampled for stable isotope analysis (Table 3) and there was a large amount of overlap in the isotope signatures of these groups. The most enriched $\delta^{15}N$ was found in 1+ salmon sampled from the littoral area of Lough Feeagh, while 0+ river trout had the least. Interestingly, both cyclopoids and mayflies sampled in Lough Feeagh had SI ratios in the same range as those of fish. Although there is a lot of overlap in the SI signatures of the groups of fish, significant differences do appear between species, habitat and age class. $\delta^{15}N$ was less enriched in river fish when compared to lake fish (ANOVA, $p < 0.01$, $F = 21.5$), trout had significantly lower $\delta^{15}N$ than salmon (ANOVA, $p < 0.01$, $F = 14.0$) and fish became more enriched

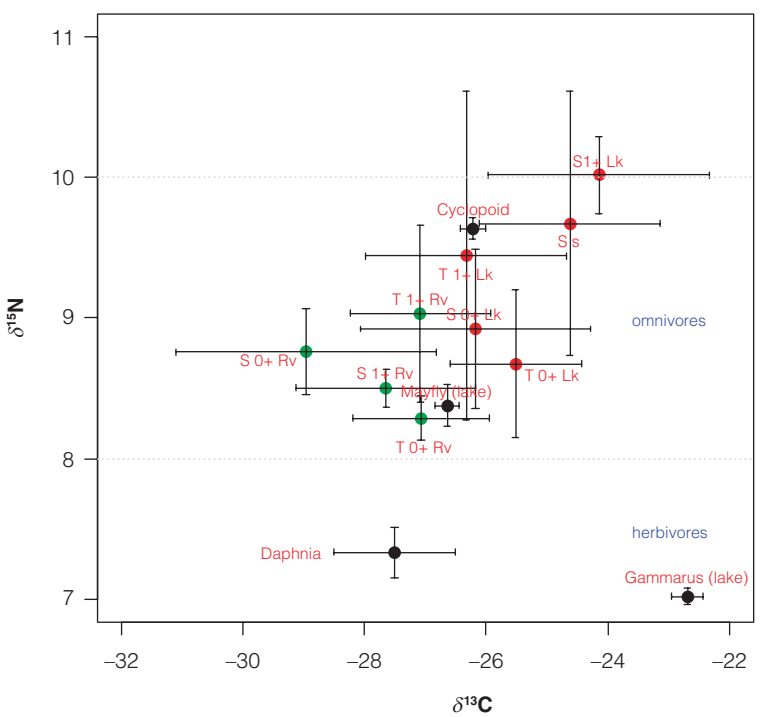

Figure 6—Dual isotope plot ($\delta^{13}C$ and $\delta^{15}N$) for invertebrates and fish (Salmon – S; Trout – T; 0+ and 1+ and s – 2+ smolt) sampled in the Burrishoole catchment. Grey dashed lines indicate arbitrary ranges for trophic groups ($\delta^{15}N$) from Jardine et al. (Jardine *et al.*, 2003) and are for indicative purposes only. Green circles are river fish (Rv), red are lake fish (Lk) and black are invertebrates for reference. Error bars indicate one standard deviation.

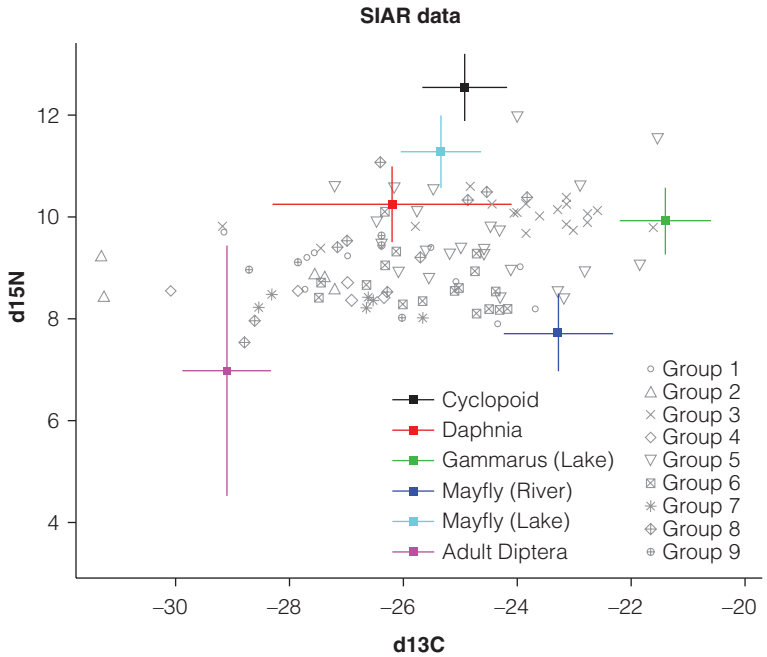

Figure 7—Raw isotope data for sources and consumers (lake fish) as a bi-plot. Trophic enrichment factors have been applied to the sources. Group 1 = Salmon 0+, group 2 = salmon 1+, group 3 = salmon smolts, group 4 = trout 0+ and group 5 = trout 1+.

in $\delta^{15}N$ as they grew from 0+ to 1+ (ANOVA, $p < 0.01$, $F = 11.2$). Although salmon smolts (2+) had higher $\delta^{15}N$ than 0+ salmon, it was actually lower than the $\delta^{15}N$ signature of 1+ lake salmon. $\delta^{13}C$ did not vary as much as $\delta^{15}N$ amongst groups, with the only significant difference being between habitat (ANOVA, $p < 0.01$, $F = 39$) where river fish were significantly depleted in $\delta^{13}C$ in comparison to lake fish. $\delta^{13}C$ did not vary with species or age class.

We used the R package SIAR to ascertain the likely food sources of groups of fish. In the isotopic $\delta^{15}N$ - $\delta^{13}C$ biplot, all lake fish fell within the area bounded by their prey items, all of which had been found during stomach content analysis (Fig 7). The results from the Bayesian model indicated varying prey items were important for each group of fish. Riverine mayflies and adult flies were the most important prey items for 0+ salmon sampled from the littoral region of the lake (S.I.). Riverine mayflies were also important in the diet of 1+ salmon in the lake, but adult flies were not. Instead, *Gammarus* made up approximately one third of the diet of these fish. Both riverine mayflies and *Gammarus* were also important components of smolt diets. It is of note that *Daphnia* did not appear, from the SIA, to be an important part of the diet of smolts migrating out of the lake, even though stomach content analysis of the same fish showed that *Daphnia* were the most numerous prey items at the time of capture, with the stomachs containing an average of 200 individuals.

The diet of 0+ lake trout was roughly similar to that of 0+ salmon, with riverine mayflies and adult flies making up approximately one third each of their diet. Finally, adult flies make up the biggest proportion of the diet of 1+ trout in Lough Feeagh, followed by riverine mayflies and *Daphnia*. The diet of 1+ trout is the only place where *Daphnia* appears to be somewhat important, indicating that perhaps these fish spend some time in the pelagic zone (S.I.).

The biplot of the river dwelling salmonids with their prey items indicates that we may have missed some important prey items when conducting our field sampling, as there were no prey items bounding the upper limit of the $\delta^{15}N$ range (Fig. 8). However, based on this initial analysis, the data indicate that mayflies and adult flies can contribute significant energy to salmonids in the rivers leading into Lough Feeagh. In particular, adult flies may constitute about 80% of the diet of 0+ salmon in the Srahrevagh and Lodge rivers (S.I.).

DISCUSSION

The food items found in the stomachs of salmon and trout in Burrishoole were generally as we would expect from literature. Salmonids in Ireland are known to feed primarily on both the larval and adult life stages of EPT taxa and Diptera (Frost 1938;

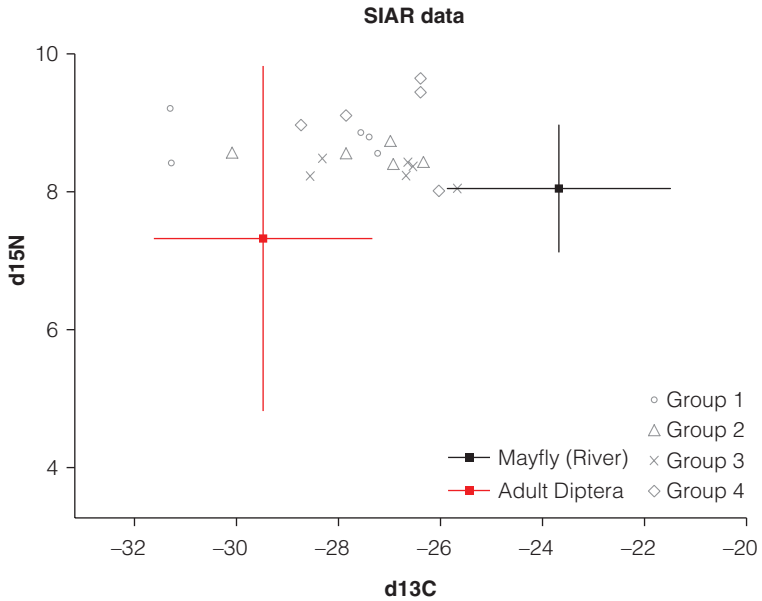

Figure 8—Raw isotope data for sources and consumers (river fish) as a bi-plot. Trophic enrichment factors have been applied to the sources. Group 1 = Salmon 0+, group 2 = salmon 1+, group 3 = trout 0+ and group 4 = trout 1+.

Stinson 1957; Lehane *et al.* 2001) and our results support this. While some studies report a considerable amount of molluscs and crustaceans in trout diets (Dauod, Bolger and Bracken 1986; Byrne, Poole and McGinnity 2000), we did not find this to be the case, with the exception of some *Gammarus* in five out of 33 trout sampled, all from the lake. This is probably a reflection of the acidic nature of the Burrishoole catchment and its underlying geology, which has low alkalinity, and low concentrations of base cations such as calcium. Occurrences of invertebrate taxa that require lots of calcium are therefore rare, apart from small pockets in Lough Feeagh and some of the rivers draining the east side of the catchment where there are veins of well buffered rocks. Previous studies have concluded that the importance of terrestrial insects becomes greater with increasing age of fish (Kelly-Quinn and Bracken 1990; Dineen, Harrison and Giller 2007), and this may account for some of the differences in stomach contents with age class in both salmon and trout in this study. However, the largest difference in diet, according to SCA, was associated with habitat. The stomach contents of lake and river dwelling fish of both species were significantly different, likely reflecting the differing availability of prey items in lentic and lotic habitats.

One surprising feature of the SCA was the predominance of *Daphnia* in the stomachs of salmon migrating through Lough Feeagh. Salmon can successfully feed and grow on a diet of Cladocera (Holm and Møller 1984), and some previous studies have reported *Daphnia* in the stomach contents of juvenile lake dwelling salmonids (Morrison 1983). However, we were unable to find much literature describing the binge-feeding that we observed in this study. According to the SIA results, both riverine mayflies and *Gammarus* were important components of the diet of salmon smolts, which seems counter-intuitive when compared with the SCA data which implied a predominantly pelagic lake diet. It may be that the smolts we sampled had come straight out of the upstream rivers into the lake, without spending enough time in the lake to accumulate a 'lake' diet signal. We note that it could take up to three months for the isotopic composition of new prey items to be detectable in consumers (Persson and Hansson 1999; Davis *et al.* 2018) and is more useful in assessing diets over weeks to months. Our combined SCA and SIA results indicate that even though smolts were feeding almost exclusively on *Daphnia* as they migrated through the lake, it was over a relatively short period of time, and most of their energy was previously derived from benthic invertebrates. It is currently unknown what proportion of Burrishoole smolts have spent the whole previous year in the lake (i.e. when they migrate permanently out of the upstream rivers into Lough Feeagh). However, these results imply that their migration time through the lake might only be a couple of days or weeks, rather than months. As we sampled the smolts over the whole migration period, we assume we sampled the variation in lake dwelling that occurs in Burrishoole salmon, and we conclude that salmon in this system generally use the lake habitat for only a very short period of time, immediately prior to their migration

to sea. Sampling these smolts at a later stage may elucidate the contribution of this binging on *Daphnia* to their overall lifetime success. In general, *Daphnia* are present in Lough Feeagh around the same time as the smolt run (late spring into early summer), raising the question of what would happen in years where there is a mismatch between the smolt run and *Daphnia* bloom. One serious shortcoming of our study is that the SIA of *Daphnia* reported here was carried out on samples which were obtained several months prior to the smolt sampling (October 2015 vs May 2016), and it is quite likely that the SI signature of *Daphnia* in May is different from that obtained in October of the previous year. Previous analysis of the SI signature of *Daphnia* in Lough Feeagh displayed some seasonal variation, with $\delta^{13}C$ varying between -25.2‰ in October 2011 and -27.3‰ in May 2012, and $\delta^{15}N$ increasing from 6.7‰ to 7.8‰ (Ryder 2015). The results from this study measured -27.5‰ and 7.34‰, which were actually nearer to the values recorded in May 2012 than those of October 2011. We therefore conclude that the *Daphnia* signal used in our SIAR analysis gives a fair indication of the occurrence of *Daphnia* in smolt diet.

While SIA is not a new technique, studies of the stable isotope signatures of Irish salmon and trout are rather rare. We found reference to five other Irish studies (Table 4), some unpublished. Dineen (2005) measured $\delta^{13}C$ and $\delta^{15}N$ in salmon and trout from various rivers in North Mayo, including several in the Burrishoole catchment. $\delta^{15}N$ values in salmon were comparable to those reported here, ranging between 7.8‰ and 11.8‰. Our salmon results ranged between 8.5‰ and 10.0‰, indicting fish feeding at similar trophic levels in both studies. However, the $\delta^{15}N$ in trout reported in Dineen (2005) was slightly higher, indicting an additional trophic level in that study, possibly encompassing 2+ fish, or higher levels of nitrogen in the system. All the trout in our study were relatively small 0+ and 1+ fish and their $\delta^{15}N$ reflects this. Some of the larger values of $\delta^{15}N$ found across Ireland and Scotland (Table 4) can be partially attributed to the size of the fish (e.g. Keaveney, Reimer and Foy 2015), as trout become progressively more ^{15}N-enriched with fish length, particularly as they move to a more piscivorous diet (Grey 2001). When comparing $\delta^{15}N$ amongst fish from different systems however, it is important to note that one of the primary determinants of $\delta^{15}N$ will be the nutrient status of the aquatic habitat, and so any comparisons will be more informative when the baseline conditions are taken into account.

The range of $\delta^{13}C$ measured across Ireland is large, particularly for salmon, indicating large variation in the food sources of salmonids across the country. Even data from the most comparable study (Dineen 2005) indicated a slightly more enriched carbon signature than that recorded in this study, with values of -22‰ recorded in some rivers (in comparison to our highest value of -24.2‰). This may be owing to the inclusion of fish from more productive rivers in north Mayo, where significant biofilms can provide a source of nutrition. It may also be owing to the fact that sampling occurred slightly earlier in the year than in the present study, and we know that SI signatures can vary significantly with time (Syväranta, Hämäläinen and Jones 2006; Ryder 2015). Some of the very low values in $\delta^{13}C$ (e.g. salmon in the river Outeragh) can be attributed

Table 4—Average stable isotope signatures of juvenile salmon and trout in Irish and Scottish waterbodies.

	Country	*Species*	*δ13C ‰*	*δ15N ‰*	*Source*
This study	Ireland	Salmon	-28.9 to -24.2	8.5 to 10.0	
Mayo rivers	Ireland	Salmon	-29.8 to -22.0	7.8 to 11.8	(Dineen 2005)
Outeragh River	Ireland	Salmon	-39.2 to -35.3	9.4 to 10.7	(Graham *et al.* 2013)
Lough Neagh	Ireland	Salmon	-30.2 to -28.7	10.8 to 15.7	(Harrod unpublished)
River Inny	Ireland	Salmon	-33.4 to -27.7	11.8 to 15.0	(Maguire *et al.* 2011)
Upper Lough Corrib	Ireland	Salmon	-28.5 to -26.6	12.5 to 14.0	(Maguire *et al.* 2011)
This study	Ireland	Trout	-27.1 to -25.5	8.3 to 9.4	
Mayo rivers	Ireland	Trout	-29.3 to -22.4	8.4 to 11.0	(Dineen 2005)
River Awbeg	Ireland	Trout	-29.4 to -26.4	10.5 to 12.4	(Graham *et al.* 2013)
Lough Neagh	Ireland	Trout	-28.8 to -20.0	12.3 to 16.8	(Harrod unpublished)
River Inny	Ireland	Trout	-32.6 to -26.7	11.1 to 17.8	(Maguire *et al.* 2011)
Upper Lough Corrib	Ireland	Trout	-31.2 to -24.8	8.4 to 15.6	(Maguire *et al.* 2011)
Lough Erne	Ireland	Trout	-32.6 to -28.8	14.1 to 19.4	(Keaveney *et al.* 2015)
Lough Lomond	Scotland	Trout	-27.7 to -17.8	8.4 to 14.4	(Etheridge *et al.* 2008)
River Enrick	Scotland	Trout	-26.0 to -22.5	7.5 to 9.9	(Grey 2001)
Loch Ness	Scotland	Trout	-27.9 to -21.1	8.0 to 14.2	(Grey 2001)

to the calcareous nature of the system, with possible fixation of methane by primary producers leading to depleted carbon isotope ratios (Graham, Harrison and Harrod, 2013).

The results from this study show that salmonids in Burrishoole are supported by a wide range of carbon energy sources, with the main split along the allochthony / autochthony gradient occurring as fish move downstream out of the headwater rivers and into Lough Feeagh. The shift in $\delta^{13}C$ between river and downstream lake habitats is consistent with the stream continuum concept whereby consumers are highly dependent on allochthonous carbon sources in headwaters, and that this dependence shifts more to autochthonous sources in downstream habitats (Doucett *et al.* 1996). This is not to say that allochthonous sources of energy in downstream lakes (e.g. lake litter) are not important, but rather that in-lake processing of organic matter and the addition of aquatic primary production (lake phytoplankton and phytobenthos) may lessen this importance. Determining the exact contribution of allochthonous and autochthonous sources to the diet of salmonids in Burrishoole was not possible with the data collected during this study, although the results presented here provide a very informative first step in designing a follow-up study with more targeted fieldwork. This might include trying to physically isolate phytoplankton and phytobenthic samples and hence accurately measure the baseline autochthonous isotopic signature required in models detecting the carbon source utilized in food web studies (Wilkinson *et al.* 2013; Keaveney *et al.* 2015).

The inclusion of allochthonous sources, and microbial processing of organic matter is likely to be the main reason for the range of trophic levels that we observed in the salmonid food web of Burrishoole. Primary producers (plants) are clearly separated at the base of the food web, with $\delta^{15}N$ values less than 0‰, while fish are grouped together at the top, with $\delta^{15}N$ between 8 and 10‰. In the middle of these two extremes are invertebrate consumers and a mix of periphyton, soils and sediments perhaps colonised with complex microbial assemblages. Using both periphyton and primary consumers as baselines for trophic position calculation placed salmonids somewhere between 2 and 3.5. Determination of trophic position is heavily influenced by the baseline $\delta^{15}N$ that is used (Anderson and Cabana, 2007), and it may be that either the periphyton or the primary consumers which we used as our baselines in both river and lake habitats were not the true baselines. In upstream rivers, we found a large gap in the trophic position between our baseline consumer (mayflies) and the fish, and it is likely that we missed some secondary consumers in this food chain. Lake periphyton may not truly represent the first trophic level of the lake food chain, as it may already have been colonised by a wide range of microinvertebrates and microbes. For example, had we used decomposing leaf litter as our baseline, salmonids would have been assigned to a trophic position greater than three. The wide range of observed trophic positions assigned to juvenile salmon and trout in Burrishoole is likely to be a consequence of omnivory, but differences in fractionation of nitrogen from one trophic level may also play a part (Jones and Waldron 2003). It also hints at food web complexity in both Lough Feeagh and the upstream rivers. Fish are functionally multi-chain omnivores, deriving energy from both periphyton- and phytoplankton-based food chains (Vadeboncoeur *et al.* 2005), as demonstrated by the wide range of $\delta^{13}C$ values recorded amongst fish cohorts (min=-31.3‰, max = -21.5‰), indicating wide utilisation of allochthonous and autochthonous sources.

The combination of stomach content analysis (SCA) and stable isotope analysis (SIA) is informative at several levels. For salmon, SCA indicated clear separation between the diets of fish from the three habitats: river, lake littoral and lake pelagic, and also a separation between the diet of 0+ and 1+ salmon in the lake littoral region. This distinction by habitat and/or age corresponded with a significant difference in $\delta^{13}C$ amongst salmon occupying the two habitats, and also manifested as a difference in $\delta^{15}N$ amongst groups. This change in $\delta^{15}N$ is consistent with fish changing their trophic position with habitat and age, perhaps as they grow larger, and are able to eat larger prey items. Although separation was less obvious in the trout samples examined for SCA, there was some differentiation between the diets of river and lake fish, but not between trout of different ages.

According to the SIA, 1+ trout are the only cohort apart from the salmon smolts where *Daphnia* appears to be somewhat important, indicating that perhaps these fish spend some time in the pelagic zone. The suggestion from this analysis is that riverine mayflies are a more likely source of energy to lake fish than mayfly living in the lake. This is rather surprising, but perhaps understandable when we look at the position of these lake mayflies in the isotope biplots (Fig. 6), where they are situated very close to the 0+ lake fish. It is possible that these lake mayflies are too big for juvenile salmonids to eat (they were all large *Heptagenia* sp. individuals), and we may have missed characterising smaller mayfly for this analysis. In contrast, the riverine mayfly samples comprise a mix of three species, including the smaller *Baetis rhodani*, which is probably a more palatable prey item for these small fish. Had we known the results from the stomach content analysis before we carried out the fieldwork, we would have paid more attention to characterising the prey items found in the river fish. For example, we decided to collect mayfly in the rivers as a signal of aquatic invertebrates, but these were not actually

found in the stomachs of the river salmon. Inclusion of some Trichoptera or Plecoptera might have given us more accurate end-members for the Bayesian mixing model conducted with SIAR. Similarly, the fact that riverine mayflies appear to be important in the diet of lake fish indicates either that the lake fish were moving in and out of areas in the lakes where smaller mayflies (with a riverine signal) were available for consumption, or alternatively, that we missed sampling an important portion of the food web that matches the SI signature of riverine mayflies. Nevertheless, the SCA and SIA both confirm the reliance of many salmonids on adult flies as a source of energy. The two analyses also show that there is clear separation between age classes and species as fish move between different habitats. The combination of SCA and SIA also highlights the swift binging of the smolts on zooplankton as they move downstream through Lough Feeagh to the sea, and indicates that this may be a very short lived, but likely important, phenomenon. The SIA has allowed us to construct a first draft of the food web supporting salmonids in Burrishoole, and this will support future research on determining how changes in land use and climate may affect different trophic levels, and hence fish production.

ACKNOWLEDGMENTS

We thank the Atlantic Salmon Trust who provided funding for the stable isotope analysis presented here. The field staff of the Marine Institute (Michael Murphy, Pat Nixon, Pat Hughes, Davy Sweeney and Joseph Cooney) assisted us with the collection of samples. Clive Trueman, Phil McGinnity and Andrew Jackson provided helpful advice while we were designing this study, and we gratefully acknowledge their time and support. Finally, Thomas Cummins (UCD), Tom Reed (UCC) and Jans-Robert Baars (UCD) facilitated the work of Niall King, Ross Finlay and Lauren Sibigtroth in this collaborative effort, and we thank them for their time and interest.

REFERENCES

Allott, N., McGinnity, P. and O'Hea, B. 2005 Factors influencing the downstream transport of sediment in the Lough Feeagh catchment, Burrishoole, Co. Mayo, Ireland. *Freshwater Forum* **23**, 126–38.

Anderson, C. and Cabana, G. 2007 Estimating the trophic position of aquatic consumers in river food webs using stable nitrogen isotopes. *Journal of the North American Benthological Society* **26**, 273–85. https://doi.org/10.1899/0887–3593(2007)26[273:ETTPOA]2.0.CO;2

Asmala, E., Carstensen, J. and Räike, A. 2019 Multiple anthropogenic drivers behind upward trends in organic carbon concentrations in boreal rivers. *Environmental Research Letters* **14**, 124018. https://doi.org/10.1088/1748–9326/ab4fa9

Bartels, P., Cucherousset, J., Steger, K., Eklöv, P., Tranvik, L.J. and Hillebrand, H. 2012 Reciprocal subsidies between freshwater and terrestrial ecosystems structure consumer resource dynamics. *Ecology* **93**, 1173–82. https://doi.org/10.1890/11–1210.1

Blenckner, T., Adrian, R., Livingstone, D.M., Jennings, E., Weyhenmeyer, G.A., George, D.G., *et al.* 2007 Large-scale climatic signatures in lakes across Europe: a meta-analysis. *Global Change Biology* **13**, 1314–26. https://doi.org/10.1111/j.1365–2486.2007.01364.x

Bonn, A., Allott, T., Hubacek, K. and Stewart, J. 2009 Managing change in the uplands - challenges in shaping the future. In: *Drivers of environmental change in uplands* (Eds A. Bonn, T. Allott, K. Hubacek and J. Stewart), 475–94. Routledge, London and New York.

Byrne, C., Poole, R. and McGinnity, P. 2000 Food consumed by wild and stocked brown trout, Salmo trutta L., and salmon, Salmo salar L., in an Irish lake. *SIL Proceedings, 1922–2010* **27**, 185–88. https://doi.org/10.1080/03680770.1998.11901223

Couture, S., Houle, D. and Gagnon, C. 2012 Increases of dissolved organic carbon in temperate and boreal lakes in Quebec, Canada. *Environmental Science and Pollution Research* **19**, 361–71. https://doi.org/10.1007/s11356–011–0565–6

Dalton, C., O'Dwyer, B., Taylor, D., de Eyto, E., Jennings, E., Chen, G., *et al.* 2014 Anthropocene environmental change in an internationally important oligotrophic catchment on the Atlantic seaboard of western Europe. *Anthropocene* **5**, 9–21. https://doi.org/10.1016/j.ancene.2014.06.003

Dauod, H.A., Bolger, T. and Bracken, J.J. 1986 Age, Growth and Diet of the brown trout Salmo Trutta L. in the Roundwood Reservoir System

Davis, M.J., Woo, I., Ellings, C.S., Hodgson, S., Beauchamp, D.A., Nakai, G., *et al.* 2018 Integrated Diet Analyses Reveal Contrasting Trophic Niches for Wild and Hatchery Juvenile Chinook Salmon in a Large River Delta. *Transactions of the American Fisheries Society* **147**, 818–41. https://doi.org/10.1002/tafs.10088

Dekar, M.P., King, R.S., Back, J.A., Whigham, D.F. and Walker, C.M. 2011 Allochthonous inputs from grass-dominated wetlands support juvenile salmonids in headwater streams: evidence from stable isotopes of carbon, hydrogen, and nitrogen. *Freshwater Science* **31**, 121–32. https://doi.org/10.1899/11–016.1

Dineen, G. 2005 *Terrestrial Energy Subsidies for Salmonids*. University College Cork, Cork.

Dineen, G., Harrison, S.S.C. and Giller, P.S. 2007 Diet partitioning in sympatric Atlantic salmon and brown trout in streams with contrasting riparian vegetation. *Journal of Fish Biology* **71**, 17–38. https://doi.org/10.1111/j.1095–8649.2007.01441.x

Doucett, R.R., Power, G., Barton, D.R., Drimmie, R.J. and Cunjak, R.A. 1996 Stable isotope analysis of nutrient pathways leading to Atlantic salmon. *Canadian Journal of Fisheries and Aquatic Sciences* **53**, 2058–66. https://doi.org/10.1139/f96–132

Doyle B.C., Eyto E. de, Dillane M., Poole R., McCarthy V., Ryder E., *et al.* 2019 Synchrony in catchment

stream colour levels is driven by both local and regional climate. *Biogeosciences* **16**, 1053–71. https://doi.org/10.5194/bg-16–1053–2019

Etheridge, E.C., Harrod, C., Bean, C. and Adams, C.E. 2008 Continuous variation in the pattern of marine v. freshwater foraging in brown trout Salmo trutta L. from Loch Lomond, Scotland. *Journal of Fish Biology* **73**, 44–53. https://doi.org/10.1111/j.1095–8649.2008.01905.x

de Eyto, E., Dalton, C., Dillane, M., Jennings, E., McGinnity, P., O'Dwyer, B., *et al.* 2016a The response of North Atlantic diadromous fish to multiple stressors, including land use change: a multidecadal study. *Canadian Journal of Fisheries and Aquatic Sciences* **73**, 1759–69. https://doi.org/10.1139/cjfas-2015–0450

de Eyto, E., Jennings, E., Ryder, E., Sparber, K., Dillane, M., Dalton, C., *et al.* 2016b Response of a humic lake ecosystem to an extreme precipitation event: physical, chemical and biological implications. *Inland Waters* **6**, 483–98. https://doi.org/10.1080/IW-6.4.875

Fealy, R., Allott, N., Broderick, C., de Eyto, E., Dillane, M., Erdil, R.M., *et al.* 2014 *RESCALE: Review and Simulate Climate and Catchment Responses at Burrishoole*. Galway.

Finstad, A.G., Helland, I.P., Ugedal, O., Hesthagen, T. and Hessen, D.O. 2014, Unimodal response of fish yield to dissolved organic carbon. *Ecology letters* **17**, 36–43

Freeman, C., Evan, C.D., T.M.D., Reynolds, B. and Fenner, N. 2001 Export of organic carbon from peat soils. *Nature* **412**, 785

Frost W.E. 1938 River Liffey Survey: II. The Food Consumed by the Brown Trout (Salmo trutta Linn.) in Acid and Alkaline Waters. *Proceedings of the Royal Irish Academy. Section B: Biological, Geological, and Chemical Science* **45**, 139–206

Gallego-Sala, A.V., Clark, J.M., House, J.I., Orr, H.G., Prentice, I.C., Smith, P., *et al.* 2010 Bioclimatic envelope model of climate change impacts on blanket peatland distribution in Great Britain. *Climate Research* **45**, 151–62. https://doi.org/10.3354/cr00911

Graham, C.T., Harrison, S.S.C. and Harrod, C. 2013 Development of non-lethal sampling of carbon and nitrogen stable isotope ratios in salmonids: effects of lipid and inorganic components of fins. *Isotopes in Environmental and Health Studies* **49**, 555–66. https://doi.org/10.1080/10256016.2013.808635

Grey, J. 2001 Ontogeny and dietary specialization in brown trout (Salmo trutta L.) from Loch Ness, Scotland, examined using stable isotopes of carbon and nitrogen. *Ecology of Freshwater Fish* **10**, 168–76. https://doi.org/10.1034/j.1600–0633.2001.100306.x

Holm, J. Chr. and Møller, D. 1984 Growth and prey selection by Atlantic salmon yearlings reared on live freshwater zooplankton. *Aquaculture* **43**, 401–12. https://doi.org/10.1016/0044–8486(84)90248–5

Ise, T., Dunn, A.L., Wofsy, S.C. and Moorcroft, P.R. 2008 High sensitivity of peat decomposition to climate change through water-table feedback. *Nature* **1**, 763–66

Jardine, T.D., McGeachy, S.A., Paton, C.M., Savoie, M. and Cunjak, R.A. 2003 Stable isotopes in aquatic systems: Sample preparation, analysis, and interpretation. *Can. Manuscr. Rep. Fish. Aquat. Sci.* **2656**, 1–39

Jennings, E., Allott, N., McGinnity, P., Poole, R., Quirke, W., Twomey, H., *et al.* 2000 The North Atlantic Oscillation: Effects on Freshwater Systems in Ireland. *Biology and Environment: Proceedings of the Royal Irish Academy* **100B**, 149–57

Jennings, E., Jarvinen, M., Allott, N., Arvola, L., Moore, K., Naden, P., *et al.* 2010 Impacts of climate on the flux of dissolved organic carbon from catchments. In: *The Impact of Climate Change on European Lakes*. Aquatic Ecology Series, (Ed. G. George), 199–20. Springer, London.

Jones, J.I. and Waldron, S. 2003 Combined stable isotope and gut contents analysis of food webs in plant-dominated, shallow lakes. *Freshwater Biology* **48**, 1396–407. https://doi.org/10.1046/j.1365–2427.2003.01095.x

Jones, M.B., Donnelly, A. and Albanito, F. 2006 Responses of Irish vegetation to future climate change. *Biology and Environment: Proceedings of the Royal Irish Academy* **106B**, 323–34

Karlsson, J., Berggren, M., Ask, J., Byström, P., Jonsson, A., Laudon, H., *et al.* 2012 Terrestrial organic matter support of lake food webs: Evidence from lake metabolism and stable hydrogen isotopes of consumers. *Limnology and Oceanography* **57**, 1042–48. https://doi.org/10.4319/lo.2012.57.4.1042

Keaveney, E.M., Reimer, P.J. and Foy, R.H. 2015 Young, Old, and Weathered Carbon—Part 2: Using Radiocarbon and Stable Isotopes to Identify Terrestrial Carbon Support of the Food Web in an Alkaline, Humic Lake. *Radiocarbon* **57**, 425–38

Kelly-Quinn, M. and Bracken, J.J. 1990 A seasonal analysis of the diet and feeding dynamics of brown trout, Salmo trutta L., in a small nursery stream. *Aquaculture Research* **21**, 107–24. https://doi.org/10.1111/j.1365–2109.1990.tb00386.x

Layer, K., Hildrew, A.G., Jenkins, G.B., Riede, J.O., Rossiter, S.J., Townsend, C.R., *et al.* 2011 Chapter Two - Long-Term Dynamics of a Well-Characterised Food Web: Four Decades of Acidification and Recovery in the Broadstone Stream Model System. In: *Advances in Ecological Research*. (Ed. G. Woodward), pp. 69–117. Academic Press.

Lehane, B.M., Walsh, B., Giller, P.S. and O'Halloran, J. 2001 The influence of small-scale variation in habitat on winter trout distribution and diet in an afforested catchment. *Aquatic Ecology* **35**, 61–71. https://doi.org/10.1023/A:1011467711628

Maguire, C., Gallagher, K., Maggs, C., Dick, J., Caffrey, J.M., O'Flynn, C., *et al.* 2011 *Alien Invasive Species in Irish Water Bodies*. EPA report 2007-W-MS-2-S1. Wexford.

Manetta, G.I., Benedito-Cecilio, E. and Martinelli, M. 2003 Carbon sources and trophic position of the main species of fishes of Baía River, Paraná River floodplain, Brazil. *Brazilian Journal of Biology* **63**, 283–90. https://doi.org/10.1590/S1519–69842003000200013

McArdle B.H. and Anderson M.J. 2001 Fitting Multivariate Models to Community Data: A Comment on Distance-Based Redundancy Analysis. *Ecology* **82**, 290–97. https://doi.org/10.1890/0012–9658(2001)082[0290:FMMTCD]2.0.CO;2

McGinnity, P., Jennings, E., de Eyto, E., Allott, N., Samuelsson, P., Rogan, G., *et al.* 2009 Impact of naturally spawning captive-bred Atlantic salmon on wild populations: depressed recruitment and increased

risk of climate-mediated extinction. *Proceedings of the Royal Society of London B: Biological Sciences* **283**, 3601–10

Meyers, P.A. 2003 Applications of organic geochemistry to paleolimnological reconstructions: a summary of examples from the Laurentian Great Lakes. *Organic Geochemistry* **34**, 261–89. https://doi.org/10.1016/S0146–6380(02)00168–7

Morrison, B.R.S. 1983 Observations on the food of juvenile Atlantic salmon, Salmo salar L, reared in a Scottish hill loch. *Journal of Fish Biology* **23**, 305–13. https://doi.org/10.1111/j.1095–8649.1983.tb02909.x

O'Gorman, R., Lantry, B.F. and Schneider, C.P. 2004 Effect of Stock Size, Climate, Predation, and Trophic Status on Recruitment of Alewives in Lake Ontario, 1978–2000. *Transactions of the American Fisheries Society* **133**, 855–67. https://doi.org/10.1577/T03–016.1

Oksanen, J., Blanchet, F.G., Kindt, R., Legendre, P., Minchin, P.R., O'Hara, R.B., *et al*. 2015 *vegan: Community Ecology Package. R package version 2.2–1.*

Parnell, A., Inger, R., Bearhop, S. and Jackson, A. 2008 SIAR: stable isotope analysis in R. *The Comprehensive R Archive Network) Available at http://cran.r-project.org/web/packages/siar/index.html* [Verified 15 July 2012]

Persson, A. and Hansson, L.-A. 1999 Diet shift in fish following competitive release. *Canadian Journal of Fisheries and Aquatic Sciences* **56**, 70–78. https://doi.org/10.1139/f98–141

Poole, W.R., Dillane, M., de Eyto, E., Rogan, G., McGinnity, P. and Whelan, K. (2006). Characteristics of the Burrishoole Sea Trout Population: Census, Marine Survival, Enhancement and Stock-Recruitment Relationship, 1971–2003. In: *Sea Trout: Biology, Conservation and Management* (Eds G. Harris and N. Milner), pp. 279–306. Blackwell, Oxford.

Poole, W.R., Diserud, O.H., Thorstad, E.B., Durif, C.M., Dolan, C., Sandlund, O.T., *et al.* 2018 Long-term variation in numbers and biomass of silver eels being produced in two European river systems. *ICES Journal of Marine Science*. https://doi.org/10.1093/icesjms/fsy053

Post, D.M., Layman, C.A., Arrington, D.A., Takimoto, G., Quattrochi, J. and Montaña, C.G. 2007 Getting to the fat of the matter: models, methods and assumptions for dealing with lipids in stable isotope analyses. *Oecologia* **152**, 179–89. https://doi.org/10.1007/s00442–006–0630-x

Renou-Wilson, F., Bolger, T., Bullock, C., Convery, F., Curry, J., Ward, S., *et al.* 2011 BOGLAND: Sustainable Management of Peatlands in Ireland. *STRIVE Report Series*, 181

Ryder, E. 2015 *Estimating Carbon Pools and Processing in a Humic Lake*. Dundalk Institute of Technology, Dundalk.

Ryder, E., de Eyto, E., Dillane, M., Poole, R. and Jennings, E. 2014 Identifying the role of environmental drivers in organic carbon export from a forested peat catchment. *Science of The Total Environment* **490**, 28–36. https://doi.org/10.1016/j.scitotenv.2014.04.091

Solomon, C.T., Carpenter, S.R., Clayton, M.K., Cole, J.J., Coloso, J.J., Pace, M.L., *et al.* 2011 Terrestrial, benthic, and pelagic resource use in lakes: results from a three-isotope Bayesian mixing model. *Ecology* **92**, 1115–25. https://doi.org/10.1890/10–1185.1

Sparber, K. 2012 *Neo- and palaeolimnological investigations in a humic and a clear water lake in the west of Ireland*. Mary Immaculate College, University of Limerick.

Stinson, N.E. 1957 The Food and Growth of Brown Trout (Salmo trutta L.) in Three Rivers in Co. Tyrone. *Proceedings of the Royal Irish Academy. Section B: Biological, Geological, and Chemical Science* **59**, 129–54

Syväranta, J., Hämäläinen, H. and Jones, R.I. 2006 Within-lake variability in carbon and nitrogen stable isotope signatures. *Freshwater Biology* **51**, 1090–02. https://doi.org/10.1111/j.1365–2427.2006.01557.x

Tanentzap, A.J., Szkokan-Emilson, E.J., Kielstra, B.W., Arts, M.T., Yan, N.D. and Gunn, J.M. 2014 Forests fuel fish growth in freshwater deltas. *Nature Communications* **5**, 4077. https://doi.org/10.1038/ncomms5077

Trueman, C.N., Johnston, G., O'Hea, B. and MacKenzie, K.M. 2014 Trophic interactions of fish communities at midwater depths enhance long-term carbon storage and benthic production on continental slopes. *Proceedings of the Royal Society B: Biological Sciences* **281**, 20140669

Vadeboncoeur, Y., McCann, K.S., Zanden, M.J.V. and Rasmussen, J.B. 2005 Effects of Multi-chain Omnivory on the Strength of Trophic Control in Lakes. *Ecosystems* **8**, 682–93. https://doi.org/10.1007/s10021–003–0149–5

Vander Zanden, M.J. and Rasmussen, J.B. 2001 Variation in δ15N and δ13C trophic fractionation: Implications for aquatic food web studies. *Limnology and Oceanography* **46**, 2061–66. https://doi.org/10.4319/lo.2001.46.8.2061

Wieczorek, A.M., Power, A.M., Browne, P. and Graham, C.T. (2018). Stable-isotope analysis reveals the importance of soft-bodied prey in the diet of lesser spotted dogfish Scyliorhinus canicula. *Journal of Fish Biology* **93**, 685–93. https://doi.org/10.1111/jfb.13770

Wilkinson, G.M., Carpenter, S.R., Cole, J.J., Pace, M.L. and Yang, C. 2013 Terrestrial support of pelagic consumers: patterns and variability revealed by a multilake study. *Freshwater Biology* **58**, 2037–49. https://doi.org/10.1111/fwb.12189

PLOS ONE

RESEARCH ARTICLE

Impacts of a record-breaking storm on physical and biogeochemical regimes along a catchment-to-coast continuum

Seán Kelly[1,2]*, **Brian Doyle**[1,2], **Elvira de Eyto**[2], **Mary Dillane**[2], **Phil McGinnity**[2,3], **Russell Poole**[2], **Martin White**[4], **Eleanor Jennings**[1]

1 Centre for Freshwater and Environmental Studies, Dundalk Institute of Technology, Louth, Ireland, **2** Marine Institute, Furnace, Newport, Mayo, Ireland, **3** School of Biological, Earth & Environmental Sciences, University College Cork, Cork, Ireland, **4** Earth & Ocean Science, National University of Ireland Galway, Galway, Ireland

* sean.kelly@dkit.ie

Citation: Kelly S, Doyle B, de Eyto E, Dillane M, McGinnity P, Poole R, et al. (2020) Impacts of a record-breaking storm on physical and biogeochemical regimes along a catchment-to-coast continuum. PLoS ONE 15(7): e0235963. https://doi.org/10.1371/journal.pone.0235963

Editor: A. P. Dimri, Jawaharlal Nehru University, INDIA

Received: December 16, 2019

Accepted: June 25, 2020

Published: July 28, 2020

Peer Review History: PLOS recognizes the benefits of transparency in the peer review process; therefore, we enable the publication of all of the content of peer review and author responses alongside final, published articles. The editorial history of this article is available here: https://doi.org/10.1371/journal.pone.0235963

Data Availability Statement: All meteorological and hydrological data files used in the analyses presented in this study are available for download from: http://data.marine.ie/geonetwork/srv/eng/

Abstract

The impacts of changes in climate are often most readily observed through the effects of extremes in local weather, effects that often propagate through multiple ecosystem levels. Precise effects of any extreme weather event depend not only on the type of event and its timing, but also on the ecosystem affected. Here the cascade of effects following the arrival of an atmospheric river (directed by record-breaking Storm Desmond) across terrestrial, freshwater and coastal zones is quantified, using the Burrishoole system on the Atlantic coast of Ireland as a natural observatory. We used a network of high-frequency *in-situ* sensors to capture in detail the effects of an unprecedented period of rainfall, high wind speeds and above-average winter air temperatures on catchment and estuarine dynamics. In the main freshwater lake, water clarity decreased and acidity increased during Storm Desmond. Surface heat input, due to a warm and moist above-lake air mass, was rapidly distributed throughout the water column. River discharge into the downstream coastal basin was estimated to be the highest on record (since 1976), increasing the buoyancy flux by an order of magnitude and doubling the water column stratification stability. Entrainment of salt into the outflowing freshwater plume exported resident salt from the inner estuarine basin, resulting in net salt loss. Here, the increased stratification markedly reinforced isolation of the bottom waters, promoting deoxygenation. Measurements of current between the inner estuarine basin and the adjacent coastal waters indicated a 20-fold increase in the volume of seaward flowing low-salinity water, as a result of storm rainfall over the watershed. Storm impacts spanned the full catchment-to-coast continuum and these results provide a glimpse into a potential future for hydrological systems where these severe hydroclimatic events are expected to occur more frequently.

catalog.search#/metadata/ie.marine.data:dataset.3979.

Funding: SK was funded under the Marine Research programme by the Irish Government (Cullen Fellowship CF/15/03 and BEYOND 2020 PBA/FS/16/02). PMcG was also supported by the Marine Institute under the Marine Research Programme (RESPI/FS/16/01). https://www.marine.ie/Home/home. The funders had no role in study design, data collection and analysis, decision to publish, or preparation of the manuscript.

Competing interests: The authors have declared that no competing interests exist.

Introduction

The attribution of individual extreme weather events to directional climate change is highly complex, given natural climatic variability and the overall rarity of such events [1,2]. However the magnitude and frequency of extreme weather events are projected to increase given anthropogenically-influenced changes in atmospheric conditions [3]. Changes in long-term mean temperatures, for example, are also likely to be associated with changes in heat extremes (e.g. more severe heatwaves) [2,4]. For precipitation, an increase in the intensity and frequency of heavy rainfall and flood events is consistent with expectations given increasing atmospheric water vapour [5,6]. Relationships between observed trends in storm and cyclone activity and climate forcing are more nuanced and uncertain [5]. Evidence does suggest, however, that increased storm magnitude over the past number of decades is linked to warmer tropical sea surface temperatures [7] and model projections indicate that more hurricane-force storms may be experienced in western Europe due to rising sea surface temperatures in the Atlantic [8]. Therefore, while not singularly attributing such events to climate change, occurrences of extreme weather represent the most tangible way in which the public perceive and recognise climate change. These events thus represent important opportunities to motivate public concern for climate action and policy to mitigate continued carbon dioxide emissions [9,10]. Furthermore, quantifying the impacts of episodic weather events across ecosystems can provide a valuable insight into how these systems respond and can serve as a tool for predicting which specific geographical areas and ecosystems may be most vulnerable to increased frequency or intensity of different types of extreme weather events. However due to their short-lived and unpredictable nature, knowledge of the consequences of extreme events for physical, chemical or biological regimes is scarce and often very difficult to capture [11,12].

Freshwater systems (lakes and their surrounding catchments) represent ideal candidate systems for observing the effects of climate and extreme weather events and have developed a reputation as 'sentinels' of climate change [13,14]. This is due to their intrinsic relationship with the overlying atmosphere and surrounding landscape, with lakes integrating changes in meteorological (e.g. air temperature, wind dynamics, solar radiation, precipitation) and terrestrial (e.g. catchment run-off) conditions. Large magnitude, short-lived changes in any of these variables have the capacity to affect biotic and abiotic conditions in lakes, although the precise changes depend on the category and timing (season) of the event as well as lake-type (e.g. oligotrophic versus eutrophic, shallow versus deep, mixed versus stratified etc) [12]. For example, in thermally stratified lakes storm events may modify the thermal structure by destabilising the water column and deepening the biologically-productive surface layer [15–17]. Such changes may reduce water clarity (e.g. [11]) or cause exchange between epilimnetic and nutrient-rich, oxygen-poor hypolimnetic waters [18]. In contrast, in mixed lakes without significant vertical thermal gradients such events may have less of an impact on whole-lake mixing and thus ecological regimes. Heavy rainfall, by increasing rates of catchment run-off, can deliver particulate and dissolved organic matter from the surrounding catchment, which can increase rates of primary-producer respiration [19] and reduce light penetration [20]. The extent to which lake ecosystems can recover (resiliency) depends on the type of surrounding catchment area as well as current nutrient status of the lake, with clear-water, oligotrophic lakes perhaps likely to undergo more significant changes than eutrophic or humic lakes [11,17,19].

Estuarine environments also tend to respond rapidly to extreme weather events also, although in addition to being influenced by atmospheric and terrestrial conditions, estuaries integrate changes in the adjacent marine environment, making them one of the most sensitive habitats to extreme weather events and climate change in general [21]. How estuarine systems respond to extreme climate events varies between individual sites, with classification based on

geomorphology (depth, width), salinity structure (well-mixed through to stratified) and tidal range [22]. As with lakes, generalisation of the effects of extreme weather events on estuaries can also be difficult–here we consider the effects of storms and floods which subject estuarine systems to wind-forcing and large volumes of freshwater input.

Heavy rainfall events may influence salinity structure, with river runoff potentially pushing the salinity intrusion limit down-estuary, exporting nutrients and salt in the process [23,24] and generating stratification in shallow well-mixed estuaries [25]. In deeper, semi-enclosed lagoonal and fjordic estuaries, which are subject to relatively weaker tidal forcing, high river flow following precipitation could reinforce stratification, increasing renewal time of deep-water masses and prompting concern over deoxygenation [26]. If the same floods lead to an influx of organic matter and nutrients from runoff, heightened respiration may compound the risk of bottom water oxygen depletion and coastal water quality in general is likely to decline [27,28]. The way in which estuarine stratification dynamics, such as the baroclinic flow fields, adjust to large quantities of freshwater input is of fundamental importance to estuarine physics and salt balance regulation [29–31]. An added complexity to the stabilising effects of freshwater input is that strong winds are often associated with storm events and serve to destabilise the water column potentially mixing saltwater and freshwater layers. In estuaries with deoxygenated deep-water, such storms could enhance upwelling of suboxic waters to shallower zones inhabited by aerobic organisms [32].

The frequency and severity of storm category weather events during winter 2015/16 in Ireland and the Britain was considered exceptional, peaking with the extratropical cyclone Storm Desmond during 4–6 December [33]. Rainfall during Desmond broke the 24- and 48-hour British rainfall records and multiple rivers throughout Ireland and Britain recorded highest ever peak discharge [34]. Desmond was caused by enhanced horizontal water vapour transport from the Atlantic Ocean, with the plume of moist air generating an 'atmospheric river' and causing extreme precipitation following orographic lifting along mountainous western Irish and British coastlines [35]. The increased heat content of the North Atlantic has led to long-term increases in atmospheric humidity, which could cause more extreme precipitation events like Desmond to occur over Ireland, Britain and western Europe [35,36]. In this study, we used *in-situ* high frequency sensor equipment to investigate the impacts of this remarkable succession of winter storms and floods on the contiguous habitats of a catchment-lake-estuarine system. We also analysed the extent to which these episodic events modified the physical and biogeochemical regimes in the system and which ecosystems were most affected by this extreme winter flood. Our study site, the Burrishoole catchment, is representative of many upland peat catchments that occur throughout Ireland and the United Kingdom, particularly along western seaboards. Thus we envisage that the results from this analysis could be generalised to many similar systems that are also anticipated to face the same increased occurrence of extreme rainfall events.

Methods

Site description

The Burrishoole catchment (~100 km^2) is a predominantly upland blanket peat, oligotrophic catchment located within the Nephin Beg mountain range on the west Atlantic coast of Ireland (Fig 1). Rivers and streams are generally acidic or neutral and water chemistry depends on local and regional climate as well as surrounding soil composition in each of the sub-catchments [37]. Given its coastal proximity, the catchment generally experiences a temperate climate with mild winters (mean December-February 2005–18 air temperature of 6.0˚ C) and summers (mean June-August 2005–18 air temperature of 14.3˚ C) and a diurnal sea breeze

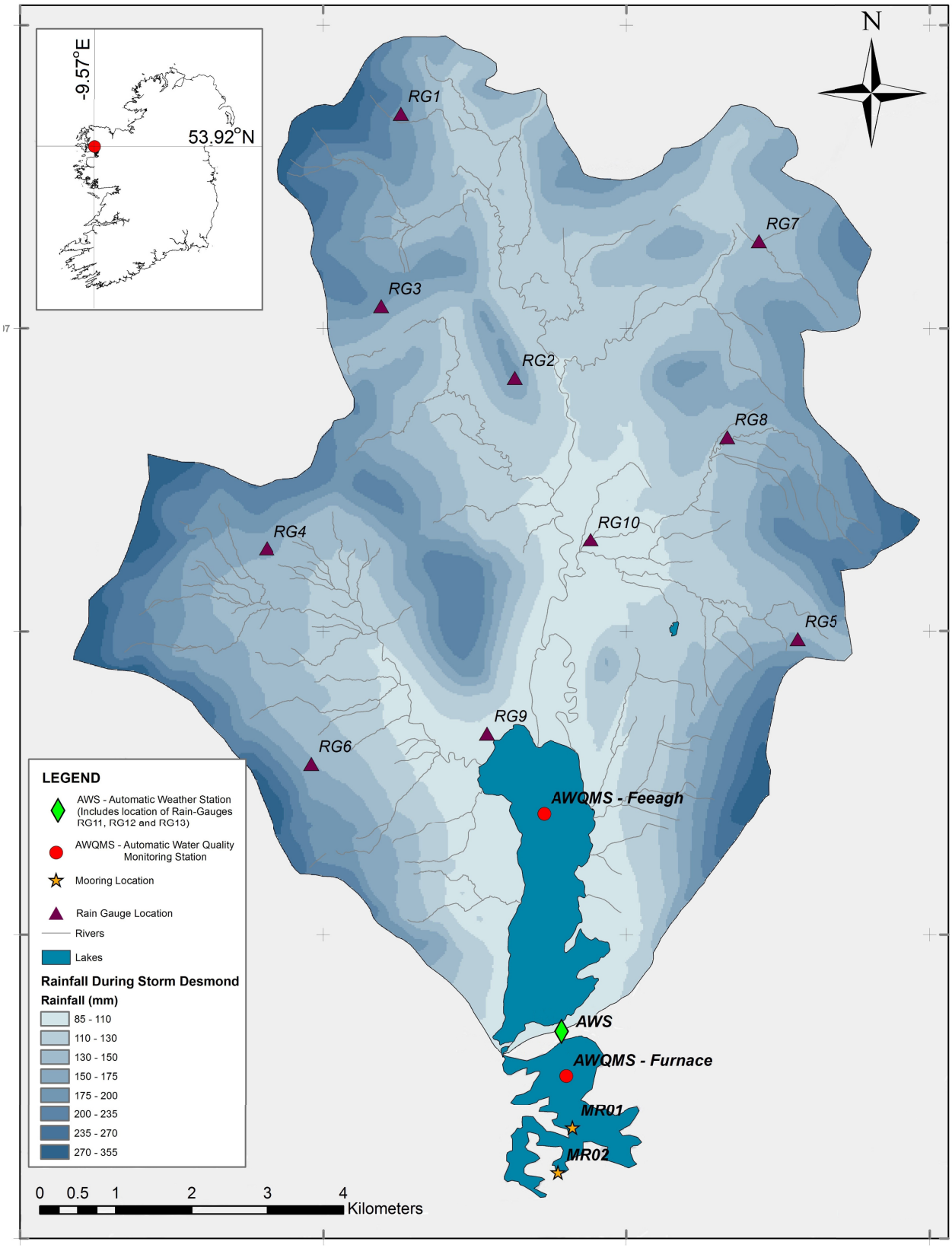
N
-9.57°E
53.92°N
RG1
RG7
RG3
RG2
RG8
RG4
RG10
RG5
RG9
RG6
AWQMS - Feeagh
AWS
AWQMS - Furnace
MR01
MR02
LEGEND
AWS - Automatic Weather Station (Includes location of Rain-Gauges RG11, RG12 and RG13)
AWQMS - Automatic Water Quality Monitoring Station
Mooring Location
Rain Gauge Location
Rivers
Lakes
Rainfall During Storm Desmond
Rainfall (mm)
85 - 110
110 - 130
130 - 150
150 - 175
175 - 200
200 - 235
235 - 270
270 - 355
0 0.5 1 2 3 4
Kilometers

Fig 1. Spatial distribution of rainfall over Burrishoole catchment during storm Desmond. Measured by 13 rain gauges (RG) (note that RG 11, 12 and 13 are situated in the vicinity of the Automatic Weather Station (AWS)). Also shown are the locations of the Automatic Water Quality Monitoring Stations (AWQMS) on Lough Feeagh and Lough Furnace and the additional instrumented moorings MR01 and MR02 on Furnace, described in the text. Shapefiles used for lakes and rivers shown here are available at: http://gis.epa.ie/GetData/Download.

https://doi.org/10.1371/journal.pone.0235963.g001

with mean wind speeds of ~5 m s^{-1} [38]. Burrishoole's primary lake basin is Lough Feeagh, with a surface area of 3.95 km^2, max depth of 46 m, mean depth of 14.5 m and volume of 5.9 x 10^7 m^3. The water of Feeagh is oligotrophic and humic, with a mean secchi disk depth of 1.7 m, pH of 6.6 and annual mean total nitrogen and phosphorus of 430 μg l^{-1} and 6.1 μg l^{-1} respectively [39]. Feeagh is located at the base of the Burrishoole catchment, draining a ~84 km^2 watershed into Lough Furnace through two short outflows, the Salmon Leap and (man-made) Mill Race rivers. Furnace is a deep lagoonal estuary (M_2 semi-diurnal tide dominant) with a surface area of 1.5 km^2, max depth of 21 m and mean depth of 7.9 m. The system comprises a main inner basin (volume of 6.75 x 10^6 m^3) connected to the open coastal waters of Clew Bay by a 1-km-long shallow and narrow channel. Tidal currents transporting coastal water must traverse this channel and two narrow topographic constrictions before reaching the inner basin [38]. The inner Furnace basin is notable for its strong saline stratification and deep anoxia, resembling a meromictic saline lake, although ventilation of the bottom water by dense tidal inflows occurs irregularly [38]. A research station operated by the Marine Institute is situated on the northern shore of Furnace and has served primarily as an international index site for migratory fish populations (Atlantic salmon (*Salmo salar* L.), trout (*Salmo trutta* L). and European eel (*Anguilla Anguilla* L.)) in the North Atlantic for half a century [40,41]. The upper parts of the catchment have Special Area of Conservation (SAC) status for the conservation of Atlantic salmon and otter (*Lutra lutra*), two species listed in Annex II of the EU Habitats Directive. Lough Furnace is part of the Clew Bay Complex Special Area of Conservation (SAC site code 001482).

Data collection and processing

This study relied on data sources routinely collected as part of the Marine Institute's long-term environmental monitoring programme in Burrishoole. Spatial extent of rainfall over the entire Burrishoole catchment was recorded by 13 tipping bucket rain gauges (Davis Instruments Corp, Hayward, CA, USA) located throughout the catchment and lake and lagoon levels were monitored by pressure sensors (OTT, Kempton, Germany) recording every 15 minutes (Fig 1). Automatic water quality monitoring stations (AWQMS) were located on Feeagh and Furnace (Fig 1). Each AWQMS was instrumented with on-lake meteorological arrays recording wind speed and direction, air temperature, shortwave radiation and surface pressure at 2-minute intervals. A multi-parameter sonde (Hydrolab DS5, OTT, Kempton, Germany) was suspended from each AWQMS; on Feeagh this sonde was kept at 0.9 m below the surface recording every 2 minutes whilst on Furnace the sonde was attached to an undulating winch profiler, recording 4 full water column profiles daily (at 00:00, 06:00, 12:00 and 18:00 hours). Parameters measured on each sonde included temperature, conductivity, pH and dissolved oxygen. The Feeagh AWQMS also contained a surface nephelometer (Chelsea Technologies Group Ltd, Surrey, UK) and thermistors (Labfacility Ltd., Bognor Regis, UK) that spanned the full water column at depth intervals of 2.5, 5, 8, 11, 14, 16, 18, 20, 22, 27, 32, 42 m, recording every 2 minutes. An additional automatic weather station (AWS) maintained by Met Éireann since 2005 was situated on the shoreline between both loughs, which recorded relative humidity and rainfall in addition to the same over-water meteorological variables recorded at each AWQMS (Fig 1).

On Furnace two additional instrumented moorings were located at the entrance channel into the main inner basin (Fig 1). MR01 (S1 Fig) contained a bottom-mounted, upward looking 1-MHz Nortek Aquadopp three-beam current profiler (ADCP) (Nortek AS, Rud, Norway). The ADCP sensor head, with a 25˚ beam angle to the vertical, was mounted at 0.2 m above the bed. The ADCP recorded in 0.5 m bin intervals, with a 0.4 m blanking distance and a velocity measure averaged over a 60 second ping interval. Two temperature and conductivity sensors (T/C) were attached to the same mooring (SBE-37 MicroCATs (Sea-Bird Scientific, Bellevue, Washington, USA)). One T/C sensor was mounted on the bottom ADCP frame and the second positioned ~1 m below the surface on an L-shaped mooring. An additional T/C, also recording pressure, was located further downstream (MR02, Fig 1). All of these instruments had synchronised internal clocks and logged measurements every 30 minutes from 13:30:00 November 26th 2015 until 11:30:00 January 21st 2016.

CTD downcasts from the Furnace AWQMS were extrapolated onto a standard depth grid spanning the water column from 0.6 m– 12.9 m in 0.15 m depth increments. Practical salinity (derived from actual conductivity and temperature) and water density (derived from salinity and temperature) were computed according to the UNESCO algorithm [42] for all sensors recording temperature and conductivity.

ADCP velocity vectors were low-pass filtered with a 6 hour cut-off frequency to remove higher frequency tidal harmonics. Low-passed horizontal velocity vectors were then rotated into along- (v) and across-channel (u) components using principal components analysis (PCA) [43]. Whilst the standard ADCP bin sizes spanned 0.5 m in the vertical, the lowest bin was weighted to account for the bottom 1.1 m of the channel (i.e. 0.5 m bin size + 0.4 m blanking distance + 0.2 m frame height above the bed). For each individual ADCP profile, the uppermost usable bin was defined as the shallowest bin below the computed depth of sidelobe interference with contaminated shallower measurements discarded. In order to account for this portion of the upper water column not measured (~10–15%), each current profile was extrapolated to the surface level using a constant velocity from the uppermost usable bin.

Data analysis

Precipitation recorded by each of the 13 rain gauges throughout the catchment were summed to 24 hour totals. To estimate the total rainfall volume that fell in the catchment within a specific time period, the raster calculator routine in the 'Spatial Analyst' toolbox in the GIS Software ArcMap 10 [44] was used. The raster calculator routine allows mathematical calculations to be conducted on existing raster data sets, in this case a raster map of the topography of the catchment. The topographic raster data comprised a 10 by 10 metre grid of the catchment with an altitude above sea level value at the centre of each grid square. To estimate rainfall volumes during Storm Desmond, an altitude-rainfall regression equation was calculated for the time period 4–6 December 2015. The rainfall volumes for each grid square were summed to get the total rainfall volume. However, the altitude-rainfall volume relationship during storm Desmond (R^2 = 0.32) was not strong when compared to a 14-year study period, 2004–2017 (R^2 = 0.82). Analysis of rainfall volumes during the storm showed that lower volumes of rainfall were recorded in the rain gauges at higher altitudes in the catchment than would otherwise be expected. Presumably the breakdown of the altitude-rainfall volume relationship at higher elevations in the catchment is a result of high wind speeds causing 'under-catch' of rainwater during the storm. Under-catch is a common phenomenon affecting the accuracy of rain gauges, where high wind speeds during storms cause wind flow deflections and turbulence patterns around the gauge funnel which in turn cause some of the raindrops to be ejected from the funnel system [45].

To correct for this, the rainfall volumes for the three rain gauges at the greatest altitudes were revised. Using the AWS rain gauge (Fig 1A) as an index site, the rainfall volume measured at this site during Storm Desmond was used to estimate the rain volumes at the three highest altitude sites. Coefficients between the index site and each of the high altitude sites were calculated over the 14 year period for which rain gauge data was available. The rainfall volume at AWS was multiplied by each of the rainfall volume coefficients for the three highest altitude sites to adjust for under-catch. Following adjustment, the altitude-rainfall volume relationship during the specific Storm Desmond timeframe improved to give an R^2 value of 0.73 and a revised total rainfall during Storm Desmond was estimated using this method.

Storm effects on dynamical transfer processes of heat and momentum across the air-water interface on both Feeagh and Furnace were assessed by calculating the net surface heat flux and energy input due to wind stress. The surface heat flux (Q_{shf}, W m^{-2}) over the month of December 2015 was calculated following [46]:

$$Q_{shf} = Q_{swin} + Q_{lwin} + Q_{lwout} + Q_h + Q_e \quad (1)$$

where Q_{swin} (W m^{-2}) is the net incoming shortwave solar radiation (accounting for reflected shortwave due to surface albedo) and Q_{lwin} and Q_{lwout} are the incoming and outgoing thermal radiation (W m^{-2}). Q_h (W m^{-2}) is the sensible heat flux, $Q_h = \rho_a C_{Pa} C_H W_z (T_s - T_z)$, and Q_e (W m^{-2}) is latent heat flux, $Q_e = \rho_a L_v C_E W_z (q_s - q_z)$, where ρ_a is the density of air at the air-sea interface (kg m^{-3}), C_{Pa} is the specific heat of air (J kg^{-1}°C^{-1}), C_H the turbulent transfer coefficient for heat, W_z the wind speed at height Z above the water (m s^{-1}), T_s the surface water temperature (°C), T_z the air temperature at height Z above the water surface (°C), L_v the latent heat of vaporization (J kg^{-1}), C_E is the turbulent transfer coefficient for humidity, q_s the saturated specific humidity (kg kg^{-1}) at T_s and q_z the specific humidity of unsaturated air (kg kg^{-1}) at height Z above the water surface. One caveat relating to the heat flux calculations presented herein is that the humidity measurements were only available from the shoreline meteorological station and not directly above either Feeagh or Furnace water surface. Positive values of each variable in Eq (1) indicate downward flux of heat; negative values indicate loss of heat to the atmosphere.

Mechanical energy transfer from the wind to the water was parameterised as the rate of work per unit area by wind stress at 10m above the water surface (W m^{-2}) [47]:

$$E_{10} = \rho_a C_D W_{10}^3 \quad (2)$$

where C_D is the surface drag coefficient. Turbulent transfer coefficients for heat (C_H), momentum (C_D) and humidity (C_E) were scaled to 10m above the water surface by correcting for atmospheric stability [46,48].

An informative measure for saline Furnace was to estimate a buoyancy flux associated with the storm through the surface, B_f (m^2 s^{-3}), including a moisture flux term (*e.g.* [49]):

$$B_f = g\left(\frac{\alpha}{\rho_0 C_P} Q_{shf} + \beta S_0 \left(\frac{Q_f}{A_s} + P - E\right)\right) \quad (3)$$

where g is gravity (m s^{-2}), ρ_0 is surface water density (kg m^{-3}), C_P the specific heat capacity of water (J kg^{-1} K^{-1}), α and β are the thermal expansion ($\alpha = \rho_0^{-1} \partial\rho/\partial T$) and haline contraction ($\beta = \rho_0^{-1} \partial\rho/\partial S$) coefficients, S_0 is surface salinity and freshwater flux (m^3 s^{-1}) is given by river discharge (Q_f) plus direct precipitation (P) minus evaporation (E) over the surface area of the lough (A_s, m^2). Positive B_F indicates buoyancy gained at the water surface.

How storm events influenced full water column stability in each water body was assessed by calculating the Schmidt stability index (S_s, J m^{-2}) [50]:

$$S_s = gA_s^{-1} \int_0^{Z_{max}} (z - \bar{z})(\rho(z) - \bar{\rho})A(z)dz \quad (4)$$

where $\bar{z}$ is the depth (m) at which mean density occurs, $\rho(z)$ is density at depth z, $\bar{\rho}$ is volume weighted mean density and $A(z)$ is basin area at depth z. S_s estimates the amount energy needed to fully mix the water column, providing a good quantitative measure of stratification and destratification processes.

In Feeagh, which is destratified by December, the total lake heat content (H_{tot}, J m^{-2}) was identified as a potentially more informative measure of internal lake response to atmospheric forcing compared to S_s:

$$H_{tot} = \rho_0 C_P A_s^{-1} \int_0^{Z_{max}} T(z)A(z)dz \quad (5)$$

In Furnace, storm winds would be anticipated to destabilise the stratified water column yet the large volumes of freshwater discharge would be anticipated to reinforce vertical stratification through a positive buoyancy input. An appropriate parameterisation of the wind-driven response of the semi-enclosed (i.e. finite-dimension), 2-layered Furnace basin during the storms is the dimensionless Wedderburn number (W_b) (e.g. [51]):

$$W_b = \frac{R_i}{(l'/h)} \quad (6)$$

where R_i is the surface-layer Richardson number $R_i = g'h/u_*^2$, with g' the reduced acceleration of gravity across the pycnocline ($g' = g(\Delta\rho/\rho_0)$), h the depth of the surface layer (m) and u_* the surface water shear velocity (m s^{-1}) given as $u_* = \left(\left(\frac{\rho_a}{\rho_0}\right) C_D W_{10}^2\right)^{0.5}$. Wind speeds were low-pass filtered with a cut-off frequency of ¼ the fundamental mode internal wave period [32]. l'/h is the aspect ratio of the basin, with the effective length scale l' defined here as the length of the unbroken pycnocline along the NE-SW axis, the direction of wind stress during Desmond.

In general, large W_b values (> 10) imply a sharp, flat interface is maintained; smaller values ($1 < W_b < 10$) indicate partial upwelling of the pycnocline at the upwind basin end and subsequent internal seiching following wind cessation; $W_b \approx 1$ implies full pycnocline upwelling whilst still smaller values (e.g. < 0.5) indicate full surfacing of sub-pycnocline waters with formation of longitudinal density gradients and ultimately basin-scale overturns [51–53].

Estuarine exchange flow through the connecting channel between Furnace and Clew Bay controls transport dynamics in and out of the main inner Furnace basin and links the Burrishoole watershed to the coastal ocean. Modification of salt content of dense bottom inflows due to mixing with lower salinity surface outflows regulates the residence time of saline water masses in the inner basin and thus the oxygen content of deep waters [38]. The impact of the storms on diapycnal mixing in this region was investigated using ADCP profiles (MR01 Fig 1), with squared shear computed as:

$$S^2 = \left(\frac{\partial u}{\partial z}\right)^2 + \left(\frac{\partial v}{\partial z}\right)^2 \quad (7)$$

where z is depth in the channel. As only two measures of density were available at the surface and bottom near the ADCP, we computed a full water column 'bulk' buoyancy frequency N

as:

$$N = \left[-\left(\frac{g}{\rho_0}\right)\left(\frac{\partial \rho}{\partial z}\right) \right]^{0.5} \quad (8)$$

S^2 was averaged over the full water column and the gradient Richardson number calculated as (e.g. [54]):

$$Ri_g = \frac{N^2}{S^2} \quad (9)$$

It was envisaged that Ri_g would provide a simple diagnosis of the dynamic stability of flow through this important section of the system, integrating the effects of wind, river flow and tidal currents on shear and stratification. $Ri_g > 0.25$ is one criterion for the occurrence of flow instabilities [54].

To compute volume and salt fluxes in and out of the inner Lough Furnace basin, the full entrance cross-section at MR01 was divided into subsections in order to overcome the limited spatial coverage of the sensors (S1 Fig). An echosounder transect provided accurate bathymetry. Firstly, the entranceway was divided laterally into a deeper trough section and shallower section to the east. The deeper channel region was divided vertically in 3 sections, with section averaged salinity in the uppermost and lowermost sections set equal to the values recorded by the T/C sensors; an interpolated salinity value was used for the intermediate section. A corresponding set of along-channel, area-averaged velocity vectors were computed from the ADCP profiles. To account for the unmonitored shallower (~2m) east section we used a simplistic approach and extrapolated across the salinity and velocity from the uppermost section in the deep channel, with the caveat that the resulting volume and salt flux values represented a first-order estimate.

Thus, within each subsection i, a timeseries of area A_i, along-channel velocity v_i and salinity S_i were derived. The net salt flux (S_f) was computed as the sum of flow rate and salinity through each area of the cross-section:

$$S_f = \langle \sum_i v_i S_i A_i \rangle \quad (10)$$

A_i for the top section in the deep channel and for the shallow side section increased or decreased with changing water level as measured by the ADCP pressure sensor. Angled brackets indicate averaging over a complete M_2 tidal cycle. Positive values indicate fluxes into the inner Furnace basin and negative values indicate fluxes out (seaward). Volume fluxes were estimated by omitting the salinity term in Eq (10).

Results

Using the standard and revised rainfall-altitude relationships for the catchment rain gauges described in the Methods section, the total estimated rainfall volume over the Burrishoole watershed during Storm Desmond was in the range $12x10^6$ - $14x10^6$ m^3 (Fig 1). In terms of these rainfall volumes, Storm Desmond was a true record-breaker. Six out of thirteen rain-gauges recorded their historical maximum cumulative daily rainfall total during one day of the storm (5th December); the greatest daily rainfall total (135.9 mm d^{-1}) of any of these rain gauges was recorded at RG7 (Fig 1). For context, the mean daily rainfall total at RG7 during December 2004–2017 was 7.5 mm d^{-1} and the historical maximum daily total (excluding December 2015) was 59.4 mm d^{-1}.

On Lough Feeagh the two single highest mean daily lake levels recorded since records began in 1976 occurred in November and December 2015, just 3 weeks apart (1.65 m on 15th

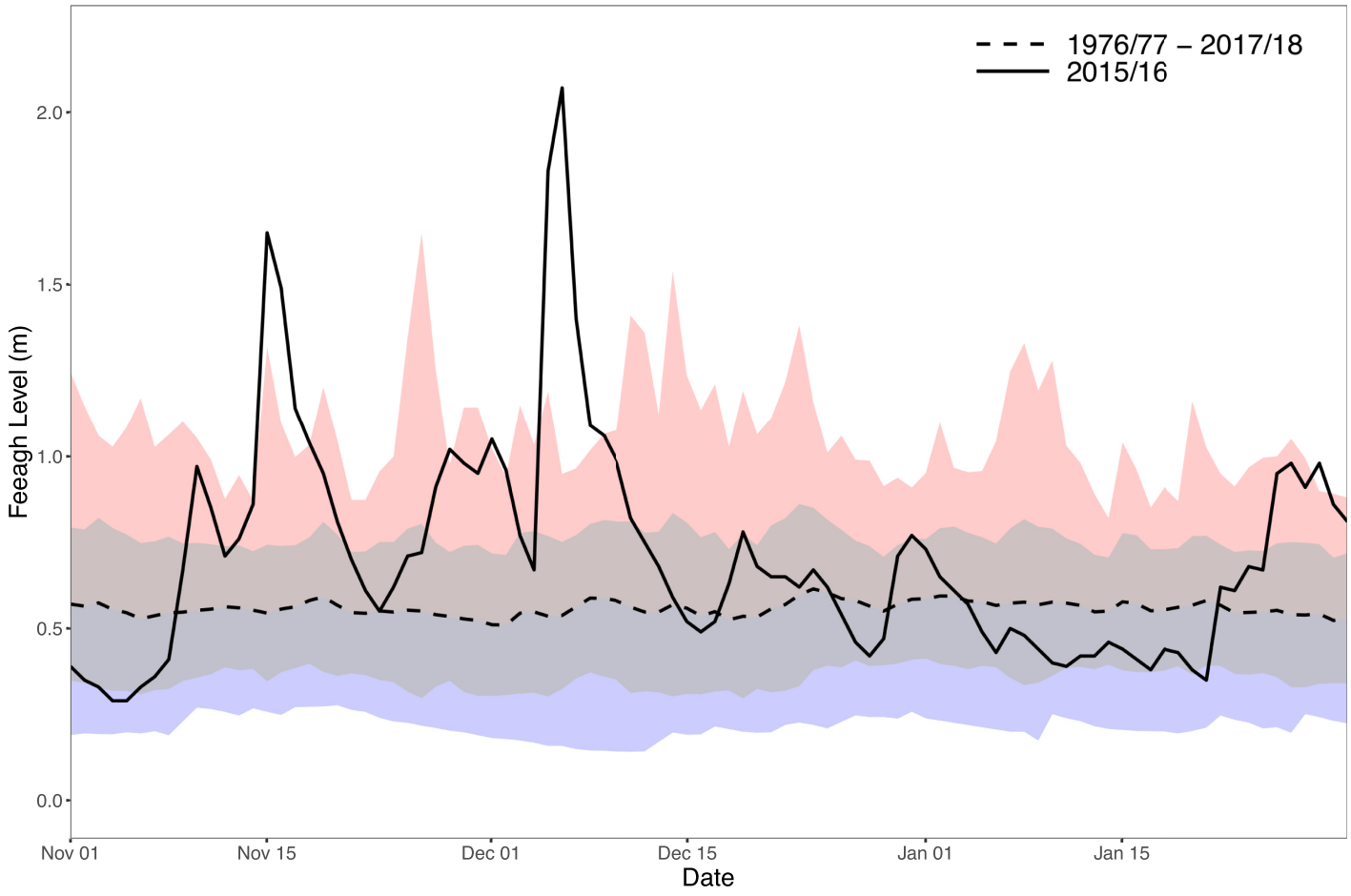

Fig 2. Surface water levels (m) on Lough Feeagh. Solid black line is daily mean November-January 2015/16; dashed black line is daily mean November-January 1976/77-2018/19 (grey shading is standard deviation around the mean). Red shaded area is historic max daily mean 1976–2018 and blue shaded area is historic min daily mean 1976–2018.

https://doi.org/10.1371/journal.pone.0235963.g002

November and 2.07 m on 6th December (Fig 2)). It should be noted that during Desmond, the Lough Feeagh basin filled beyond carrying capacity and spilled over-land into downstream Furnace. This flood caused extensive structural damage to the Marine Institute's aquaculture research and migratory fish trapping facilities [55]. In addition to intense precipitation, a comparison of the mean December air temperature and wind speeds recorded at AWS (Fig 1) to monthly December averages over the period 2005–2018 revealed that mean air temperature (8.2˚C 2015; 6.5˚C 2005–2018) and wind speed (7.1 m s^{-1} 2015; 5.6 m s^{-1} 2005–2018) were both the higher than average. Following Desmond, two additional storm category weather events occurred on the 23rd ('Eva') and 29th ('Frank') December.

Persistent heavy rainfall throughout November ensured that catchment soils would have already been saturated when Desmond occurred; with very little storage capacity the rainfall over the 4–6 December would have followed overland routes, resulting in the drastic rise in water levels (Fig 2 and Fig 3A). Turbidity increased and pH decreased at the surface of Feeagh in the immediate aftermath of Desmond on 6th December (Fig 3B). In addition, total lake heat content increased by ~30 MJ m^{-2}, despite the overall seasonal decrease in water temperatures

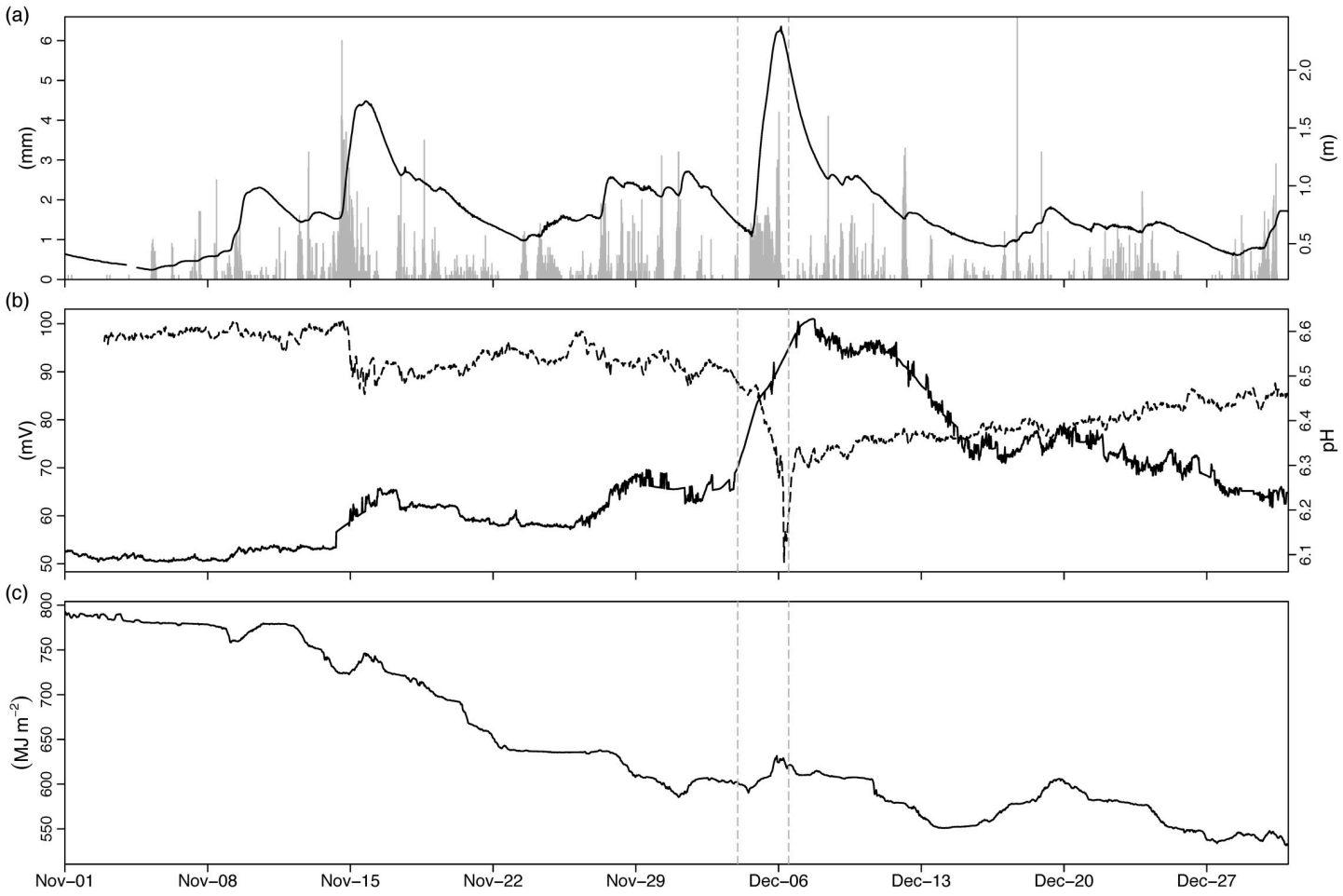

Fig 3. 30 minute timeseries showing storm impacts on Lough Feeagh. (A) rainfall (mm) recorded at AWS (grey bars) and Feeagh surface lake level (m) (B) surface pH (dashed line) and turbidity (mV) on Feeagh, (C) total heat content (MJ m^{-2}) of full Feeagh water column. Dashed vertical lines denote Storm Desmond.

https://doi.org/10.1371/journal.pone.0235963.g003

from November onward (Fig 3C, black line). S_s values were very low during this winter period, as the Feeagh water column is generally isothermal and fully-mixed.

Analysis of air-water transfer processes on Feeagh confirmed that a net positive transfer of heat (typically ~100–200 W m^{-2}) occurred during Desmond and other high wind events in December (Fig 4). Heat input from solar radiation was very slight and short-lived given the cloudy sky conditions and short day length during this time of year (Fig 4A). More important drivers of heat flux into the water appeared to be a slight net positive heating by thermal radiation (Fig 4B), an increase in sensitive heat flux due to increased over-lake air temperature (Fig 4C) and an increase in latent heat flux due to condensation of atmospheric water vapour at the surface of Feeagh (Fig 4E).

On Furnace the effects of large volumes of rainfall in the winter of 2015 were apparent as early as November, with a notable deepening of the halocline (red line, Fig 5A). Between 01 November and 06 December, the halocline had deepened by ~6 m (over 25% of the total water depth). Crucially, this haline stratification influenced the vertical distribution of temperature and dissolved oxygen (Fig 5B and 5C). The warm, anoxic sub-halocline basin water was completely isolated from the upper freshwater layer following Desmond, due to increased sharpness of oxygen and (inverse) thermal gradients. The strength of the stratification stability,

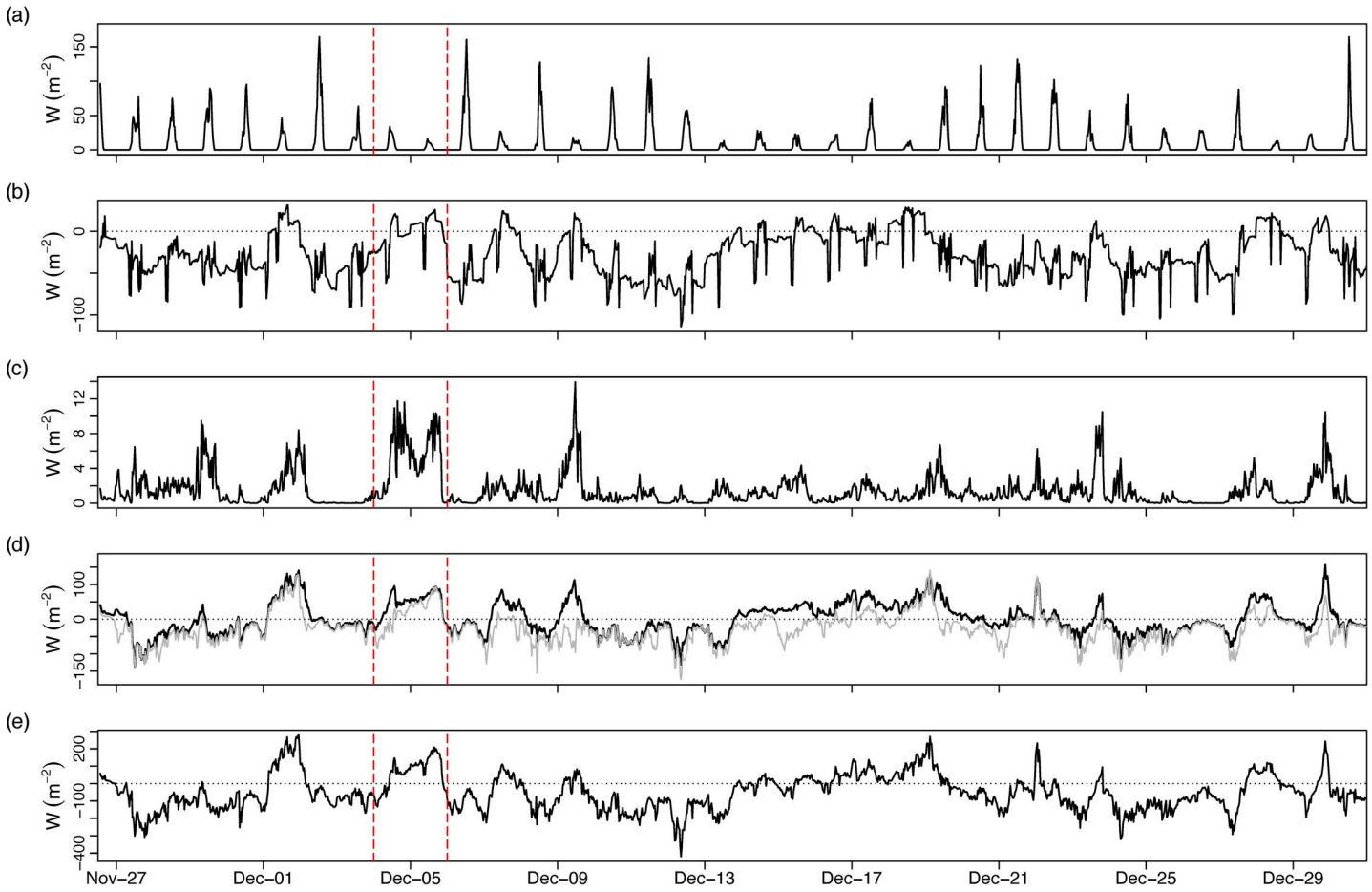

Fig 4. 30 minute timeseries of atmosphere-water interaction on Feeagh during winter storms 2015. (A) solar radiation (W m^{-2}), (B) thermal radiation (W m^{-2}), (C) energy input from wind stress (W m^{-2}), (D) latent (grey line) and sensible (black line) heat flux (W m^{-2}), (E) total surface heat flux (W m^{-2}). Positive values denote downward flux into the lake. Dashed vertical lines denote Storm Desmond.

https://doi.org/10.1371/journal.pone.0235963.g004

as indicated by S_s values, more than doubled over the course of the winter floods (~800 J m^{-2} to ~2000 J m^{-2}) (Fig 5D).

The large quantities of rainfall leading up to and including Desmond culminated in a buoyant surface plume that increased the buoyancy flux into Furnace by an order of magnitude (Fig 6A). The stabilising effect of this buoyancy input increased the baroclinic restoring force and despite large wind stress values being reached during and after Desmond (Fig 6B), only partial upwelling occurred as indicated by non-critical (*i.e.* > 1) values of the inverse W_b number (Fig 6C). The upper and lower dashed lines in Fig 6C represent a range of values over which partial upwelling is expected (equivalent to standard W_b values in the range 3–6). On only one occasion did W_b indicate significant upwelling of the pycnocline toward the surface (in the midst of Desmond) and on several occasions during particularly strong winds smaller upwelling events occurred. Inverse W_b values falling in this range are indicative of subsequent internal seiche activity [53].

Timeseries of the instruments moored at MR01 and MR02 provided valuable insight into how the storm-related floods modified estuarine hydrodynamics at the entranceway to Furnace inner basin (Fig 7). Firstly, along-channel currents showed atypical dynamics during Desmond with strong seaward flow (negative values, denoted by blue) occupying the full extent of

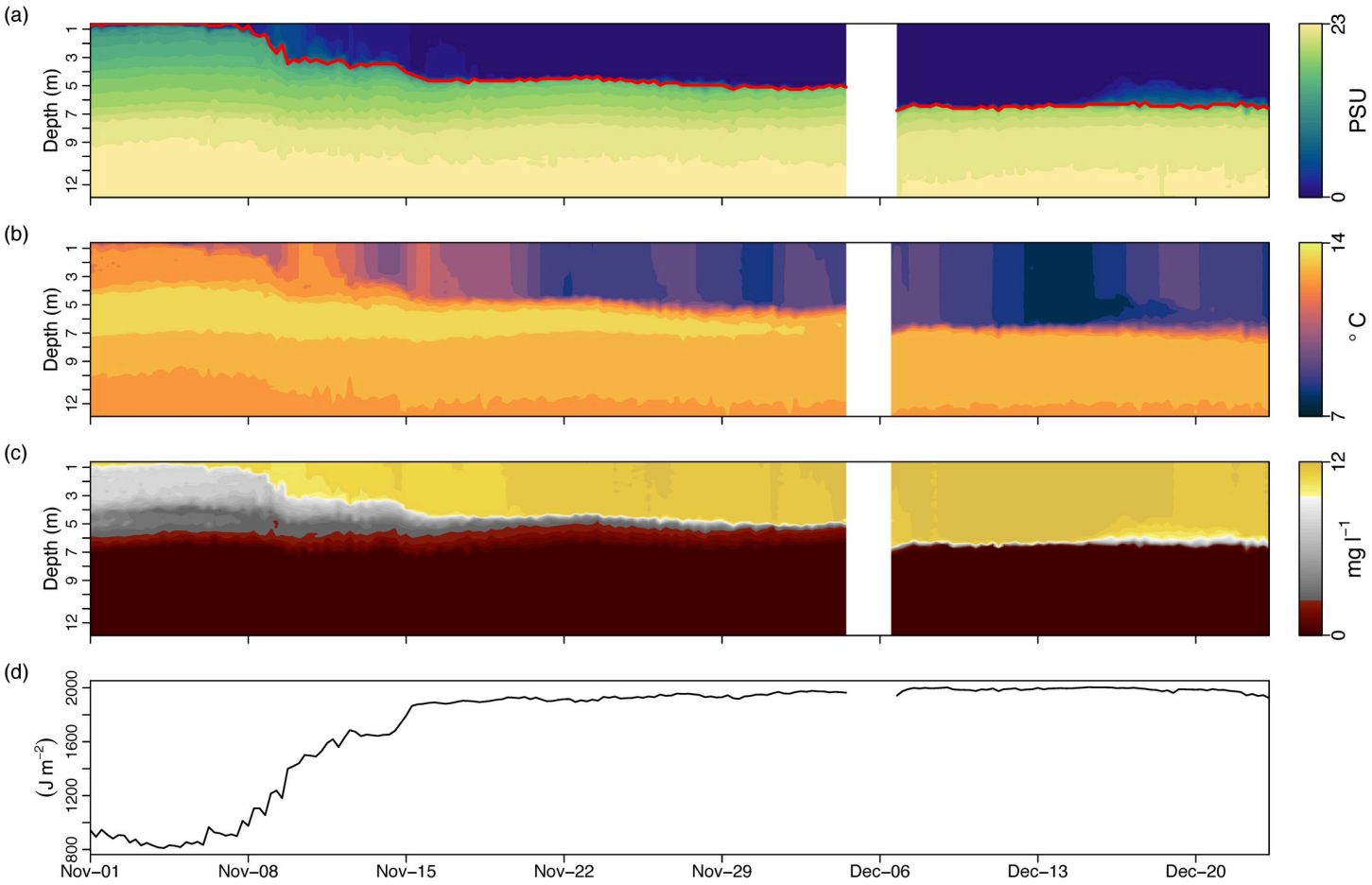

Fig 5. Water column profiles (taken every 6 hours) on Lough Furnace pre- and post-Storm Desmond. (A) salinity, (B) temperature (˚C), (C) dissolved oxygen (mg l^{-1}), (D) Schmidt stability (J m^{-2}). Note that the automated profiler malfunctioned during Storm Desmond (white gap, 4–6 December 2015).

https://doi.org/10.1371/journal.pone.0235963.g005

the channel depth (Fig 7A). It should be noted that Desmond occurred during neap tides, meaning that only weak inflows (positive values, denoted by red) to Furnace would typically occur at this time. (Spring-neap tidal phase is indicated by the water level (black line, Fig 7A) as well as the salinity timeseries at MR02 (black line, Fig 7B)). Water level in the channel rose in the immediate aftermath of Desmond and fell again quickly, as the initial pulse of freshwater exited the system (Fig 7A). Surface (blue line), bottom (red line) and even lower estuary (black line) water was essentially comprised of freshwater from the end of November until spring tides on the 11th December, when saltwater inflows were observed along the channel bottom (Fig 7A and 7B). Curiously, a slight increase in surface and bottom salinity was detectable in the midst of Desmond (Fig 7B). Salinity at the surface remained almost at 0 for the remainder of the month and into January 2016, whilst bottom salinities rose gradually on each successive spring tidal phase causing restratification to occur. Aside from clear bottom inflow during spring tides, current profiles revealed that the flow direction in the upper water column (< 2 m from the surface) was dominated by along-channel wind direction (Fig 7A and 7C). The predominant wind direction during December was up-estuary, which opposed the outflowing flood water direction, causing surface flow reversals. Up-estuary winds forced outflow at intermediate depths and when this occurred during spring tides, a 3-layered exchange flow was

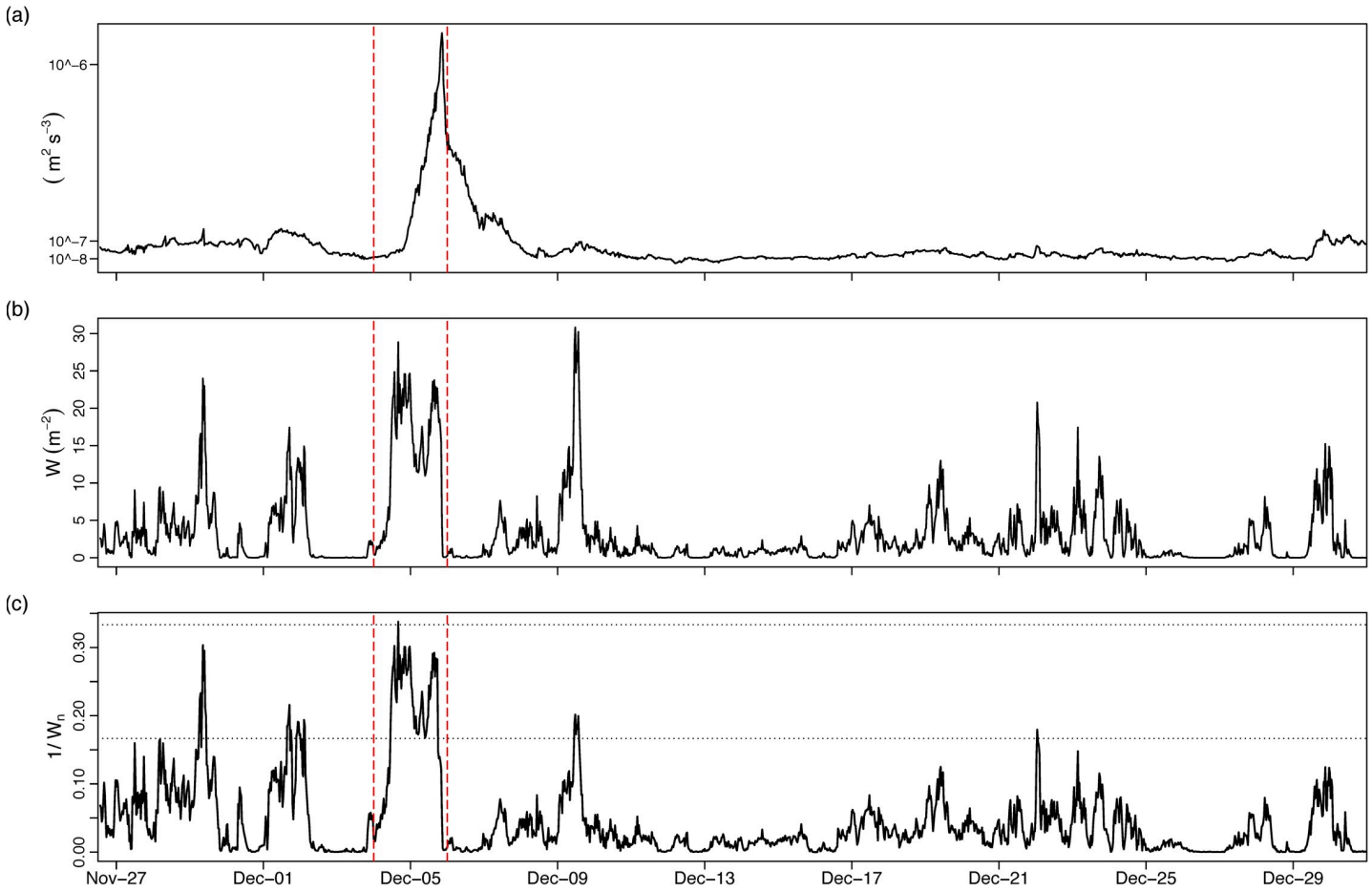

Fig 6. 30 minute timeseries showing rain and wind impacts on Furnace. (A) surface buoyancy flux ($m^2 s^{-3}$) (positive values indicate buoyancy input at surface), (B) energy input from wind stress ($W m^{-2}$), (C) inverse Wedderburn number (horizontal dashed lines denote partial and full upwelling limits). Dashed vertical lines denote Storm Desmond.

https://doi.org/10.1371/journal.pone.0235963.g006

observed with bottom and surface inflow and intermediate outflow (*e.g.* December 11–18; December 25-January 01).

Intense shear was observed near the surface during strong wind events throughout December and January (Fig 7D). However in the lead up to and immediate aftermath of Desmond, only very weak and sporadic shear was observed further down in the water column. It was not until the restratification associated with the subsidence of the Desmond flood waters and the onset of spring tides (Fig 7E) that occasions of intense shear were supported near the channel bottom (*e.g.* ~December 18th, ~Jan 5th, Fig 7D). Analysis of S^2 and bulk water column N^2 (Fig 7E) and Ri_g (Fig 7F) provided insight into relative contributions to flow stability during and after the floods. During the flood, stratification was absent and flow was completely turbulent through the entranceway, which had not been observed previously in this section [77]. However during the subsequent restratification, flow went through phases of stability and instability denoted by Ri_g falling below 0.25 (dashed horizontal line). Instability was generally related to strong winds and tidal currents and was most critical just prior to 25th December, when stratification had weakened during neap tides. As the stratification continued to increase post-flood with successive spring tides, flow became increasingly stable and in January, despite occasions of wind- and tidally-driven shear, Ri_g values remained above 0.25.

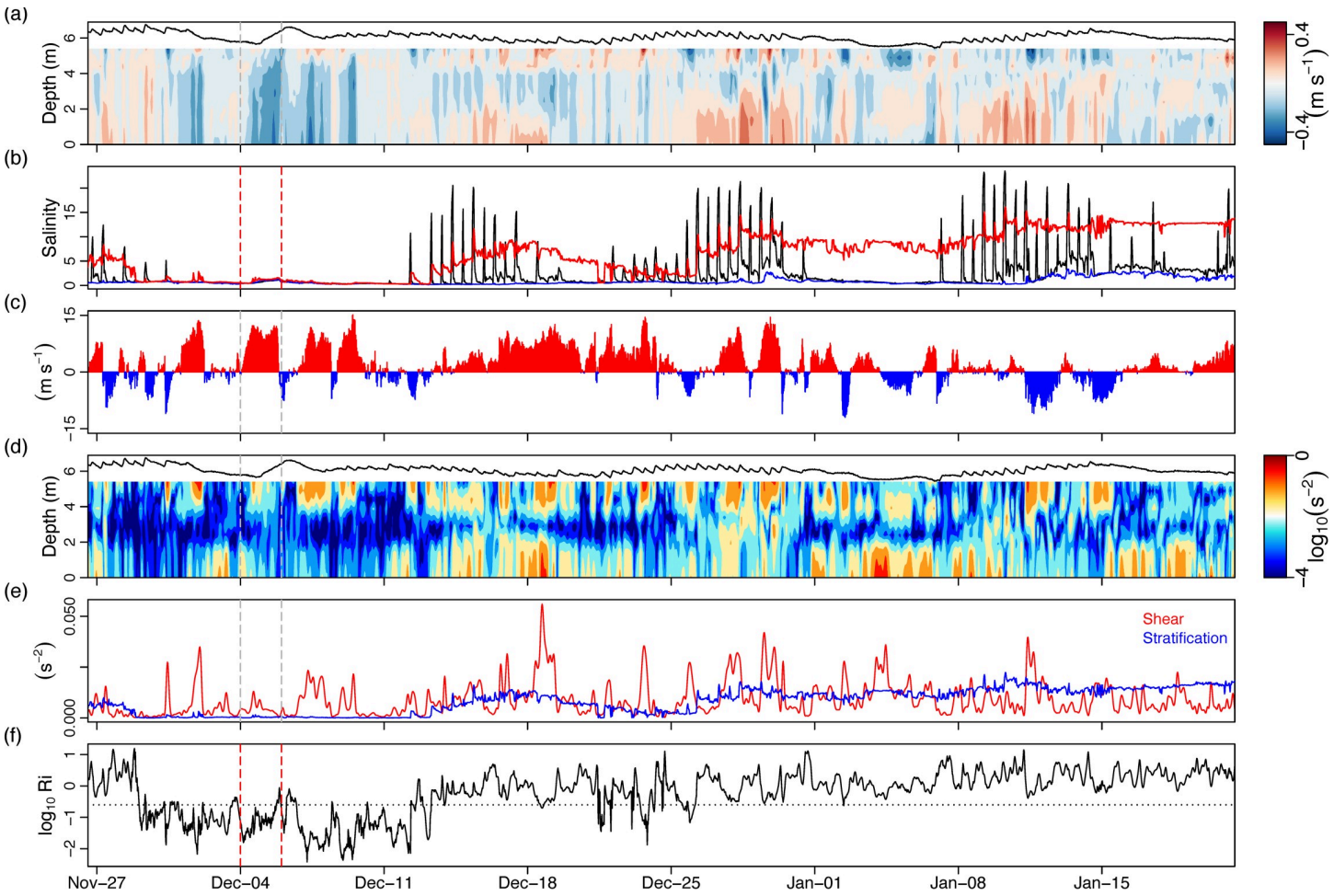

Fig 7. 30 minute timeseries showing storm impacts on estuarine hydrodynamics. (A) along-channel (350˚T) current velocities (m s^{-1}) at MR01 (black line is water surface; positive values indicate flow into Furnace inner basin, negative values indicate seaward flow), (B) surface (blue) and bottom (red) salinities at MR01, bottom salinity (black) at MR02, (C) along-channel winds (positive values indicate winds blowing toward Furnace inner basin), (D) squared shear (s^{-2}), (E) mean squared shear (s^{-2}) (red) and squared buoyancy frequency (s^{-2}) (blue) and (F) gradient Richardson number at MR01. (A) and (D) are plotted with respect to height above the bottom and velocity vectors are 6-hour low-passed. Dashed vertical lines denote Storm Desmond.

https://doi.org/10.1371/journal.pone.0235963.g007

Averaged over a complete tidal cycle, volume fluxes highlighted that net transport was predominantly seaward during the deployment period (negative values represent outward volume fluxes, Fig 8A). A mean net volume flux of -15.8 m^3 s^{-1} was estimated during December, with volume fluxes of up to -80 m^3 s^{-1} estimated during Desmond. For comparison, a volume flux estimate made using an ADCP over summer 2010 had a mean value of—3 m^3 s^{-1} [38]. Positive volume fluxes (into Furnace) were largely attenuated during early December with inward volume transport occurring during spring tides and up-estuary winds later in the month (Fig 8B). However larger outflow volumes for the remainder of December and January ensured that volume transport was predominantly seaward with only occasional, short-lived periods of net positive fluxes (Fig 8A and 8B).

The tidally-averaged total salt flux was generally negative (seaward) for most of early December with no net positive influx until spring tides just prior to 18th December (black line, Fig 8C). Following this point, the salt flux showed a pronounced spring-neap oscillation with net influx during springs and outflux during neaps, which was most apparent when the salt flux was low-passed to remove oscillations with periods smaller than 5 days (red line, Fig 8C).

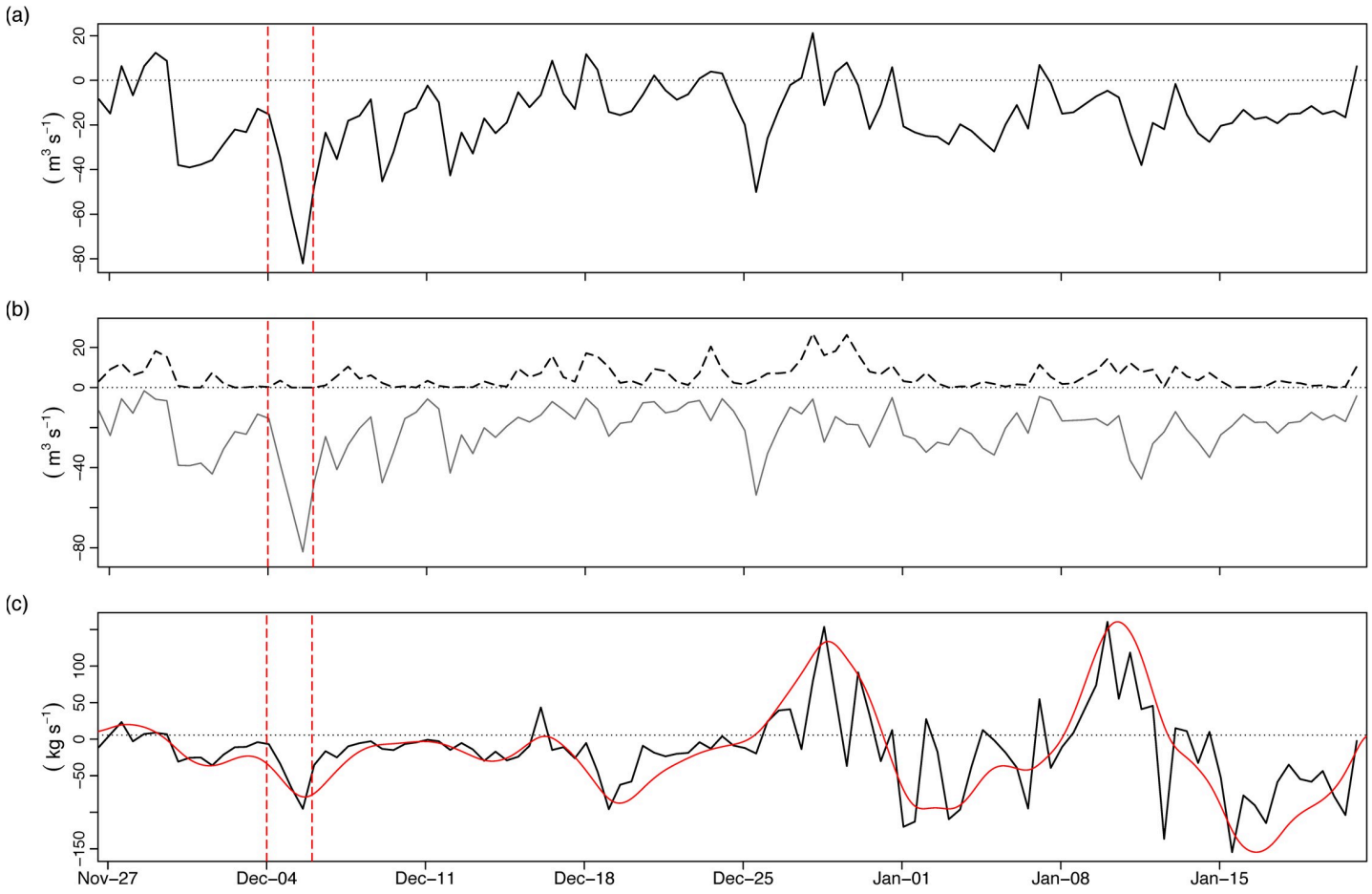

Fig 8. Tidally-averaged volume and salt fluxes in/out of Lough Furnace. (A) net volume flux ($m^3 s^{-1}$) in/out of Furnace inner basin through MR01 (positive values indicate flux into Furnace; negative values outward flux), (B) partitioned volume fluxes into positive (dashed line) and negative (solid line) components, (C) salt flux (kg s^{-1}) in (positive) and out (negative) (red line is 5-day low-passed). Dashed vertical lines denote Storm Desmond.

https://doi.org/10.1371/journal.pone.0235963.g008

Of particular importance then was that at peak flooding (4–6 December), salt export increased despite only small quantities of residual salt in the bottom of the channel from the prior spring tides (Fig 7B); this implies that the steady-state salt balance was modified and there was a net loss of salt from the inner Furnace basin during the flood period.

Discussion

A number of recent reports suggest that the intensity of extreme rainfall and storm events is expected to increase in response to increases in atmospheric heat and moisture [5,6,56]. Thus, documenting how different aquatic ecosystems react to the varying magnitude and timing of episodic events is crucial, as biogeochemical processes and ecological communities may be perturbed. This study has quantified the cascading impacts from successive heavy rainfall events during a single winter on a catchment, its freshwater lake and its downstream estuarine waters, with an emphasis on one exceptional event, the extratropical North Atlantic cyclone Storm Desmond. Most importantly, it has shown how synchronicity between storm-specific forcing factors (precipitation intensity, wind speeds and onshore wind direction) and antecedent local conditions (pre-saturated catchment ground and high water levels from prior rainfall) can amplify environmental impacts. Of particular note was how the magnitude of storm

impacts varied between the linked aquatic ecosystems, despite their spatial proximity. Results highlight the relative contribution of conditions associated with large-scale atmospheric variability (e.g. a high-moisture winter storm originating in the North Atlantic) and local factors (e.g. isothermal, winter-mixed freshwater lake versus saline stratified estuarine system) to the nature of the environmental or ecosystem disturbance experienced.

Storm impacts on catchment and freshwater lake habitats

Analysis of the rain gauge data during Storm Desmond showed that the rainfall was extremely heavy, continuous and spatially distributed throughout the catchment. This was in contrast to an extreme precipitation event documented in this catchment previously, when a much shorter and intensive rainfall event exhibited a notable asymmetry and led to particularly destructive flooding on the eastern side of the catchment [17]. In Lough Feeagh, the most notable shift was the sudden increase in surface water acidity following Desmond. This was likely a consequence of the mobilisation of organic matter from the predominantly peatland catchment area [37] with a potential contribution from the direct rainfall over the lake surface. Whilst Feeagh is normally slightly acidic, post-flood values were noticeably lower than the annual mean pH (6.1 compared to 6.6). River plumes resulting from major flood events have been shown to cause decreases in lake pH relative to non-plume waters, with this effect related primarily to the soil-type surrounding the river [57,58]. These results are applicable to lake systems situated in other upland peat catchments around Ireland and the United Kingdom, that are likely to experience more of these high intensity rainfall events which are projected for these regions [35,36,59]. Significant increases in post-flood turbidity and decreased water clarity have been documented for other lakes [11,20]. Biological consequences of increased riverine input may include increased respiration [17,19,60] whilst decreased water clarity following storms may substantially decrease lake primary productivity [61]. However, as the event described here occurred in winter, when primary productivity was low, and changes in water clarity, inputs of organic material and even loss of plankton communities to bulk advection by flood waters are less likely to cause major ecological change [12,17]. Monthly measurements of water colour, total nitrogen and total phosphorus in our study did not deviate noticeably from usual winter values.

Apart from biogeochemical changes, Feeagh also underwent net warming during the storm due to positive (downward) heat fluxes (Figs 3D and 4). Our results represent a rare quantification of the direct transfer of properties from an 'atmospheric river' [35] directly to surface and interior lake waters. The magnitude of warming was small however and heat was rapidly redistributed throughout the water column. Thus, the winter setting was again important in terms of how effectively air-water energy transfer was circulated to interior waters, as Feeagh is fully mixed and isothermal by December. In contrast, an extreme flood event during summer 2009 when Feeagh was stratified had more drastic impacts on water column hydrodynamics, causing a decrease in stratification stability and deepening the epilimnion [17].

Storm impacts on estuarine and coastal habitats

The largest storm impacts occurred on the downstream Lough Furnace. Here, storm event timing had less impact hydrodynamically, as this system is stratified year-round [38]. Prior to Desmond, heavy rainfall throughout November had caused river discharge to increase the thickness of the freshwater surface layer, resulting in a large salinity (*viz*. density) gradient with depth and a doubling in stratification strength. The major consequence of a deepening halocline is that it reinforces stagnant, anoxic conditions in the bottom basin water. Whilst Furnace does not overturn vertically, occasional lateral inflows of dense, oxygenated coastal

water can ventilate the bottom anoxic water [38]. Similar deep-water ventilation processes are documented for stratified coastal basins such as fjords and sea-lochs [62] and play a fundamental role in oxygen dynamics (e.g. [63]), microbial activity (e.g. [64]) and primary production (e.g. [65]). In Furnace, deep-water ventilation has been observed to occur only following prolonged dry periods with little river flow, allowing tidal inflows of coastal water to reach the bottom of the inner basin. The large freshwater plume that occurred during winter 2015 blocked communication between the deep basin water and external coastal water, the only potential supplier of oxygenated replacement water. Initially the surface freshwater layer occupied the full depth extent of the connecting channel inhibiting any landward inflows.

Consequently, this absence of stratification in the connecting channel leading up to and during Storm Desmond minimised shear, particularly below the wind-influenced surface layer (Fig 7D). Subsidence of the initial flood and onset of spring tides gave rise to an evolving and highly dynamic flow environment. Tidal currents and strong winds generated intense shear near the surface and bottom, supported by the restratification, with indication of turbulent mixing in the entrance channel (Fig 7F). However the large amount of residual freshwater and successive spring tides meant that increasingly strong stratification ultimately suppressed large-scale turbulence and gave way to a stratified exchange flow regime. Flow structure and turbulence in this section is noteworthy, as it sets the composition of fluid entering and leaving Furnace. This has implications for exchange of resident interior water [38] and influxes of nutrients or planktonic seed populations [66] and also establishes the initial density of the estuarine outflow, which can influence far field plume dynamics in the coastal ocean [67]. The development of stratified flow resulted in the dilution of incoming tidal water as it met largely unmixed low salinity surface outflow in the shallow area between MR01 and MR02 (Figs 1 and 7B); this resulted in only intermediate depth water replacement in the main Furnace basin in the months following the flood event.

More broadly, modified freshwater runoff climatology has been implicated in exacerbating dissolved oxygen depletion in estuarine and coastal systems globally [68]. This is largely due to the mechanism explored here: intensified vertical stratification and isolation of deeper waters from lateral inflows. Additionally, rivers may cause nutrient enrichment which stimulates primary productivity or directly transport organic matter to coastal zones, which both heighten respiration rates and increase oxygen demand [26]. At the largest scale, bottom oxygen dynamics in the Baltic Sea are generally controlled by deep water inflows from the contiguous North Sea; changes in precipitation intensity over North-West Europe in recent decades has been implicated in a reduction in ventilation frequency due to large freshwater outflows attenuating dense inflows [69]. In semi-enclosed coastal systems similar to Furnace with restricted connections to adjacent coastal areas, large seaward river flows can inhibit ventilation of deep waters (e.g. [70,71]). Thus, a very likely consequence of changing patterns of precipitation intensity, especially the kind of extreme flood events recounted here, could significantly reinforce stagnant bottom water conditions in deep estuarine basins, promoting anoxia.

In several studies of stratified basins during storms, upwelling of sub-pycnocline water in nearshore areas was documented [15,18,72] and in general upwelling plays a pivotal role in generating turbulent flux pathways around lateral boundaries [73,74]. Partial upwellings occurred in Furnace during individual storm events throughout December, with the stable stratification preventing complete surfacing of lower layer water (Fig 6C). Pycnocline destabilisation results in energy transfer to the internal wave field, with the ratio of h/H and range of inverse Wb in Furnace during December implying that most of the resulting standing waves were linearly damped [53]. In systems with deep anoxia, internal seiche-related upwelling can have added significance, exposing nearshore areas to drastically fluctuating oxygen levels [32,53,75].

Catchment-to-coast volume fluxes

A ratings curve developed for the Mill Race and Salmon Leap rivers (Fig 1) provided a useful reference for the anticipated freshwater outflow volumes from the Burrishoole catchment during December (although it should be noted that the ratings curve relationship almost certainly breaks down for the extreme flows that occurred during Desmond). The mean river discharge into Furnace during the month of December was 13.7 $m^3 s^{-1}$. This compared reasonably well to the mean volume flux estimated from the ADCP of—15.8 $m^3 s^{-1}$, which also would have integrated volumetric fluxes from direct precipitation over Furnace as well as additional surface and groundwater inflows from the surrounding land area. Thus, using the ADCP estimates, the mean volumetric flux leaving the Burrishoole system during Storm Desmond (4–6 December) was (O)43 $m^3 s^{-1}$, with instantaneous fluxes potentially as high as (O)88 $m^3 s^{-1}$ at peak flooding. Based on the Feeagh lake level records, this was most likely the highest volume of water leaving Burrishoole since 1976 when records began (Fig 2). Mean annual discharge from Feeagh into Furnace is only 3–5 $m^3 s^{-1}$ [38]. Furthermore, the total volume of rainfall estimated from analysis of the catchment rain gauges over the 72 hour period (4–6 December) gave a volumetric rainfall flux of 46–54 $m^3 s^{-1}$, which again compares reasonably well to the ADCP estimate. The mismatch may be attributed to measurement error and calculation uncertainty attributed to each method and also that not all of the rainfall would have instantaneously exited the system (for example Feeagh lake level took ~10 days to fall back to typical mean December levels after the 6th December (Fig 2)).

Using the average volume flux of 43 $m^3 s^{-1}$ as a representative transport of water through the catchment during Desmond, the renewal time of the Feeagh lake basin ($T_R = Vol/Q$) was reduced to 15.8 days. The average renewal time of Feeagh is ~170 days; a previous extreme flood event during summer 2009 indicated that the renewal time of Feeagh also reduced to (O) 15 days [17]. However a major difference was that peak flow rates used to estimate this reduced renewal time during the summer flood lasted only ~3 hours, whereas our estimate for the Desmond volume flux is representative of a 3 day period, meaning that at least 20% of the volume of fully-mixed Feeagh was displaced over the 4–6 December, if a 100% exchange efficiency is assumed.

These values provide a first order estimate of the quantity of freshwater that ultimately reached Clew Bay and the coastal ocean from one single watershed in the aftermath of Desmond. Considering additional sources of river discharge around Clew Bay, it is likely that such elevated freshwater discharge would have affected stratification dynamics in the short term and may have delivered large quantities of terrestrial-source water properties over a very short time span (e.g. [27,28]). Numerical modelling of the impact of such extreme rainfall and flood events on the oceanography and biogeochemistry of Clew Bay could offer insight into how large coastal embayments respond to such climate-related extreme events.

Storm impacts on estuarine salt balance

In estuarine basins, the salinity budget is maintained by the competing influences of seaward and landward salt transport and depends on tidal, wind and freshwater flow [76]. In stratified estuaries such as Furnace, spring-neap oscillations in salt transport are often the dominant factor in determining the longer-term salt balance (e.g. [29]). For example, in the inner basin of Furnace, steady-state conditions in relation to salt and volume are on average achieved over a complete spring-neap cycle [77]. However large pulses of freshwater may disrupt the longer-term salt balance, especially in lagoonal estuaries with restricted horizontal connection to oceanic water. The Furnace salt balance was modified during Desmond with net export of salt which was not replenished immediately by spring tides. Perhaps most importantly, this salt

flux did not appear to be imported salt from the prior spring tides, as the surface and bottom salinities at MR01 were almost zero prior to Desmond yet both increased slightly during the middle of Desmond (Fig 7B). To assess whether this exported salt came from sub-halocline water in the deep inner basin, we invoked some practical assumptions about the mean volumetric flux during Desmond (Q_{mean}≈43 m^3 s^{-1}), the salinity of the water above the halocline at the mouth of the basin (S_1≈0, recorded at MR01) and salinity below the halocline (S_2≈16; Fig 5A), and estimated an entrainment flux (Q_{We}, m^{-3} s^{-1}) of sub-halocline water by the outflowing plume as $Q_{We} = Q_{mean}(S_1/S_2–S_1)$. This provided a mean estimate of Q_{We} during the flood of 2.8 m^3 s^{-1}. Using the approximate basin area at the depth of the halocline gives a mean entrainment velocity of 5 x 10^{-6} m s^{-1}. Thus for S_2≈16, a simplistic estimate of mean upward salt flux across the halocline gives 45 kg s^{-1}; over the 4–6 December the mean salt flux through the entranceway based on Eq 10 was– 42 kg s^{-1} (although the large range of values in the salt flux timeseries must be acknowledged, with max values of– 90 kg s^{-1} at peak flow (Fig 8C)). Thus we tentatively conclude that salt loss from Furnace during the peak of the freshwater flood was from older resident salt reserves located beneath the halocline and below sill depth. This is an important dynamic, as in topographically constrained estuaries like Furnace, the deep basin water below sill depth is normally detached from the wind, estuarine and tidal circulation that takes place above the sill (e.g. [62]). Large flood events may be capable of freshening semi-enclosed coastal basins such as Furnace not only by limiting salt import during flood tides but also by exporting resident salt through entrainment.

Conclusions

Here we have quantified the impacts from a succession of heavy rainfall events that spanned a catchment-lake-estuarine system and shown that, in large part due to the timing (winter) and event conditions (rain and wind), the coastal estuarine system underwent the most significant changes. The timing of such events over the annual cycle is less important for estuarine systems in temperate climates and in some respects winter floods may have larger impacts, as extreme rainfall is superposed on higher seasonal freshwater input. A logical next phase to the results presented here would be to quantify how additional biogeochemical and biological parameters not monitored during the flood would respond, as well as tracking plume impacts further offshore. One potential approach toward this would be forcing coupled physical-biogeochemical models using volume and air-sea fluxes quantified here as boundary conditions.

Supporting information

S1 Fig. Cross-sectional profile of entranceway into Furnace inner basin at MR01. Shown is the instrumentation configuration of this mooring (acoustic doppler current profiler and temperature-conductivity sensor (bottom triangle); temperature-conductivity sensor (surface triangle)). Black lines indicate borders of 4 regions used to compute volume and salt fluxes through the entranceway.
(EPS)

Acknowledgments

The long-term environmental monitoring programme in Burrishoole is facilitated by the technical staff of the Marine Institute Newport (Joseph Cooney, Michael Murphy, Pat Hughes, Pat Nixon, Davy Sweeney) and Martin Rouen (Lakeland Instrumentation Ltd.). The work on Lough Furnace was only possible thanks to field and technical support from Sheena Fennell (Earth and Ocean Science Department, NUI Galway).

Author Contributions

Conceptualization: Seán Kelly, Brian Doyle, Elvira de Eyto.

Data curation: Seán Kelly, Elvira de Eyto, Mary Dillane.

Formal analysis: Seán Kelly, Brian Doyle.

Funding acquisition: Phil McGinnity, Martin White, Eleanor Jennings.

Investigation: Seán Kelly, Elvira de Eyto, Mary Dillane.

Methodology: Martin White.

Project administration: Phil McGinnity, Eleanor Jennings.

Supervision: Russell Poole, Martin White, Eleanor Jennings.

Visualization: Seán Kelly.

Writing – original draft: Seán Kelly.

Writing – review & editing: Seán Kelly, Brian Doyle, Elvira de Eyto, Mary Dillane, Phil McGinnity, Russell Poole, Martin White, Eleanor Jennings.

References

1. Otto FEL, Massey N, Oldenborgh GJ van, Jones RG, Allen MR. Reconciling two approaches to attribution of the 2010 Russian heat wave. Geophys Res Lett. 2012; 39(4).
2. Stott PA, Stone DA, Allen MR. Human contribution to the European heatwave of 2003. Nature. 2004 Dec; 432(7017):610–4. https://doi.org/10.1038/nature03089 PMID: 15577907
3. Trenberth KE. Framing the way to relate climate extremes to climate change. Clim Change. 2012 Nov 1; 115(2):283–90.
4. Imada Y, Shiogama H, Takahashi C, Watanabe M, Mori M, Kamae Y, et al. Climate Change Increased the Likelihood of the 2016 Heat Extremes in Asia. Bull Amer Meteor Soc. 2018 Jan 1; 99(1):S97–101.
5. Kunkel KE, Karl TR, Brooks H, Kossin J, Lawrimore JH, Arndt D, et al. Monitoring and Understanding Trends in Extreme Storms: State of Knowledge. Bull Amer Meteor Soc. 2012 Aug 8; 94(4):499–514.
6. Coumou D, Rahmstorf S. A decade of weather extremes. Nature Climate Change. 2012 Jul; 2(7):491–6.
7. Emanuel K. Increasing destructiveness of tropical cyclones over the past 30 years. Nature. 2005 Aug; 436(7051):686–8. https://doi.org/10.1038/nature03906 PMID: 16056221
8. Haarsma RJ, Hazeleger W, Severijns C, Vries H de, Sterl A, Bintanja R, et al. More hurricanes to hit western Europe due to global warming. Geophys Res Lett. 2013; 40(9):1783–8.
9. Deryugina T. How do people update? The effects of local weather fluctuations on beliefs about global warming. Clim Change. 2013 May 1; 118(2):397–416.
10. Myers TA, Maibach EW, Roser-Renouf C, Akerlof K, Leiserowitz AA. The relationship between personal experience and belief in the reality of global warming. Nat Clim Change. 2013 Apr; 3(4):343–7.
11. Kasprzak P, Shatwell T, Gessner MO, Gonsiorczyk T, Kirillin G, Selmeczy G, et al. Extreme Weather Event Triggers Cascade Towards Extreme Turbidity in a Clear-water Lake. Ecosystems. 2017 Dec 1; 20(8):1407–20.
12. Jennings E, Jones S, Arvola L, Staehr PA, Gaiser E, Jones ID, et al. Effects of weather-related episodic events in lakes: an analysis based on high-frequency data. Freshw Biol. 2012 Mar 1; 57(3):589–601.
13. O'Reilly CM, Sharma S, Gray DK, Hampton SE, Read JS, Rowley RJ, et al. Rapid and highly variable warming of lake surface waters around the globe. Geophys Res Lett. 2015; 42(24):10,773–10,781.
14. Adrian R, O'Reilly CM, Zagarese H, Baines SB, Hessen DO, Keller W, et al. Lakes as sentinels of climate change. Limnol Oceanogr. 2009 Nov; 54(6):2283–97. https://doi.org/10.4319/lo.2009.54.6_part_2.2283 PMID: 20396409
15. Woolway RI, Simpson JH, Spiby D, Feuchtmayr H, Powell B, Maberly SC. Physical and chemical impacts of a major storm on a temperate lake: a taste of things to come? Clim Change. 2018 Nov 1; 151(2):333–47. https://doi.org/10.1007/s10584-018-2302-3 PMID: 30930507

16. Giling DP, Nejstgaard JC, Berger SA, Grossart H-P, Kirillin G, Penske A, et al. Thermocline deepening boosts ecosystem metabolism: evidence from a large-scale lake enclosure experiment simulating a summer storm. Glob Chang Biol. 2017; 23(4):1448–62. https://doi.org/10.1111/gcb.13512 PMID: 27664076

17. de Eyto E, Jennings E, Ryder E, Sparber K, Dillane M, Dalton C, et al. Response of a humic lake ecosystem to an extreme precipitation event: physical, chemical, and biological implications. Inland Waters. 2016a Jan 1; 6(4):483–98.

18. Imboden DM, Stotz B, Wüest A. Hypolimnic mixing in a deep alpine lake and the role of a storm event. Int. Ver. The. 1988 Jan; 23(1):67–73.

19. Sadro S, Melack JM. The Effect of an Extreme Rain Event on the Biogeochemistry and Ecosystem Metabolism of an Oligotrophic High-Elevation Lake. Arct Antarct Alp Res. 2012 May 1; 44(2):222–31.

20. Perga M-E, Bruel R, Rodriguez L, Guénand Y, Bouffard D. Storm impacts on alpine lakes: Antecedent weather conditions matter more than the event intensity. Glob Chang Biol. 2018; 24(10):5004–16. https://doi.org/10.1111/gcb.14384 PMID: 29974996

21. Robins PE, Skov MW, Lewis MJ, Giménez L, Davies AG, Malham SK, et al. Impact of climate change on UK estuaries: A review of past trends and potential projections. Estuar Coast Shelf Sci. 2016 Feb 5; 169:119–35.

22. Dyer KR. Estuaries: a physical introduction. 2nd ed. New Jersey: John Wiley. 1997.

23. Yang Z, Wang T, Voisin N, Copping A. Estuarine response to river flow and sea-level rise under future climate change and human development. Estuar Coast Shelf Sci. 2015 Apr 5; 156:19–30.

24. Robins PE, Lewis MJ, Simpson JH, Howlett ER, Malham SK. Future variability of solute transport in a macrotidal estuary. Estuar Coast Shelf Sci. 2014 Dec 5; 151:88–99.

25. Lee SB, Birch GF. Utilising monitoring and modelling of estuarine environments to investigate catchment conditions responsible for stratification events in a typically well-mixed urbanised estuary. Estuar Coast Shelf Sci. 2012 Oct 1; 111:1–16.

26. Rabalais NN, Díaz RJ, Levin LA, Turner RE, Gilbert D, Zhang J. Dynamics and distribution of natural and human-caused hypoxia. Biogeosciences. 2010 Feb 12; 7(2):585–619.

27. Voynova YG, Brix H, Petersen W, Weigelt-Krenz S, Scharfe M. Extreme flood impact on estuarine and coastal biogeochemistry: the 2013 Elbe flood. Biogeosciences. 2017 Feb 6; 14(3):541–57.

28. Wetz MS, Yoskowitz DW. An 'extreme' future for estuaries? Effects of extreme climatic events on estuarine water quality and ecology. Mar Pollut Bull. 2013 Apr 15; 69(1):7–18.

29. Bowen MM, Geyer WR. Salt transport and the time-dependent salt balance of a partially stratified estuary. J Geophys Res Oceans. 2003; 108(C5).

30. Monismith SG, Kimmerer W, Burau JR, Stacey MT. Structure and Flow-Induced Variability of the Subtidal Salinity Field in Northern San Francisco Bay. J Phys Oceanogr. 2002 Nov 1; 32(11):3003–19.

31. MacCready P. Estuarine Adjustment to Changes in River Flow and Tidal Mixing. J Phys Oceanogr. 1999 Apr 1; 29(4):708–26.

32. Kelly S, Eyto E de, Poole R, White M. Ecological consequences of internal seiches in a semi-enclosed, anoxic coastal basin. Mar Ecol Prog Ser. 2018a Sep 17; 603:265–72.

33. McCarthy M, Spillane S, Walsh S, Kendon M. The meteorology of the exceptional winter of 2015/2016 across the UK and Ireland. Weather. 2016 Dec 1; 71(12):305–13.

34. Barker L, Hannaford J, Muchan K, Turner S, Parry S. The winter 2015/2016 floods in the UK: a hydrological appraisal. Weather. 2016; 71(12):324–33.

35. Matthews T, Murphy C, McCarthy G, Broderick C, Wilby RL. Super Storm Desmond: a process-based assessment. Environ Res Lett. 2018 Jan; 13(1):014024.

36. Lavers DA, Allan RP, Villarini G, Lloyd-Hughes B, Brayshaw DJ, Wade AJ. Future changes in atmospheric rivers and their implications for winter flooding in Britain. Environ Res Lett. 2013 Jul; 8 (3):034010.

37. Doyle BC, de Eyto E, Dillane M, Poole R, McCarthy V, Ryder E, et al. Synchrony in catchment stream colour levels is driven by both local and regional climate. Biogeosciences. 2019 Mar 15; 16(5):1053–71.

38. Kelly S, Eyto E de, Dillane M, Poole R, Brett G, White M. Hydrographic maintenance of deep anoxia in a tidally influenced saline lagoon. Mar Freshwater Res. 2018b Mar 21; 69(3):432–45.

39. Marine Institute. Newport Research Facility Annual Report, No. 62, 2018. Marine Institute, Newport, Mayo, 2019.

40. Poole WR, Diserud OH, Thorstad EB, Durif CM, Dolan C, Sandlund OT, et al. Long-term variation in numbers and biomass of silver eels being produced in two European river systems. ICES J Mar Sci. 2018 Oct 1; 75(5):1627–37.

41. de Eyto E., Dalton C., Dillane M., Jennings E., McGinnity P., O'Dwyer, et al. The response of North Atlantic diadromous fish to multiple stressors, including land use change: a multidecadal study, Can. J. Fish. Aquat. Sci., 73, 1759–1769. https://doi.org/10.1139/cjfas-2015-0450, 2016b.

42. Fofonoff NP, Millard RC. Algorithms for Computation of Fundamental Properties of Seawater. Endorsed by Unesco/SCOR/ICES/IAPSO Joint Panel on Oceanographic Tables and Standards and SCOR Working Group 51. Unesco Technical Papers in Marine Science, No. 44. 1983

43. Emery WJ, Thomson RE. Data analysis methods in physical oceanography. 2nd ed. New York: Elsevier. 2001.

44. ArcGIS Desktop: Release 10, Environmental Systems Research Institute, CA, USA, 2011.

45. Sieck LC, Burges SJ, Steiner M. Challenges in obtaining reliable measurements of point rainfall. Water Resour Res. 2007; 43(1). https://doi.org/10.1029/2005wr004773 PMID: 20300476

46. Woolway RI, Jones ID, Hamilton DP, Maberly SC, Muroaka K, Read JS, et al. Automated calculation of surface energy fluxes with high-frequency lake buoy data. Environ Modell Softw. 2015; 70:191198.

47. Kullenberg GEB. On vertical mixing and the energy transfer from the wind to the water. Tellus. 1976 Jan 1; 28(2):159–65.

48. Zeng X, Zhao M, Dickinson RE. Intercomparison of Bulk Aerodynamic Algorithms for the Computation of Sea Surface Fluxes Using TOGA COARE and TAO Data. J Climate. 1998 Oct 1; 11(10):2628–44.

49. Gill A.E. Atmosphere-ocean dynamics. International geophysics series. New York: Academic Press. 1982.

50. Schmidt W. Über Die Temperatur- Und Stabili-Tätsverhältnisse Von Seen. Geogr Ann. 1928 Aug 1; 10 (1–2):145–77.

51. Shintani T, Fuente A de la, Fuente A de la, Niño Y, Imberger J. Generalizations of the Wedderburn number: Parameterizing upwelling in stratified lakes. Limnol Oceanogr. 2010; 55(3):1377–89.

52. Niño Y, Caballero R, Reyes L. Mixing and interface dynamics in a two-layer stratified fluid due to surface shear stress. J Hydraul Res. 2003 Nov 1; 41(6):609–21.

53. Horn DA, Imberger J, Ivey GN. The degeneration of large-scale interfacial gravity waves in lakes. J Fluid Mech. 2001 May; 434:181–207.

54. Thorpe SA, Jiang R. Estimating internal waves and diapycnal mixing from conventional mooring data in a lake. Limnol Oceanogr. 1998; 43(5):936–45.

55. Marine Institute. Newport Research Facility Annual Report, No. 60, 2015 Marine Institute, Newport, Mayo, 2016.

56. Schaller N, Kay AL, Lamb R, Massey NR, van Oldenborgh GJ, Otto FEL, et al. Human influence on climate in the 2014 southern England winter floods and their impacts. Nature Climate Change. 2016 Jun; 6(6):627–34.

57. Cooney EM, McKinney P, Sterner R, Small GE, Minor EC. Tale of Two Storms: Impact of Extreme Rain Events on the Biogeochemistry of Lake Superior. J Geophys Res Biogeosci. 2018; 123(5):1719–31. https://doi.org/10.1029/2017JG004216 PMID: 30800557

58. Haapala H, Sepponen P, Meskus E. Effect of Spring Floods on Water Acidity in the Kiiminkijoki Area, Finland. Oikos. 1975; 26(1):26–31.

59. Otto FEL, Wiel K van der, Oldenborgh GJ van, Philip S, Kew SF, Uhe P, et al. Climate change increases the probability of heavy rains in Northern England/Southern Scotland like those of storm Desmond—a real-time event attribution revisited. Environ Res Lett. 2018 Jan; 13(2):024006.

60. Bouffard D, Perga M-E. Are flood-driven turbidity currents hot spots for priming effect in lakes? Biogeosciences. 2016 Jun 20; 13(12):3573–84.

61. Havens KE, Beaver JR, Casamatta DA, East TL, James RT, Mccormick P, et al. Hurricane effects on the planktonic food web of a large subtropical lake. J Plankton Res. 2011 Jul 1; 33(7):1081–94.

62. Farmer DM, Freeland HJ. The physical oceanography of Fjords. Prog Oceanogr. 1983 Jan 1; 12 (2):147–219.

63. Thomson RE, Spear DJ, Krassovski MV, Hourston RAS, Juhász TA, Mihály SF. Buoyancy-driven coastal current blocks ventilation of an anoxic fjord on the Pacific coast of Canada. J Geophys Res Oceans. 2017 Apr 1; 122(4):2976–98.

64. Pakhomova S, Braaten HFV, Yakushev E, Skei J. Biogeochemical consequences of an oxygenated intrusion into an anoxic fjord. Geochem Trans. 2014 Apr 28; 15:5. https://doi.org/10.1186/1467-4866-15-5 PMID: 24872727

65. Watts LJ, Rippeth TP, Edwards A. The Roles of Hydrographic and Biogeochemical Processes in the Distribution of Dissolved Inorganic Nutrients in a Scottish Sea-loch: Consequences for the Spring Phytoplankton Bloom. Estuar Coast Shelf Sci. 1998 Jan 1; 46(1):39–50.

66. de Eyto E, Kelly S, Ryder E, Dillane M, Archer L, O'Cathain D, et al. High frequency monitoring reveals fine scale spatial and temporal dynamics of the deep chlorophyll maximum of a stratified coastal lagoon. Estuar Coast Shelf Sci. 2019 Mar 5; 218:278–91.

67. Valle-Levinson A, Klinck JM, Wheless GH. Inflows/outflows at the transition between a coastal plain estuary and the coastal ocean. Cont Shelf Res. 1996 Dec 1; 16(14):1819–47.

68. Breitburg D, Levin LA, Oschlies A, Grégoire M, Chavez FP, Conley DJ, et al. Declining oxygen in the global ocean and coastal waters. Science. 2018 Jan 5; 359(6371):eaam7240. https://doi.org/10.1126/science.aam7240 PMID: 29301986

69. Schinke H, Matthäus W. On the causes of major Baltic inflows—an analysis of long time series. Cont Shelf Res. 1998 Apr 24; 18(1):67–97.

70. Allen GL, Simpson JH. Deep Water Inflows to Upper Loch Linnhe. Estuar Coast Shelf Sci. 1998 Oct 1; 47(4):487–98.

71. Gillibrand PA, Turrell WR, Elliott AJ. Deep-Water Renewal in the Upper Basin of Loch Sunart, a Scottish Fjord. J Phys Oceanogr. 1995 Jun 1; 25(6):1488–503.

72. Laval BE, Morrison J, Potts DJ, Carmack EC, Vagle S, James C, et al. Wind-driven Summertime Upwelling in a Fjord-type Lake and its Impact on Downstream River Conditions: Quesnel Lake and River, British Columbia, Canada. J Great Lakes Res. 2008 Jan 1; 34(1):189–203.

73. Cossu R, Wells MG. The Interaction of Large Amplitude Internal Seiches with a Shallow Sloping Lakebed: Observations of Benthic Turbulence in Lake Simcoe, Ontario, Canada. PLoS One. 2013; 8 (3).

74. Lorke A, Umlauf L, Mohrholz V. Stratification and mixing on sloping boundaries. Geophys Res Lett. 2008; 35(14).

75. Chikita K. Dynamic behaviours of anoxic saline water in Lake Abashiri, Hokkaido, Japan. Hydrol Process. 2000; 14(3):557–74.

76. Vaz N, Silva JDL e, Dias JM. Salt Fluxes in a Complex River Mouth System of Portugal. PLOS ONE. 2012 Oct 10; 7(10):e47349. https://doi.org/10.1371/journal.pone.0047349 PMID: 23071793

77. Kelly, S. Marine and freshwater influences on the hydrography, oxygen dynamics and ecology of an anoxic lagoonal estuary, Lough Furnace, Mayo, Ireland, Ph.D. thesis, National University of Ireland Galway, Ireland. 2019.

Received: 7 September 2020 | Revised: 18 November 2020 | Accepted: 24 November 2020

DOI: 10.1111/jbi.14052

RESEARCH ARTICLE

Journal of Biogeography | WILEY

Abundance and biogeography of methanogenic and methanotrophic microorganisms across European streams

Magdalena Nagler[1] | Nadine Praeg[1] | Georg H. Niedrist[2] | Katrin Attermeyer[3,4] | Núria Catalán[5,6] | Francesca Pilotto[7,8] | Catherine Gutmann Roberts[9] | Christoph Bors[10] | Stefano Fenoglio[11,12] | Miriam Colls[5,6] | Sophie Cauvy-Fraunié[13] | Brian Doyle[14] | Ferran Romero[5,6] | Björn Machalett[15,16] | Thomas Fuss[17] | Adam Bednařík[18] | Marcus Klaus[19] | Peter Gilbert[20] | Dominique Lamonica[13] | Anna C. Nydahl[3] | Clara Romero González-Quijano[17] | Lukas Thuile Bistarelli[17] | Lyubomir Kenderov[21] | Elena Piano[11] | Jordi-René Mor[5,6] | Vesela Evtimova[22] | Elvira deEyto[23] | Anna Freixa[5,6] | Martin Rulík[18] | Josephine Pegg[24,9] | Sonia Herrero Ortega[17] | Lea Steinle[25] | Pascal Bodmer[10,26]

[1]Department of Microbiology, Universität Innsbruck, Innsbruck, Austria

[2]Department of Ecology, Universität Innsbruck, Innsbruck, Austria

[3]Limnology/Department of Ecology and Genetics, Uppsala University, Uppsala, Sweden

[4]WasserCluster Lunz, Lunz am See, Austria

[5]Catalan Institute for Water Research (ICRA), Girona, Spain

[6]Universitat de Girona (UdG), Girona, Spain

[7]Senckenberg Research Institute and Natural History Museum Frankfurt, Gelnhausen, Germany

[8]Umeå University, Historical, Philosophical and Religious studies, Umeå, Sweden

[9]Bournemouth University, Bournemouth, United Kingdom

[10]University of Koblenz-Landau, Landau in der Pfalz, Germany

[11]DBIOS - Università degli Studi di Torino Via Accademia Albertina, 13, 10123 Torino

[12]ALPSTREAM, Italy

[13]Riverly Lab, Irstea Centre de Lyon-Villeurbanne, Saint Martin d'Heres, France

[14]Dundalk Institute of Technology, Centre for Freshwater and Environmental Studies (CFES), Dundalk, Ireland

[15]Humboldt-Universität zu Berlin, Institute of Geography, Climatology Group, Berlin, Germany

[16]Department of Geosciences, University of Massachusetts Amherst, Amherst, MA, USA

[17]Leibniz-Institute of Freshwater Ecology and Inland Fisheries (IGB), Berlin, Germany

[18]Department of Ecology and Environmental Sciences, Palacký University, Olomouc, Czechia

[19]Department of Ecology and Environmental Science, Umeå University, Umeå, Sweden

[20]University of Highlands and Islands, Thurso, UK

[21]Faculty of Biology, Sofia University "St. Kliment Ohridski", Sofia, Bulgaria

[22]Bulgarian Academy of Sciences, Institute of Biodiversity and Ecosystem Research, Sofia, Bulgaria

[23]The Marine Institute, Newport, Ireland

[24]South African Institute for Aquatic Biodiversity, Makhanda, South Africa

[25]University of Basel, Basel, Switzerland

[26]Département des Sciences Biologiques, Groupe de Recherche Interuniversitaire en Limnologie, Université du Québec à Montréal, Montreal, Canada

Correspondence
Magdalena Nagler, Universität Innsbruck, Department of Microbiology, Innsbruck, Austria.
Email: Magdalena.Nagler@uibk.ac.at

Funding information
German Research Foundation, Grant/Award Number: BO 5050/ and 1-1

Handling Editor: Jani Heino

Abstract

Aim: Although running waters are getting recognized as important methane sources, large-scale geographical patterns of microorganisms controlling the net methane balance of streams are still unknown. Here we aim at describing community compositions of methanogenic and methanotrophic microorganisms at large spatial scales and at linking their abundances to potential sediment methane production (PMP) and oxidation rates (PMO).

Location: The study spans across 16 European streams from northern Spain to northern Sweden and from western Ireland to western Bulgaria.

Taxon: Methanogenic archaea and methane-oxidizing microorganisms.

Methods: To provide a geographical overview of both groups in a single approach, microbial communities and abundances were investigated via 16S rRNA gene sequencing, extracting relevant OTUs based on literature; both groups were quantified via quantitative PCR targeting mcrA and pmoA genes and studied in relation to environmental parameters, sediment PMP and PMO, and land use.

Results: Diversity of methanogenic archaea was higher in warmer streams and of methanotrophic communities in southern sampling sites and in larger streams. Anthropogenically altered, warm and oxygen-poor streams were dominated by the highly efficient methanogenic families *Methanospirillaceae*, *Methanosarcinaceae* and *Methanobacteriaceae*, but did not harbour any specific methanotrophic organisms. Contrastingly, sediment communities in colder, oxygen-rich waters with little anthropogenic impact were characterized by methanogenic *Methanosaetaceae*, *Methanocellaceae* and *Methanoflorentaceae* and methanotrophic *Methylococcaceae* and *Cd*. Methanoperedens. Representatives of the methanotrophic *Crenotrichaceae* and *Methylococcaceae* as well as the methanogenic *Methanoregulaceae* were characteristic for environments with larger catchment area and higher discharge. PMP increased with increasing abundance of methanogenic archaea, while PMO rates did not show correlations with abundances of methane-oxidizing bacteria.

Main conclusions: Methanogenic and methanotrophic communities grouping into three habitat types suggest that future climate- and land use changes may influence the prevailing microbes involved in the large-scale stream-related methane cycle, favouring the growth of highly efficient hydrogenotrophic methane producers. Based on these results, we expect global change effect on PMP rates to especially impact rivers adjacent to anthropogenically disturbed land uses.

KEYWORDS
inland waters, methane-oxidizing bacteria, methanogenic archaea, potential methane oxidation, potential methane production, stream sediments

1 | INTRODUCTION

Methane (CH_4) has a global warming potential 34 times higher than carbon dioxide (CO_2) (Ciais et al., 2013) due to its efficiency in absorbing infrared radiation (Etminan et al., 2016). While sources of CH_4 are manifold and may be natural or anthropogenic, current estimates suggest that 35%–50% of global CH_4 emissions originate from natural sources (Ciais et al., 2013). Among these sources, natural wetlands are the largest, followed by geological sources and freshwaters (running waters and lakes), with running waters contributing 3% of the global release or 15%–40% of the efflux from wetlands and lakes (Stanley et al., 2016).

Biogenic CH_4 is almost exclusively produced by methanogenic archaea (MA) during the final step of anaerobic degradation of organic matter. MA mainly produce CH_4 either from H_2 and CO_2 (hydrogenotrophic pathway) or from acetate cleavage (acetoclastic

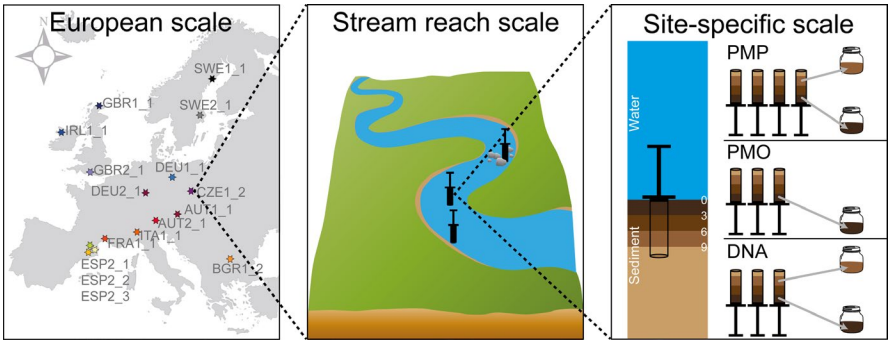

FIGURE 1 Conceptual figure of the sampling design at European, stream reach and site-specific scale. PMP = samples retrieved for potential methane production measurements, PMO = samples retrieved for potential methane oxidation measurements, DNA = samples retrieved for qPCR and sequencing. Map in Lambert Conformal Conic projection

pathway) (Nazaries et al., 2013). Lotic waters represent important components of the global carbon cycle through carbon mineralization into CO_2 and CH_4 (Stanley et al., 2016) and first studies on river sediments revealed the dominance of *Methanosarcinales* and *Methanomicrobiales* (Chaudhary et al., 2017).

Environments facilitating the occurrence of communities producing CH_4 are also typical habitats for methane-oxidizing microorganisms (MOX) (Kalyuzhnaya et al., 2019), which consume the newly synthesized CH_4 as a carbon and energy source. Some MOX belong to archaea, perform anaerobic methane oxidation (ANME) and involve three distinct methanotrophic groups. Of these groups (ANME-1 to ANME-3), ANME-2 is further divided into four subgroups ANME-2 a, b, c, and *Candidatus* (*Cd.*) Methanoperedens (Boetius et al., 2000). Furthermore, anaerobic CH_4 oxidation can be performed by several bacterial species belonging to the phylum NC10 (Ettwig et al., 2010). Aerobic CH_4 oxidation, however, is carried out by a heterogeneous group of obligate or facultative methanotrophic bacteria (MOB) usually divided into three main types: Gammaproteobacteria (type I or type X), Alphaproteobacteria (type II) and Verrucomicrobia (type III), all with different pathways of utilizing CH_4 (Kalyuzhnaya et al., 2019). Aerobic MOX, often inhabiting anoxic–oxic interfaces such as the upper sediment layers, are known to support a high potential for CH_4 oxidation in riverbeds (Trimmer et al., 2015). Furthermore, a large-scale study on methanotrophic communities in boreal inland waters in Canada highlighted a clear niche differentiation between type I and type II methanotrophs in water and river sediments (Crevecoeur et al., 2019). Besides these works on specific groups, however, the taxonomic composition/distribution of both, methanogens and methanotrophs and the respective predominant key players in different streams across ecoregions have not yet been examined.

While molecular approaches are helpful in analysing community compositions and abundances of MA and MOX, studying the net CH_4 balance of an ecosystem also requires the quantification and investigation of CH_4 production and oxidation processes. Studies measuring potential methane production (PMP) in streams, rivers (Bednařík et al., 2017) or river impoundments (Wilkinson et al., 2019) are scarce and do not necessarily link PMP rates with MA abundances. However, some recent studies on PMP in stream sediments (Chaudhary et al., 2017; Mach et al., 2015) reported two depth-related PMP maxima along sediment profiles dominated by hydrogenotrophic methanogenesis. While these studies could not prove a relationship between MA abundance and PMP, others (Crawford et al., 2017) observed highest PMP rates in sediments enriched in the methane-producing *mcrA*-gene. Data on potential CH_4 oxidation (PMO) in freshwater ecosystems are also scarce (e.g. Oswald et al., 2015), but it was shown that PMO from river sediments increased with decreasing gravel size (Bodmer et al., 2020). Additional drivers of such distributions and rates in stream sediments have not been identified so far.

To our knowledge, an in-depth investigation of taxonomic distributions and abundances of both microbial groups involved in the CH_4 cycle and of underlying environmental conditions has not been carried out on large continental (European) scale. Thus, the present study aims to (a) describe the biogeography of MA and MOX in stream sediments, (b) identify the dominant species within each functional group, (c) examine the links between environmental conditions and the distribution of both MA and MOX and (d) compare the absolute abundances of MA and MOX with their potential metabolic activities across 16 European streams.

2 | MATERIALS AND METHOD

2.1 | Sampling design

We sampled sediments from 16 streams across 10 European countries (Table S1, Appendix S2), using the EuroRun network (Bodmer et al., 2019; Bravo et al., 2018). Within a representative 50 m section of the investigated stream three patches were sampled based on their sediment grain size: (a) coarse (gravel, >0.2 cm to 2 cm), (b) medium (sand/mud, >6 µm to 2 mm), and (c) fine (silt/loam/clay, <6 µm; Figure 1). If not applicable, sediment patches with the widest range of sediment grain size were selected (coarse, medium and fine sediment). Particle size distributions were additionally measured in the laboratory to assure for a comparability of the categories across the streams. In most cases, the categories did not completely match with the measured grain sizes and, therefore, the three areas were considered as replicates of the same stream. Sediment surface area (measured) was used as parameter describing the within-stream sediment heterogeneity (see chapter 2.2.)

From each of the three stream replicates (patches), 10 sediment cores were sampled with cut-off 100 mL syringes (diameter: 3.6 cm), avoiding sediment vertical profile disturbance or compression. To

gain insight into microbial spatial preferences resulting from oxygen availability, cores were split into two samples from different depths (0–3 cm and 6–9 cm below the surface water interface), and transferred to 30 mL glass vials. Samples were stored at 4°C and shipped to the respective laboratories (University of Koblenz-Landau, Germany: PMP, sediment nitrogen and organic carbon content; University of Basel, Switzerland: PMO; University Innsbruck, Austria: molecular work) the following day. Three parallel samples of each sediment layer per patch were combined to form one composite sample of each depth, and an aliquot was taken for DNA extraction ($n = 96$; stored at −20°C; processed 7–21 days after sampling; Figure 1). Furthermore, three 0-3cm sediment samples per sediment patch were used for PMO measurements ($n = 144$; stored at 3°C; processed 5–8 days after sampling), and both sediment layers of four sediment samples per patch were used for PMP measurements ($n = 384$; stored at 4°C; processed 3–10 days after sampling; Figure 1).

2.2 | Physical and chemical parameters

The upstream catchment area, elevation (metres above sea level), Strahler stream order (Strahler, 1952), and land use within the catchment were taken from Bravo et al. (2018), which covered the same sites (Table S1, Appendix S2). Land use within the catchment was further simplified after inspection via principal component analysis (PCA; see section 2.7) by unifying the classes 'urban' and 'agriculture' as well as 'forest' and 'others' into 'anthropogenically altered' and 'natural' respectively. As those two variables represented co-correlating values, only 'natural' was used for those analyses influenceable by correlating descriptor variables (i.e. redundancy analysis; RDA and generalized linear mixed models; GLMMs). Besides these landscape variables, hydromorphological features were measured with standard methods (see Method S1, Appendix S3), including wetted stream width (m), cross-sectional area (m^2), water depth (m), stream area (m^2), discharge ($m^3\ s^{-1}$), mean flow velocity (ms^{-1}) and channel slope (%).

Physical and chemical parameters (pH, surface water oxygen concentration [mg/L], conductivity [μScm^{-1}] and temperature [°C]) were measured with standard methods during daytime in the middle of the stream (Table S2, Appendix S2 for devices used at individual sites).

Particle size distribution was measured from a subsample of each PMP sample at the Thuringian Particle Size Laboratory using a Beckman-Coulter LS 13,320 PIDS following (Machalett et al. 2008; Method S2, Appendix S3). To estimate the area potentially colonizable by microorganisms, sediment surface area ($cm^2\ cm^{-3}$) was calculated using the mean size of each particle class assuming a spherical particle shape.

Sediment nitrogen and organic carbon content (expressed as weight percent of dry sediment) was measured from PMP samples after the incubation period by dry combustion (Vario MICRO Cube, Elementar Analysensysteme GmbH), assuming the consumption under anoxic conditions in this period of time to be negligible (Method S3, Appendix S3).

2.3 | Potential methane production and potential methane oxidation

PMP was measured according to Wilkinson et al. (2019) and PMO according to Steinle et al. (2016) and Su et al. (2019). In brief, for PMP, the sediment was incubated for 5 weeks in an air-tight vial at 16°C in the dark. Headspace gas samples were analysed weekly with an ultraportable greenhouse gas analyser and PMP was calculated from the linear increase in CH_4 partial pressure over time (g CH_4 m^{-3} fresh sediment d^{-1}).

For PMO, fresh sediment samples were amended with trace amounts of ^{14}C-labelled aqueous CH_4 and incubated in the dark for ~3 days at room temperature. Incubations were stopped with 20 mL 2.5% sodium hydroxide and PMO (%CH_4 d^{-1}) was assessed by $^{14}CH_4$ combustion and $^{14}CO_2$ acidification. Further details are given in the supplement (Method S4, Appendix S3).

2.4 | DNA extraction

DNA was extracted from approx. 500 mg fresh composite sediment sample for each depth using the Nucleo Spin® Soil Kit (Macherey-Nagel). DNA quality was checked on 1% (w/v) agarose gels using GelGreen™ staining (Biotium Inc.,) and quantity was measured using a Quantus™Fluorometer and the QuantiFluor® Dye System for double-stranded DNA (dsDNA; Promega).

2.5 | qPCR

Quantitative PCR (qPCR) was conducted using the SensiFast™ SYBR No-Rox Kit (Bioline, UK) on a Corbett Life Science Rotor-GeneTMQ system (Qiagen). Total *mcrA*-genes of MA were determined using the primer set mlas/mcrA-rev (469bp) (Steinberg and Regan, 2009) and the abundance of *pmoA* gene of type Ia and type II methane-oxidizing bacteria with the primer pairs A189f/Mb601r (432bp) and II223f/II646r (444bp) (Kolb et al., 2003; Cai et al., 2016; Praeg et al., 2020; see Table S3, Appendix S2 for cycling conditions). Detailed qPCR-related information is given in the supplement (Method S5, Appendix S3). In contrast to the sequencing, the qPCR approach does not include ANME and the quantified group targeted with the *pmoA* is thus abbreviated as MOB (without archaea). Thereby, the separate investigation of type I and type II MOB provides (more) detailed information on methanotrophic physiology (Trimmer et al., 2015) and total methanotrophs can be quantified to a large extend by the aforementioned primer pairs (Cai et al., 2016; Kolb et al., 2003; Praeg et al., 2020). Thus, gene copies of type Ia and type II MOB were summed to represent an approximation to the total MOB gene copy number.

2.6 | 16S rRNA gene sequencing and bioinformatics

For this first study investigating the biogeography and diversity of all microorganisms driving the CH_4 cycle within stream sediments across Europe, we sequenced the 16S rRNA gene as a target, providing a broad overview of all present microbial taxa including MA and MOX in equal measure. The gained rarefaction curves (Figure S1, Appendix S1) exhibited a high depth of 16S rRNA gene sequencing suitable for in-depth interpretation. Although targeting of functional marker genes might yield more informative sequence reads, the used primer set makes the results highly comparable to existing 16S rRNA-based studies and a careful interpretation of the results offers noticeable first insights on the diversity of methanogens and methanotrophs across European stream sediments.

A total of 96 DNA extracts resulting from (composite) triplicates of 16 streams and two depths was subjected to high-throughput amplicon sequencing on an Illumina MiSeq platform (v2) performing a 300 bp paired-end run and simultaneously targeting bacteria and archaea via the V4 region of the 16S SSU rRNA gene (StarSEQ) using the 515f/806r primer system (Caporaso et al., 2011).

Sequence data were processed applying the CoMA pipeline, a pipeline for amplicon sequencing data analysis based on various applications such as Qiime, Mothur and others (Hupfauf et al., 2020). In brief, merging of paired-end reads and trimming of barcodes and primers were done using the recommended settings. High-quality reads were selected to show <5% deviation from the mode sequence length and at least 99.7% base call accuracy (phred score ≥25). Sequences were aligned applying a 97% similarity level and assigned taxonomically using the blast algorithm against *SILVA SSU* (release 132) and *Greengenes* (release 13_5) as primary and backup databases respectively. Operational taxonomic units (OTUs) represented by only one read within all samples were excluded and samples were subsampled to 73'249 reads after rarefaction analysis, thereby dropping two samples (FRA1_1_2_B and FRA1_1_2_C) with considerably lower read numbers (37'630 and 34'099 reads, respectively). After even-sampling, OTUs assigned to MA and methane-oxidizing microorganisms (containing both, archaea and bacteria and therefore abbreviated as MOX) as listed in recent literature (Kalyuzhnaya et al., 2019; Nazaries et al., 2013) were extracted and used for subsequent analyses.

2.7 | Data analysis

2.7.1 | Environmental data

To reduce the dimensions of the multivariate dataset and explore the environmental conditions of the streams, a PCA was performed using the *FactoMineR* and *factoextra* packages (Kassambra & Mundt, 2017; Lê et al., 2008; R Core Team, 2018).

2.7.2 | Community data

Differences among the community structure of all sequenced OTUs from different sediment depths (0–3 cm, 6–9 cm) and variation in community composition as a function of stream and depth were tested with one-way and two-way PERMANOVA (using Adonis function) with 9,999 permutations, based on Bray–Curtis dissimilarity matrix of both MA and MOX communities using the *vegan* package (Oksanen et al., 2019). As sampling depth had no significant influence on the community composition of MA or MOX, subsequent analyses were performed on sequencing data of both sampling depths combined (n = 96); α-diversity was inspected calculating Shannon index and OTU richness (Chao-index) using the *Mothur* software pipeline v.1.39.0 (Schloss et al., 2009) and averaging their distribution on family-level in each stream (i.e. combining the three composite samples per sediment depth of the three sampled patches). The top 5 families in each stream were determined by calculating mean ranks of all families, and β-diversities were studied performing an NMDS with Bray–Curtis dissimilarities on OTU-level of MA and MOX including both sediment layers.

Univariate relationships between log-transformed relative read numbers of MA and MOX families with each other and with environmental variables were examined with Pearson correlation tables using the *corrplot* package and a significance level of 1% (Wei et al., 2017). Correlation between environmental variables and MA and MOX communities were determined via redundancy analyses (RDA) with 499 unrestricted permutations on log-transformed read numbers using the default interactive forward selection mode in Canoco5 (Šmilauer & Lepš, 2014), considering only one representative of each co-correlating group of environmental variables (identified in the PCA, see above).

2.7.3 | Gene abundance data

Relationships between abundance of MA and MOB, between PMP and MA, and between PMO and MOB were explored using generalized linear models (GLMs) on log-transformed data. Differences in gene copy numbers at different depths were tested using pairwise comparisons (paired student's t test) in all technical replicate samples with the package *ggpubr* (Kassambra, 2018). Since the depth effect was negligible (small significant effect for MOX only, see results section 3.5), both depth levels were combined for subsequent analyses. Differences of gene copy numbers between individual streams were evaluated using Kruskal–Wallis rank sum test and best correlating stream-scale variables were identified with GLMs on the data aggregated by stream (n = 16) with forward selection based on Bayesian information criterion, using a log link function and considering multicollinearity between predictors. Generalized linear mixed models (GLMMs) were used to disentangle the site-specific environmental drivers of MA and MOB gene copy numbers, while considering stream-scale differences (n = 96). Hence, stream

identity was considered as a random effect and the following site-specific variables were included as fixed effects: sediment nitrogen and organic carbon content, sediment surface area, and sediment C:N ratio. Various models with different combinations of fixed effects were constructed using the packages *lme4* (Bates et al., 2015) and *r2glmm* (Jaeger, 2017), while avoiding multicollinearity (checked using the package *corrplot;* Wei et al., 2017). The final GLMM for the two dependent microbial communities (MA and MOB) was selected based on the GLMMs fit by examining both the mixed effect models conditional R^2 (Nakagawa & Schielzeth, 2012) and the prediction quality of gene copy numbers (correlation between observed and predicted gene copies). The importance of each environmental variable was evaluated using the percentage of explained variation.

3 | RESULTS

3.1 | Environmental data

The PCA (Figure 2; Tables S1, S4 in Appendix S2) revealed the influence of hydromorphological stream characteristics and physicochemical water properties on the first axis (Figure 2). The second axis discriminated the samples based on grain size distributions and sediment organic carbon content. Axis 1 ordered samples according to site and latitude and axis 2 separated different sediment types within streams (i.e. coarse, medium and fine sediment patches).

3.2 | Alpha- and beta-diversity of MA and MOX communities in streams across Europe

Total 16S rRNA read numbers ranged from 73'249 to 140'000 per sample. Of all reads, a mean of 728 (1.0%) belonged to MA and 799 (1.1%) to MOX. There were no significant differences in overall microbiome composition of all sequenced operational taxonomic units (OTUs; including all bacteria and archaea) between samples from 0–3 cm and 6–9 cm sediment depths, as tested with PERMANOVA.

MA reads were assigned to 11 families, with *Methanoregulaceae*, *Methanosaetaceae*, *Methanosarcinaceae* and *Methanobacteriaceae* being relatively most abundant (Figure 3a,c), based on the number of reads. MA diversity ranged from 10 to 33 OTUs and over a Shannon index from 1.6 to 2.9 (Figure 3a; Table S5 in Appendix S2). MA species richness and diversity were positively correlated with water temperature (Pearson`s r = 0.45, $p < 0.01$) and catchment area (Pearson`s r = 0.48, $p < 0.01$), respectively, while they were negatively correlated with increasing natural land cover percentages within the catchment (r = −0.48 and r = −0.5, resp., $p < 0.01$; Figure S2 in Appendix S1).

For MOX, OTUs were assigned to eight different families, with bacterial *Methylococcaceae*, unclassified *Methylococcales*, *Methylocystaceae*, *Cd.* Methylomirabilis and the archaeal clade *Cd.* Methanoperedens being most abundant (Figure 3b,d; Table S5, Appendix S2). Within MOX, significant differences in read numbers between both sampling depths (0–3 versus. 6–9 cm) were found for *Cd.* Methanoperedens as well as *Cd.* Methylomirabilis, yielding higher relative abundances in deeper sediment samples (Mann–Whitney U, $p < 0.01$, Table S5, Appendix S2). For other families including *Methylocystaceae*, CABC2E06, *Crenotrichaceae* and plW-20, differences were less pronounced ($p = 0.014$, $p = 0.017$, $p = 0.034$ and $p = 0.023$, respectively), but all families displayed lower read numbers in the deeper sediment layer. Similarly, read numbers of anaerobic methane oxidizers (i.e. the sum of *Cd.* Methanoperedens + *Cd.* Methylomirabilis reads) were significantly higher within the deeper sediment layer (Mann–Whitney U, $p < 0.01$), while read numbers of aerobic methane oxidizers did not differ significantly between both sampling depths. MOX OTU numbers ranged from 12 to 64 and diversities from 0.5 to 2.7, with diversity being significantly correlated with geographical latitude (Pearson`s r = −0.51, $p < 0.01$), stream area (Pearson`s r = 0.51, $p < 0.01$), wetted stream width (Pearson`s r = 0.49, $p < 0.01$) and channel slope (Pearson`s r = 0.46, $p < 0.01$, Figure S2, Appendix S1).

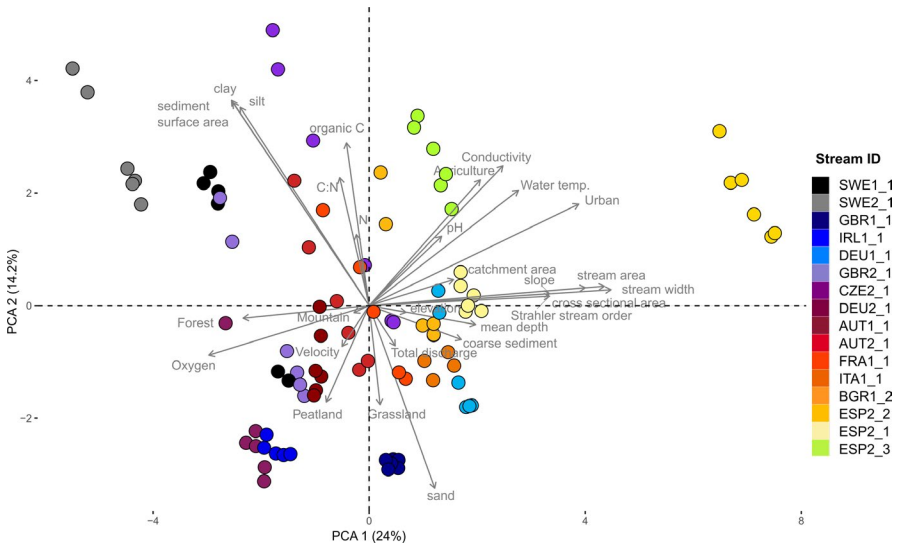

FIGURE 2 Principal component analysis plot of the first two dimensions based on all combined environmental data collected at two depths (0–3 and 6–9 cm depth) of three patches in each stream. Sample sites are coloured according to geographical latitude with SWE1_1 representing the northernmost and ESP2_3 the southernmost sampling points. Further information about units is listed in Tables S1 and S4 in Appendix S2. Proportions of explained variance of both dimensions are given in brackets

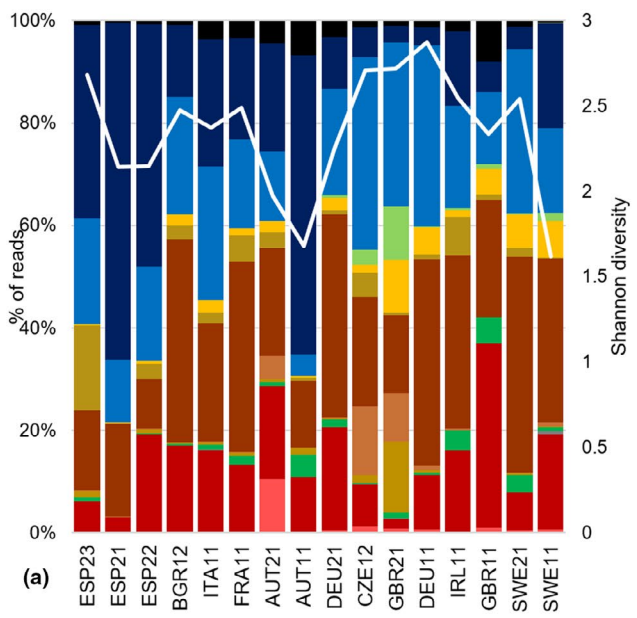

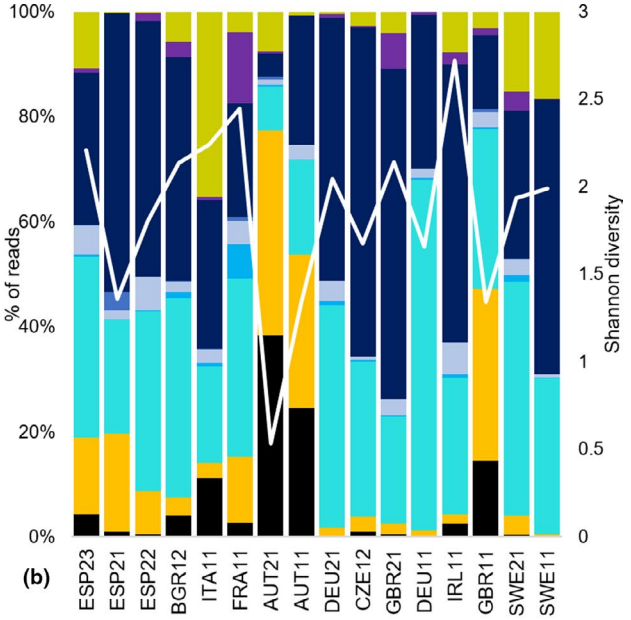

Order	Family
Thermoplasmata	Incertae Sedis
Methanosarcinales	Methanosarcinaceae
	Methanosaetaceae
Methanomicrobiales	Cd. Methanoflorentaceae
	MHLsu47-B8A
	Methanospirillaceae
	Methanoregulaceae
	Methanomicrobiaceae
	unclassified
Methanocellales	Methanocellaceae
Methanobacteriales	Methanobacteriaceae
Unclassified Methanomicrobia	

Order	Family
Methanosarcinales	Cd. Methanoperedens
Methylococcales	pLW-20
	Methylococcaceae
	Marine Methylotrophic group
	Crenotrichaceae
	CABC2E06
	unknown
Rhizobiales	Methylocystaceae
Nitrospirales	Cd. Methylomirabilis

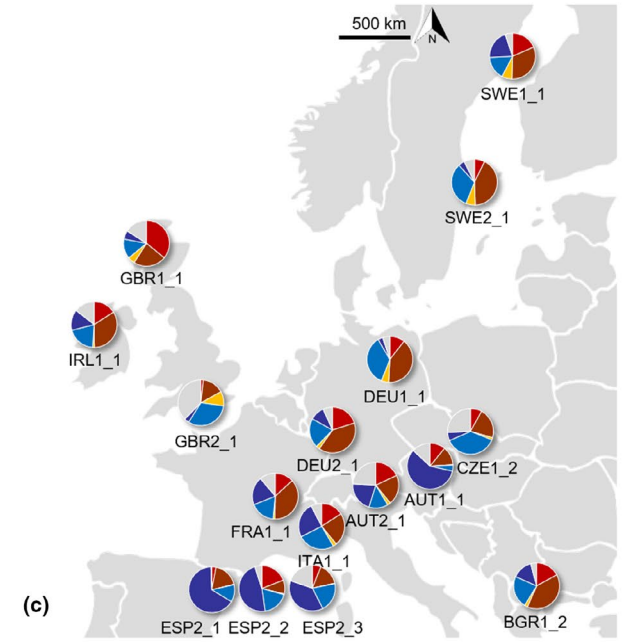

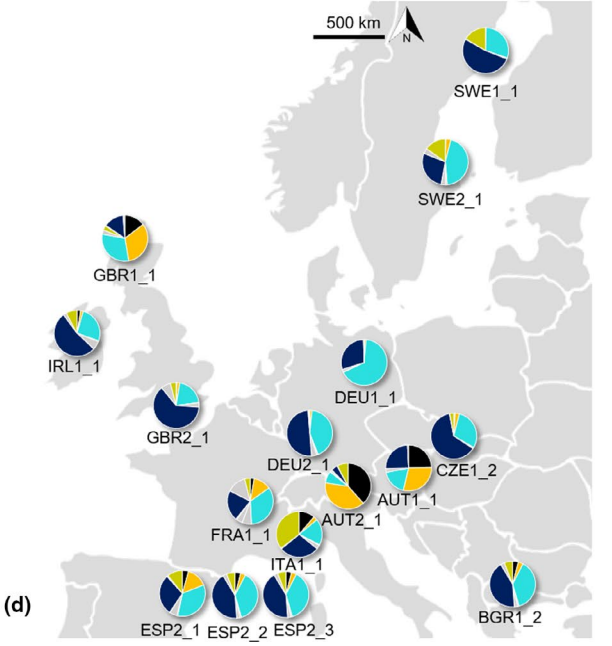

FIGURE 3 Mean biogeography of (a,c) methanogenic archaea (MA) and (b,d) methane-oxidizing bacteria and archaea (MOX) based on combined data from 0 to 3 and from 6 to 9 cm sediment depth in streams across Europe. a) and b) show relative α-diversities at family level with sampling sites ordered by geographical latitude. The line represents the Shannon Index. (c and d) show the top 5 families across European streams selected by mean rank of each family among all sites. Pie charts show percentages of reads belonging to MA or MOX. Map in Lambert Conformal Conic projection

3.3 | Correlations among taxonomic groups and with environmental variables

The separation of communities via NMDS illustrated a more homogeneous composition of MA compared to MOX. The latter formed clusters that are more distinct among sampling sites and roughly grouped according to their geographical latitude (Figure S3, Appendix S1), but both groups exhibited a wide range of within-stream variability, which is linked to both the sampling depth and patch-specific environmental constraints. According to the two-way PERMANOVA, the affiliation to a certain stream had a significant effect on both, MA and MOX (PERMANOVA, $p < 0.01$), while the sampling depth was found to be marginally influential only for MOX (PERMANOVA, $p = 0.032$) and no significant interaction effect was found.

The best (and significant) subset of the environmental variables to summarize the variation in species composition (identified via interactive forward selection in RDA) accounted for an adjusted explained variation of 39.5% (MA) and 55.4% (MOX; Figure 4a,b). MA communities in more anthropogenically altered and warm environments with increased pH were represented by various *Methanospirillum* spp., by members of the family *Methanosarcinaceae* and by a variety of taxa belonging to *Methanobacteriaceae* (Figure 4a), while no representative MOX community was established within comparable environments (Figure 4b).

Communities in well-oxygenated streams in natural land cover dominated catchments were characterized by MA groups *Methanosaeta* spp., *Methanocellaceae* and *Methanoflorentaceae*, and by many MOX of the family *Methylococcaceae*, of unassigned *Methylococcales* and, interestingly, by various *Cd.* Methanoperedens (Figure 4a,b).

For both, MA and MOX, another well-separated community was also found in streams draining larger catchments with high discharge (mainly sampling site DEU1_1) featuring MA representatives *Methanosaeta* spp., *Methanolinea* spp. and *Mehanoregula* spp. and MOX representatives *Methylocaldum* spp. and *Crenothrix* spp. (Figure 4a,b).

Generally, relative read numbers of MA were mostly influenced by environmental parameters reflecting climatic conditions such as latitude and water temperature, while MOX read numbers correlated with surface water oxygen saturation and stream area (Figure S2a, Appendix S1). Moreover, identified positive and negative relationships within and between MA and MOX families are reflecting the grouping in the RDA (Figure S3, Appendix S1).

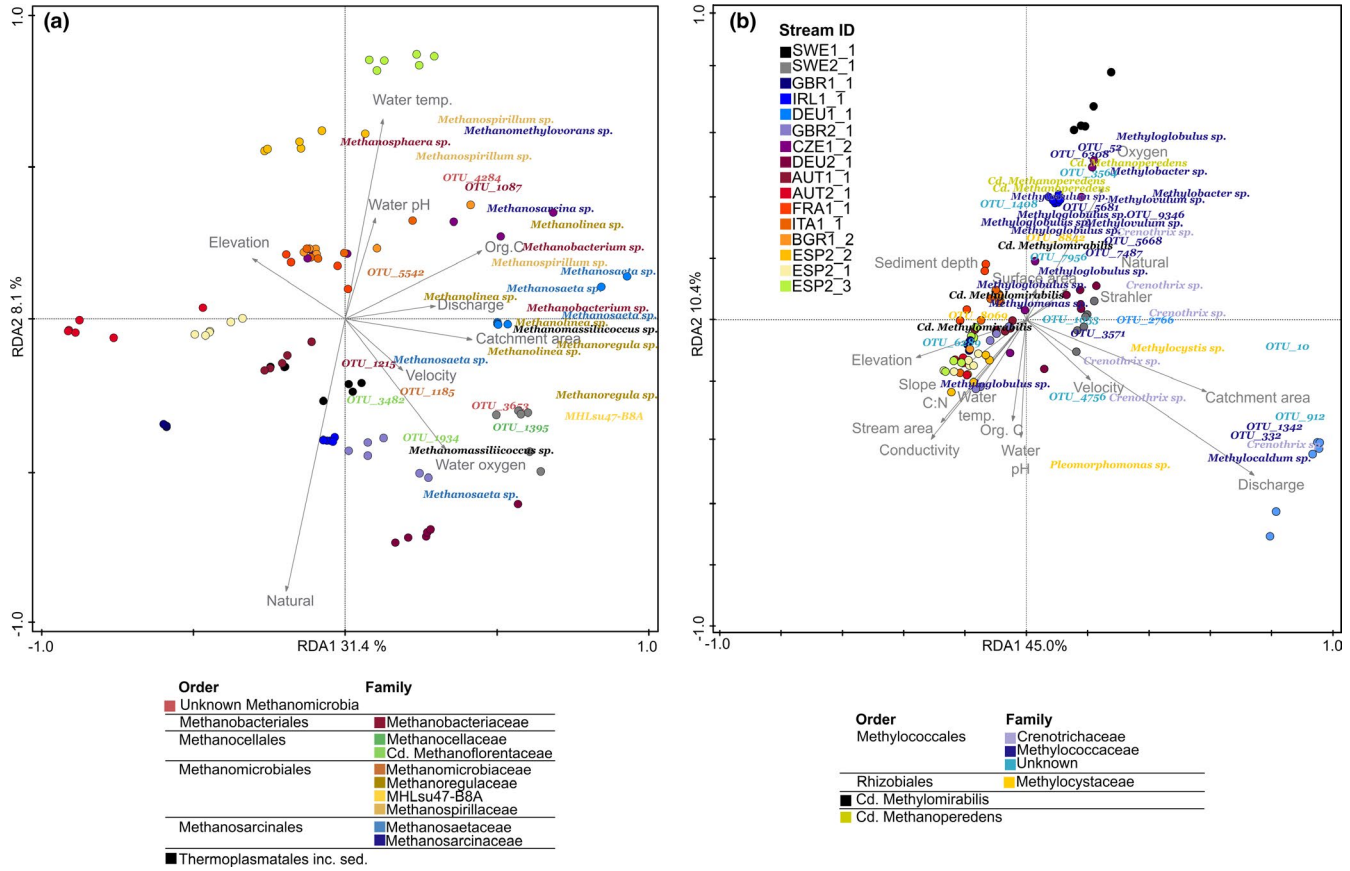

FIGURE 4 Triplots of redundancy analysis (RDA) of MA (top) and MOX (bottom) sequences from stream sediments in 0–3 and in 6–9 cm depth. Significant environmental parameters selected by forward selection are depicted and are grouping operational taxonomic units (OTU) as well as samples (sediment patch and depth) towards their predominant environmental characteristics and preferred habitats respectively. Explained variations of each axis are given as percentage of all eigenvalues. The stream-ID colour code refers to circles and the OTU colour code to labels

3.4 | Methane production and oxidation potentials

PMP rates ranged from 9.7×10^{-5} g CH_4 $m^{-3}d^{-1}$ (IRL1_1) to 9.46 g CH_4 $m^{-3}d^{-1}$ (CZE1_2) and PMO rates from 1.7×10^{-4}% CH_4 d^{-1} (SWE1_1) to 0.32% CH_4 d^{-1} (IRL1_1; Table S5, Appendix S2). PMP rates did not differ significantly between both sediment depths, with mean values of 1.61 ± 0.69 at 0–3 cm and 0.56 ± 1.58g CH_4 $m^{-3}d^{-1}$ at 6–9 cm.

3.5 | Gene abundance data

Abundance of *mcrA*-gene ranged from 3.1×10^1 to 3.2×10^7 gene copies g fresh weight^{-1}, type Ia MOB gene abundances from 2.82×10^2 to 2.55×10^7 and type II MOB from 5.98×10^2 to 6.8×10^7 gene copies g fresh weight^{-1} (Table S5, Appendix S2). While mean copy numbers of all genes were lower in the deeper sediment samples (mcrA: 2.6×10^6 versus. 2.5×10^6 type Ia: 3.3×10^6 versus. 2.1×10^6 type II: 4.3×10^6 versus. 2.1×10^6), the effect of sampling depth was not significant.

Gene copy numbers of *mcrA*-genes were correlated with both single MOB-deriving gene abundances ($R^2 = 0.670$, $p < 0.001$ for type Ia; $R^2 = 0.348$, $p < 0.001$ for type II; Figure 5a,b) and to the cumulative MOB gene copy numbers ($R^2 = 0.594$, $p < 0.001$ Figure 5c), forming a LOG–LOG relationship. Similarly, *mcrA*-gene copy numbers showed a positive LOG–LOG correlation with PMP rates ($R^2 = 0.394$, $p < 0.001$, Figure 5d). A correlation between PMO rates and both MOB-related gene abundances was not detected (Figure 5e,f).

Cumulative MOB gene copy numbers were significantly higher in upper sediment layers of each sample (paired Student's *t* test, $p < 0.01$, Figure S5, Appendix S1), although the difference was only marginal.

Gene abundances of MA and cumulative MOB differed among sampled streams (Kruskal–Wallis $\chi^2 = 59$ and 46, $p < 0.05$), with higher numbers in streams draining larger catchment areas (linear model, $p < 0.05$; Table S6, Appendix S2). Discharge correlated positively with catchment area and was therefore not considered as potential predictor. Within streams, the number of MA gene copies was positively related to sediment organic carbon content and sediment surface area, while MOB gene copies were positively related with sediment organic carbon content (Table S6, Appendix S2). Overall, the increasing explanatory power of GLMMs due to the inclusion of site-scale variables (increasing R^2, from 0.55 to 0.65 for MA and

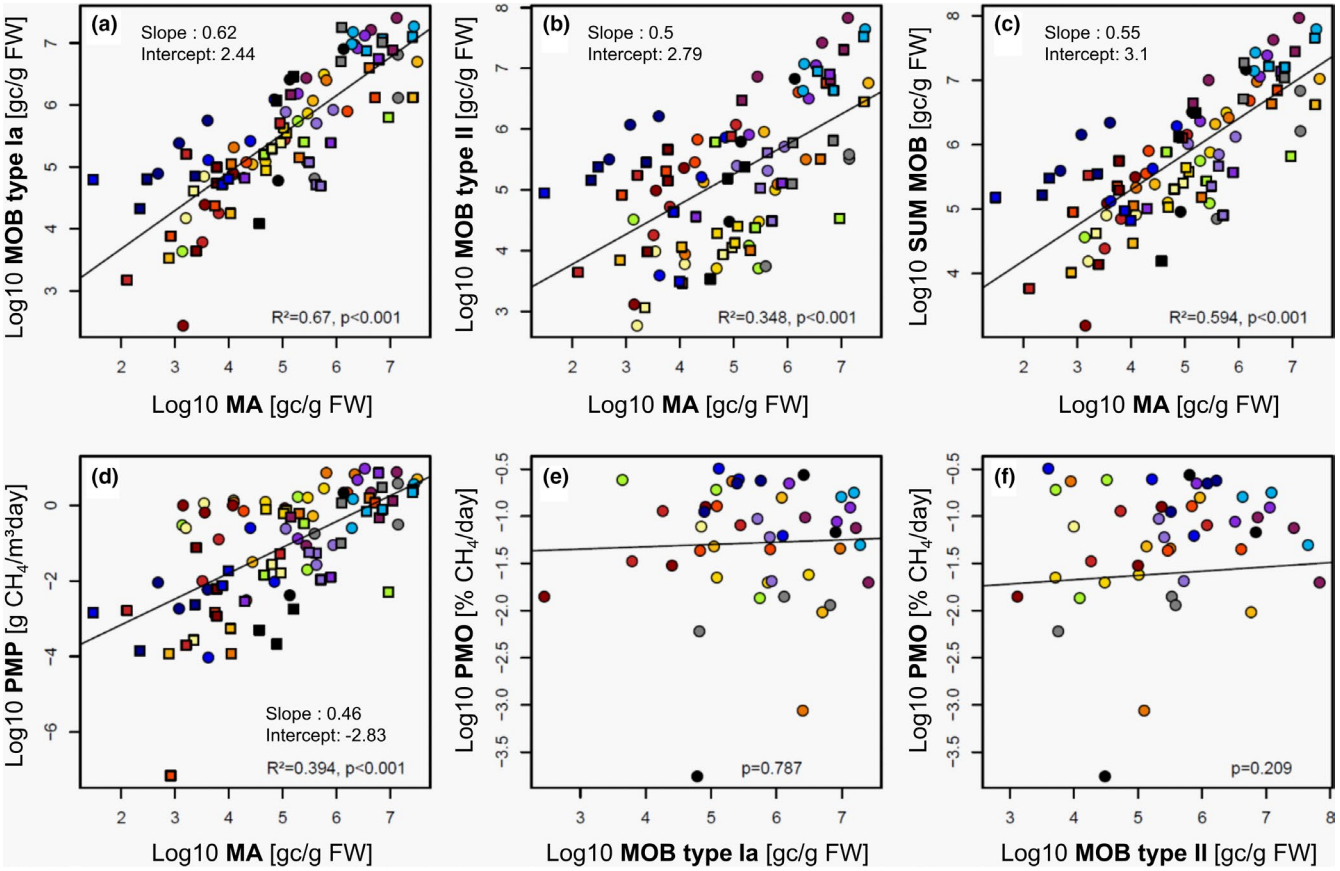

FIGURE 5 Correlations of log-transformed mcrA-gene abundances of methanogenic archaea and type Ia MOB (a), type II MOB (b), cumulative MOB (c) and potential methane production rates (PMP) (d). Relation of type Ia (e) and type II MOB (f) and potential methane oxidation rates (PMO). MOB = methane-oxidizing bacteria. MA = methanogenic archaea. Colours refer to sampled streams described in Figure 2, circles to sediments sampled at 0–3 cm depth and squares to sediments sampled at 6–9 cm depth. Slope and intercept of the fitted lines are only reported for significant ($p < 0.05$) relationships

from 0.44 to 0.54 for MOB; Table S6, Appendix S2) indicated positive correlations between gene copies and organic carbon content and/or surface area within streams, while the overall gene copy number differed among streams. No other parameter showed significant relationships with response measures, but nitrogen content was significantly correlated with organic carbon content and was therefore excluded from the model.

4 | DISCUSSION

4.1 | Environmental constraints

A major interest in microbial ecology is the identification of biogeography, shaped by processes such as habitat filtering, dispersal, drift and mutation. In that context, we demonstrate a biogeographic pattern of methanotrophic and methanogenic communities associated with geographic dispersal and environmental influences, identify dominant taxa within each functional group, and compare the absolute abundance of MA and MOX with their potential activities within 16 stream sediments across a latitudinal and longitudinal distance of 2'700 km. Streams were separated in two groups based on environmental conditions (first PCA component, Figure 2). '**Environment 1'** represents warm streams with large stream areas, high conductivity and low surface water oxygen concentrations, draining catchments with high proportions of agricultural and urban land cover . In contrast, '**Environment 2'** is cold, medium- to small-sized streams with low conductivity and pH, high surface water oxygen concentrations and less agricultural and urban land use within their catchment (Figure S4, Appendix S1). These two most diverging environments should be kept in mind for the following discussion, which evaluates if these encountered habitat diversities are mirrored in MA and MOX biogeography.

4.2 | MA and MOX biogeography and diversity

4.2.1 | Methanogenic archaea

The four dominating MA families were comparable to those found in other sediment-related studies (Mach et al., 2015): *Methanoregulaceae* are ubiquitous and abundant in many habitats (Yang et al., 2017). They perform hydrogenotrophic methanogenesis similar to *Methanobacteriaceae*, the dominant archaeal group within lake ecosystems (Fan & Xing, 2016). Across the studied streams, relative abundances of *Methanosarcinaceae* and *Methanosaetaceae* were negatively correlated, probably due to their shared capacity to perform acetoclastic methanogenesis and the resulting competition for the same niche. Of these, relative abundance of *Methanosarcinaceae* was higher in southern sampling sites, probably due to their versatile metabolic capabilities that allow them to adapt to the presence of other substrates besides acetate (Nazaries et al., 2013). Furthermore, they likely experience growth advantages over *Methanosaetaceae*, as acetate has been shown to be a major precursor of CH_4 particularly under low-temperature conditions (Nozhevnikova et al., 2007).

The higher MA diversity and richness (Figure S2a, Appendix S1) at higher temperatures and larger catchment areas are probably due to a higher variability in nutrient sources and niches to be exploited. Similarly, lower anthropogenic influence generally limits the nutrient input into streams (Withers & Lord, 2002), explaining the overall lower diversity and richness of MA in streams with higher natural catchment proportions.

4.2.2 | Methane-oxidizing microorganisms

In accordance with previous studies, the predominant family of MOX across European streams was represented by *Methylococcaceae* (Costello et al., 2002), whereas a considerable number of OTUs (30) was unassigned *Methylococcales* (Figure 3). The order and the family are both type I MOB, while *Methylobacteriaceae*, the second most abundant family, is a representative of type II MOB, each type inhabiting a different niche. The general predominance of type I over type II MOB in freshwater sediments is consistent with previous findings (Costello et al., 2002). In contrast, the increased relative abundances of type II over type I MOB applied to all Spanish and Austrian samples (and GBR_1_1) was also reflected in the MOX community since the aforementioned streams clustered separately in the NMDS (Figure S3b, Appendix S1). For Spanish sites within mostly agricultural catchments, this might be explained by a potential eutrophication favouring type II MOB (Yang et al., 2019). Next to the aerobic type I and type II MOB, anaerobic CH_4-oxidizing archaeal *Cd*. Methanoperedens occupied anaerobic niches as corroborated by their higher abundance in deeper sediment layers. Deeper layers are typically supplied with less oxygen than the layers at the sediment-water interface, which also explains the higher abundance of the second anaerobic MOX representative, *Cd*. Methylomirabilis. Accordingly, *Cd*. Methanoperedens seems to benefit from higher surface areas (i.e. smaller particle sizes), leading to more anaerobic niches within those sites.

The diversity of MOX was mainly correlated with variables describing stream size (e.g. wetted stream width, stream area) and geographical latitude, with larger, southern streams exhibiting a higher diversity, probably due to a higher spatiotemporal variability in nutrients inputs of such streams draining larger catchments (Wilhelm et al., 2015).

4.3 | Climate and land use drive methanogenic and methanotrophic community compositions

4.3.1 | Methanogenic archaea

Compared to MOX, MA showed a more homogeneous distribution across European streams, although PERMANOVA confirmed that there were significant differences among sampled streams. On

the one hand, 'environment 1' streams showed MA communities mostly harbouring hydrogenotrophic members (*Methanospirillaceae* and *Methanobacteriaceae*) and the metabolically and physiologically versatile *Methanosarcinaceae*, which were negatively correlated with geographical latitude. On the other hand, acetoclastic *Methanosaetaceae* and hydrogenotrophic *Methanocellaceae* occurred in 'environment 2' streams (Figure S4, Appendix S1). The occurrence of methanogens in partly oxygenated soils and sediment has been acknowledged in upland soils (Angel et al., 2011), wetland sediments (Angle et al., 2017; Steinle et al., 2017) and lakes (Grossart et al., 2011) and in many cases they are dominated by the order *Methanocella*, due to its ability to detoxify reactive oxygen species (Angel et al., 2011).

Land use and land cover changes generally increased over the past decades and are mainly attributed to conversion of natural ecosystems to agricultural or urban areas (Hurtt et al., 2011). In that context, our results suggest that an ongoing increase of anthropogenic catchment alteration might result in altered MA communities with increased abundances of species characteristic for the defined 'environment 1'. Due to their diverse metabolic capacities and since their metabolic activity depends on the type and quantity of present substrates, altered CH_4-production rates are difficult to estimate. Our results suggest, however, that increasing stream temperatures lead to higher abundances of methanogens that use CO_2 and H_2 as substrates, a highly efficient CH_4-production pathway (Lackner et al., 2018). On the other hand, relative abundances of *Methanocellaceae* and *Cd*. Methanoflorentaceae, the latter being a hydrogenotrophic group dominating partially thawed and cold environments (Mondav et al., 2014), typically decrease with increasing stream temperatures, and might, thus, be negatively impacted by climate change.

Irrespective of water temperature and human impact, sediments of high-discharge streams featuring large catchments ('environment 3'; Figure S4, Appendix S1) harboured a high proportion of the methanogenic family *Methanoregulaceae*, dominated by the genera *Methanolinea* and *Methanoregula*. The large catchment areas may provide more diverse nutrients, promoting the aforementioned genera. In addition, the family *Methanoregulaceae* is used as a proxy for freshwater influence in the marine realm (Yang et al., 2017). Since the occurrences of this family were higher in high-discharge streams, *Methanoregulaceae* might be an indicator family of fresh water supply also in streams.

4.3.2 | Methane-oxidizing microorganisms

As the major biological sink for CH_4, MOX attenuate the rivers' CH_4 production within the water column and the sediment (Shelley et al., 2015). In this study, MOX communities were more distinct among streams than MA communities (Figure S3, Appendix S1). In addition, the sampling depth influenced the species composition, most probably due to the changed oxygen supply. Indeed, redundancy analysis identified oxygen as important environmental parameter shaping the MOX community composition. Typical representatives of oxygen-rich 'environment 2' streams were *Methyloglobulus* spp. and other representatives of the family *Methylococcaceae* (Figure 4), all belonging to type I MOB, performing the ribulose monophosphate pathway for carbon assimilation and requiring oxygen for CH_4 activation (Kits et al., 2015). Oshkin et al. (2014) showed that type I MOB dominate cold floodplains of Siberian rivers and feature a large proportion of psychrotolerant methanotrophs, which fits to their higher abundance in the 'environment 2'. MOX utilize CH_4 as their sole carbon and energy source at the sediment-water interface when oxygen from bottom waters is available as electron acceptor. In case of oxygen depletion and the presence of alternative electron acceptors, methane oxidation can be performed by anaerobically (ANME). The redox state, driven significantly by oxygen concentration, is a major environmental factor influencing microbial activity and diversity. ANME is mostly coupled to the reduction of iron, manganese, sulphate and nitrate (Boetius et al., 2000). Interestingly, *Cd*. Methanoperedens was also a typical representative of oxygen-rich environments in this study, although it is an ANME methanotroph mediating nitrate-dependent anaerobic CH_4 oxidation. It featured, however, higher abundances in the deeper sediment layer. This genus can counteract oxidative damage and adapt to regular oxygen exposure (Guerrero-Cruz et al., 2018).

Referring to the generally ongoing land use changes, increasing the agricultural and urban land cover in many European stream catchments (Hurtt et al., 2011), together with the accelerated warming of stream water, the here presented MOX community of 'environment 1' may gain importance in the future. This finding is supported by a recent study postulating that climate controls microbial functional gene diversity in streams at large spatial scales (Picazo et al., 2020). However, 'environment 1' did not harbour any conspicuous MOX except a few representatives of *Cd*. Methylomirabilis and of the genus *Methylogobulus* (*Methylococcaceae*), probably reflecting the importance of other drivers that we did not measure. Rather, MOX communities formed an additional cluster including high-order and high discharge streams draining large catchments ('environment 3'; Figure S4, Appendix S1). This environment is preferentially inhabited by *Methylocaldum* spp., a genus able to fix CO_2 in addition to CH_4 (Group X), and *Crenothrix* spp., an important type I MOB described in Swiss lakes (Oswald et al., 2017).

4.4 | Gene abundances and their relation to PMO and PMP

The logarithmic relationship between MA and MOB gene copies suggests a close dependency of CH_4-oxidizing bacteria with the occurrence of methane-producing archaea (Figure 5). However, type I MOB showed a higher dependency on the occurrence of MA than type II MOB. One possible explanation is that some representatives of type II MOB (e.g. *Methylocystis* and all *Methylobacteriaceae)* are facultative methanotrophs and capable of growing on carbon sources other than CH_4 (Dedysh & Dunfield, 2011), while sufficient CH_4 availability is a prerequisite for the proliferation of type I MOB. Further, the 'low-affinity' CH_4 oxidation kinetics of type I methanotrophs, enabling

high oxidation of CH_4 at concentrations well above atmospheric levels might additionally explain this different relationship. In contrast, type II MOB has their niche in resource limited habitats (Cai et al., 2016).

According to the GLMM, organic carbon supply and thus nutrient availability within streams is positively related to the abundance of both, MA and MOB, while MA abundance additionally depends on sediment surface area. The latter dependency may reflect the general affinity of MA to anaerobic microhabitats formed to a higher degree in fine sediments (Higashino, 2013). The significant positive relationship between gene abundance and catchment area indicates that streams draining larger catchments receive more diverse nutrient species and provide higher nutrient availability and number of present niches for a wider range of organisms (Kosek et al., 2019).

Across European stream sediments, gene abundances of MA showed a significant positive correlation with PMP rates (Figure 5d), clearly linking the microbial abundances to its function by forming a LOG–LOG relationship. However, a slope of <1 suggests that with more methanogenic gene copies, the PMP is slightly lower as compared to smaller gene copy numbers. Thus, increased gene copy numbers within the investigated environmental DNA are not linearly correlated with activity. This is most probably due to extracellular DNA being produced with increasing activity, and/or due to changing counts of *mcrA*-gene copies in the genome of different MA species (Nagler et al., 2018). Similarly, Mach et al. (2015) were not able to link PMP and *mcrA*-gene copy numbers in river sediments due to a regulation of PMP on the MA RNA or activity level rather than their absolute abundance.

In contrast to these findings, no significant relationship was found between PMO rates and MOB gene abundances. This finding, however, must be interpreted with care as not all MOX have been targeted with the qPCR and type Ib MOB (mostly represented by *Methylocaldum* spp. and *Cd*. Methanoperedens) have not been quantified although they might represent an important share of all MOB according to the sequencing results. Besides this, there are several possible explanations for a lack of a clear relationship between PMO and MOB: (a) RNA or activity level of MOB might be a better indicator than absolute abundance (Mach et al., 2015), (b) alternative pathways might be carried out to gain energy since many MOB are non-obligatory CH_4 oxidizers, (c) current methods are unable to distinguish aerobic from anaerobic PMO, while the sediment composition might lead to a higher proportion of either aerobic or anaerobic PMO through differences in oxygen availability (Higashino, 2013). Hence, the different pathways and efficiencies of aerobic and anaerobic PMO might not allow a simple relationship between abundance and PMO.

4.5 | Conclusions

Our results demonstrate that the methanogenic and methanotrophic communities of the investigated European streams mainly group into three habitat types characterized by different abiotic conditions and catchment characteristics. Such distinguishable microbial communities suggest, that future climate- and land use changes may influence the prevailing microbes involved in the large-scale stream-related CH_4 cycle. Increasing water temperatures as consequence of climate change in combination with agricultural intensification and urban land use might thereby lead to higher abundances of highly efficient hydrogenotrophic CH_4 producers (i.e. *Methanospirillaceae*, *Methanobacteriaceae* and *Methanosarcinaceae*), while the expected changes for CH_4 consumers are less clear and seem to be more dependent on site specificities. In that context, this study gives a first overview of MA and MOX biogeographical patterns in stream sediments. However, additional in-depth studies are needed to further affirm our findings. The links between sediment organic carbon content and MA/MOB abundance, and between MA abundances and PMP rates emphasize the importance of nutrient input for the CH_4 cycle in streams, with potential consequences for the overall CH_4 emissions from running waters. While many previous studies highlighted the general importance of nutrient effects on CH_4 cycling (reviewed by Stanley et al., 2016), our results suggest, that these effects are mediated by changes within the microbial communities, whose composition and activity regulate this cycle.

ACKNOWLEDGEMENTS

We thank Jihyeon Kim, Christian Noss, Merlin Rosner and Haiying Xia for their support during the campaign preparations, laboratory work and raw data processing. Furthermore, we thank Sebastian Hupfauf, Andreas Lorke and Jeremy Wilkinson for their input regarding bioinformatics, study design and technical questions. The authors declare no conflict of interest. This study was financially supported by the German Research Foundation (grant BO 5050/1-1).

DATA AVAILABILITY STATEMENT

The datasets supporting the conclusions of this article are available in the NCBI repository under BioProject PRJNA578023, BioSample accessions from SAMN13046387 to SAMN13046482 and SRA IDs from 13,046,387 to 13,046,482 respectively (https://www.ncbi.nlm.nih.gov/sra/PRJNA578023). Sampling was conducted in compliance with collecting permits that applied for the various countries.

ORCID

Magdalena Nagler https://orcid.org/0000-0002-4165-7290

REFERENCES

Angel, R., Claus, P., & Conrad, R. (2011). Methanogenic archaea are globally ubiquitous in aerated soils and become active under wet anoxic conditions. *The Isme Journal*, *6*, 847. https://doi.org/10.1038/ismej.2011.141

Angle, J. C., Morin, T. H., Solden, L. M., Narrowe, A. B., Smith, G. J., Borton, M. A., Rey-Sanchez, C., Daly, R. A., Mirfenderesgi, G., Hoyt, D. W., Riley, W. J., Miller, C. S., Bohrer, G., & Wrighton, K. C. (2017). Methanogenesis in oxygenated soils is a substantial fraction of wetland methane emissions. *Nature Communications*, *8*, 1567. https://doi.org/10.1038/s41467-017-01753-4

Bates, D., Mächler, M., Bolker, B., & Walker, S. (2015). Fitting linear mixed-effects models using lme4. *Journal of Statistical Software*, *67*, 1–48.

Bednařík, A., Blaser, M., Matoušů, A., Hekera, P., & Rulík, M. (2017). Effect of weir impoundments on methane dynamics in a river. *Science of the Total Environment*, *584–585*, 164–174. https://doi.org/10.1016/j.scitotenv.2017.01.163

Bodmer, P., Attermeyer, K., Pastor, A., & Catalán, N. (2019). Collaborative projects: Unleashing early career scientists' power. *Trends in Ecology & Evolution*, *34*, 871–874. https://doi.org/10.1016/j.tree.2019.07.016

Bodmer, P., Wilkinson, J., & Lorke, A. (2020). Sediment properties drive spatial variability of potential methane production and oxidation in small streams. *Journal of Geophysical Research: Biogeosciences*, *125*. https://doi.org/10.1029/2019JG005213

Boetius, A., Ravenschlag, K., Schubert, C. J., Rickert, D., Widdel, F., Gieseke, A., Amann, R., Jørgensen, B. B., Witte, U., & Pfannkuche, O. (2000). A marine microbial consortium apparently mediating anaerobic oxidation of methane. *Nature*, *407*, 623–626. https://doi.org/10.1038/35036572

Bravo, A. G., Kothawala, D. N., Attermeyer, K., Tessier, E., Bodmer, P., Ledesma, J. L. J., Audet, J., Casas-Ruiz, J. P., Catalán, N., Cauvy-Fraunié, S., Colls, M., Deininger, A., Evtimova, V. V., Fonvielle, J. A., Fuß, T., Gilbert, P., Herrero Ortega, S., Liu, L., Mendoza-Lera, C., … Amouroux, D. (2018). The interplay between total mercury, methylmercury and dissolved organic matter in fluvial systems: A latitudinal study across Europe. *Water Research*, *144*, 172–182. https://doi.org/10.1016/j.watres.2018.06.064

Cai, Y., Zheng, Y., Bodelier, P. L. E., Conrad, R., & Jia, Z. (2016). Conventional methanotrophs are responsible for atmospheric methane oxidation in paddy soils. *Nature Communications*, *7*, 11728. https://doi.org/10.1038/ncomms11728

Caporaso, J. G., Lauber, C. L., Walters, W. A., Berg-Lyons, D., Lozupone, C. A., Turnbaugh, P. J., Fierer, N., & Knight, R. (2011). Global patterns of 16S rRNA diversity at a depth of millions of sequences per sample. *Proceedings of the National Academy of Sciences*, *108*, 4516–4522. https://doi.org/10.1073/pnas.1000080107

Chaudhary, P. P., Rulík, M., & Blaser, M. (2017). Is the methanogenic community reflecting the methane emissions of river sediments?—comparison of two study sites. *MicrobiologyOpen*, *6*, e00454.

Ciais, P., Sabine, C., Bala, G., Bopp, L., Brovkin, V., Canadell, J., Thornton, P. (2013) Carbon and other biogeochemical cycles. In T. F. Stocker, D. Qin, G.-K. Plattner, M. Tignor, S. K. Allen, J. Boschung, & P. M. Midgley (Eds), *Climate Change 2013: The physical science basis. Contribution of Working Group I to the Fifth Assessment Report of the Intergovernmental Panel on Climate Change*. Intergovernmental Panel on Climate Change.

Costello, A. M., Auman, A. J., Macalady, J. L., Scow, K. M., & Lidstrom, M. E. (2002). Estimation of methanotroph abundance in a freshwater lake sediment. *Environmental Microbiology*, *4*, 443–450.

Crawford, J. T., Loken, L. C., West, W. E., Crary, B., Spawn, S. A., Gubbins, N., & Stanley, E. H. (2017). Spatial heterogeneity of within-stream methane concentrations. *Journal of Geophysical Research: Biogeosciences*, *122*, 1036–1048.

Crevecoeur, S., Ruiz-González, C., Prairie, Y. T., & del Giorgio, P. A. (2019). Large-scale biogeography and environmental regulation of methanotrophic bacteria across boreal inland waters. *Molecular Ecology*, *28*, 4181–4196.

Dedysh, S. N., & Dunfield, P. F. (2011). Chapter three - facultative and obligate methanotrophs: How to identify and differentiate them. In A. C. Rosenzweig & S. W. Ragsdale (Eds.), *Methods in Enzymology* (pp. 31–44). Academic Press.

Etminan, M., Myhre, G., Highwood, E. J., & Shine, K. P. (2016). Radiative forcing of carbon dioxide, methane, and nitrous oxide: A significant revision of the methane radiative forcing. *Geophysical Research Letters*, *43*, 12614–12623.

Ettwig, K. F., Butler, M. K., Le Paslier, D., Pelletier, E., Mangenot, S., Kuypers, M. M. M., & Strous, M. (2010). Nitrite-driven anaerobic methane oxidation by oxygenic bacteria. *Nature*, *464*, 543.

Fan, X., & Xing, P. (2016). Differences in the Composition of archaeal communities in sediments from contrasting zones of Lake Taihu. *Frontiers in Microbiology*, *7*.

Grossart, H.-P., Frindte, K., Dziallas, C., Eckert, W., & Tang, K. W. (2011). Microbial methane production in oxygenated water column of an oligotrophic lake. *Proceedings of the National Academy of Sciences of the United States of America*, *108*, 19657–19661.

Guerrero-Cruz, S., Cremers, G., van Alen, T. A., Op den Camp, H. J. M., Jetten, M. S. M., & Vaksmaa, A. (2018). Response of the anaerobic methanotroph *Candidatus* methanoperedens nitroreducens" to oxygen stress. *Applied and Environmental Microbiology*, *84*, e01832–e1918.

Higashino, M. (2013). Quantifying a significance of sediment particle size to hyporheic sedimentary oxygen demand with a permeable stream bed. *Environmental Fluid Mechanics*, *13*, 227–241.

Hupfauf, S., Etemadi-Shalamzari, M., Fernández-Delgado Juárez, M., Gómez-Brandón, M., Insam, H., & Podmirseg, S. M. (2020). CoMA – an intuitive and user-friendly pipeline for amplicon-sequencing data analysis. *Plos ONE*. Available at: https://www.uibk.ac.at/microbiology/services/coma.html accessed 29.10.2020. https://doi.org/10.1371/journal.pone.0243241.

Hurtt, G. C., Chini, L. P., Frolking, S., Bett, R. A., Feddema, J., Fischer, G., & Wang, Y. P. (2011). Harmonization of land-use scenarios for the period 1500–2100: 600 years of global gridded annual land-use transitions, wood harvest, and resulting secondary lands. *Climatic Change*, *109*, 117–161.

Jaeger, B. (2017) 2glmm: Computes R Squared for Mixed (Multilevel) Models.

Kalyuzhnaya, M. G., Gomez, O. A., & Murrell, J. C. (2019). The Methane-oxidizing bacteria (Methanotrophs). In T. J. Mcgenity (Ed.), *Taxonomy, Genomics and Ecophysiology of Hydrocarbon-Degrading Microbes* (pp. 1–34). Springer International Publishing.

Kassambra, A. (2018) ggpubr: "ggplot2" Based Publication Ready Plots.

Kassambra, A., & Mundt, F. (2017) factoextra: Extract and Visualize the Results of Multivariate Data Analyses.

Kits, K. D., Campbell, D. J., Rosana, A. R., & Stein, L. Y. (2015). Diverse electron sources support denitrification under hypoxia in the obligate methanotroph Methylomicrobium album strain BG8. *Frontiers in Microbiology*, *6*.

Kolb, S., Knief, C., Stubner, S., & Conrad, R. (2003). Quantitative detection of methanotrophs in soil by novel pmoA-targeted real-time PCR assays. *Applied and Environmental Microbiology*, *69*, 2423–2429.

Kosek, K., Luczkiewicz, A., Kozioł, K., Jankowska, K., Ruman, M., & Polkowska, Ż. (2019). Environmental characteristics of a tundra river system in Svalbard. Part 1: Bacterial abundance, community structure and nutrient levels. *Science of the Total Environment*, *653*, 1571–1584.

Lackner, N., Hintersonnleitner, A., Wagner, A. O., & Illmer, P. (2018). Hydrogenotrophic methanogenesis and autotrophic growth of *Methanosarcina thermophila*. *Archaea*, *2018*, 4712608.

Lê, S., Josse, J., & Husson, F. (2008). FactoMineR: An R package for multivariate analysis. *Journal of Statistical Software*, *1*(1).

Mach, V., Blaser, M. B., Claus, P., Chaudhary, P. P., & Rulík, M. (2015). Methane production potentials, pathways, and communities of methanogens in vertical sediment profiles of river Sitka. *Frontiers in Microbiology*, *6*.

Machalett, B., Oches, E. A., Frechen, M., Zöller, L., Hambach, U., Mavlyanova, N. G., & Endlicher, W. (2008). Aeolian dust dynamics in central Asia during the Pleistocene: Driven by the long-term migration, seasonality, and permanency of the Asiatic polar front. *Geochemistry, Geophysics, Geosystems*, *9*, https://doi.org/10.1029/2007GC001938

Mondav, R., Woodcroft, B. J., Kim, E.-H., McCalley, C. K., Hodgkins, S. B., Crill, P. M., & Tyson, G. W. (2014). Discovery of a novel methanogen prevalent in thawing permafrost. *Nature Communications*, *5*, 3212.

Nagler, M., Podmirseg, S. M., Griffith, G. W., Insam, H., & Ascher-Jenull, J. (2018). The use of extracellular DNA as a proxy for specific microbial activity. *Applied Microbiology and Biotechnology*, *102*, 2885–2898.

Nakagawa, S., & Schielzeth, H. (2012). A general and simple method for obtaining R^2 from generalized linear mixed-effects models. *Methods in Ecology and Evolution*, *4*, 133–142.

Nazaries, L., Murrell, J. C., Millard, P., Baggs, L., & Singh, B. K. (2013). Methane, microbes and models: Fundamental understanding of the soil methane cycle for future predictions. *Environmental Microbiology*, *15*, 2395–2417.

Nozhevnikova, A. N., Nekrasova, V., Ammann, A., Zehnder, A. J. B., Wehrli, B., & Holliger, C. (2007). Influence of temperature and high acetate concentrations on methanogenensis in lake sediment slurries. *FEMS Microbiology Ecology*, *62*, 336–344.

Oksanen, J., Blanchet, F. G., Friendly, M., Kindt, R., Legendre, P. D. M., Minchin, P. R., O'Hara, B., Simpson, G. L., Solymos, P., Stevens, H., & Wagner, H. (2019). vegan: Community Ecology Package.

Oshkin, I. Y., Wegner, C. C. L., Glagolev, M. V., Fillipov, I. V., Pimenov, N. V., Liesack, W., & Dedysh, S. N. (2014). Gammaproteobacterial methanotrophs dominate cold methane seeps in floodplains of West Siberian Rivers. *Microbial Ecology*, *80*, 5944–5954.

Oswald, K., Graf, J. S., Littmann, S., Tienken, D., Brand, A., Wehrli, B., & Milucka, J. (2017). Crenothrix are major methane consumers in stratified lakes. *The Isme Journal*, *11*, 2124.

Oswald, K., Milucka, J., Brand, A., Littmann, S., Wehrli, B., Kuypers, M. M. M., & Schubert, C. J. (2015). Light-Dependent Aerobic methane oxidation reduces methane emissions from seasonally stratified lakes. *PLoS One*, *10*, e0132574.

Picazo, F., Vilmi, A., Aalto, J., Soininen, J., Casamayor, E. O., Liu, Y., & Wang, J. (2020). Climate mediates continental scale patterns of stream microbial functional diversity. *Microbiome*, *8*, 92.

Praeg, N., Schwinghammer, L., & Illmer, P. (2020). Larix decidua and additional light affect the methane balance of forest soil and the abundance of methanogenic and methanotrophic microorganisms. *FEMS Microbiology Letters*, *366*.

R Core Team (2018). *R: A language and environment for statistical computing*. R Foundation for Statistical Computing.

Schloss, P. D., Westcott, S. L., Ryabin, T., Hall, J. R., Hartmann, M., Hollister, E. B., & Weber, C. F. (2009). Introducing mothur: Open-Source, platform-independent, community-supported software for describing and comparing microbial communities. *Applied and Environmental Microbiology*, *75*, 7537–7541.

Shelley, F., Abdullahi, F., Grey, J., & Trimmer, M. (2015). Microbial methane cycling in the bed of a chalk river: Oxidation has the potential to match methanogenesis enhanced by warming. *Freshwater Biology*, *60*, 150–160.

Šmilauer, P., & Lepš, J. (2014). *Multivariate Analysis of Ecological Data using CANOCO 5* (2nd ed.). Cambridge University Press.

Stanley, E. H., Casson, N. J., Christel, S. T., Crawford, J. T., Loken, L. C., & Oliver, S. K. (2016). The ecology of methane in streams and rivers: Patterns, controls, and global significance. *Ecological Monographs*, *86*, 146–171. https://doi.org/10.1890/15-1027

Steinle, L., Maltby, J., Treude, T., Kock, A., Bange, H. W., Engbersen, N., Zopfi, J., Lehmann, M. F., & Niemann, H. (2017). Effects of low oxygen concentrations on aerobic methane oxidation in seasonally hypoxic coastal waters. *Biogeosciences*, *14*, 1631–1645. https://doi.org/10.5194/bg-14-1631-2017

Steinle, L., Schmidt, M., Bryant, L., Haeckel, M., Linke, P., Sommer, S., & Niemannn, H. (2016). Linked sediment and water-column methanotrophy at a man-made gas blowout in the North Sea: Implications for methane budgeting in seasonally stratified shallow seas. *Limnology and Oceanography*, *61*, S367–S386.

Strahler, A. N. (1952). Hypsometric (area-altitude) analysis of erosional topography. *GSA Bulletin*, *63*, 1117–1142.

Su, G., Niemann, H., Steinle, L., Zopfi, J., & Lehmann, M. F. (2019). Evaluating radioisotope-based approaches to measure anaerobic methane oxidation rates in lacustrine sediments. *Limnology and Oceanography: Methods*, *17*, 429–438.

Trimmer, M., Shelley, F. C., Purdy, K. J., Maanoja, S. T., Chronopoulou, P.-M., & Grey, J. (2015). Riverbed methanotrophy sustained by high carbon conversion efficiency. *The ISME Journal*, *9*, 2304–2314. https://doi.org/10.1038/ismej.2015.98

Wei, T., Simko, V., Levy, M., Xie, Y., Jin, Y., & Zemla, J. (2017). Corrplot: Visualisation of a Correlation Matrix.

Wilhelm, L., Besemer, K., Fragner, L., Peter, H., Weckwerth, W., & Battin, T. J. (2015). Altitudinal patterns of diversity and functional traits of metabolically active microorganisms in stream biofilms. *The Isme Journal*, *9*, 2454. https://doi.org/10.1038/ismej.2015.56

Wilkinson, J., Bodmer, P., & Lorke, A. (2019). Methane dynamics and thermal response in impoundments of the Rhine River, Germany. *Science of the Total Environment*, *659*, 1045–1057. https://doi.org/10.1016/j.scitotenv.2018.12.424

Withers, P. J. A., & Lord, E. I. (2002). Agricultural nutrient inputs to rivers and groundwaters in the UK: Policy, environmental management and research needs. *Science of the Total Environment*, *282–283*, 9–24. https://doi.org/10.1016/S0048-9697(01)00935-4

Yang, S., Liebner, S., Winkel, M., Alawi, M., Horn, F., Dörfer, C., & Wagner, D. (2017). In-depth analysis of core methanogenic communities from high elevation permafrost-affected wetlands. *Soil Biology and Biochemistry*, *111*, 66–77.

Yang, Y., Chen, J., Tong, T., Li, B., He, T., Liu, Y., & Xie, S. (2019). Eutrophication influences methanotrophic activity, abundance and community structure in freshwater lakes. *Science of the Total Environment*, *662*, 863–872.

BIOSKETCH

Magdalena Nagler is an early career postdoctoral microbiologist interested in the description of microbial biogeographical patterns with a special focus on anaerobic pro- and eukaryota including methanogenic archaea and anaerobic fungi. Furthermore, she studies the influence of extracellular DNA on the indicator quality of environmental DNA in ecological assessments.

Author contribution: MN analysed the DNA samples, performed bioinformatics and statistics and wrote the major part of the manuscript, NP performed laboratory work, performed bioinformatics and statistics, helped with the interpretation of the results and wrote parts of the manuscript, GHN and NC performed statistical tests and wrote parts of the manuscript, KA generated the conceptual figures and gave major inputs to the manuscript, BM performed laboratory analyses, LS performed laboratory analyses and wrote parts of the manuscript, PG performed language editing, and PB coordinated the project, was responsible for the study design, wrote major parts of the manuscript and discussed and interpreted the results. Besides NP, BM and LS, all authors selected sites, participated in the sampling campaign and data collection, and contributed to the different versions of the manuscript

SUPPORTING INFORMATION

Additional supporting information may be found online in the Supporting Information section.

How to cite this article: Nagler M, Praeg N, Niedrist GH, et al. Abundance and biogeography of methanogenic and methanotrophic microorganisms across European streams. *J Biogeogr*. 2020;00:1–14. https://doi.org/10.1111/jbi.14052

Substantial carbon dioxide flux changes from day to night across European streams

Katrin Attermeyer[1,2,3], Joan Pere Casas-Ruiz[4,5], Thomas Fuss[6], Ada Pastor[4,5,7], Sophie Cauvy-Fraunié[8], Danny Sheath[9,10], Anna C. Nydahl[1], Alberto Doretto[11,12], Ana Paula Portela[13,14], Brian C. Doyle[15], Nikolay Simov[16], Catherine Gutmann Roberts[9], Georg H. Niedrist[17], Xisca Timoner[4,5], Vesela Evtimova[18], Laura Barral-Fraga[5], Tea Bašić[9,19], Joachim Audet[20,21], Anne Deininger[22,23], Georgina Busst[9], Stefano Fenoglio[12,24], Núria Catalán[4,5,25], Elvira de Eyto[26], Francesca Pilotto[22,27], Jordi-René Mor[4,28], Juliana Monteiro[29], David Fletcher[9], Christian Noss[30], Miriam Colls[4,5], Magdalena Nagler[31], Liu Liu[30,32], Clara Romero González-Quijano[6], Ferran Romero[4,5], Nina Pansch[32], José L. J. Ledesma[20,33], Josephine Pegg[9,34], Marcus Klaus[22,35], Anna Freixa[4,5], Sonia Herrero Ortega[32], Clara Mendoza-Lera[8], Adam Bednařík[36], Jérémy A. Fonvielle[32], Peter Gilbert[37], Lyubomir A. Kenderov[38], Martin Rulík[36], Pascal Bodmer[30,39,40]*

1 Limnology/Department of Ecology and Genetics, Uppsala University, 75236 Uppsala, Sweden

2 WasserCluster Lunz, 3293 Lunz am See, Austria

3 Department of Functional and Evolutionary Ecology, University of Vienna, 1090 Vienna, Austria

4 Catalan Institute for Water Research (ICRA), 17003 Girona, Spain

5 Department of Environmental Sciences, University of Girona (UdG), 17003 Girona, Spain

6 Ecohydrology, Leibniz-Institute of Freshwater Ecology and Inland Fisheries (IGB), 12587 Berlin, Germany

7 current address: Department of Biology, Aarhus University, 8000 Aarhus C, Denmark

8 INRAE, UR Riverly, Centre de Lyon-Villeurbanne, Villeurbanne Cedex, France

9 Department of Life and Environmental Sciences, Bournemouth University, BH12 5BB, UK

10 current address: Institute of Global Health, Faculty of Medicine, University of Geneva, Campus Biotech, 1211 Geneva, Switzerland

11 Department of Sciences and Technological Innovation, University of Piemonte Orientale, 15121 Alessandria, Italy

12 ALPSTREAM – Alpine Stream Research Center, 12030 Ostana, Italy

13 Research Centre in Biodiversity and Genetic Resources (CIBIO-InBIO), University of Porto, 4485-661 Vila do Conde, Portugal

14 Faculty of Sciences, University of Porto, 4169-007 Porto, Portugal

15 Centre for Freshwater and Environmental Studies, Dundalk Institute of Technology, Dundalk, Co Louth, A91 K584, Ireland

16 National Museum of Natural History, Bulgarian Academy of Sciences, 1000 Sofia, Bulgaria

17 River and Conservation Research, Institute of Ecology, University of Innsbruck, 6020 Innsbruck, Austria

18 Department of Aquatic Ecosystems, Institute of Biodiversity and Ecosystem Research, Bulgarian Academy of Sciences, 1000 Sofia, Bulgaria

18

19 current address: Centre for Environment, Fisheries and Aquaculture Science (Cefas), Pakefield Road, Lowestoft, Suffolk NR33 OHT, UK

20 Department of Aquatic Sciences and Assessment, Swedish University of Agricultural Sciences, 75007 Uppsala, Sweden

21 current address: Department of Bioscience, Aarhus University, 8600 Silkeborg, Denmark

22 Department of Ecology and Environmental Science, Umeå University, 90736 Umeå, Sweden

23 current address: Norwegian Institute for Water Research, 0349 Oslo, Norway

24 Department of Life Sciences and Systems Biology, University of Turin, 10124 Turin, Italy

25 current address: Laboratoire des Sciences du Climat et de l'Environnement (LSCE), CEA, CNRS, UVSQ, 91191 Gif-Sur-Yvette, France / United States Geological Survey, Boulder, CO 80303, USA

26 Marine Institute, Furnace, Newport, Co Mayo F28 PF65, Ireland

27 current address: Environmental Archaeology Lab, Department of Historical, Philosophical and Religious studies, Umeå University, 90736 Umeå, Sweden

28 Department of Evolutionary Biology, Ecology and Environmental Sciences, Faculty of Biology, University of Barcelona (UB), 08028 Barcelona, Spain

29 Centre for Ecology, Evolution and Environmental Changes (cE3c), Faculdade de Ciências, Universidade de Lisboa, 1749-016 Lisboa, Portugal

30 Institute for Environmental Sciences, University of Koblenz-Landau, 76829 Landau, Germany

31 Institute of Microbiology, University of Innsbruck, 6020 Innsbruck, Austria

32 Experimental Limnology, Leibniz-Institute of Freshwater Ecology and Inland Fisheries (IGB), 16775 Stechlin, Germany

33 Center for Advanced Studies of Blanes, Spanish National Research Council, 17300 Blanes, Spain

34 South African Institute of Aquatic Biodiversity, Makhanda, 6139, South Africa

35 current address: Department of Forest Ecology and Management, Swedish University of Agricultural Sciences, 90183 Umeå, Sweden

36 Department of Ecology and Environmental Sciences, Palacky University in Olomouc, 77146 Olomouc, Czech Republic

37 Environmental Research Institute, University of Highlands and Islands (UHI), Thurso KW14 7JD, Scotland, UK

38 Department of General and Applied Hydrobiology, Sofia University "St. Kliment Ohridski", 1164 Sofia, Bulgaria

39 Chemical Analytics and Biogeochemistry, Leibniz-Institute of Freshwater Ecology and Inland Fisheries, 12587 Berlin, Germany

40 current address: Groupe de Recherche Interuniversitaire en Limnologie, Département des Sciences Biologiques, Université du Québec à Montréal, Montréal H3C 3J7, Canada

*Corresponding author: Katrin Attermeyer (katrin.attermeyer@wcl.ac.at)

Author order except first, second, and last author was computed randomly

Globally, inland waters emit over 2 Pg of carbon (C) per year as carbon dioxide (CO_2), of which 90% originates from streams and rivers. Despite the global significance of fluvial CO_2 emissions, little is known about their diel dynamics. Here, we present the first large-scale, year-round assessment of day- and night-time CO_2 fluxes at the water-air interface. Fluxes were directly measured once per season using drifting chambers in 34 streams across 11 European countries. Median CO_2 fluxes amounted to 1.4 mmol m^{-2} h^{-1} at midday and 2.1 mmol m^{-2} h^{-1} at midnight with night fluxes exceeding those during day by 39% across all seasons. Diel CO_2 flux variability matched the diel amplitude of water partial pressure of CO_2 (pCO_2), suggesting biogeochemical sources and sinks of CO_2 are more important than turbulence to explain CO_2 flux variability. Our results highlight substantial fluvial CO_2 flux changes from day to night, which need to be considered to more accurately assess global fluvial CO_2 emissions.

Main text

Inland waters are important sources of atmospheric CO_2 partially offsetting the terrestrial carbon sink [1,2]. Streams and rivers therein represent major CO_2 emitters, contributing 90% of the total flux from inland waters [3]. Fluvial CO_2 fluxes are primarily controlled by the gas exchange velocity at the water-air interface (k) and the gradient between the water and atmospheric partial pressures of CO_2 (pCO_2) [4]. Both parameters are highly variable in space and time [5,6], causing uncertainty in the magnitude of regional and global fluvial CO_2 emissions [2].

The high spatiotemporal variability of k and water pCO_2 can be attributed to a complex interplay of underlying controls. While k in streams is mostly driven by water turbulence created by variations in flow and stream morphology [7], the water pCO_2 is influenced by the degree of hydrological connectivity between the stream and the adjacent riparian soils [8] as well as by in-stream processes (e.g., stream metabolism). The supply of CO_2 from external sources, such as soil water or groundwater, into streams varies with reach and season [5,9]. Furthermore, seasonal and diel changes in stream pCO_2 are attributed to stream metabolism driven by temperature and solar radiation [10–13]. Ecosystem respiration, a source of CO_2 into the stream, takes place throughout the whole day, and gross primary production, a sink of CO_2, occurs only during daylight. Temperature and solar radiation also directly influence water pCO_2, the former by changing the solubility of the gas and the latter due to photomineralization [14]. However, the magnitude and relative drivers of seasonal and diel fluctuations of CO_2 fluxes in streams remain open questions.

Presently, most fluvial CO_2 emission values are derived from k estimates based on water velocity and stream channel slope and on water pCO_2 values indirectly calculated from alkalinity, pH, and temperature [3]. This approach fails to capture the high spatiotemporal variability observed for k and pCO_2 and therefore incorrectly estimates CO_2 fluxes [15,16]. Direct field observations provide the means to improve estimates and understanding of the drivers behind spatiotemporal variability, and thus the dynamics of CO_2 outgassing from running waters. However, beside some local studies that indirectly infer CO_2 fluxes from pCO_2 concentrations and k [11,12,17,18], no direct measurements exist that compare day- and night-time CO_2 fluxes from streams on a larger spatial scale across seasons.

The aim of this study was to assess the magnitude and drivers of stream CO_2 flux variations between day and night across European streams and across seasons. We hypothesized that CO_2 fluxes differ between day and night likely due to diel variations in terrestrial inorganic carbon inputs, *in situ* metabolism, and

temperature. As higher temperatures and solar radiation may favor differences in pCO_2, we expected a higher difference between day- and night-time fluxes in spring and summer (temporal) and at lower latitudes (spatial). Hence, we measured day and night-time fluxes of CO_2 once every season from 34 streams (Strahler stream orders from 1 to 6) in 11 countries across Europe following a standardized procedure. CO_2 fluxes were measured at midday (11am Greenwich Mean Time (GMT)) and midnight (11pm GMT) with drifting flux chambers equipped with CO_2 sensors as described in Bastviken et al. (2015) [19].

Substantial CO_2 flux variation from day to night

Midday CO_2 fluxes at the water-air interface ranged from -2.7 (uptake) to 19.9 mmol m^{-2} h^{-1} (emission) (1.4 [0.5, 3.1]; median [interquartile range (IQR)]; n = 107) and midnight fluxes ranged from -0.3 to 25.6 mmol m^{-2} h^{-1} (2.1 [0.9, 3.7]; n = 107) (Fig. 1). Our measured fluxes are comparable to other studies conducted in temperate and boreal streams that used chambers [20,21] or empirical models [12,22,23], although they were in the lower range of the numbers modelled in Hotchkiss et al. (2015) [23] (Fig. S5). This might be due to the lack of tributary inflows, large woody debris and strong hydraulic jumps in the selected stream sections (Supplementary Hand Out protocol). Similarly, the median standardized gas exchange velocity (k_{600}) was 1.68 m d^{-1} for both, day and night, and thus 70% lower than the global average of 5.7 m d^{-1} estimated in Raymond et al. (2013) [3] for streams and rivers.

To assess stream CO_2 flux variations between day and night, we computed the difference of night- minus day-time fluxes for each stream and season, where positive numbers indicate an increase from day to night and vice versa (Fig. 1). Differences in CO_2 fluxes amounted to 0.5 mmol m^{-2} h^{-1} [0.1, 1.4] (n = 107) across all sites and seasons, which is equivalent to a relative increase of 39% [4%, 100%] (n = 101; n reduced due to exclusion of relative comparisons to zero flux at day-time) (Fig. 2a). Based on estimation statistics with bootstrap sampling, the most probable day-to-night change in CO_2 fluxes amounted to 26% [9.3%, 38.9%] (Fig. S4). For comparison, in the lower Mississippi River, the relative increase of the CO_2 evasion rates during hours of darkness was only of 10-25% [18]. Our estimates are likely conservative as we compared fixed time points at midday and midnight, while largest diel differences in stream pCO_2 concentrations have generally been detected at the end of the day compared to the end of the night [12,18,24].

Diel differences in CO_2 fluxes varied among streams and seasons. In 34.6% of the comparisons (37 out of 107) we found a significant increase from midday to midnight (Fig. 2b). In 19% of these increases, the stream even switched from a sink of CO_2 at midday to a source of CO_2 to the atmosphere at midnight (Table S3). In 45% of the comparisons (48 out of 107) no statistically significant changes were detected, whereas some streams (7.5%; 8 out of 107) surprisingly showed significantly lower CO_2 fluxes at midnight (Fig. 2b). This proportion (significant decreases from midday to midnight) could be expected to occur by chance in a series of multiple independent comparisons (see Supplementary Methods and Results). We therefore regard the significant night-time decreases to be an artifact of multiple comparisons, while the night-time increase reflects an ecologically relevant pattern. A rough annual extrapolation of fluxes from our study sites (Supplementary Methods) shows that the inclusion of night-time fluxes increases annual estimates of stream CO_2 emissions by on average 16% (Table S4 and Supplementary Methods). Hence, our measurements and the simplified extrapolation of our data emphasize the need to collect and integrate night-time CO_2 flux data into sampling protocols as well as regional and global upscaling efforts.

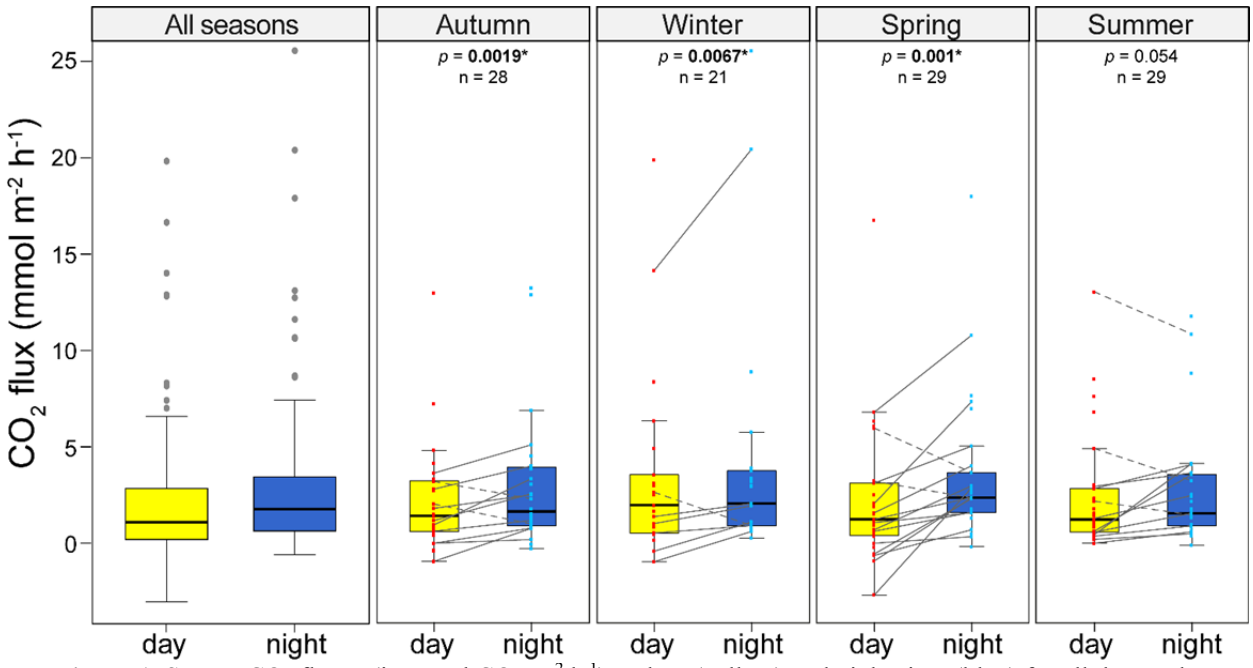

Figure 1. Stream CO_2 fluxes (in mmol CO_2 m^{-2} h^{-1}) at day- (yellow) and night-time (blue) for all data and separately for each season. In the panel including all seasons, gray dots indicate outliers outside the range of 1.5 * inter-quartile ranges. In the seasonal comparisons, CO_2 fluxes for individual stream sites are indicated by red (day) and light blue (night) dots. Gray continuous lines indicate significant increases from day to night and gray dashed lines indicate significant decreases from day to night. The boxplots visualize the median of all stream sites (line), the first and third quartiles (hinges), and the 1.5 * inter-quartile ranges (whiskers). The differences in the CO_2 fluxes in mmol CO_2 m^{-2} h^{-1} from day to night are for autumn: 0.5 [0.1, 1.2]; winter: 0.5 [0.3, 0.9]; spring: 1.1 [0.1, 2.3]; summer: 0.3 [-0.2, 1.1] (median [IQR]). On top are *p* values retrieved from paired comparisons of median CO_2 fluxes tested by Wilcoxon signed rank tests and the sample size (n). Significant *p* values with $p < 0.05$ are in bold with an asterisk.

Highest diel CO_2 flux differences in Southern Europe and in spring

On the spatial scale, we found that the diel differences in CO_2 fluxes were significantly negatively related to latitude (Table 1A), with substantial diel variation more likely in Southern Europe. This might be explained by higher temperatures and solar radiation boosting in-stream primary production [25]. However, substantial diel changes in CO_2 emissions have also been recorded in Arctic streams [13] highlighting the need for further research to investigate latitudinal patterns. Currently, it is difficult to compare our measurements with other studies as, to our knowledge, there are no studies using flux chambers to measure CO_2 fluxes and compare those fluxes at day- and night-time on such a large spatial scale.

We found no significant differences in the magnitude of diel differences in CO_2 fluxes between seasons for the aggregated dataset (Table 1A) using a linear mixed-effect model (LME). However, comparing the CO_2 fluxes at midday to midnight in each season separately, we detected significant diel changes in CO_2 fluxes in autumn, winter, and spring (Fig. 1). Contrary to our hypothesis, we did not detect significant changes from day to night in summer (Fig. 1), during which period the lowest changes in absolute numbers were recorded (0.3 mmol m^{-2} h^{-1}; Fig. 1). The highest differences of CO_2 fluxes from day to night were measured during spring (1.1 mmol m^{-2} h^{-1}), followed by winter (0.5 mmol m^{-2} h^{-1}) and autumn (0.5 mmol m^{-2} h^{-1}). Lower day-night changes in summer could be explained by increased riparian shading reducing in-stream metabolism [26,27]. For example, reduced in-stream metabolism in summer compared to

spring has been shown for a subalpine stream network [27] or a temperate forested headwater stream [26]. However, comparing the canopy cover of the streams and the differences in CO_2 fluxes from day to night (Fig. S6) revealed no clear pattern whilst concurrent decreases from midday to midnight in oxygen and pH in summer indicate higher ecosystem respiration, thus rejecting shade as a limiting factor (Fig. 3, Fig. S7c, f). A probable alternate explanation is that CO_2 production via photomineralization during the day counteracted a decrease via CO_2 fixation by photosynthesis[28] and diminished diel pCO_2 and ultimately CO_2 flux changes. This highlights the complex interplay between different light-dependent processes in streams influencing pCO_2 concentrations on a diel scale.

The importance of year-round measurement is highlighted by the winter data set containing the second highest diel CO_2 flux changes. European ice-free streams may be perceived "dormant" during these periods and representative CO_2 flux estimates are thus often missing [3]. Our winter data showed a magnitude of flux comparable to the rest of the year across the European streams as well as a high diel variability in CO_2 fluxes (Fig. 1). This may be attributed in part to the latitudinal coverage of our study as we included streams from the boreal to the Mediterranean. For example, the water temperatures of the Spanish streams were still relatively high in winter around 2.8 - 9.5°C during the day whereas Swedish streams showed these temperatures in autumn and spring. A study in the coterminous US looking into stream pCO_2 variability also reports varying strengths of diel pCO_2 variability, dependent on the investigated stream and time [29]. Hence, diel pCO_2 and CO_2 flux variability can be large in streams of the northern hemisphere, stressing the need to unravel the site-specific drivers of and mechanisms behind these diel changes.

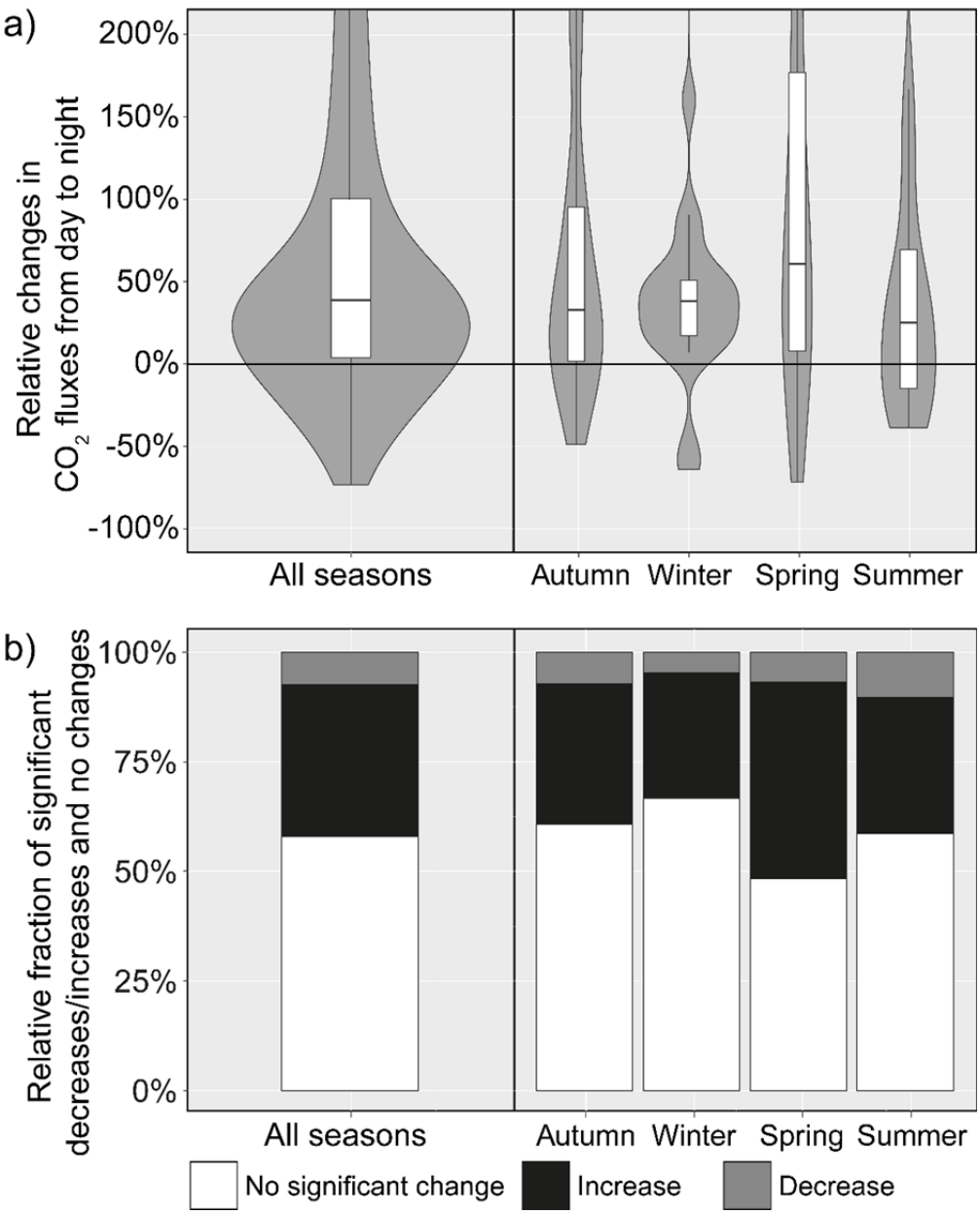

Figure 2. Relative changes in CO_2 fluxes from day to night (expressed as a %-change of the day-time values) for all data together and for each season (a) and relative fraction of significant increases, decreases, and no statistically significant changes from day to night (b), given for all comparisons and each season separately. A positive value in a) indicates an increase in CO_2 fluxes during the night and vice versa. Outliers (> 1.5 * IQR) for a) were excluded for illustration purposes as the large relative variation in these fluxes was due to minor absolute variation in fluxes close to zero. The median relative changes were positive throughout all seasons, ranging from 32% [0.6%, 95%] in autumn, 38% [16%, 50%] in winter, 60% [7%, 177%] in spring, to 24% [-16%, 69%] in summer (median [IQR]; n = 26, 21, 28, and 26, respectively).

Diel CO_2 flux variability driven by changes in water pCO_2

To understand the mechanisms behind the observed changes in CO_2 fluxes from day to night, we selected the measured biochemical parameters that vary on a diel scale (Table 1B; Fig. S7) and explored the influence of these parameters on CO_2 flux using a LME. The diel CO_2 flux variability in European streams could be mostly attributed to changes in water pCO_2 (Table 1B), whereas changes in the gas exchange velocity k appeared less important. In fact, we did not measure significant variations in k from day to night in our streams (Fig. 3; Supplementary Fig. S7h).

Increased water pCO_2 during the night has been attributed to in-stream metabolic signals [13,18], although a recent study suggests that the adjacent groundwater can show measurable but less pronounced diel pCO_2 variations [30]. In the absence of associations with variables related to in-stream metabolism (e.g., O_2) and no significant diel changes of O_2 in autumn, winter, and spring, external sources may explain the amplitude of water pCO_2. However, the CO_2 sources in streams can vary with size and our sampling streams covered a wide size range. In small streams, CO_2 concentrations are mostly driven by terrestrially-derived inputs of CO_2 [23], which can show diel variability linked to riparian evapotranspiration or temperature [31,32]. In larger streams and rivers *in situ* metabolism contributes to CO_2 supersaturation and evasion [23], however even in small streams, it can act on a seasonal or diel scale [10–13]. We did not find any trend in CO_2 flux changes with stream order as a proxy for size (Fig. S8) although other studies suggest changes over a size gradient [23,33]. Hence, further research is needed on diel variability of the sources of pCO_2 in streams and the occurrence across different sizes.

Table 1. Results of the linear mixed model testing effects of latitude and season (A) and the effect of day-to-night differences of physical and biogeochemical data (Δ = night minus day values) (B) on the day-to-night difference of CO_2 fluxes. Stream ID was included as a random effect on the intercept. Significances of fixed effects were assessed with likelihood ratio tests with degrees of freedom = 1. The slope direction (sign) of the effect is indicated with – or + when significant. Significant p values <0.05 are in bold.

Response variable	Fixed effect	χ^2 (1)	p	sign
A) Testing spatial and temporal hypotheses				
CO_2 flux difference from day to night	Latitude	8.1913	**0.004**	-
	Season	3.0897	0.378	
	Latitude * Season	5.1331	0.162	
B) Testing physical and biogeochemical drivers				
CO_2 flux difference from day to night	Δ water O_2 concentration	0.0140	0.906	
	Δ pH	0.2560	0.613	
	Δ conductivity	0.1280	0.721	
	Δ Tw-Ta* (proxy for heat flux)	0.1895	0.663	
	Δ water pCO_2	4.0232	**0.045**	+
	Δ gas transfer velocity k	0.4974	0.481	
	Δ water temperature	0.2490	0.618	

* Heat flux calculated as water temperature (Tw) minus air temperature (Ta).
A) Marginal $R^2 = 0.14$, conditional $R^2 = 0.23$, sample size =107.
B) Marginal $R^2 = 0.08$, conditional $R^2 = 0.09$, sample size = 72.

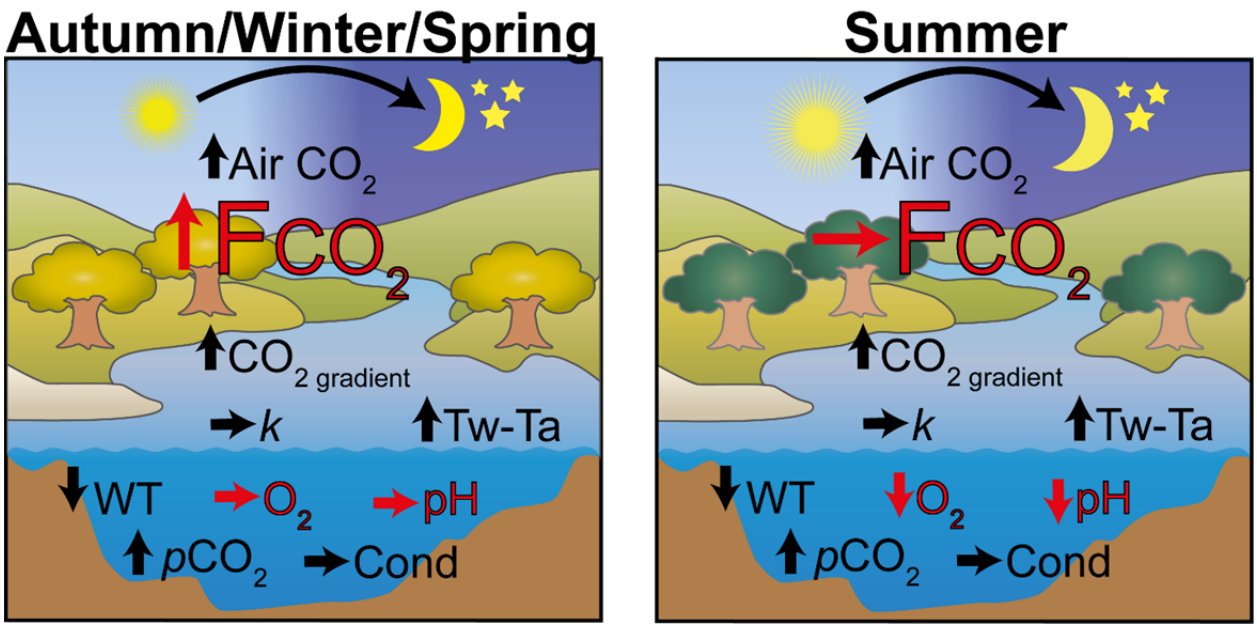

Figure 3. Diel changes in CO_2 fluxes (F_{CO_2}) and other physical and chemical parameters for autumn/winter/spring and summer, respectively. The physical and chemical parameters comprise atmospheric CO_2 (Air CO_2), the differences of CO_2 concentrations in the water minus the air ($CO_{2\ gradient}$), the water-air gas transfer velocity (k), the differences of temperatures in the water minus the air (Tw-Ta), the water temperature (WT), the oxygen concentration in the water (O_2), pH in the water, the partial pressure of CO_2 in the water (pCO_2), and conductivity (Cond). The arrows indicate significant increases (↑) or significant decreases (↓) from day to night as well as no significant change (→) tested by a Wilcoxon signed rank test (see Supplementary Fig. S7 for more information). The differences between the seasons autumn/winter/spring (right) and summer (left) detected in our study are highlighted in red.

Hotspots of diel variation in CO_2 fluxes to refocus future research efforts

With the aim to inform future studies where hotspots of diel variation in CO_2 fluxes can be expected, we used our dataset to predict what characterizes streams where CO_2 fluxes significantly vary from day to night. We developed several binomial regression models that predict whether diel CO_2 fluxes change significantly or not based on catchment variables and selected the best model based on the Akaike information criterion (AIC). The best model indicated that the likelihood of finding significant changes in CO_2 fluxes from day to night is high in streams that have a smaller subcatchment area and a lower percentage of forest land (Table S5). Indeed, high-frequency monitoring of CO_2 concentrations in an agricultural lowland stream in Sweden with a small catchment has revealed the most pronounced diel dynamics reported to date [34]. Thus, special attention should be given to these types of streams. It is worth noting that currently our model has a misclassification error of 40% (median of 1000 model runs, 95% confidence interval ranges between 23 and 53%; see Table S5). Hence, additional mechanistic studies are needed to better predict where and when diel changes of stream CO_2 fluxes will occur.

While our results provide a first insight into the drivers of day-night differences in CO_2 fluxes, the high uncertainty in the model as well as the sometimes opposing patterns - increases and decreases from day to night in different streams and seasons - point towards different drivers varying on a temporal and spatial scale. The physical and chemical variables (Fig. 3) were surprisingly poor predictors of day to night differences in CO_2 fluxes across all streams and seasons (see R^2 in Table 1), further suggesting a complex

combination of factors governing diel patterns across large spatial scales. Despite the high spatiotemporal scale of our study, there was no relationship between CO_2 fluxes and other biogeochemical factors than water pCO_2, which does not exclude the potential existence of relationships at other scales (e.g., at even higher resolutions).We recommend that future study designs incorporate high-frequency CO_2 data together with biogeochemical variables from the stream (i. e., O_2) and the atmosphere (i. e., CO_2 or temperature) [35]. Additionally, we recommend including radioactive or stable carbon isotope signatures to track potential sources of CO_2 and their changes in streams [36,37] to better assess terrestrial-aquatic linkages. Linking temporal patterns of CO_2 fluxes with its drivers across large spatial scales is a path towards a more accurate understanding of their role in regional and global carbon cycles. Our results demonstrate that, in many streams across Europe, night-time CO_2 fluxes substantially exceed day-time, and are thus critical for accurate daily and annual estimates of CO_2 emissions from inland waters.

Methods

The project included 16 teams distributed across 11 European countries. Every team sampled one to three streams every three months within a time frame of two weeks for a whole year to cover the seasons autumn, winter, spring, and summer. In total, 34 stream sites (Fig. S1) were visited each season during the specified two weeks' time frame except for 11 streams in winter that were frozen during the sampling weeks (Table S3).

CO_2 fluxes were measured once every season with drifting flux chambers equipped with CO_2 sensors. This method has proven to be a reliable and least biased direct measurement of CO_2 fluxes at the water-air interface in streams [19,38]. CO_2 concentrations in the chamber headspace were logged every 30 seconds over a period of 5 to 10 minutes during each run, and CO_2 fluxes were calculated based on the rate of change over time in pCO_2 in the chamber headspace. At each stream, we measured CO_2 fluxes with the flux chamber (5 times), pCO_2 concentration in the atmosphere and water with the CO_2 sensors in the flux chamber (details described in Supplementary Methods), pH, temperature, conductivity, and oxygen in the water with a multiprobe (Table S2) at midday and midnight. Stream width, depth, and discharge were determined during the day. In addition, the following information were collected for each stream once during the study: stream order, climate zone, catchment area until the endpoint of the investigated stream site and the percentage of coverage of different land use classes in this catchment area, and predominant geology (Table S1).

Flux rates were obtained from the linear slopes of the pCO_2 in the chamber headspace over time and a flux was accepted if the coefficient of determination (R^2) of the slope was at least 0.65 [39]. An exception was made in cases where the slope was close to zero and the pCO_2 concentrations in the atmosphere and water (measured at the same time) were at equilibrium. These fluxes were set to zero. Final flux rates F (mmol CO_2 m^{-2} h^{-1}) were calculated according to Eq. (1) [40]:

$$F = S * 10^{-3} \frac{PV}{RTA} * 60 * 60, \quad (1)$$

where S is the slope (ppm s^{-1}), P is the pCO_2 concentration in the atmosphere (atm), V is the volume (mL) of the drifting chamber, R is the gas constant (82.0562 mL atm K^{-1} mol^{-1}), T is the chamber air temperature (K), A is the bottom area of the chamber (m^2), and the last term is the conversion from seconds to hours. In this study, we followed the sign convention whereby positive values indicate a CO_2 flux from the stream to the atmosphere (source) and negative values indicate a flux from the atmosphere to the stream (sink). The magnitudes of variations between day- and night-time measurements are additionally stated as percent increases, which were computed by dividing the difference between the

values at night minus day by the value at day and expressing the result as a percent change from day to night.

We used F (Eq. 1) to calculate the gas transfer velocity (k in cm h^{-1}) by inverting the equation for Fick's law of gas diffusion, according to Eq. (2):

$$k = \frac{F}{kH\left(CO_{2_{water}} - CO_{2_{air}}\right)} * 100, \quad (2)$$

where kH is Henry's constant (in mol L^{-1} atm^{-1}) adjusted for temperature [41].

For comparison of transfer velocities between sites and seasons and with the literature, k (Eq. 2) was standardized to k_{600} (Eq. 3):

$$k_{600} = k\left(\frac{600}{S_c}\right)^{-0.5}, \quad (3)$$

where k is the transfer velocity at *in situ* temperature (T), Sc is the Schmidt number for *in situ* temperature T, and the Schmidt number for 20°C in freshwater is 600 and representing a hydrodynamically rough water surface to be expected in streams, the exponent of -0.5 was chosen [42].

All statistical analyses were performed with median values of three to five floating chamber runs per day and night, respectively, using the statistical programming language R [43] (version 3.5.1). Samplings that generated less than three values for either day or night due to an R^2 of the slope <0.65 [39] were excluded from further analysis reducing the number from 136 to 107 day-night comparisons. For our statistical tests, the alpha level was set to $\alpha = 0.05$. Significant differences between day- and night-time measurements for each season across all streams were tested with Wilcoxon signed rank tests [44] where median day- and night-time values for each stream site were paired (Fig. 1). The same tests were conducted for the other biogeochemical variables measured at midday and midnight (see Fig. 3; Fig. S7). To test significant changes between CO_2 fluxes of day and night for each stream and season separately, we used Wilcoxon rank sum tests ("wilcox.test" function). We thereby assumed that day- and night-time measurements are independent since we were measuring different water parcels. We tested each hypothesis (H0 = day and night-time CO_2 fluxes are the same) separately without correcting for multiple comparisons, e. g., Bonferroni. Especially in small data sets (like ours), reducing the type I error for null hypotheses with rather conservative corrections increases the type II error for those hypotheses that are not null [45]. Instead, we evaluated whether the observed number of significant day-to-night changes could have simply occurred by chance by comparing it to the expected number of type I errors simulated using the Bernoulli equation. In addition, we estimated the most likely difference using bootstrap-coupled estimations to avoid the pitfalls of significance testing (see Supplementary Methods 4 and Results 1).

A first linear mixed-effect model (LME) tested the latitudinal effect and differences between seasons of CO_2 flux differences from day to night. A second LME was built to evaluate the biochemical factors potentially influencing the differences of night- minus day-time fluxes. For these tests, we used the "lmer" function of the R-package "lme4" [46] with Maximum Likelihood estimation. Fixed effects for the LME with biogeochemical parameters for CO_2 flux differences from day to night included absolute differences from day to night of oxygen concentration in the water, pH, conductivity, temperature gradient of atmosphere and water, water pCO_2, gas transfer velocity k, and water temperature. For the LMEs we included stream ID as a random effect allowing different intercepts for each stream to account for pseudoreplication (one data point per season per stream) and z-scaled all fixed effects with the "scale"

function before running the models. Statistical significances of fixed effects were assessed with likelihood ratio tests using the function "drop1" [47]. The respective LMEs were followed by a model validation, checking the residuals for normal distribution and homogeneity of variances. A separation of the dataset to check if drivers between increases from day to night and decreases from day to night differ, did not reveal acceptable models in terms of model validation (i.e. residuals were not normally distributed). Although our dataset provided a large spatial coverage on day-night differences in CO_2 fluxes in European streams, it did not have the statistical power to test for significant drivers separately for increases and decreases.

In another approach, we aimed to explore the variables that best predict significant changes from day to night in CO_2 fluxes by a binomial regression model with two groups: 1) significant changes from day to night (either increase or decrease) or 2) no significant changes. For the binomial regression analysis, we used the "multinom" function of the R package "nnet" [48]. Briefly, the full dataset gets randomly subset in a training dataset (70% of the observations) and a test dataset (30% of the observations). The misclassification error expresses the prediction accuracy of the model built with the training dataset when applied to the test dataset. Since the misclassification error is depending on the randomly selected training and test dataset, we run the model 1000 times and report the median and 95% confidence interval for the relevant model parameters (Table S5). We used variables that can be obtained remotely (e.g., extracted from GIS shape files) in order to be able to predict hot spots of diel CO_2 flux variability. The initial full model included the fixed effects stream order, catchment area, the land cover categories forest, agriculture, and urban, altitude, latitude, climate zone after Köppen Geiger (determined by the package "kgc" in R [49]), surface lithology, and geology (see Supplementary Methods for details on definitions and classifications of lithology and geology). Fixed effects were excluded stepwise while comparing the AIC of individual models. The best model included catchment area, the proportion of forested land cover, and latitude (Table S5). As for the linear mixed effect model, stream ID was included as a random effect and the continuous fixed effects were z-scaled beforehand.

References

1. Butman, D. E. *et al.* Aquatic carbon cycling in the conterminous United States and implications for terrestrial carbon accounting. *Proc. Natl. Acad. Sci.* **113**, 58–63 (2016).

2. Drake, T. W., Raymond, P. A. & Spencer, R. G. M. Terrestrial carbon inputs to inland waters: A current synthesis of estimates and uncertainty. *Limnol. Oceanogr. Lett.* **3**, 132–142 (2018).

3. Raymond, P. A. *et al.* Global carbon dioxide emissions from inland waters. *Nature* **503**, 355–359 (2013).

4. MacIntyre, S., Wanninkhof, R. & Chanton, J. P. Trace gas exchange in freshwater and coastal marine systems: flux across the air water interface. in *Methods in Ecology: Biogenic Trace Gases: Measuring Emissions from Soil and Water* 52–97 (Blackwell Publishing, 1995).

5. Duvert, C., Butman, D. E., Marx, A., Ribolzi, O. & Hutley, L. B. CO2 evasion along streams driven by groundwater inputs and geomorphic controls. *Nat. Geosci.* **11**, 813–818 (2018).

6. Rocher□Ros, G., Sponseller, R. A., Lidberg, W., Mörth, C. & Giesler, R. Landscape process domains drive patterns of CO2 evasion from river networks. *Limnol. Oceanogr. Lett.* **4**, 87–95 (2019).

7. Hall, R. O. & Ulseth, A. J. Gas Exchange in Streams and Rivers. *WIREs Water* e1391 (2019).

doi:10.1002/wat2.1391

8. Hope, D., Palmer, S. M., Billet, M. F. & Dawson, J. J. C. Variations in dissolved CO2 and CH4 in a first-order stream and catchment: an investigation of soil-stream linkages. *Hydrol. Process.* **18**, 3255–3275 (2004).

9. Horgby, Å., Gómez-Gener, L., Escoffier, N. & Battin, T. J. Dynamics and potential drivers of CO2 concentration and evasion across temporal scales in high-alpine streams. *Environ. Res. Lett.* **14**, 124082 (2019).

10. Guasch, H., Armengol, J., Martí, E. & Sabater, S. Diurnal variation in dissolved oxygen and carbon dioxide in two low-order streams. *Water Res.* **32**, 1067–1074 (1998).

11. Lynch, J. K., Beatty, C. M., Seidel, M. P., Jungst, L. J. & DeGrandpre, M. D. Controls of riverine CO2 over an annual cycle determined using direct, high temporal resolution pCO2 measurements. *J. Geophys. Res.* **115**, G03016 (2010).

12. Peter, H. *et al.* Scales and drivers of temporal pCO2 dynamics in an Alpine stream. *J. Geophys. Res. Biogeosciences* **119**, 1078–1091 (2014).

13. Rocher-Ros, G., Sponseller, R. A., Bergstr, A.-K., Myrstener, M. & Giesler, R. Stream metabolism controls diel patterns and evasion of CO2 in Arctic streams. *Glob. Chang. Biol.* **00**, 1–14 (2019).

14. Koehler, B., Landelius, T., Weyhenmeyer, G. A., Machida, N. & Tranvik, L. J. Sunlight-induced carbon dioxide emissions from inland waters. *Global Biogeochem. Cycles* **28**, 696–711 (2014).

15. Golub, M., Desai, A. R., McKinley, G. A., Remucal, C. K. & Stanley, E. H. Large Uncertainty in Estimating pCO2 From Carbonate Equilibria in Lakes. *J. Geophys. Res. Biogeosciences* **122**, 2909–2924 (2017).

16. Raymond, P. A. *et al.* Scaling the gas transfer velocity and hydraulic geometry in streams and small rivers. *Limnol. Oceanogr. Fluids Environ.* **2**, 41–53 (2012).

17. Schelker, J., Singer, G. A., Ulseth, A. J., Hengsberger, S. & Battin, T. J. CO2 evasion from a steep, high gradient stream network: importance of seasonal and diurnal variation in aquatic pCO2 and gas transfer. *Limnol. Oceanogr.* **61**, 1826–1838 (2016).

18. Reiman, J. H. & Xu, Y. J. Diel variability of pCO2 and CO2 outgassing from the lower Mississippi River: Implications for riverine CO2 outgassing estimation. *Water* **11**, 43 (2019).

19. Bastviken, D., Sundgren, I., Natchimuthu, S., Reyier, H. & Gålfalk, M. Technical Note: Cost-efficient approaches to measure carbon dioxide (CO2) fluxes and concentrations in terrestrial and aquatic environments using mini loggers. *Biogeosciences* **12**, 3849–3859 (2015).

20. Looman, A., Maher, D. T., Pendall, E., Bass, A. & Santos, I. R. The carbon dioxide evasion cycle of an intermittent first-order stream: contrasting water–air and soil–air exchange. *Biogeochemistry* **132**, 87–102 (2017).

21. Crawford, J. T. *et al.* CO2 and CH4 emission from streams: Patterns, controls, and regional significance. *Global Biogeochem. Cycles* **28**, 197–210 (2014).

22. Teodoru, C. R., Del Giorgio, P. A., Prairie, Y. T. & Camire, M. Patterns in pCO2 in boreal streams and rivers of northern Quebec, Canada. *Global Biogeochem. Cycles* **23**, GB2012 (2009).

23. Hotchkiss, E. R. *et al.* Sources of and processes controlling CO2 emissions change with the size of streams and rivers. *Nat. Geosci.* **8**, 696–699 (2015).

24. Bodmer, P., Heinz, M., Pusch, M., Singer, G. & Premke, K. Carbon dynamics and their link to dissolved organic matter quality across contrasting stream ecosystems. *Sci. Total Environ.* **553**, 574–586 (2016).

25. Demars, B. O. L. *et al.* Impact of warming on CO2 emissions from streams countered by aquatic photosynthesis. *Nat. Geosci.* **9**, 758–761 (2016).

26. Roberts, B. J., Mulholland, P. J. & Hill, W. R. Multiple scales of temporal variability in ecosystem metabolism rates: Results from 2 years of continuous monitoring in a forested headwater stream. *Ecosystems* **10**, 588–606 (2007).

27. Ulseth, A. J., Bertuzzo, E., Singer, G. A., Schelker, J. & Battin, T. J. Climate-Induced Changes in Spring Snowmelt Impact Ecosystem Metabolism and Carbon Fluxes in an Alpine Stream Network. *Ecosystems* **21**, 373–390 (2018).

28. Cory, R. M., Ward, C. P., Crump, B. C. & Kling, G. W. Sunlight controls water column processing of carbon in arctic fresh waters. *Science (80-.).* **345**, 925–928 (2014).

29. Crawford, J. T., Stanley, E. H., Dornblaser, M. M. & Striegl, R. G. CO2 time series patterns in contrasting headwater streams of North America. *Aquat. Sci.* **79**, 473–486 (2016).

30. Riml, J., Campeau, A., Bishop, K. & Wallin, M. B. Spectral Decomposition Reveals New Perspectives on CO2 Concentration Patterns and Soil-Stream Linkages. *J. Geophys. Res. Biogeosciences* **124**, 3039–3056 (2019).

31. Schwab, M., Klaus, J., Pfister, L. & Weiler, M. Diel discharge cycles explained through viscosity fluctuations in riparian inflow. *Water Resour. Res.* **52**, 8744–8755 (2016).

32. Riveros-Iregui, D. A. *et al.* A watershed-scale assessment of a process soil CO2 production and efflux model. *Water Resour. Res.* **47**, W00J04 (2011).

33. Liu, S. & Raymond, P. A. Hydrologic controls on pCO2 and CO2 efflux in US streams and rivers. *Limnol. Oceanogr. Lett.* **3**, 428–435 (2018).

34. Wallin, M. B., Audet, J., Peacock, M., Sahlée, E. & Winterdahl, M. Carbon dioxide dynamics in an agricultural headwater stream driven by hydrology and primary production. *Biogeosciences* **17**, 2487–2498 (2020).

35. Vachon, D. *et al.* Paired O2-CO2 measurements provide emergent insights into aquatic ecosystem function. *Limnol. Oceanogr. Lett.* (2019).

36. Campeau, A. *et al.* Stable Carbon Isotopes Reveal Soil-Stream DIC Linkages in Contrasting Headwater Catchments. *J. Geophys. Res. Biogeosciences* **123**, 149–167 (2018).

37. Campeau, A. *et al.* Current forest carbon fixation fuels stream CO2 emissions. *Nat. Commun.* **10**, 1–9 (2019).

38. Lorke, A. *et al.* Technical note: Drifting versus anchored flux chambers for measuring greenhouse gas emissions from running waters. *Biogeosciences* **12**, 7013–7024 (2015).

39. Tremblay, A., Varfalvy, L., Garneau, M. & Roehm, C. *Greenhouse gas Emissions-Fluxes and Processes: hydroelectric reservoirs and natural environments*. (Springer Science & Business Media, 2005).

40. Duc, N. T. *et al.* Automated Flux Chamber for Investigating Gas Flux at Water–Air Interfaces. *Environ. Sci. Technol.* **47**, 968–975 (2013).

41. Goldenfum, J. A. *GHG Measurement Guidelines for Freshwater Reservoirs: Derived From: The UNESCO/IHA Greenhouse Gas Emissions from Freshwater Reservoirs Research Project*. (International Hydropower Association (IHA), 2010).

42. Jähne, B. *et al.* On the parameters influencing air□water gas exchange. *J. Geophys. Res. Ocean.* **92**, 1937–1949 (1987).

43. R Core Team. R: A language and environment for statistical computing. *R Found. Stat. Comput. Vienna, Austria* (2018).

44. Wilcoxon, F. Individual Comparisons by Ranking Methods. *Biometrics Bull.* **1**, 80–83 (1945).

45. Rothman, K. J. No Adjustments Are Needed for Multiple Comparisons. *Epidemiology* **1**, 43–46 (1990).

46. Bates, D., Maechler, M., Bolker, B. & Walker, S. Fitting Linear Mixed-Effects Models Using lme4. *J. Stat. Softw.* **67**, 1–48 (2015).

47. Zuur, A., Ieno, E. N., Walker, N., Saveliev, A. A. & Smith, G. M. *Mixed effects models and extensions in ecology with R*. (Springer Science & Business Media, 2009).

48. Venables, W. N. & Ripley, B. D. *Modern applied statistics with S*. (Springer, 2002).

49. Bryant, C., Wheeler, N. R., Rubel, F. & French, R. H. kgc: Koeppen-Geiger Climatic Zones. *R Packag. version 1.0.2* (2017).

Acknowledgements

We thank the initiators of the first Collaborative European Freshwater Science Project for Young Researchers, the European Federation of Freshwater Sciences (EFFS) board, the European Fresh and Young Researchers (EFYR) and the representatives of the Fresh Blood for Fresh Water (FBFW) meetings. We also thank the seven national freshwater societies financing this project, namely the Iberian Association of Limnology (AIL; Spain and Portugal), Deutsche Gesellschaft für Limnologie e.V. (DGL; Germany), Swiss Society for Hydrology and Limnology (SGHL; Switzerland), Italian Association of Oceanography and Limnology (Italy), Freshwater Biological Association (FBA; United Kingdom), French Limnological Association (AFL; France), Austrian Limnological Society (SIL-Austria), as well as the Leibniz-Institute of Freshwater Ecology and Inland Fisheries for additional funds. We acknowledge Luigi Naselli-Flores and Antonio Camacho for their encouragement and support during the project. We also thank David Bastviken, Ingrid Sundgren, and Thanh Duc Nguyen for the introduction to the logger and chamber construction and advice for measurements of CO_2 fluxes with the chamber and Vincent Fugère for his help in setting up the linear mixed models. Furthermore, we are very thankful to Rafael Marcé for his thoughtful comments on the manuscript.

Author contributions

K. A. and P.B. conceived the study design, coordinated the project and contributed equally to this work; all authors collected and analyzed the field data and K.A. and P.B. gathered and performed the quality check of all data; K.A., P.B. and J.P.C.-R. co-wrote the paper with the help of M.K., G.H.N., and N.C. All authors commented on the manuscript.

Competing financial interests

The authors declare no competing financial interests.

Data availability statement

The data that support the findings of this study are openly available in figshare at http://doi.org/10.6084/m9.figshare.12717188.